

Summary of the Bulletin of the International Seismological Centre

2016

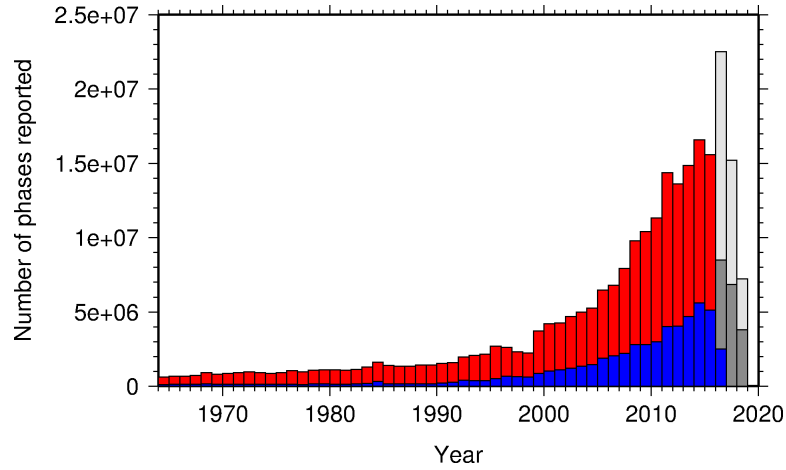
January – June

Volume 53 Issue I

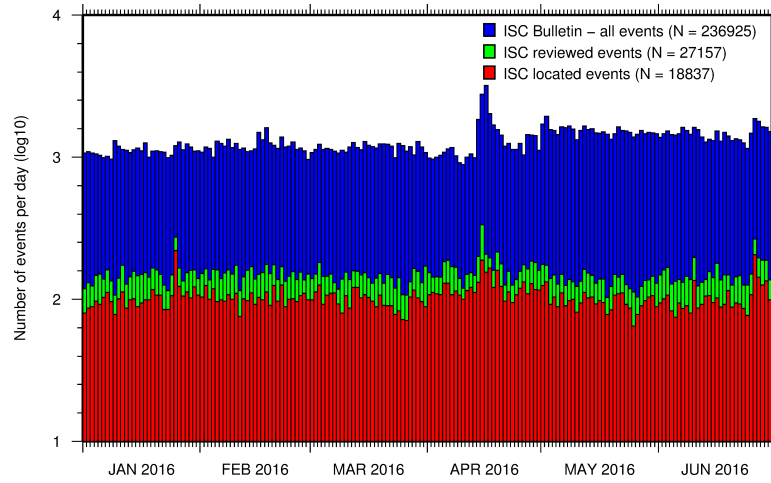
www.isc.ac.uk

ISSN 2309-236X

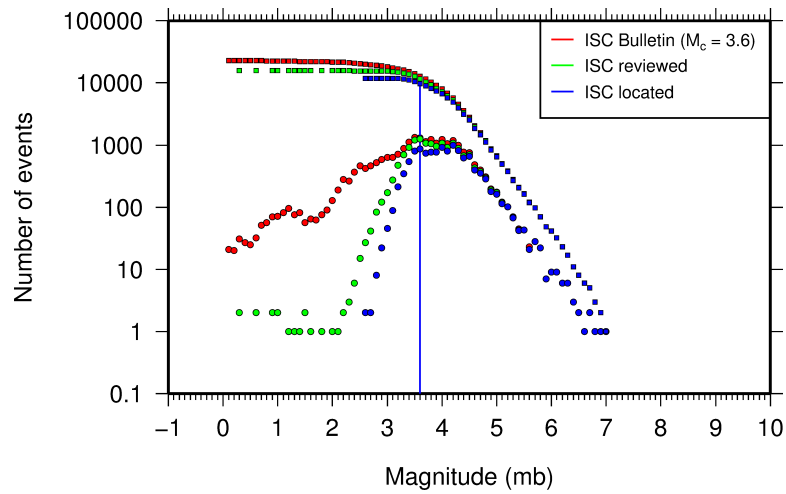
2019



The number of phases (red) and number of amplitudes (blue) collected by the ISC for events each year since 1964. The data in grey covers the current period where data are still being collected before the ISC review takes place and are accurate at the time of publication. See Section 8.3.



The number of events within the Bulletin for the current summary period. The vertical scale is logarithmic. See Section 9.1.



Frequency and cumulative frequency magnitude distribution for all events in the ISC Bulletin, ISC reviewed events and events located by the ISC. The magnitude of completeness (M_C) is shown for the ISC Bulletin. Note: only events with values of m_b are represented in the figure. See Section 9.4.

Summary of the Bulletin of the International Seismological Centre

2016

January - June

Volume 53 Issue I

Produced and edited by:

Kathrin Lieser, James Harris and Dmitry Storchak

Published by
International Seismological Centre



ISC Data Products

<http://www.isc.ac.uk/products/>

ISC Bulletin:

<http://www.isc.ac.uk/iscbulletin/search>

ISC Bulletin and Catalogue monthly files, to the last reviewed month in FFB or ISF1 format:

[ftp://www.isc.ac.uk/pub/\[isf|ffb\]/bulletin/yyyy/yyyymm.gz](ftp://www.isc.ac.uk/pub/[isf|ffb]/bulletin/yyyy/yyyymm.gz)

[ftp://www.isc.ac.uk/pub/\[isf|ffb\]/catalogue/yyyy/yyyymm.gz](ftp://www.isc.ac.uk/pub/[isf|ffb]/catalogue/yyyy/yyyymm.gz)

Datafiles for the ISC data before the rebuild:

[ftp://www.isc.ac.uk/pub/prerebuild/\[isf|ffb\]/bulletin/yyyy/yyyymm.gz](ftp://www.isc.ac.uk/pub/prerebuild/[isf|ffb]/bulletin/yyyy/yyyymm.gz)

[ftp://www.isc.ac.uk/pub/prerebuild/\[isf|ffb\]/catalogue/yyyy/yyyymm.gz](ftp://www.isc.ac.uk/pub/prerebuild/[isf|ffb]/catalogue/yyyy/yyyymm.gz)

ISC-EHB Bulletin:

<http://www.isc.ac.uk/isc-ehb/search/>

IASPEI Reference Event List (GT bulletin):

<http://www.isc.ac.uk/gtevents/search/>

ISC-GEM Global Instrumental Earthquake Catalogue:

<http://http://www.isc.ac.uk/iscgem/download.php>

ISC Event Bibliography:

http://www.isc.ac.uk/event_bibliography/bibsearch.php

International Seismograph Station Registry:

<http://www.isc.ac.uk/registries/search/>

Seismological Contacts:

<http://www.isc.ac.uk/projects/seismocontacts/>

Copyright © 2019 by International Seismological Centre

Permission granted to reproduce for personal and educational use only. Commercial copying, hiring, lending is prohibited.

International Seismological Centre

Pipers Lane

Thatcham

RG19 4NS

United Kingdom

www.isc.ac.uk

ISSN 2309-236X

Printed and bound in Wales by Cambrian Printers.

Contents

1	Preface	1
2	The International Seismological Centre	2
2.1	The ISC Mandate	2
2.2	Brief History of the ISC	3
2.3	Former Directors of the ISC and its U.K. Predecessors	4
2.4	Member Institutions of the ISC	5
2.5	Sponsoring Organisations	9
2.6	Data Contributing Agencies	11
2.7	ISC Staff	18
3	Availability of the ISC Bulletin	24
4	Citing the International Seismological Centre	25
5	Operational Procedures of Contributing Agencies	27
5.1	Monitoring System of the Institute of Geophysical Research of the Ministry of Energy of the Republic of Kazakhstan	27
5.1.1	Regional Seismicity and Station Network	27
5.1.2	Data Processing and Data Availability	32
5.1.3	References	36
6	The ISC Bulletin Rebuild Project: 1980 – 1984	39
7	Summary of Seismicity, January – June 2016	41
8	Statistics of Collected Data	47
8.1	Introduction	47
8.2	Summary of Agency Reports to the ISC	47
8.3	Arrival Observations	52
8.4	Hypocentres Collected	59
8.5	Collection of Network Magnitude Data	61
8.6	Moment Tensor Solutions	67
8.7	Timing of Data Collection	69
9	Overview of the ISC Bulletin	71

9.1	Events	71
9.2	Seismic Phases and Travel-Time Residuals	80
9.3	Seismic Wave Amplitudes and Periods	85
9.4	Completeness of the ISC Bulletin	88
9.5	Magnitude Comparisons	89
10	The Leading Data Contributors	93
10.1	The Largest Data Contributors	93
10.2	Contributors Reporting the Most Valuable Parameters	96
10.3	The Most Consistent and Punctual Contributors	100
11	Appendix	102
11.1	ISC Operational Procedures	102
11.1.1	Introduction	102
11.1.2	Data Collection	102
11.1.3	ISC Automatic Procedures	103
11.1.4	ISC Location Algorithm	107
11.1.5	Review Process	117
11.1.6	History of Operational Changes	118
11.2	IASPEI Standards	119
11.2.1	Standard Nomenclature of Seismic Phases	119
11.2.2	Flinn-Engdahl Regions	126
11.2.3	IASPEI Magnitudes	133
11.2.4	The IASPEI Seismic Format (ISF)	137
11.2.5	Ground Truth (GT) Events	139
11.2.6	Nomenclature of Event Types	141
11.3	Tables	142
12	Glossary of ISC Terminology	162
13	Acknowledgements	166
	References	167

1

Preface

Dear Colleague,

This is the first 2016 issue of the Summary of the ISC Bulletin, which remains the most fundamental reason for continued operations at the ISC. This issue covers earthquakes and other seismic events that occurred during the period from January to June 2016. The full annual DVD-ROM will be sent together with the second 2016 issue. In the mean time, the monthly files for January to June period are available from the ISC ftp site. For instructions, please see the www.isc.ac.uk/iscbulletin/.

This publication contains information on the ISC, its staff, Members, Sponsors and Data providers. It offers analysis of the data contributed to the ISC by many seismological agencies worldwide as well as analysis of the data in the ISC Bulletin itself. This issue also includes seismological standards and procedures used by the ISC in its operations.

Notably, this issue contains information on the recently released portion of the Rebuilt ISC Bulletin for the period 1980-1984 that replaced the original ISC Bulletin data.

We continue publishing invited articles describing the history, current status and operational procedures at those networks that contribute data to the ISC. This time it is the turn for the seismic network run by the Kazakhstan National Data Centre in Almaty.

We hope that you find this publication useful in your work. If your home-institution or company is unable, for one reason or another, to support the long-term international operations of the ISC in full by becoming a Member or a Sponsor, then, please, consider subscribing to this publication by contacting us at admin@isc.ac.uk.

With kind regards to our Data Contributors, Members, Sponsors and users,

Dr Dmitry A. Storchak

Director

International Seismological Centre (ISC)

2

The International Seismological Centre

2.1 The ISC Mandate

The International Seismological Centre (ISC) was set up in 1964 with the assistance of UNESCO as a successor to the International Seismological Summary (ISS) to carry forward the pioneering work of Prof. John Milne, Sir Harold Jeffreys and other British scientists in collecting, archiving and processing seismic station and network bulletins and preparing and distributing the definitive summary of world seismicity.

Under the umbrella of the International Association of Seismology and Physics of the Earth Interior (IASPEI/IUGG), the ISC has played an important role in setting international standards such as the International Seismic Bulletin Format (ISF), the IASPEI Standard Seismic Phase List (SSPL) and both the old and New IASPEI Manual of the Seismological Observatory Practice (NMSOP-2) (www.iaspei.org/projects/NMSOP.html).

The ISC has contributed to scientific research and prominent scientists such as John Hodgson, Eugene Herrin, Hal Thirlaway, Jack Oliver, Anton Hales, Ola Dahlman, Shigeji Suehiro, Nadia Kondorskaya, Vit Karnik, Stephan Müller, David Denham, Bob Engdahl, Adam Dziewonski, John Woodhouse and Guy Masters all considered it an important duty to serve on the ISC Executive Committee and the Governing Council.

The current mission of the ISC is to maintain:

- the ISC **Bulletin** – the longest continuous definitive summary of World seismicity (collaborating with 130 seismic networks and data centres around the world). (www.isc.ac.uk/iscbulletin/)
- the International Seismographic Station Registry (**IR**, jointly with the World Data Center for Seismology, Denver). (www.isc.ac.uk/registries/)
- the IASPEI Reference Event List (Ground Truth, **GT**, jointly with IASPEI). (www.isc.ac.uk/gtevents/)

These are fundamentally important tasks. Bulletin data produced, archived and distributed by the ISC for almost 50 years are the definitive source of such information and are used by thousands of seismologists worldwide for seismic hazard estimation, for tectonic studies and for regional and global imaging of the Earth's structure. Key information in global tomographic imaging is derived from the analysis of ISC data. The ISC Bulletin served as a major source of data for such well known products as the ak135 global 1-D velocity model and the EHB (*Engdahl et al.*, 1998) and Centennial (*Engdahl and Villaseñor*, 2002) catalogues. It presents an important quality-control benchmark for the Comprehensive Nuclear-Test-Ban Treaty Organization (CTBTO). Hypocentre parameters from the ISC Bulletin are used

by the Data Management Center of the Incorporated Research Institutions for Seismology (IRIS DMC) to serve event-oriented user-requests for waveform data. The ISC-GEM Bulletin is a cornerstone of the ISC-GEM Global Instrumental Reference Earthquake Catalogue for Global Earthquake risk Model (GEM).

The ISC Bulletin contains over 6 million seismic events: earthquakes, chemical and nuclear explosions, mine blasts and mining induced events. At least 1.7 million of them are regional and teleseismically recorded events that have been reviewed by the ISC analysts. The ISC Bulletin contains approximately 200 million individual seismic station readings of arrival times, amplitudes, periods, SNR, slowness and azimuth, reported by approximately 17,000 seismic stations currently registered in the IR. Over 6,000 stations have contributed to the ISC Bulletin in recent years. This number includes the numerous sites of the USArray. The IASPEI GT List currently contains 8816 events for which latitude, longitude and depth of origin are known with high confidence (to 5 km or better) and seismic signals were recorded at regional and/or teleseismic distances.

2.2 Brief History of the ISC

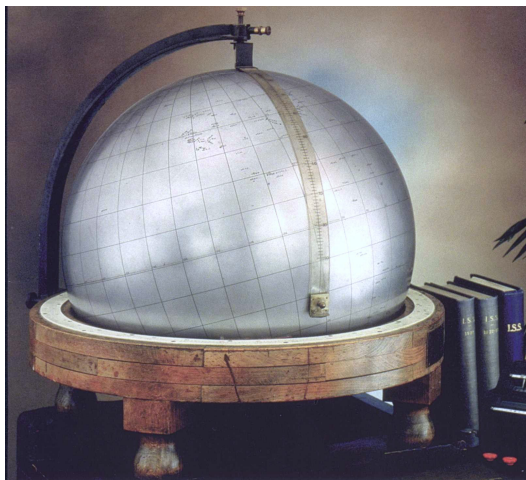


Figure 2.1: *The steel globe bearing positions of early seismic stations was used for locating positions of earthquakes for the International Seismological Summaries.*

(BCIS).

Earthquake effects have been noted and documented from the earliest times, but it is only since the development of earthquake recording instruments in the latter half of the 19th century that a proper study of their occurrence has been possible. After the first teleseismic observation of an earthquake in 1889, the need for international exchange of readings was recognised in 1895 by Prof. John Milne and by Ernst von Rebeur Paschwitz together with Georg Gerland, resulting in the publication of the first international seismic bulletins. Milne's "Slide Circulars" were issued under the auspices of the Seismological Committee of the British Association for the Advancement of Science (BAAS), while co-workers of Gerland at the Central Bureau of the International Association of Seismology worked independently in Strasbourg

Following Milne's death in 1913, Seismological Bulletins of the BAAS were continued under Prof. H.H. Turner, later based at Oxford University. Upon formal post-war dissolution of the International Association of Seismology in 1922 the newly founded Seismological Section of the International Union of Geodesy and Geophysics (IUGG) set up the International Seismological Summary (ISS) to continue at Oxford under Turner, to produce the definitive global catalogues from the 1918 data-year onwards, under the auspices of IUGG and with the support of the BAAS.

ISS production, led by several professors at Oxford University, and Sir Harold Jeffreys at Cambridge

University, continued until it was superseded by the ISC Bulletin, after the ISC was formed in Edinburgh in 1964 with Dr P.L. Willmore as its first director.

During the period 1964 to 1970, with the help of UNESCO and other international scientific bodies, the ISC was reconstituted as an international non-governmental body, funded by interested institutions from various countries. Initially there were supporting members from seven countries, now there are almost 60, and member institutions include national academies, research foundations, government departments and research institutes, national observatories and universities. Each member, contributing a minimum unit of subscription or more, appoints a representative to the ISC's Governing Council, which meets every two years to decide the ISC's policy and operational programme. Representatives from the International Association of Seismology and Physics of the Earth's Interior also attend these meetings. The Governing Council appoints the Director and a small Executive Committee to oversee the ISC's operations.



Figure 2.2: *ISC building in Thatcham, Berkshire, UK.*

In 1975, the ISC moved to Newbury in southern England to make use of better computing facilities there. The ISC subsequently acquired its own computer and in 1986 moved to its own building at Pipers Lane, Thatcham, near Newbury. The internal layout of the new premises was designed for the ISC and includes not only office space but provision for the storage of extensive stocks of ISS and ISC publications and a library of seismological observatory bulletins, journals and books collected over many tens of years.

In 1997 the first set of the ISC Bulletin CD-ROMs was produced (not counting an earlier effort at USGS). The first ISC website appeared in 1998 and the first ISC database was put in day-to-day operations from 2001.

Throughout 2009-2011 a major internal reconstruction of the ISC building was undertaken to allow for more members of staff working in mainstream ISC operations as well as major development projects such as the CTBTO Link, ISC-GEM Catalogue and the ISC Bulletin Rebuild.

2.3 Former Directors of the ISC and its U.K. Predecessors



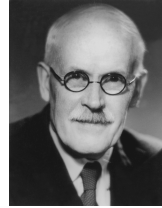
John Milne
Publisher of the Shide Circular Reports on Earthquakes
1899-1913



Herbert Hall Turner
Seismological Bulletins of the BAAS
1913-1922
Director of the ISS
1922-1930



Harry Hemley Plaskett
Director of the ISS
1931-1946



Harold Jeffreys
Director of the ISS
1946-1957



Robert Stoneley
Director of the ISS
1957-1963



P.L. (Pat) Willmore
Director of the ISS
1963-1970
Director of the ISC
1964-1970



Edouard P. Arnold
Director of the ISC
1970-1977



Anthony A. Hughes
Director of the ISC
1977-1997



Raymond J. Willemann
Director of the ISC
1998-2003



Avi Shapira
Director of the ISC
2004-2007

2.4 Member Institutions of the ISC

Article IV(a-b) of the ISC Working Statutes stipulates that any national academy, agency, scientific institution or other non-profit organisation may become a Member of the ISC on payment to the ISC of a sum equal to at least one unit of subscription and the nomination of a voting representative to serve on the ISC's governing body. Membership shall be effective for one year from the date of receipt at the ISC of the annual contribution of the Member and is thereafter renewable for periods of one year.

The ISC is currently supported with funding from its 62 Member Institutions and a four-year Grant Award EAR-1811737 from the US National Science Foundation.

Figures 2.3 and 2.4 show major sectors to which the ISC Member Institutions belong and proportional

financial contributions that each of these sectors make towards the ISC's annual budget.

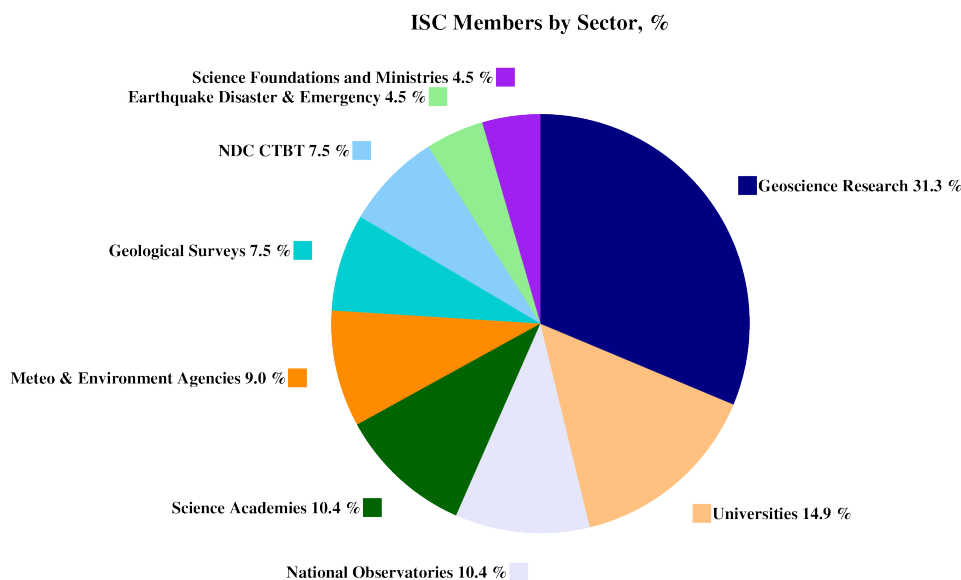


Figure 2.3: Distribution of the ISC Member Institutions by sector in year 2013 as a percentage of total number of Members.

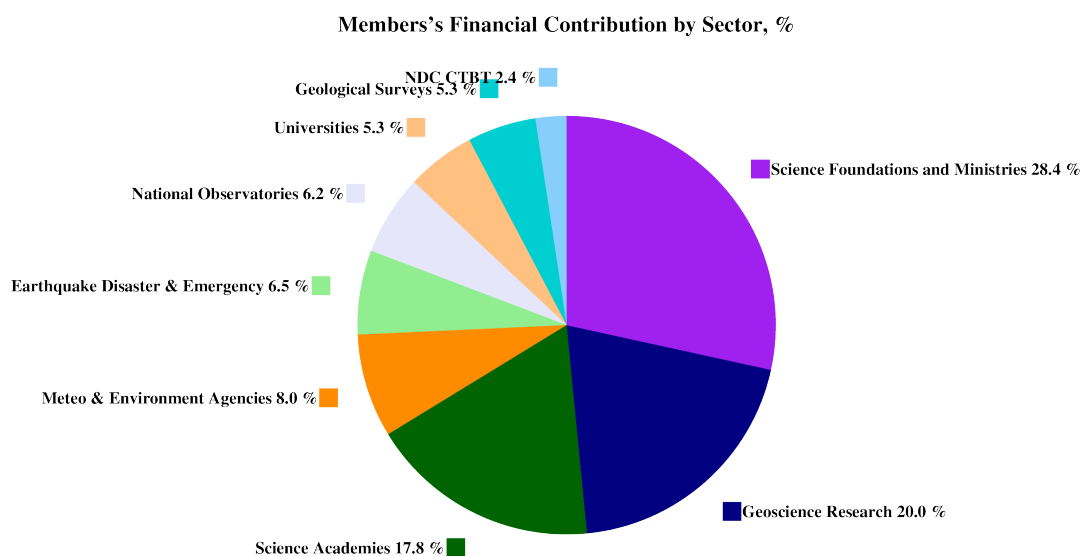


Figure 2.4: Distribution of Member's financial contributions to the ISC by sector in year 2013 as a percentage of total annual Member contributions.

There follows a list of all current Member Institutions with a category (1 through 9) assigned according to the ISC Working Statutes. Each category relates to the number of membership units contributed.



Centre de Recherche
en Astronomie, As-
trophysique et Géo-
physique (CRAAG)
Algeria
www.craag.dz
Category: 1



Instituto Nacional de
Prevención Sísmica (IN-
PRES)
Argentina
www.inpres.gov.ar
Category: 1



Geoscience Australia
Australia
www.ga.gov.au
Category: 4



Bundesministerium
für Wissenschaft,
Forschung und
Wirtschaft (BMFWF)
Austria
www.bmbwk.gv.at
Category: 2



Centre of Geophysical
Monitoring (CGM) of
the National Academy
of Sciences of Belarus
Belarus
www.cgm.org.by
Category: 1



Belgian Science Policy
Office (BELSPO)
Belgium
Category: 1



Seismological Observa-
tory, Institute of Geo-
sciences, University of
Brasilia
Brazil
www.obsis.unb.br
Category: 1



Universidade de São
Paulo, Centro de Sis-
mologia
Brazil
www.sismo.iag.usp.br
Category: 1



The Geological Survey
of Canada
Canada
gsc.nrcan.gc.ca
Category: 4



Centro Sismologico Na-
cional, Universidad de
Chile
Chile
ingenieria.uchile.cl
Category: 1



China Earthquake Ad-
ministration
China
www.cea.gov.cn
Category: 4



Institute of Earth Sci-
ences, Academia Sinica
Chinese Taipei
www.earth.sinica.edu.tw
Category: 1



Geological Survey De-
partment
Cyprus
www.moa.gov.cy
Category: 1



Institute of Geophysics,
Academy of Sciences of
the Czech Republic
Czech Republic
www.avcr.cz
Category: 1



Geological Survey of
Denmark and Green-
land (GEUS)
Denmark
www.geus.dk
Category: 2



National Research Insti-
tute for Astronomy and
Geophysics (NRIAG),
Cairo
Egypt
www.nriag.sci.eg
Category: 1



The University of
Helsinki
Finland
www.helsinki.fi
Category: 2



Laboratoire de Dé-
tection et de Géo-
physique/CEA
France
www-dase.cea.fr
Category: 2



Institute National des
Sciences de l'Univers
France
www.insu.cnrs.fr
Category: 4



GeoForschungsZentrum
Potsdam
Germany
www.gfz-potsdam.de
Category: 2



Bundesanstalt für Ge-
owissenschaften und
Rohstoffe
Germany
www.bgr.bund.de
Category: 4



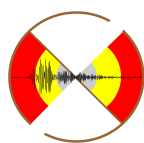
The Seismological Insti-
tute, National Observa-
tory of Athens
Greece
www.noa.gr
Category: 1



The Hungarian
Academy of Sciences
Hungary
www.mta.hu
Category: 1



The Icelandic Meteoro-
logical Office
Iceland
www.vedur.is
Category: 1



National Centre for
Seismology, Ministry of
Earth Sciences of India
India
www.moes.gov.in
Category: 4



Iraqi Meteorological Or-
ganization and Seismol-
ogy
Iraq
www.imos-tm.com
Category: 1



Dublin Institute for Ad-
vanced Studies
Ireland
www.dias.ie
Category: 1



The Geophysical Insti-
tute of Israel
Israel
www.gii.co.il
Category: 1



Soreq Nuclear Research
Centre (SNRC)
Israel
www.soreq.gov.il
Category: 1



Istituto Nazionale di
Geofisica e Vulcanologia
Italy
www.ingv.it
Category: 3



Istituto Nazionale di
Oceanografia e di Ge-
ofisica Sperimentale
Italy
www.ogs.trieste.it
Category: 1



University of the West
Indies at Mona
Jamaica
www.mona.uwi.edu
Category: 1



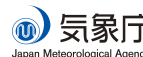
Earthquake Research
Institute, University of
Tokyo
Japan
www.eri.u-tokyo.ac.jp
Category: 3



Japan Agency for
Marine-Earth Science
and Technology (JAM-
STEC)
Japan
www.jamstec.go.jp
Category: 2



National Institute of Po-
lar Research (NiPR)
Japan
www.nipr.ac.jp
Category: 1



The Japan Meteorologi-
cal Agency (JMA)
Japan
www.jma.go.jp
Category: 5



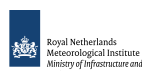
Royal Scientific Society
Jordan
www.rss.jo
Category: 1



Centro de Investigación
Científica y de Edu-
cación Superior de Ense-
ñada (CICESE)
Mexico
resnom.cicese.mx
Category: 1



Institute of Geophysics,
National University of
Mexico
Mexico
www.igeofcu.unam.mx
Category: 1



The Royal Netherlands
Meteorological Institute
(KNMI)
Netherlands
www.knmi.nl
Category: 2



GNS Science
New Zealand
www.gns.cri.nz
Category: 3



Stiftelsen NORSAR
Norway
www.norsar.no
Category: 2



The University of
Bergen
Norway
www.uib.no
Category: 2



Institute of Geophysics,
Polish Academy of Sci-
ences
Poland
www.igf.edu.pl
Category: 1



Instituto Português do
Mar e da Atmosfera
Portugal
www.ipma.pt
Category: 2



Red Sismica de Puerto
Rico
Puerto Rico
redsismica.uprm.edu
Category: 1



Korean Meteorological
Administration
Republic of Korea
www.kma.go.kr
Category: 1



National Institute for
Earth Physics
Romania
www.infp.ro
Category: 1



Russian Academy of Sci-
ences
Russia
www.ras.ru
Category: 5



Earth Observatory of
Singapore (EOS), an
autonomous Institute of
Nanyang Technological
University
Singapore
www.earthobservatory.sg
Category: 1



Environmental Agency
of Slovenia
Slovenia
www.arso.gov.si
Category: 1



Council for Geoscience
South Africa
www.geoscience.org.za
Category: 1



Institute of Earth Sci-
ences Jaume Almera
Spain
www.ictja.csic.es
Category: 1



Institut Cartogràfic i
Geològic de Catalunya
(ICGC)
Spain
www.icgc.cat
Category: 1



Uppsala Universitet
Sweden
www.uu.se
Category: 2



National Defence Re-
search Establishment
(FOI)
Sweden
www.foi.se
Category: 1



The Swiss Academy of
Sciences
Switzerland
www.scnat.ch
Category: 2



The Seismic Research
Centre, University of
the West Indies at St.
Augustine
Trinidad and Tobago
www.uwiseismic.com
Category: 1



Kandilli Observatory
and Earthquake Re-
search Institute
Turkey
www.koeri.boun.edu.tr
Category: 1



Disaster and Emergency
Management Authority
(AFAD)
Turkey
www.deprem.gov.tr
Category: 2



British Geological Sur-
vey
United Kingdom
www.bgs.ac.uk
Category: 2



AWE Blacknest
United Kingdom
www.blacknest.gov.uk
Category: 1



The Royal Society
United Kingdom
www.royalsociety.org
Category: 6



Incorporated Research
Institutions for Seismol-
ogy
U.S.A.
www.iris.edu
Category: 1



National Earthquake In-
formation Center, U.S.
Geological Survey
U.S.A.
www.neic.usgs.gov
Category: 1



Texas Seismological
Network (TexNet),
Bureau of Economic
Geology, J.A. & K.G.
Jackson School of Geo-
sciences, University of
Texas at Austin
U.S.A.
www.beg.utexas.edu
Category: 1



The National Science
Foundation of the
United States. (Grant
No. EAR-1811737)
U.S.A.
www.nsf.gov
Category: 9

In addition the ISC is currently in receipt of grants from the International Data Centre (IDC) of the Preparatory Commission of the Comprehensive Nuclear-Test-Ban Treaty Organization (CTBTO), FM Global, Lighthill risk Network, USGS (Award G15AC00202), BGR and Willis Towers Watson.



2.5 Sponsoring Organisations

Article IV(c) of the ISC Working Statutes stipulates any commercial organisation with an interest in the objectives and/or output of the ISC may become an Associate Member of the ISC on payment of an Associate membership fee, but without entitlement to representation with a vote on the ISC's governing body.

MS&AD**MS&AD InterRisk Research & Consulting**[http://www.irric.co.jp/en/
corporate/](http://www.irric.co.jp/en/corporate/)

MS&AD InterRisk Research & Consulting, Inc. is responsible for the core of risk-related service businesses in the MS&AD group. We provide services which meet various expectations of the clients, including consulting, research and investigation, seminars and publications for risk management in addition to the think-tank functions.

REF TEK
A TRIMBLE BRANDwww.reftek.com

REF TEK designs and manufactures application specific, high-performance, battery-operated, field-portable geophysical data acquisition devices for the global market. With over 35 years of experience, REF TEK provides customers with complete turnkey solutions that include high resolution recorders, broadband sensors, state-of-the-art communications (V-SAT, GPRS, etc), installation, training, and continued customer support. Over 7,000 REF TEK instruments are currently being used globally for multiple applications. From portable earthquake monitoring to telemetry earthquake monitoring, earthquake aftershock recording to structural monitoring and more, REF TEK equipment is suitable for a wide variety of application needs.

GeoSIG
swiss made to measure<http://www.geosig.com/>

GeoSIG provides earthquake, seismic, structural, dynamic and static monitoring and measuring solutions. As an ISO Certified company, GeoSIG is a world leader in design and manufacture of a diverse range of high quality, precision instruments for vibration and earthquake monitoring. GeoSIG instruments are at work today in more than 100 countries around the world with well-known projects such as the NetQuakes installation with USGS and Oresund Bridge in Denmark. GeoSIG offers off-the-shelf solutions as well as highly customised solutions to fulfil the challenging requirements in many vertical markets including the following:

- Earthquake Early Warning and Rapid Response (EEWRR)
- Seismic and Earthquake Monitoring and Measuring
- Industrial Facility Seismic Monitoring and Shutdown
- Structural Analysis and Ambient Vibration Testing
- Induced Vibration Monitoring
- Research and Scientific Applications



Güralp has been developing revolutionary force-feedback broadband seismic instrumentation for more than thirty years. Our sensors record seismic signals of all kinds, from teleseismic events occurring on the other side of the planet, to microseisms induced by unconventional hydrocarbon extraction. Our sophisticated digitisers record these signals with the highest resolution and accurate timing.

We supply individual instruments or complete seismic systems. Our services include field support such as installation and maintenance, to complete network and data management.

We design our instruments to meet increasingly complex requirements for deployment in the most challenging circumstances. As a result, you will find Güralp instruments gathering seismic data in the harshest of environments, from the Antarctic ice sheet; to boreholes 100s of metres deep; to the world's most active volcanoes and deepest ocean trenches.



























The Seismology Research Centre is an Australian earthquake observatory that began developing their own seismic recorders and data processing software in the late 1970s when digital recorders were uncommon. The Gecko is the SRC's 7th generation of seismic recorder, now available with a variety of integrated sensors to meet every monitoring requirement, including:

- Strong Motion Accelerographs
- 2Hz and 4.5Hz Blast Vibration Monitors
- Short Period 1Hz Seismographs
- Broadband 200s-1500Hz Optical Seismographs

Visit src.com.au/downloads/waves to grab a free copy of the SRC's MiniSEED waveform viewing and analysis software application, Waves.

2.6 Data Contributing Agencies

In addition to its Members and Sponsors, the ISC owes its existence and successful long-term operations to its 149 seismic bulletin data contributors. These include government agencies responsible for national seismic networks, geoscience research institutions, geological surveys, meteorological agencies, universities, national data centres for monitoring the CTBT and individual observatories. There would be no ISC Bulletin available without the regular stream of data that are unselfishly and generously contributed to the ISC on a free basis.

	East African Network EAF		The Institute of Seismology, Academy of Sciences of Albania Albania TIR		Centre de Recherche en Astronomie, Astrophysique et Géophysique Algeria CRAAG
	Universidad Nacional de La Plata Argentina LPA		Instituto Nacional de Prevención Sísmica Argentina SJA		National Survey of Seismic Protection Armenia NSSP
	Geoscience Australia Australia AUST		Curtin University Australia CUPWA		International Data Centre, CTBTO Austria IDC
	Zentralanstalt für Meteorologie und Geodynamik (ZAMG) Austria VIE		Republican Seismic Survey Center of Azerbaijan National Academy of Sciences Azerbaijan AZER		Royal Observatory of Belgium Belgium UCC
	Observatorio San Calixto Bolivia SCB		Republic Hydrometeorological Service, Seismological Observatory, Banja Luka Bosnia and Herzegovina RHSSO		Instituto Astronomico e Geofísico Brazil VAO
	Geophysical Institute, Bulgarian Academy of Sciences Bulgaria SOF		Seismological Observatory of Mount Cameroon Cameroon SOMC		Canadian Hazards Information Service, Natural Resources Canada Canada OTT
	Centro Sismológico Nacional, Universidad de Chile Chile GUC		China Earthquake Networks Center China BJI		Institute of Earth Sciences, Academia Sinica Chinese Taipei ASIES
	CWB Chinese Taipei TAP		Red Sismológica Nacional de Colombia Colombia RSNC		Sección de Sismología, Vulcanología y Exploración Geofísica Costa Rica UCR
	Seismological Survey of the Republic of Croatia Croatia ZAG		Servicio Sismológico Nacional Cubano Cuba SSNC		Cyprus Geological Survey Department Cyprus NIC



Institute of Geophysics,
Czech Academy of Sciences
Czech Republic
WBNET



The Institute of Physics
of the Earth (IPEC)
Czech Republic
IPEC



Geophysical Institute,
Academy of Sciences of
the Czech Republic
Czech Republic
PRU

Korea Earthquake Ad-
ministration
Democratic People's Re-
public of Korea
KEA



Geological Survey of
Denmark and Green-
land
Denmark
DNK



Observatorio Sismo-
logico Politecnico
Loyola
Dominican Republic
OSPL



Servicio Nacional de Sis-
mología y Vulcanología
Ecuador
IGQ



National Research Insti-
tute of Astronomy and
Geophysics
Egypt
HLW



Servicio Nacional de Es-
tudios Territoriales
El Salvador
SNET



University of Addis
Ababa
Ethiopia
AAE



Seismological Observa-
tory Skopje
FYR Macedonia
SKO



Institute of Seismology,
University of Helsinki
Finland
HEL



Laboratoire de Dé-
tection et de Géo-
physique/CEA
France
LDG



EOST / RéNaSS
France
STR



Laboratoire de Géo-
physique/CEA
French Polynesia
PPT



Institute of Earth Sci-
ences/ National Seismic
Monitoring Center
Georgia
TIF



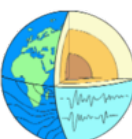
Bundesanstalt für Ge-
owissenschaften und
Rohstoffe
Germany
BGR



Alfred Wegener Insti-
tute for Polar and Ma-
rine Research
Germany
AWI



Seismological Observa-
tory Berggießhübel, TU
Bergakademie Freiberg
Germany
BRG



Geophysikalisches Ob-
servatorium Collm
Germany
CLL



National Observatory of
Athens
Greece
ATH



Department of Geo-
physics, Aristotle
University of Thessa-
loniki
Greece
THE



University of Patras,
Department of Geology
Greece
UPSL



INSIVUMEH
Guatemala
GCG



Hong Kong Observatory
Hong Kong
HKC



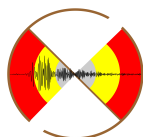
Geodetic and Geophysi-
cal Research Institute
Hungary
BUD



Geodetic and Geophysi-
cal Research Institute,
Hungarian Academy of
Sciences
Hungary
KRSZO



Icelandic Meteorological
Office
Iceland
REY



National Centre for Seis-
mology of the Ministry
of Earth Sciences of In-
dia
India
NDI



National Geophysical
Research Institute
India
HYB



Badan Meteorologi, Kli-
matologi dan Geofisika
Indonesia
DJA



Tehran University
Iran
TEH



International Institute
of Earthquake Engi-
neering and Seismology
(IIEES)
Iran
THR



Iraqi Meteorological and
Seismology Organi-
sation
Iraq
ISN



The Geophysical Insti-
tute of Israel
Israel
GII



Istituto Nazionale di
Oceanografia e di Ge-
ofisica Sperimentale
(OGS)
Italy
TRI



Laboratory of Research
on Experimental and
Computational Seimol-
ogy
Italy
RISSC



Istituto Nazionale di
Geofisica e Vulcanologia
Italy
ROM



Dipartimento per lo Stu-
dio del Territorio e delle
sue Risorse (RSNI)
Italy
GEN



MedNet Regional Cen-
troid - Moment Tensors
Italy
MED_RCMT

Station Géophysique de
Lamto
Ivory Coast
LIC



Jamaica Seismic Net-
work
Jamaica
JSN



Japan Meteorological
Agency
Japan
JMA



The Matsushiro Seismo-
logical Observatory
Japan
MAT



National Research Insti-
tute for Earth Science
and Disaster Prevention
Japan
NIED



National Institute of Po-
lar Research
Japan
SYO



Jordan Seismological
Observatory
Jordan
JSO



Seismological Experi-
mental Methodological
Expedition
Kazakhstan
SOME



National Nuclear Center
Kazakhstan
NNC

Kyrgyz Seismic Network
Kyrgyzstan
KNET



Institute of Seismology,
Academy of Sciences of
Kyrgyz Republic
Kyrgyzstan
KNET



Latvian Seismic Net-
work
Latvia
LVSN



National Council for
Scientific Research
Lebanon
GRAL



Geological Survey of
Lithuania
Lithuania
LIT

European Center for
Geodynamics and Seis-
mology
Luxembourg
ECGS



Macao Meteorological
and Geophysical Bureau
Macao, China
MCO

Antananarivo
Madagascar
TAN



Geological Survey De-
partment Malawi
Malawi
GSDM

Malaysian Meteorologi-
cal Service
Malaysia
KLM



Centro de Investigación
Científica y de Edu-
cación Superior de Ense-
nada
Mexico
ECX



Instituto de Geofísica de
la UNAM
Mexico
MEX



Institute of Geophysics
and Geology
Moldova
MOLD



Seismological Institute
of Montenegro
Montenegro
PDG



Centre National de
Recherche
Morocco
CNRM



The Geological Survey
of Namibia
Namibia
NAM



National Seismological
Centre, Nepal
Nepal
DMN



IRD Centre de Nouméa
New Caledonia
NOU



Institute of Geological
and Nuclear Sciences
New Zealand
WEL



Instituto Nicaraguense
de Estudios Territoriales
- INETER
Nicaragua
INET



University of Bergen
Norway
BER



Stiftelsen NORSAR
Norway
NAO



Sultan Qaboos Univer-
sity
Oman
OMAN



Micro Seismic Studies
Programme, PIN-
STECH
Pakistan
MSSP



Universidad de Panama
Panama
UPA



Philippine Institute of
Volcanology and Seis-
mology
Philippines
MAN



Institute of Geophysics,
Polish Academy of Sci-
ences
Poland
WAR



Instituto Geofísico do
Infante Dom Luiz
Portugal
IGIL

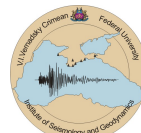
Sistema de Vigilância
Sismológica dos Açores
Portugal
SVSA



Instituto Português do
Mar e da Atmosfera, I.P.
Portugal
INMG



Centre of Geophysical
Monitoring of the Na-
tional Academy of Sci-
ences of Belarus
Republic of Belarus
BELR



Inst. of Seismology and
Geodynamics, V.I. Ver-
nadsky Crimean Federal
University
Republic of Crimea
CFUSG



Korea Meteorological
Administration
Republic of Korea
KMA



National Institute for
Earth Physics
Romania
BUC



Kola Regional Seismic
Centre, GS RAS
Russia
KOLA



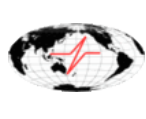
Kamchatkan Experi-
mental and Methodical
Seismological Depart-
ment, GS RAS
Russia
KRSC



Altai-Sayan Seismologi-
cal Centre, GS SB RAS
Russia
ASRS



Institute of Environ-
mental Problems of
the North, Russian
Academy of Sciences
Russia
IEPN



Geophysical Survey of
Russian Academy of Sci-
ences
Russia
MOS



Sakhalin Experimental
and Methodological
Seismological Expedi-
tion, GS RAS
Russia
SKHL



Baykal Regional Seismo-
logical Centre, GS SB
RAS
Russia
BYKL



Mining Institute of the
Ural Branch of the Rus-
sian Academy of Sci-
ences
Russia
MIRAS



Yakutiya Regional Sei-
smological Center, GS
SB RAS
Russia
YARS



North Eastern Regional
Seismological Centre,
GS RAS
Russia
NERS



Saudi Geological Survey
Saudi Arabia
SGS



Seismological Survey of
Serbia
Serbia
BEO



Geophysical Institute,
Slovak Academy of
Sciences
Slovakia
BRA



Slovenian Environment
Agency
Slovenia
LJU



Ministry of Mines, En-
ergy and Rural Electri-
fication
Solomon Islands
HNR



Council for Geoscience
South Africa
PRE



Real Instituto y Observatorio de la Armada
Spain
SFS



Instituto Geográfico Nacional
Spain
MDD



Institut Cartogràfic i Geològic de Catalunya
Spain
MRB

Sudan Seismic Network
Sudan
SSN



University of Uppsala
Sweden
UPP



Swiss Seismological Service (SED)
Switzerland
ZUR



The Seismic Research Centre
Trinidad and Tobago
TRN



Disaster and Emergency Management Presidency
Turkey
DDA



Kandilli Observatory and Research Institute
Turkey
ISK



The Global Project
U.S.A.
GCMT



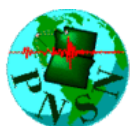
National Earthquake Information Center
U.S.A.
NEIC



Red Sísmica de Puerto Rico
U.S.A.
RSPR



IRIS Data Management Center
U.S.A.
IRIS



Pacific Northwest Seismic Network
U.S.A.
PNSN



Subbotin Institute of Geophysics, National Academy of Sciences
Ukraine
SIGU

Main Centre for Special Monitoring
Ukraine
MCSM



Dubai Seismic Network
United Arab Emirates
DSN



British Geological Survey
United Kingdom
BGS

Institute of Seismology, Academy of Sciences, Republic of Uzbekistan
Uzbekistan
ISU



Fundación Venezolana de Investigaciones Sísmológicas
Venezuela
FUNV



National Center for Scientific Research
Vietnam
PLV

Geological Survey Department of Zambia
Zambia
LSZ



Goetz Observatory
Zimbabwe
BUL

2.7 ISC Staff

Listed below are the staff (and their country of origin) who were employed at the ISC at the time of this ISC Bulletin Summary.

- Dmitry Storchak
- Director
- Russia/United Kingdom



- Lynn Elms
- Administration Officer
- United Kingdom



- James Harris
- Senior System and
Database Administrator
- United Kingdom



- Alfie James Barber
- System Administrator
- United Kingdom



- Gergely Csontos
- Web Developer
- Hungary



- John Eve
- Data Collection Officer
- United Kingdom



- Domenico Di Giacomo
- Seismologist
- Italy



- Konstantinos Lentas
- Seismologist/Developer
- Greece



- Rosemary Hulin (née Wylie)
- Analyst/Administrator
- United Kingdom



- Blessing Shumba
- Seismologist/Analyst
- Zimbabwe



- Rebecca Verney
- Analyst
- United Kingdom



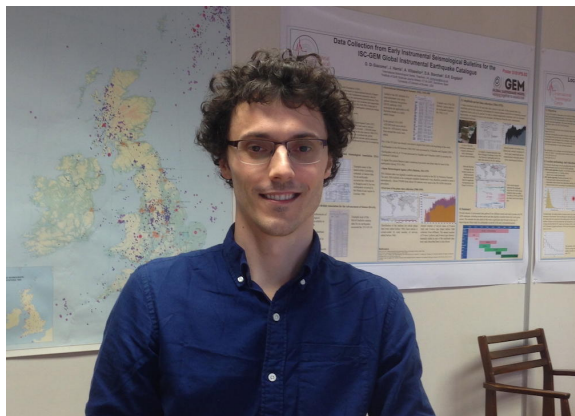
- Elizabeth Ayres (née Ball)
- Analyst/Historical Data Entry Officer
- United Kingdom



- Kathrin Lieser
- Seismologist/Analyst
- Germany



- Lonn Brown
- Seismologist/Analyst
- Canada



- Charikleia Gkarlaouni
- Seismologist/Analyst
- Greece



- Peter Franek
- Seismologist/Analyst
- Slovakia



- Angeliki Adamaki
- Seismologist/Analyst
- Greece



- Burak Sakarya
- Seismologist/Analyst
- Turkey



- Daniela Olaru
- Historical Data Entry Officer
- Romania



- Tom Garth
- Seismologist, PDRA, jointly with Department of Earth Sciences at University of Oxford
- United Kingdom



3

Availability of the ISC Bulletin

The ISC Bulletin is available from the following sources:

- Web searches

The entire ISC Bulletin is available directly from the ISC website via tailored searches.

(www.isc.ac.uk/iscbulletin/search)

(isc-mirror.iris.washington.edu/iscbulletin/search)

- Bulletin search - provides the most verbose output of the ISC Bulletin in ISF or QuakeML.
- Event catalogue - only outputs the prime hypocentre for each event, producing a simple list of events, locations and magnitudes.
- Arrivals - search for arrivals in the ISC Bulletin. Users can search for specific phases for selected stations and events.

- CD-ROMs/DVD-ROMs

CDs/DVDs can be ordered from the ISC for any published volume (one per year), or for all back issues of the Bulletin (not including the latest volume). The data discs contain the Bulletin as a PDF, in IASPEI Seismic Format (ISF), and in Fixed Format Bulletin (FFB) format. An event catalogue is also included, together with the International Registry of seismic station codes.

- FTP site

The ISC Bulletin is also available to download from the ISC ftp site, which contains the Bulletin in PDF, ISF and FFB formats. (<ftp://www.isc.ac.uk>)

(<ftp://isc-mirror.iris.washington.edu>)

Mirror service

A mirror of the ISC database, website and ftp site is available at IRIS DMC (isc-mirror.iris.washington.edu), which benefits from their high-speed internet connection, providing an alternative method of accessing the ISC Bulletin.

4

Citing the International Seismological Centre

Data from the ISC should always be cited. This includes use by academic or commercial organisations, as well as individuals. A citation should show how the data were retrieved and may be in one of these suggested forms:

Data retrieved from the ISC web site:

- International Seismological Centre, On-line Bulletin, <http://www.isc.ac.uk>, Internatl. Seismol. Cent., Thatcham, United Kingdom, 2019.

Data transcribed from the IASPEI reference event bulletin:

- International Seismological Centre, Reference Event Bulletin, <http://www.isc.ac.uk>, Internatl. Seismol. Cent., Thatcham, United Kingdom, 2019.

Data transcribed from the EHB bulletin:

- International Seismological Centre, EHB Bulletin, <http://www.isc.ac.uk>, Internatl. Seismol. Cent., Thatcham, United Kingdom, 2019.

Data copied from ISC CD-ROMs/DVD-ROMs:

- International Seismological Centre, Bulletin Disks 1-26 [CD-ROM], Internatl. Seismol. Cent., Thatcham, United Kingdom, 2019.

Data transcribed from the printed Bulletin:

- International Seismological Centre, Bull. Internatl. Seismol. Cent., 46(9-12), Thatcham, United Kingdom, 2009.

Data transcribed from the printed Summary of the Bulletin:

- International Seismological Centre, Summ. Bull. Internatl. Seismol. Cent., January - June 2016, 53(I), Thatcham, United Kingdom, 2019.

The ISC is named as a valid data centre for citations within American Geophysical Union (AGU) publications. As such, please follow the AGU guidelines when referencing ISC data in one of their journals. The ISC may be cited as both the institutional author of the Bulletin and the source from which the data were retrieved.

BibTex entry example:

```
@manual{ISCcitation2019,  
author = "International Seismological Centre",  
title = "On-line Bulletin",  
organization = "Internatl. Seismol. Cent.",  
note = "http://www.isc.ac.uk",  
address = "Thatcham, United Kingdom",  
year = "2019"  
}
```

5

Operational Procedures of Contributing Agencies

5.1 Monitoring System of the Institute of Geophysical Research of the Ministry of Energy of the Republic of Kazakhstan

Natalya N. Mikhailova and Inna N. Sokolova

Institute of Geophysical Research, Ministry of Energy of the Republic of Kazakhstan, Almaty, Kazakhstan



Natalya N. Mikhailova



Inna N. Sokolova

The seismic monitoring network of the Institute of Geophysical Research of the Ministry of Energy of the Republic of Kazakhstan (IGR ME RK) was created with the support provided by international organisations over the past two decades. This article describes the history of station installations, parameters and opportunities of the system as well as the functions and results of the Kazakhstan National Data Centre (KNDC) of IGR ME RK.

5.1.1 Regional Seismicity and Station Network

The territory of Kazakhstan and adjacent countries is seismically active especially its south-east part. The mountain ranges of the south Tien Shan, north Tien Shan and Dzhungariya have experienced earthquakes with magnitudes greater than 8. The largest earthquakes in the territory of Kazakhstan were the 1889 Chilik earthquake with $M_W=8.3$, and 1911 Kemin earthquake with $M_W=8.2$. Figure 5.1 shows a map of large earthquake epicentres that occurred in the territory of Central Asia with magnitudes greater than 5; the map was constructed by data of the EMCA (Earthquake Model Central Asia) catalogue (*Mikhailova et al.*, 2015).

In the past, the seismic stations network was created mainly at the seismically active south-east part of Kazakhstan. And only some individual stations operated in the south and east. The other regions of Kazakhstan (west, north, and centre) had almost no stations. The first station, Alma-Ata, was opened in 1927 in Alma-Ata. After that seismic stations were installed in Chimkent (1932) and Semipalatinsk

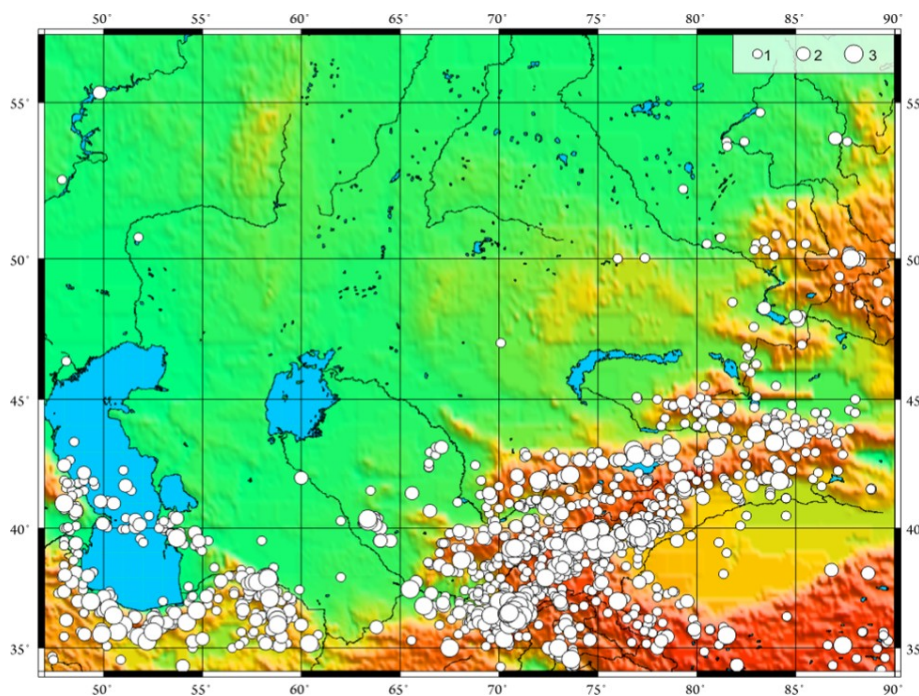
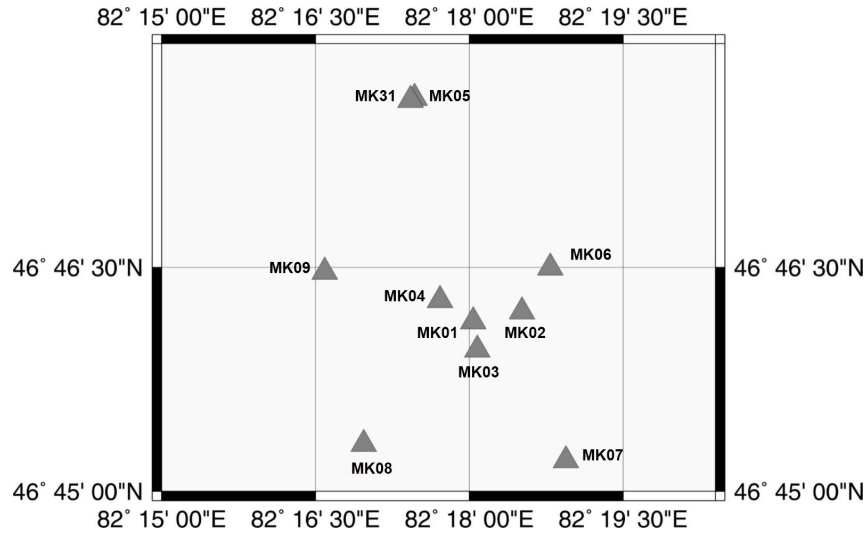


Figure 5.1: Map of large earthquake epicentres on the territory of Central Asia, $M \geq 5$ (from the ancient time to 2009). 1: $5 \leq M \leq 6$, 2: $6 < M \leq 7$, 3: $M > 7$. (Mikhailova et al., 2015)

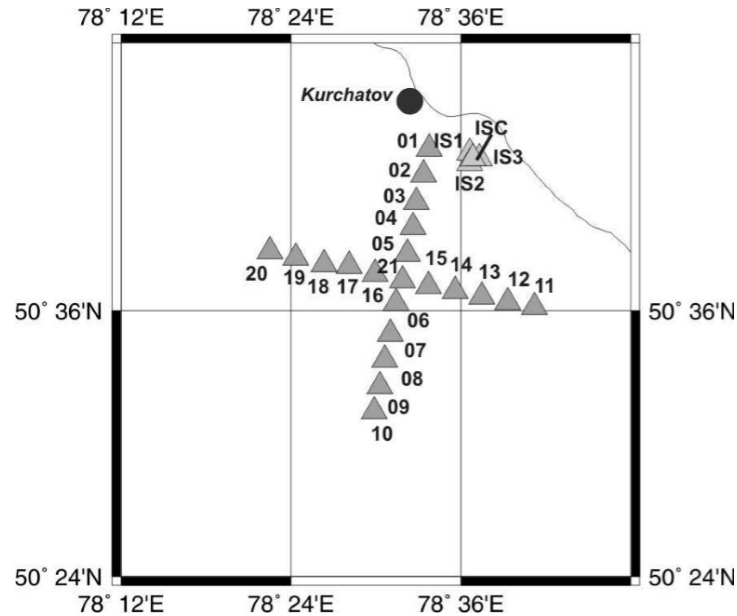
(1934). In the 1950s, after beginning to work on detailed investigations of the seismic regime, several stations were opened at the same time and formed a seismic monitoring network. The network was operated by the Institute of Physics of the Earth (IPE) of the Academy of Science (AS) of USSR until 1969. The data were processed in Talgar town by the Complex Seismological Expedition (CSE) of IPE AS USSR. In 1969 the CSE stations were transferred to the Institute of Geological Science (IGS), of AS of Kazakh SSR, and after that to the newly created Institute of Seismology (IS) of AS Kazakh SSR (1976) where the network had been developed due to the opening of new stations and observatories, and due to modernisation. From 1969, station data were processed by the processing group of the IGS, and then since 1976 by the IS AS Kazakh SSR. In 1979, the Seismological Experience-Methodical Expedition (SEME, ISC agency code SOME) was formed and operated all stations in the network. It had a group for seismic data processing and this structure still exists (Mikhailova and Kurskeyev, 1995).

The period from 1999 to 2009 was a unique stage in the seismological observations development in Kazakhstan: during this short period new seismic arrays and stations were put into operation one by one. The seismic arrays network and some other stations are operated by the Institute of Geophysical Research which was part of the National Nuclear Centre (NNC) of RK (Mikhailova, 2009). The main designation of the created seismic arrays is monitoring nuclear tests and earthquakes as part of the global monitoring networks. Three seismic arrays – Makanchi, Borovoye, and Kurchatov-Cross – are included in the International Monitoring System (IMS) created under the Comprehensive Test-Ban Treaty (CTBT) (Mikhailova, 2016). Makanchi is a primary station of the IMS, Borovoye and Kurchatov-Cross are included in the IMS network of auxiliary stations (Mikhailova, 2016). Two seismic arrays - Karatayu and Akbulak - were created together with the Air Force Technical Application Centre (AFTAC, USA) and were integrated into the network of nuclear tests monitoring of AFTAC (Mikhailova, 2016).

The seismic arrays have different configurations and apertures (Mikhailova, 2016). The configuration of



(a) MK01–MK09: elements with one-component vertical seismometers, MK31 – three-component seismometer



(b) 01–20: elements with one-component vertical seismometers; 21: three-component seismometer. IS1, IS2, IS3, IS4 are elements of the infrasound array KURIS.

Figure 5.2: Configuration of seismic arrays. a: Makanchi (same configuration as seismic arrays Borovoye, Karatayu, Akbulak); b: Kurchatov-Cross

four arrays (Makanchi, Borovoye, Karatayu, Akbulak) approximately represents a circle with nine elements installed in lines (vertical seismometers) and one central element (three-component seismometer). Their aperture is 3–4 km. These are so-called small-aperture arrays (Figure 5.2(a)). Kurchatov-Cross seismic array (Mikhailova, 2016) is configured in the form of orthogonal profiles with 21 installed elements (20 vertical seismometers, 1 central three-component seismometer, Figure 5.2(a)). The array aperture is 22.5 km. Figure 5.3 shows the site of Makanchi seismic array and Figure 5.4 of Kurchatov-Cross seismic array.



(a)



(b)

Figure 5.3: Makanchi seismic array. Left: The Central receiving Facility (CRF) for stations PS23 (MKAR), MAKZ(IRIS) and infra sound station. Inside the balls are satellite antennas. Right: Another view of CRF.



(a)



(b)

Figure 5.4: Views of Kurchatov-Cross seismic array. On the left is CRF of station AS058, on the right is an instrument vault of one of the elements.

The seismometers at all arrays are located in wells of 25 m – 60 m depth. More detailed information on seismic arrays and its aperture can be found on the web site of the Kazakhstan National Data Centre www.kndc.kz.

Data from all seismic arrays arrive at the Kazakhstan National Data Centre (KNDC), Almaty, and are transmitted or submitted after processing to international data centres (IDC, IRIS/DMC, NEIC, ISC, EMSC, GSRAS), where they are successfully used for global seismic monitoring. The data from the Kazakhstan seismic arrays are always used for processing of the largest earthquakes of the world; researchers from different countries apply this data to solve tasks in different fields of geophysics including investigation of the Earth's structure and creation of its more complete models (*Mikhailova, 2016*).

In addition to seismic arrays, the IGR network contains three-component stations among which there are two stations of the IRIS IDA network, one IRIS GSN station, one station of the IMS auxiliary network and two stations were earlier included into the network under the CAREMON project (*Mikhailova et al., 2010*).

The main dates of the IGR ME RK observation system installation are:

1994	The stations of the special control service of the former USSR – Borovoye, (BRVK) Kurchatov (KURK), Aktyubinsk (AKTK/AKTO), Makanchi (MAKZ) were transferred to the NNC RK.
1994	Installation of 8 broadband digital stations on the territory of Kazakhstan together with LDEO (AKTK, BRVK, CHKZ, KURK, MAKZ, TLG, VOS/VOSK, ZRNK).
1994 – 1996	Installation of 3 stations of IRIS/IDA and IRIS/GSN system (Borovoye, Kurchatov, Makanchi) in Kazakhstan.
1996	Kazakhstan signed the Comprehensive Test-Ban Treaty according to which the installation of 5 IMS facilities on the territory of Kazakhstan is planned.
1997	Installation of three-component seismic stations Podgornoye (PDGK/PDGN), northern Tien Shan.
1999	Opening of the Centre for acquisition and processing of data (KNDC) in Almaty.
1999 – 2000	Construction and launching of the primary IMS Makanchi station PS23 (MKAR). The station was certified in January 2002.
2000 – 2001	Construction and launching of Karatau (KKAR) station (AFTAC).
2001 – 2002	Construction and launching of the auxiliary IMS Borovoye AS057 (BVAR) station. The station was certified in December 2002.
2001	Construction and launching of Aktyubinsk infrasound station (IS31). The station was certified in November 2004.
2002 – 2003	Construction and launching of Akbulak station (AFTAC).
2005	Modernisation and launching of auxiliary IMS station, Aktyubinsk AS059 (AKTO). The station was certified in November 2005.
2006	Launching of three-component KNDC station located in Almaty.

- | | |
|------|--|
| 2006 | Launching of auxiliary IMS station, Kurchatov-Cross AS058 (KUR01-KUR21). The station was certified in 2007. |
| 2010 | Launching of three-component Ortau station (OTUK) located in the territory of Central Kazakhstan, and modernisation of three-component Podgornoye station (PDGK/PDGN), Northern Tien Shan. |
| 2016 | Launching of three-component seismic station Kaskelen (KASK) westward of Almaty city. |

Figure 5.5 shows a map of the IGR ME RK network stations location.

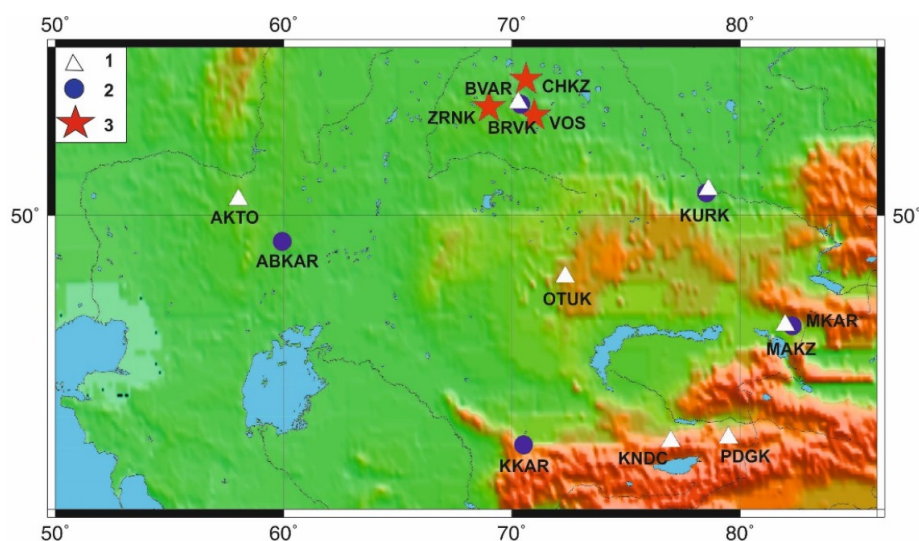


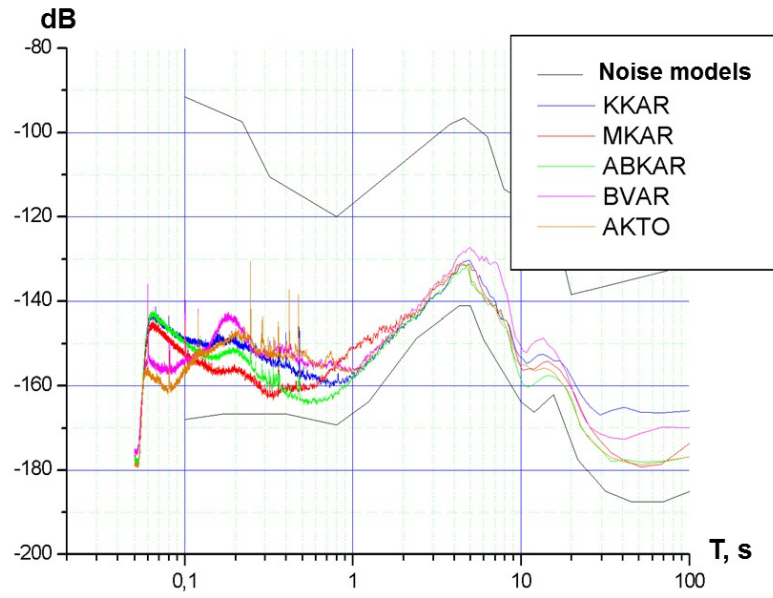
Figure 5.5: IGR seismic stations. 1: three-component seismic station, 2: seismic array, 3: seismic arrays Zerenda, Chkalovo, Vostochnaya of the large-aperture Borovoye system that are being upgraded.

Most of the seismic stations of Kazakhstan have excellent conditions for seismic signals recording. Owing to the detailed selection of sites for the stations in respect to geology and seismic noise characteristics, successful configuration of arrays, integration of broadband and short-period instruments, all stations in the system are highly sensitive to regional and teleseismic events. This allows for using the system successfully within the national and international monitoring.

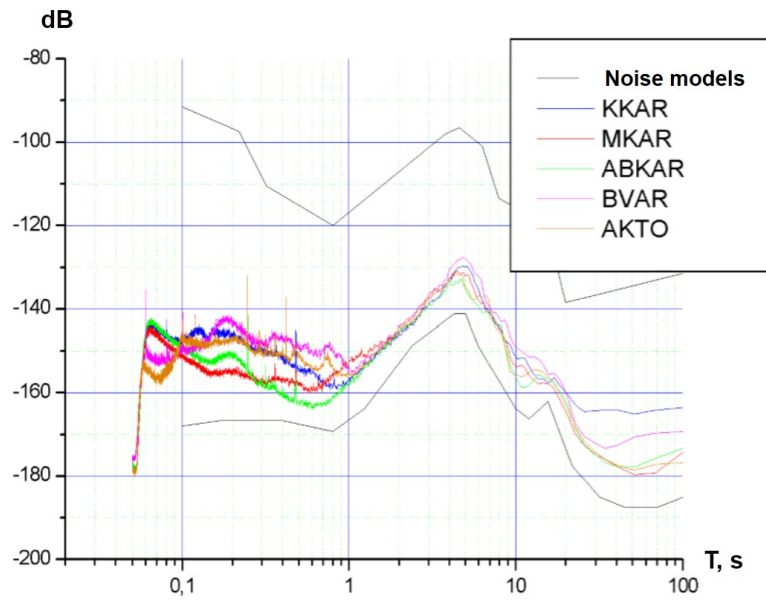
Figure 5.6 shows the seismic noise spectral density for Makanchi, Karatayu, Akbulak, Borovoye and Aktyubinsk stations for day and night time as well as the global models of seismic noise by *Peterson* (1993). It is clearly seen that curves for all stations are close to the low-level noise model (*Sinyova et al.*, 2000; *Mikhailova and Komarov*, 2006a).

5.1.2 Data Processing and Data Availability

Data from all stations arrive in real time to the Data Centre (KNDC). The KNDC tasks are acquisition and transmission of data of the network stations, processing of arriving seismic and infrasound data, storage and exchange of data with other national and international centres and research investigations in support of monitoring. Since 2009 with support from the Norwegian Centre NORSAR and Norway MFA, KNDC regularly conducts training courses on processing and interpreting seismograms in support of the CTBT for the specialists from Central Asian countries of the former USSR.



(a) Night time



(b) Day time

Figure 5.6: Spectral density of seismic noise for stations Makanchi, Karatayu, Akbulak, Borovoye, and Aktyubinsk (vertical component).

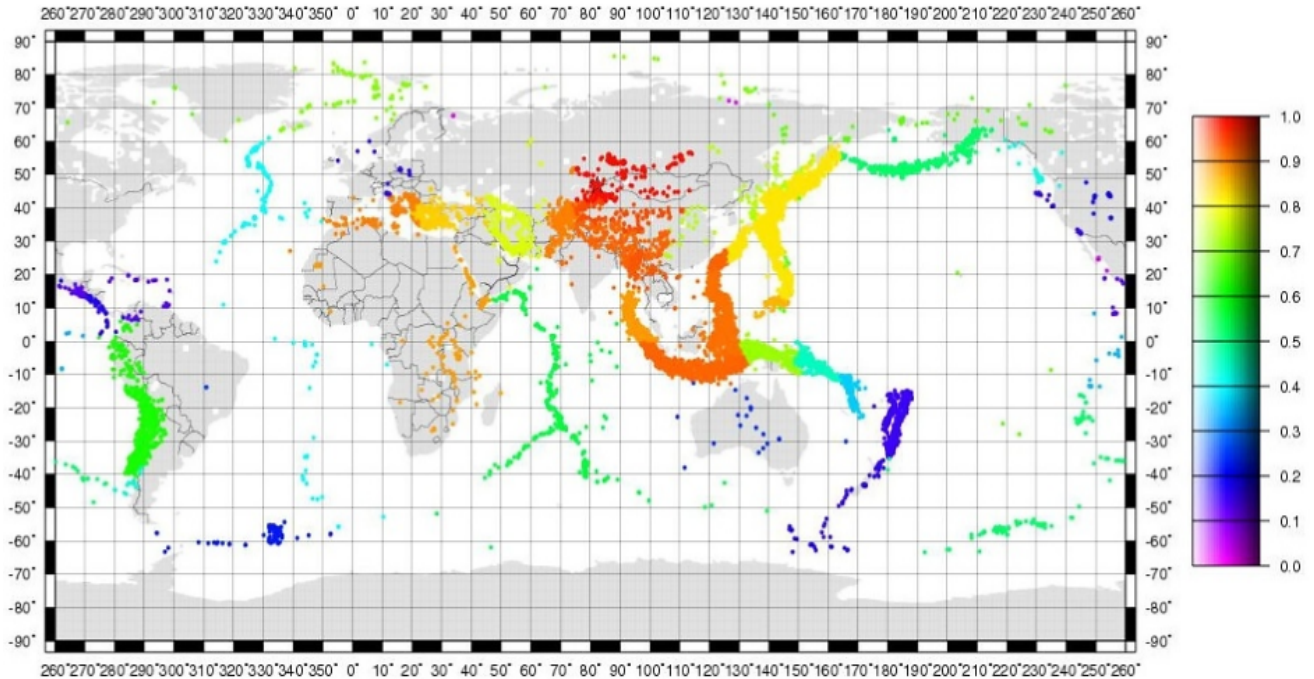


Figure 5.7: Map of Makanchi station participation in REB bulletin created by the International Data Centre. The Figure shows the part of REB with Makanchi station participation.

The Centre actively exchanges data with many research organisations in Kazakhstan and the world. Figure 5.7 shows data from Makanchi station participation in the Reviewed Event Bulletin (REB) seismological bulletin created by the International Data Centre (IDC) of the CTBTO.

Data processing in the Centre is conducted 24 hours a day, 7 days per week. The processing of seismic events is made for local and regional distances (Central Asia), we determine the arrival time, amplitudes, and periods of regional seismic phases Pn, Pg, P, Sn, S, Lg, Rg. The following types of seismic bulletins are created:

- Automated bulletin, the delay is from 40 minutes to one hour.
- Interactive regional bulletin, 1 day delay.
- Joint interactive regional bulletin (with SEME Ministry of Education and Science (MES) RK and other Central Asia stations), 2 days delay (Figure 5.8).
- Catalogue of seismic events indicating its nature, several months delay.

Note that for the creation of interactive seismic bulletins, KNDC uses data from stations belonging to several other organisations. The data arrive in real time from seismic arrays Zalesovo (Russia), Alibek (Turkmenistan), several stations in Kyrgyzstan and one SEME station. In addition, KNDC receives arrival times, amplitudes and periods in tabular form from SEME stations that are inaccessible in real time.

For the bulletin creation, 'Seatools' software (NDC USA) is used. This software is applicable for data processing from three-component stations and from seismic arrays (*Mikhailova and Sinyova, 2002b*).

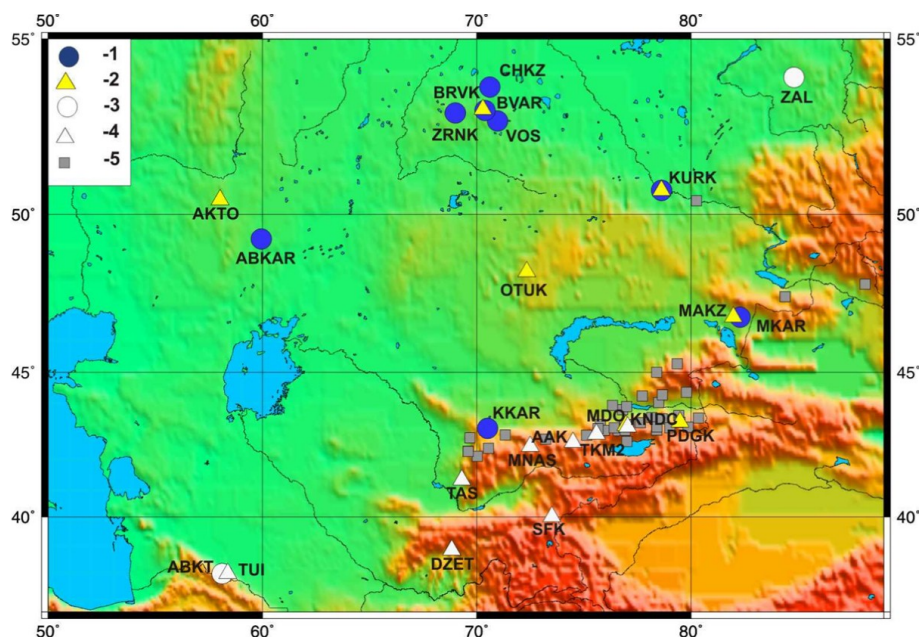


Figure 5.8: Stations used by KNDC for seismic bulletin creation. 1: seismic arrays of the IGR, 2: three-component stations of the IGR, 3: seismic arrays of neighbouring countries, 4: CAREMON stations, 5: stations of SEME MES RK which data arrive in tabular form.

The software has tools for calculating the regional mpv magnitude and energy class K (Rayutian, 1964; Mikhailova and Neverova, 1986). All processing results can be found in KNDC web-site www.kndc.kz.

The data of the IGR ME RK stations network are used for special tasks of nuclear monitoring, such as location, estimation of parameters and discrimination. In addition, the network records large amounts of earthquakes occurring on the territory of Central and South Asia. The data analysis of the IGR monitoring network allowed the revealing of earthquake sources in regions that were traditionally considered as aseismic or of low seismic activity in the territory of Kazakhstan (Figure 5.9) (Mikhailova and Sokolova, 2003a; Mikhailova et al., 2003b; Belyashova et al., 2002; Mikhailova et al., 2002a; Mikhailova et al., 2006b; Chekaninskiy, 1928; Urazayev, 1979; Kondorskaya and Shebalin, 1977; Mikhailova et al., 2003c; Mikhailova et al., 2012). Its discovery is an interesting fact which should be taken into account for seismic hazard assessment. In addition, the staff of the Data Center of the IGR ME RK has analysed retrospective historical and new data from digital stations. The availability of a huge archive of historical seismograms in the Republic containing records from the 1960s allowed us to determine the parameters of some historical earthquakes that occurred in different regions of Kazakhstan. The judgement on Kazakhstan's seismicity has been changed significantly.

New data on seismicity should effect the assessment of seismic hazard in Kazakhstan and be taken into account while compiling a new map of general seismic zoning.

The Institute of Geophysical Research supports the open data exchange policy for researchers all over the world. The waveforms of the IGR RK station network are sent to the IRIS DMC in SEED format. They contain data from three-component seismic stations, seismic arrays and KURIS infrasound station. The network code is KZ, DOI: 10.7914. This archive contains data from July 1994 onward. Some stations ABKAR, KKAR, MKAR, KURK, BRVK and MAKZ transmit data to IRIS DMC in real time mode, the rest are presented with half a year delay.

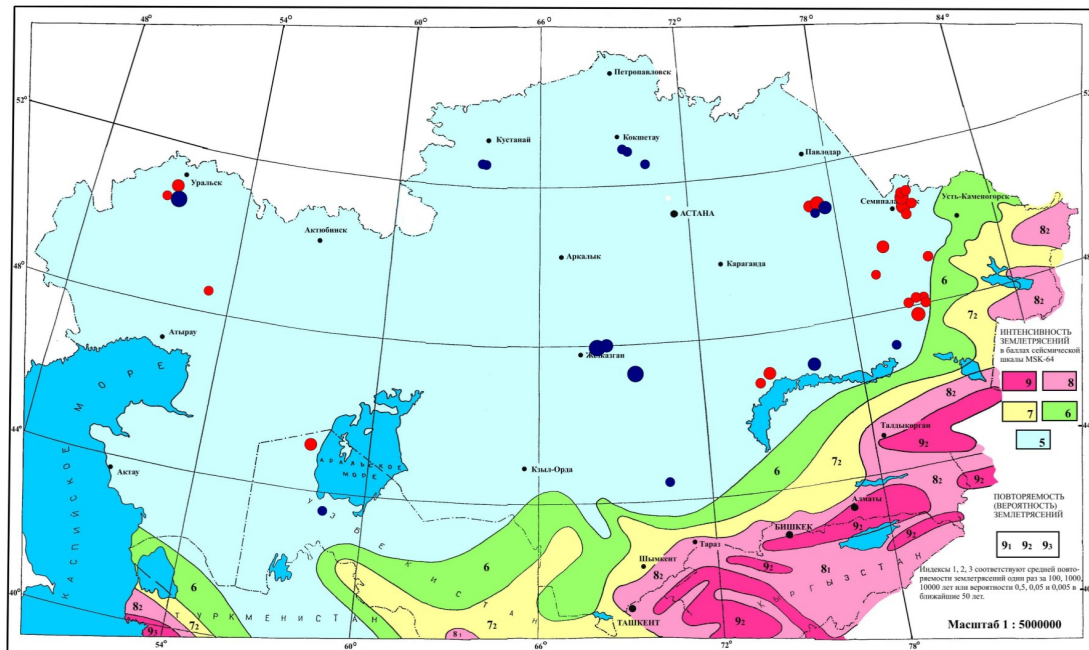


Figure 5.9: Map of seismic zoning of Kazakhstan territory (2006) with earthquake epicentres ($mPV \geq 3$) at new regions. Red circles: historical earthquakes from 19th century to 1994, blue circles: earthquakes recorded by the IGR network. Colours are earthquake intensity by MSK-64 scale. 9₁, 9₂, 9₃ correspond to earthquake recurrence or probability period, where 1, 2, 3 are the average recurrence of earthquakes: once per 100, 1000, 10000 years; or probability 0.5, 0.05 and 0.005 in the nearest 50 years. Scale 1:5.000.000. (Construction in Seismic Regions, Construction Codes and Rules, 2.03.-30-2006, Committee on Construction Affairs of the Ministry of Industry and Trade of the Republic of Kazakhstan, Almaty 2006, 80 pages).

In addition, the IGR ME RK, starting from July 2002, regularly submits the seismic bulletins to the ISC. The agency code is NNC (soon to be changed to KNDC).

5.1.3 References

- Belyashova N.N., N.N. Mikhailova and I.N. Sokolova (2002), Central and Eastern Kazakhstan, *Earthquakes of Northern Eurasia in 1996*, GS RAS, Obninsk, 71 – 75 (in Russian).
- Chekaninskiy I.V. (1928), Report on seismic phenomena at Semipalatinsk province from 1760 to 1927 (from Semipalatinsk historical archive) (in Russian).
- Kondorskaya N.V. and N.V. Shebalin (eds.) (1977), A new catalogue of large earthquakes on the territory of the USSR, *Nauka*, Moscow, (in Russian).
- Mikhailova N.N. and N.P. Neverova (1986), Calibration function to determine MPVA magnitude of Northern Tien Shan earthquakes, *Integrated investigations at Alma-Ata prognosis site*, Nauka, Moscow, 41 – 47 (in Russian).
- Mikhailova N.N. and A.K. Kurskeyev (1995), Present Status of the Network for Seismic Observations in Kazakhstan, *Journal of Earthquake Prediction Research*, 4(4), 497 – 506.
- Mikhailova N.N., A.I. Nedelkov A.I., I.N. Sokolova, Ye.N. Kazakov and A.V. Belyashov A.V (2002a), Shalgin earthquake in Central Kazakhstan of 22.08.2001, *Geophysics and problems of non-proliferation*,

- Vestnik NNC RK*, 2, 78 – 87 (in Russian).
- Mikhailova N.N. and Z.I. Sinyova (2002b), Processing of the NNC RK seismic stations data, *Geophysics and problems of non-proliferation*, *Vestnik NNC RK*, 2(10), 64– 68 (in Russian).
- Mikhailova N.N. and I.N. Sokolova (2003a), Central and East Kazakhstan, *Earthquakes of Northern Eurasia in 1997*, GS RAS, Obninsk, 89 – 91 (in Russian).
- Mikhailova N.N., I.N. Sokolova and A.I. Nedelkov A.I (2003b), New data on earthquakes at aseismic regions of Kazakhstan, *Geophysics of XXI century: year 2002*, Collection of proceedings of the Fourth Geophysical Readings after V.V. Fedynskiy, 28 February – 2 March, 2002, Moscow, 251 – 255 (in Russian).
- Mikhailova N.N., N.A. Volf and Z.I Sinyova (2003c), Seismicity of areas surrounding new seismic arrays makanchi and Karatayu, *Geophysics and problems of non-proliferation*, *Vestnik NNC RK*, 2, 94–100 (in Russian).
- Mikhailova N.N. and I.I. Komarov (2006a), Spectral parameters of seismic noise by data of Kazakhstan monitoring stations, *Vestnik NNC RK*, 2, 19 – 26 (in Russian).
- Mikhailova N.N., A.I Nedelkov, I.N. Sokolova and N.N. Poleshko (2006b), Investigation of seismicity of the former Semipalatinsk Test Site territory and its vicinity, *Geophysics of XX century: year 2006. Collection of proceedings of the Eighth Geophysical Readings after V.V. Fedynskiy*, 179 – 191 (in Russian).
- Mikhailova N.N. (2009), Kazakhstan seismic observations system of the Institute of Geophysical Research of the National Nuclear Centre and its information capabilities, *Seismic safety of Almaty: Proceedings of Scientific and Technical Conference*, ES Department. MES RK., Almaty (in Russian).
- Mikhailova N.N., A. Strollo, D. Bindi, A.Ye. Velikanov, V.G. Kunakov, I.I. Komarov and Z.I. Sinyova (2010), New Kazakhstan stations installed within CAREMON Project, *Monitoring of Nuclear Tests and Their Consequences: Reports thesis*, VI International Conference, Kurchatov, 9 – 13 August 2010, 23 – 24.
- Mikhailova N.N., I.N. Sokolova, A.Ye. Velikanov and N.N. Poleshko (2012), Seismicity of the western Kazakhstan by data of the NNC RK network, *Seismic prediction observations on the territory of Azerbaijan*, RCSS NASA, 336 – 348 (in Russian).
- Mikhailova N.N., I.L. Aristova and A.S. Mukambayev (2015), Unified earthquakes catalogue for Kazakhstan territory and adjacent regions (from ancient times to 2009), *Vestnik NNC RK*, 4, 132–143 (in Russian).
- Mikhailova N.N. (2016), Important results obtained owing to seismic arrays opening in Kazakhstan, *Vestnik NNC RK*, 2, 23–32 (in Russian).
- Peterson, J. (1993), Observation and Modeling of Seismic Background Noise, *Open-File Report 93-322*, Albuquerque, New Mexico.
- Rayutian T.G. (1964), To calculation of earthquake energy at 3000 km distance, *Proceedings of the IPE AS USSR*, 32(199), 72 – 98.

Sinyova Z.I., N.N. Mikhailova and I.I. Komarov (2000), Investigation of dynamic parameters of seismic noise by data of Kazakhstan network digital stations, *Vestnik NNC RK*, 2, 24 – 30 (in Russian).

Urazayev B.M (1979), Seismic zoning of Kazakhstan, *Nauka* (in Russian).

6

The ISC Bulletin Rebuild Project: 1980 – 1984

The ISC has completed work on the next 5 years of the Bulletin Rebuild project, covering the period from 1980 – 1984. The improved Bulletin has been uploaded to the live account and is now available for use by all interested parties.

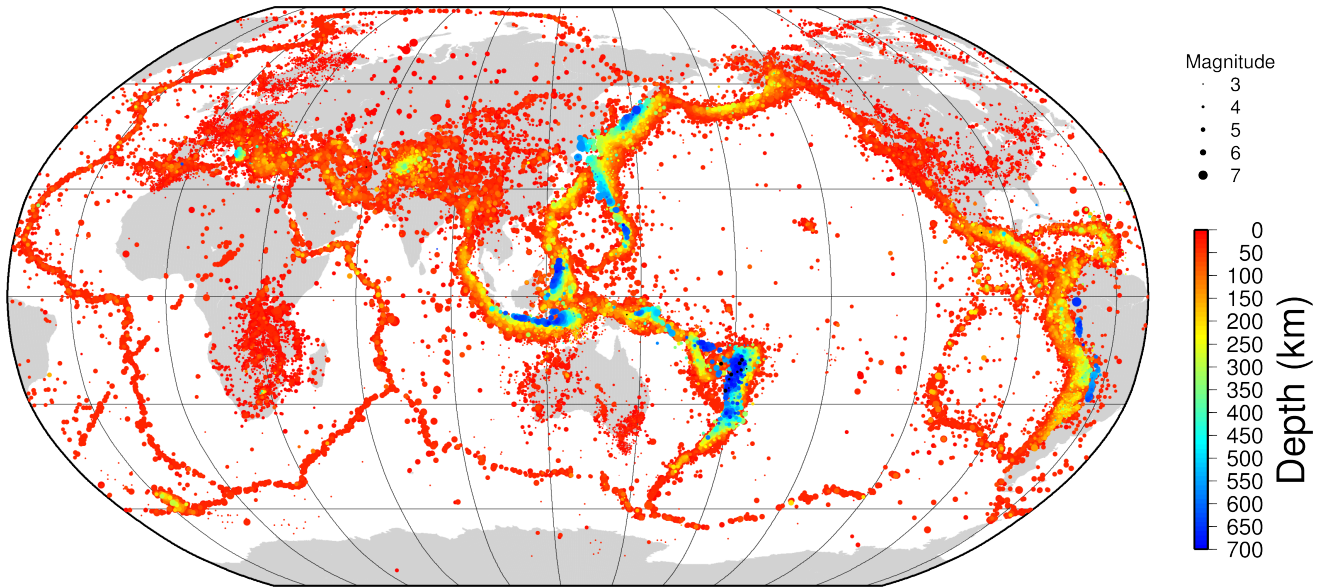
The broad aims of the Rebuild project are to update, extend and homogenise the ISC Bulletin using the same velocity model, modern methods and consistent quality criteria, as well as adding additional previously unavailable data. For a more in-depth description please see the Summary from January – June 2015 (*International Seismological Centre*, 2018) and the paper published on the data years 1964 – 1979 (*Storchak et al.*, 2017). Figure 6.1 compares the ISC locations before and after the Rebuild project for the entirety of the released rebuilt ISC Bulletin from 1964 to 1984.

To clarify, the rebuilt ISC Bulletin becomes the ISC Bulletin as we release it. If you search for events before 1985 on our website, you are now viewing the rebuilt Bulletin. We welcome any feedback.

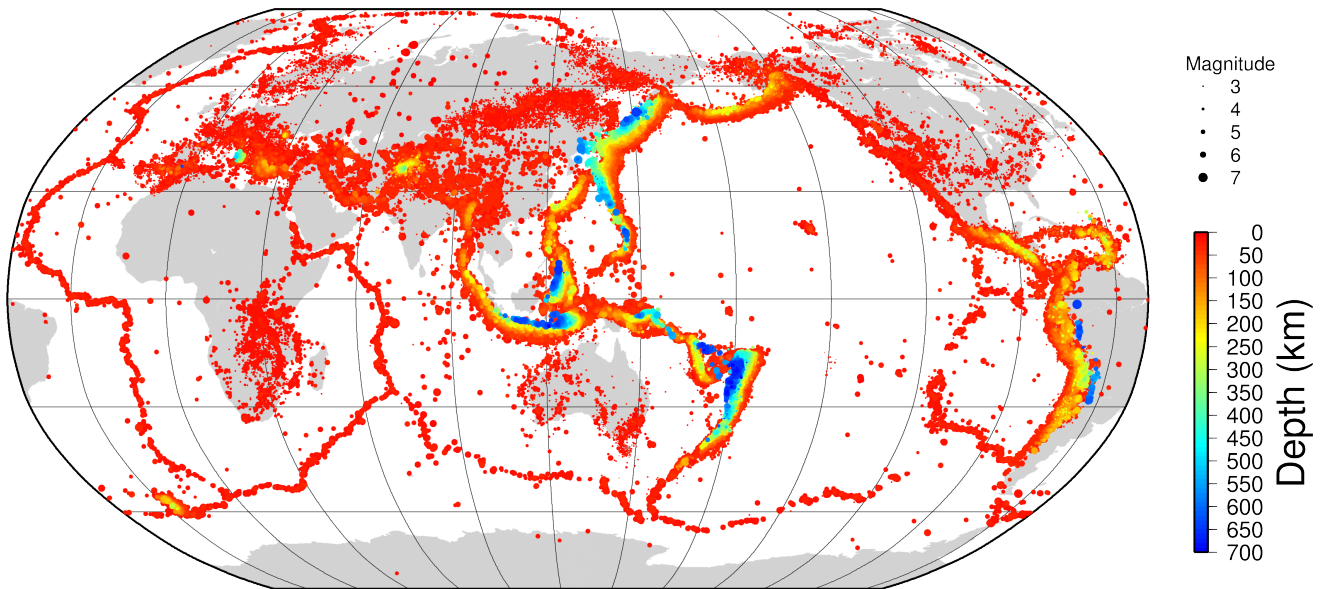
Also, please be aware that there are big plans for the Rebuild project this year and we plan to release the entire rebuild ISC Bulletin (1964 – 2010) early in 2020.

References

- International Seismological Centre (2018), January – June 2015, *Summ. Bull. Internatl. Seismol. Cent.*, 52(I), <https://doi.org/10.31905/JSWEM8MG>.
- Storchak, D.A., J. Harris, L. Brown, K. Lieser, B. Shumba, R. Verney, D. Di Giacomo and E. Korger (2017), Rebuild of the Bulletin of the International Seismological Centre (ISC), part 1: 1964-1979, *Geoscience Letters*, 4(32), <https://doi.org/10.1186/s40562-017-0098-z>.



(a) Original ISC Bulletin



(b) Rebuilt ISC Bulletin

Figure 6.1: Locations, depths and magnitudes of ISC relocated events, comparing the original ISC Bulletin (a) and the rebuilt ISC Bulletin (b). Data shown covers the period of 1964–1984.

7

Summary of Seismicity, January – June 2016

The two largest events in this Summary's time period were the M_W 7.8 Wharton Basin event south-west of Sumatra in March (02/03/2016 12:49:48.85 UTC, 4.9196°S, 94.2507°E, 26.1 km, 2624 Stations (ISC)) and the M_W 7.8 Equador event in April (16/04/2016 23:58:34.52 UTC, 0.2792°N, 79.9840°W, 8.7 km, 2855 Stations (ISC)).

The Wharton Basin event in March 2016 was a large intraplate oceanic earthquake which ruptured the basin with a magnitude of M_W 7.8 and triggered a small tsunami despite being a strike-slip event (Heidarzadeh *et al.*, 2017a; Gusman *et al.*, 2017). Large tsunamigenic events are usually associated with thrust faulting in subducting zones. The Wharton Basin lies between the Sunda Trench to the east and the Ninety East Ridge to the west in a diffuse deformation zone with several north-south trending fracture zones between the Indian and Australian Plates (Lay *et al.*, 2016; Hananto *et al.*, 2018; Heidarzadeh *et al.*, 2017a). Several large events occurred here before, e.g. in 1928 (M_W 7.7), in 1949 (M_W 6.8) and in 2000 (M_W 7.9) (Heidarzadeh *et al.*, 2017a). About 800 km to the north of the epicentre of the March 2016 event, the largest recorded intraplate oceanic strike-slip earthquake ruptured the basin on 11 April 2012 with a magnitude of M_W 8.6, followed by an aftershock of M_W 8.2 two hours later. Both events triggered small tsunamis as well (Heidarzadeh *et al.*, 2017a).

The event in April offshore northern Equador ruptured a segment of approximately 100-120 km length (Nocquet *et al.*, 2017; Ye *et al.*, 2016) of the megathrust at the Equador-Colombia subduction zone where the Nazca Plate subducts beneath the South American Plate. Several large events occurred in this area during the twentieth century. In 1906 a M_W 8.8 ($M_{S(ISC)}$ 8.2) event broke a segment approximately 500 km long that was then ruptured again by three events from south to north in 1942 ($M_{S(ISC)}$ 7.6), 1958 ($M_{S(ISC)}$ 7.5) and 1979 ($M_{S(ISC)}$ 7.6)). The 2016 earthquake shows similarities in surface wave magnitude ($M_{S(ISC)}$ 7.5), slip amount, aftershock distribution and rupture area to the 1942 event, which is at the southern end of the rupture area of the 1906 event, (Ye *et al.*, 2016; Heidarzadeh *et al.*, 2017b; Nocquet *et al.*, 2017) suggesting that the 2016 event re-ruptured a common asperity (Ye *et al.*, 2016). The 2016 event caused substantial damage to the area resulting in about 660 deaths but only triggered a relatively small tsunami which did not cause any reported damage (Heidarzadeh *et al.*, 2017b).

The event in this Summary's time period that was discussed most by the Scientific Community, especially in Japan, was the M_W 7.0 Kumamoto event on Kyushu island, Japan, with 149 entries to date in the ISC Event Bibliography (Di Giacomo *et al.*, 2014; International Seismological Centre, 2019). The Kumamoto sequence started with a series of foreshocks with two events showing a magnitude greater than 6 on 14 April. The main shock occurred on 15 April (16:25:06.02 UTC, 32.7207°N, 130.7439°E, 7.0 km, 2795 Stations (ISC)). The foreshocks ruptured the northern part of the Hinagu fault (Kobayashi, 2017) while the main shock and the aftershock sequence ruptured the adjacent Futagawa fault (e.g. Yagi *et al.*, 2016). The event caused significant surface ruptures (e.g. Shirahama *et al.*, 2016) and damage and resulted in at least 9 fatalities and 800 injuries (USGS, 2019).

A non-tectonic event that was reported by over 1000 stations around the globe was the DPR Korea underground nuclear test on 6 January 2016 (06/01/2016 01:30:00.72 UTC, 41.3144°N, 129.0461°E, 0 km, 1035 Stations (ISC)). It was the 4th test conducted at the North Korean Nuclear Test Site (NKTS) since 2006 (CTBTO, 2019).

The number of events in this Bulletin Summary categorised by type are given in Table 7.1.

Table 7.1: Summary of events by type between January and June 2016.

felt earthquake	141
known earthquake	191993
known chemical explosion	8606
known induced event	4210
known landslide	2
known mine explosion	1065
known rockburst	726
known experimental explosion	68
suspected collapse	3
suspected earthquake	24360
suspected chemical explosion	767
suspected induced event	6
suspected mine explosion	4802
suspected nuclear explosion	1
suspected rockburst	182
suspected experimental explosion	3
unknown	1
total	236936

The period between January and June 2016 produced 7 earthquakes with $M_W \geq 7$; these are listed in Table 7.2.

Table 7.2: Summary of the earthquakes of magnitude $M_W \geq 7$ between January and June 2016.

Date	lat	lon	depth	Mw	Flinn-Engdahl Region
2016-03-02 12:49:48	-4.92	94.25	26	7.8	Southwest of Sumatera
2016-04-16 23:58:34	0.28	-79.98	8	7.8	Near coast of Ecuador
2016-01-30 03:25:11	53.95	158.50	171	7.2	Near east coast of Kamchatka Peninsula
2016-05-28 09:47:00	-56.27	-26.96	89	7.2	South Sandwich Islands region
2016-01-24 10:30:29	59.69	-153.58	126	7.1	Southern Alaska
2016-04-15 16:25:06	32.72	130.74	7	7.0	Kyushu
2016-04-28 19:33:24	-16.10	167.37	25	7.0	Vanuatu Islands

Figure 7.1 shows the number of moderate and large earthquakes in the first half of 2016. The distribution of the number of earthquakes should follow the Gutenberg-Richter law.

Figures 7.2 to 7.5 show the geographical distribution of moderate and large earthquakes in various magnitude ranges.

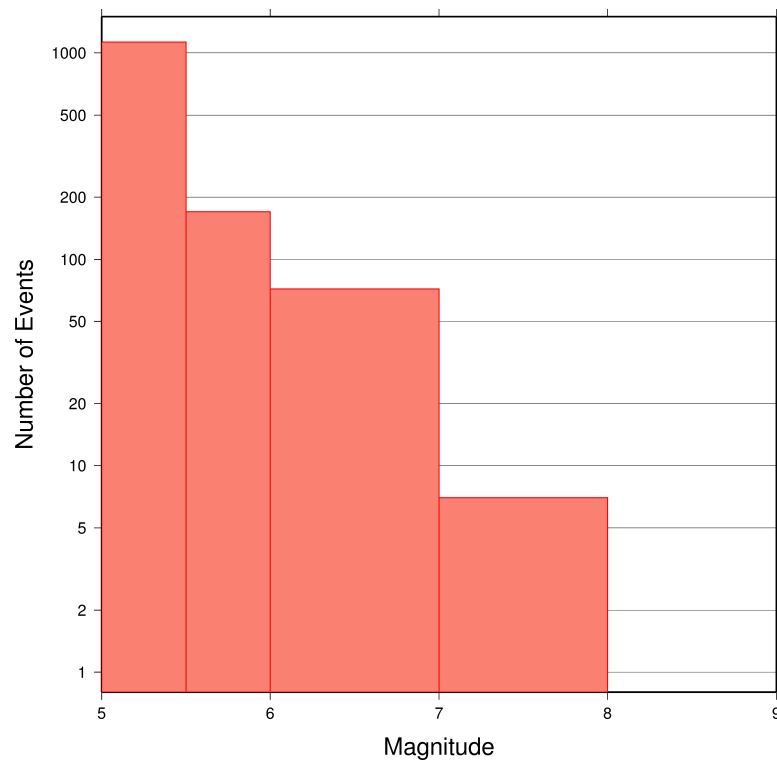


Figure 7.1: Number of moderate and large earthquakes between January and June 2016. The non-uniform magnitude bias here correspond with the magnitude intervals used in Figures 7.2 to 7.5.

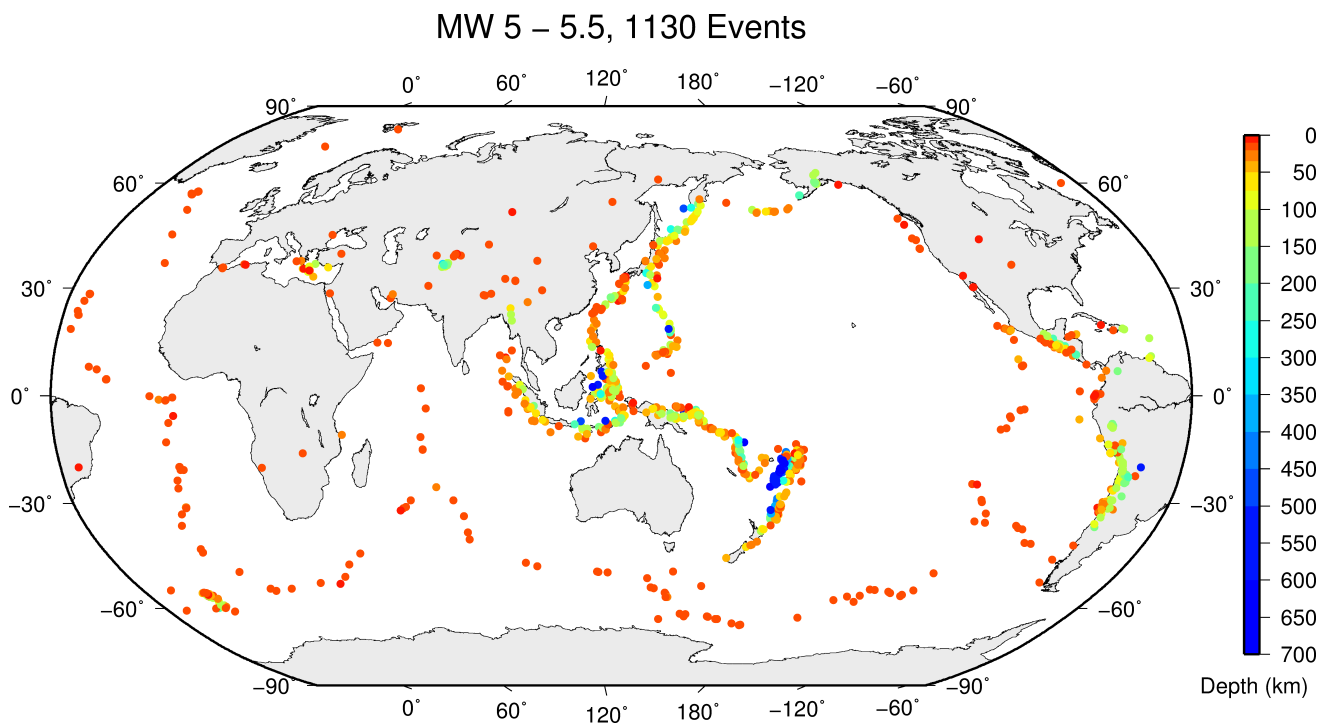


Figure 7.2: Geographic distribution of magnitude 5-5.5 earthquakes between January and June 2016.

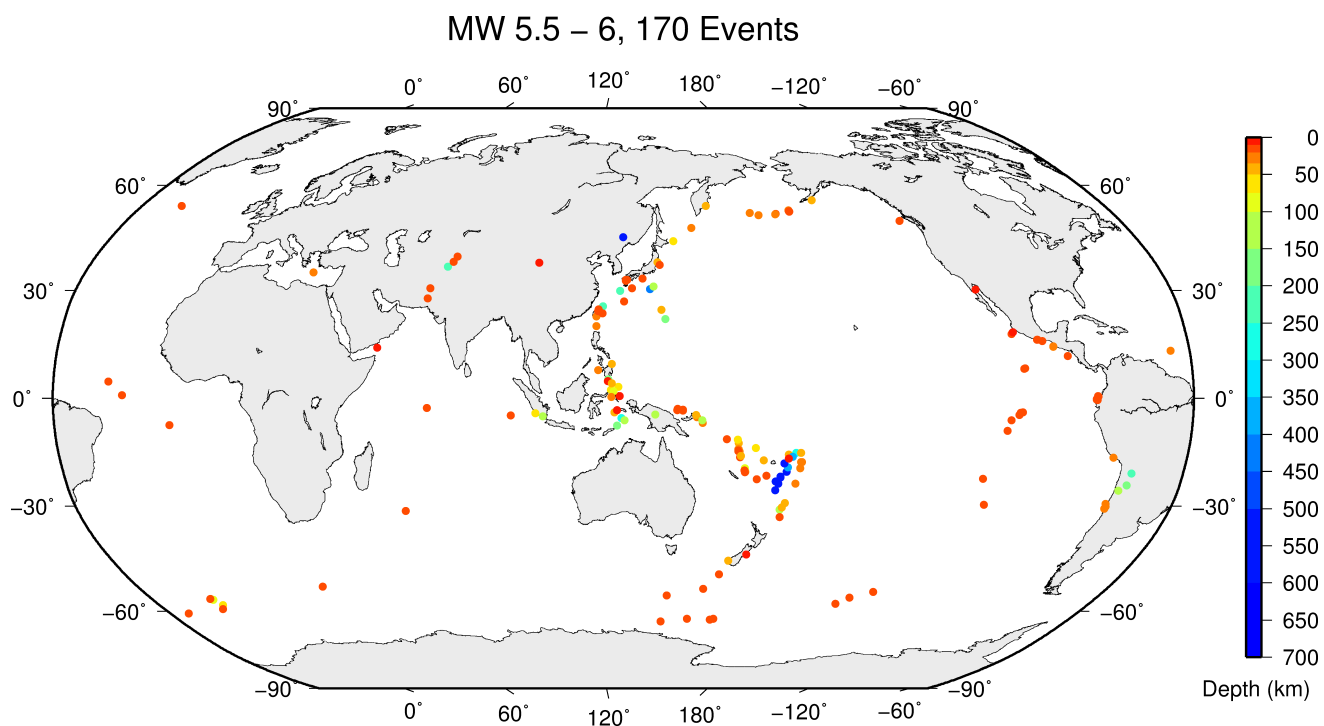


Figure 7.3: Geographic distribution of magnitude 5.5-6 earthquakes between January and June 2016.

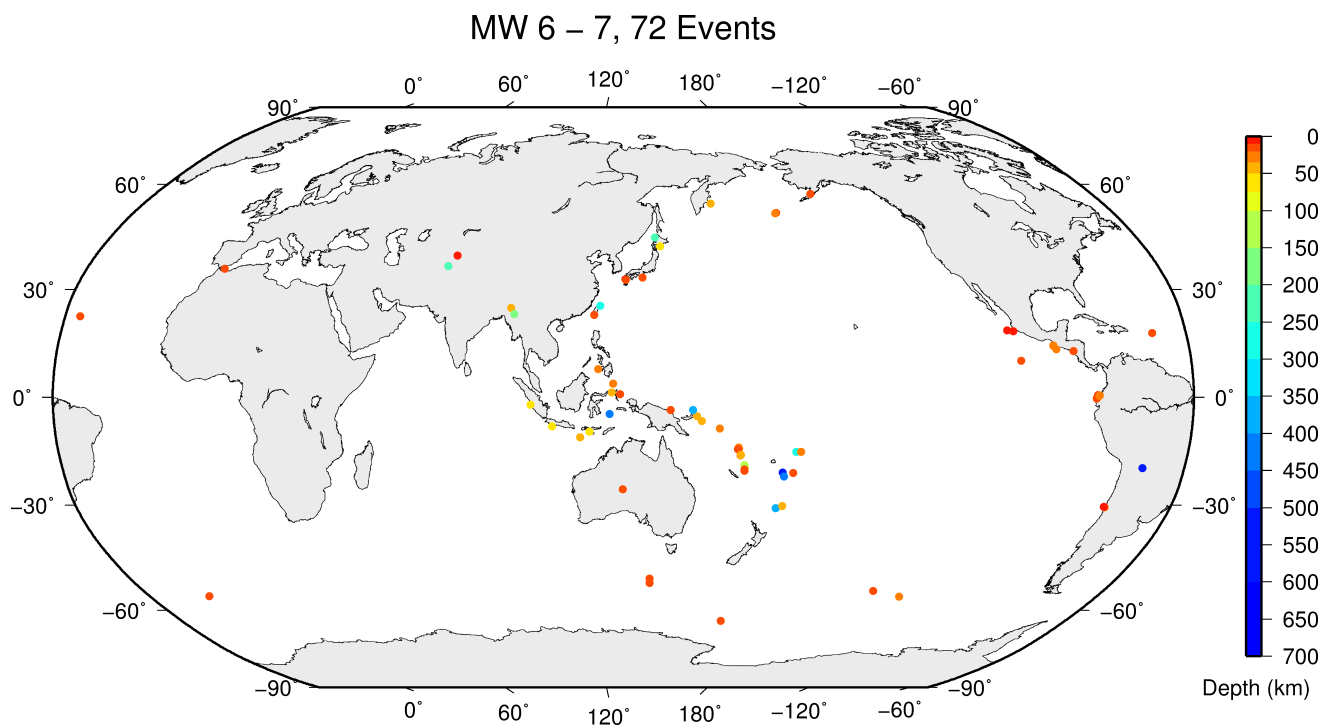


Figure 7.4: Geographic distribution of magnitude 6-7 earthquakes between January and June 2016.

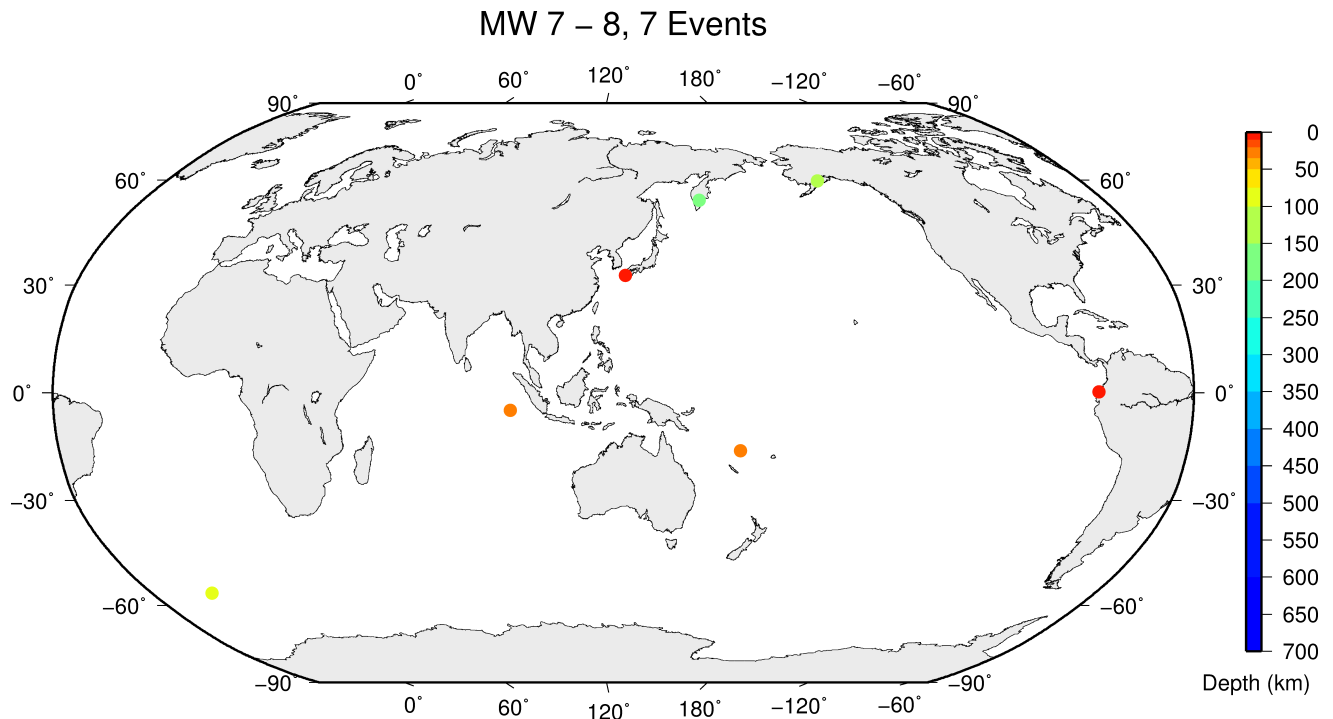


Figure 7.5: Geographic distribution of magnitude 7-8 earthquakes between January and June 2016.

References

- CTBTO (2019), Preparatory Commission for the Comprehensive Nuclear-Test-Ban Treaty Organization, <https://www.ctbto.org/the-treaty/developments-after-1996/2017-sept-dprk/> (viewed 24 January 2019).
- Di Giacomo, D., D.A. Storchak, N. Safronova, P. Ozgo, J. Harris, R. Verney and I. Bondár (2014), A New ISC Service: The Bibliography of Seismic Events, *Seismol. Res. Lett.*, **85**(2), 354–360, <https://doi.org/10.1785/0220130143>.
- Gusman, A. R., K. Satake and T. Harada (2017), Rupture process of the 2016 Wharton Basin strike-slip faulting earthquake estimated from joint inversion of teleseismic and tsunami waveforms, *Geophys. Res. Lett.*, **44**, 4082–4089, <https://doi.org/10.1002/2017GL073611>.
- Hananto, N., A. Boudarine, H. Carton, S.C. Singh, P. Avianto, J. Dymont, Y. Qin, D. Ghosal, R. Zuraida, P.E. Tapponnier and C. Deplus (2018), Evidence of pervasive trans-tensional deformation in the northwestern Wharton Basin in the 2012 earthquakes rupture area, *Earth Planet. Sci. Lett.*, **502**, 174–186, <https://doi.org/10.1016/j.epsl.2018.09.007>.
- Heidarzadeh, M., T. Harada, K. Satake, T. Ishibe and T. Takagawa (2017a), Tsunamis from strike-slip earthquakes in the Wharton Basin, northeast Indian Ocean: March 2016 Mw 7.8 event and its relationship with the April 2012 Mw 8.6 event, *Geophys. J. Int.*, **211**(3), 1601–1612, <https://doi.org/10.1093/gji/ggx395>.
- Heidarzadeh, M., S. Murotani, K. Satake, T. Takagawa and T. Saito (2017b), Fault size and depth extent of the Ecuador earthquake (Mw 7.8) of 16 April 2016 from teleseismic and tsunami data, *Geophys. Res. Lett.*, **44**, 2211–2219, <https://doi.org/10.1002/2017GL072545>.

- International Seismological Centre (2019), On-line Event Bibliography, http://www.isc.ac.uk/event_bibliography, Internatl. Seis. Cent., Thatcham, United Kingdom.
- Kobayashi, T. (2017), Earthquake rupture properties of the 2016 Kumamoto earthquake foreshocks (Mj 6.5 and Mj 6.4) revealed by conventional and multiple-aperture InSAR, *Earth Planets Space*, 69(7), <https://doi.org/10.1186/s40623-016-0594-y>.
- Lay, T., L. Ye, C. J. Ammon, A. Dunham and K. D. Koper (2016), The 2 March 2016 Wharton Basin Mw 7.8 earthquake: High stress drop north-south strike-slip rupture in the diffuse oceanic deformation zone between the Indian and Australian Plates, *Geophys. Res. Lett.*, 43, 7937–7945, <https://doi.org/10.1002/2016GL069931>.
- Nocquet, J. M., P. Jarrin, M. Vallée, P.A. Mothes, R. Grandin, F. Rolandone, B. Delouis, H. Yepes, Y. Font, D. Fuentes and M. Régnier (2017), Supercycle at the Ecuadorian subduction zone revealed after the 2016 Pedernales earthquake, *Nature Geoscience*, 10(2), 145, <https://doi.org/10.1038/NGE02864>.
- Shirahama, Y., M. Yoshimi, Y. Awata, T. Maruyama, T. Azuma, Y. Miyashita, H. Mori, K. Imanishi, N. Takeda, T. Ochi, M. Otsubo, D. Asahina and A. Miyakawa (2016), Characteristics of the surface ruptures associated with the 2016 Kumamoto earthquake sequence, central Kyushu, Japan, *Earth Planets Space*, 68(191), <https://doi.org/10.1186/s40623-016-0559-1>.
- USGS (2019), Earthquake Summary Poster, <https://earthquake.usgs.gov/archive/product/poster/20160415/us/1462205824007/poster.pdf> (viewed 31 January 2019).
- Yagi, Y., R. Okuwaki, B. Enescu, A. Kasahara, A. Miyakawa and M. Otsubo (2016), Rupture process of the 2016 Kumamoto earthquake in relation to the thermal structure around Aso volcano, *Earth Planets Space*, 68(118), <https://doi.org/10.1186/s40623-016-0492-3>.
- Ye, L., H. Kanamori, J.P. Avouac, L. Li, K.F. Cheung and T. Lay (2016), The 16 April 2016, MW 7.8 (MS 7.5) Ecuador earthquake: A quasi-repeat of the 1942 MS 7.5 earthquake and partial re-rupture of the 1906 MS 8.6 Colombia–Ecuador earthquake, *Earth Planet. Sci. Lett.*, 454, 248–258, <https://doi.org/10.1016/j.epsl.2016.09.006>.

8

Statistics of Collected Data

8.1 Introduction

The ISC Bulletin is based on the parametric data reports received from seismological agencies around the world. With rare exceptions, these reports include the results of waveform review done by analysts at network data centres and observatories. These reports include combinations of various bulletin elements such as event hypocentre estimates, moment tensors, magnitudes, event type and felt and damaging data as well as observations of the various seismic waves recorded at seismic stations.

Data reports are received in different formats that are often agency specific. Once an authorship is recognised, the data are automatically parsed into the ISC database and the original reports filed away to be accessed when necessary. Any reports not recognised or processed automatically are manually checked, corrected and re-processed. This chapter describes the data that are received at the ISC before the production of the reviewed Bulletin.

Notably, the ISC integrates all newly received data reports into the automatic ISC Bulletin (available on-line) soon after these reports are made available to ISC, provided it is done before the submission deadline that currently stands at 12 months following an event occurrence.

With data constantly being reported to the ISC, even after the ISC has published its review, the total data shown as collected, in this chapter, is limited to two years after the time of the associated reading or event, i.e. any hypocentre data collected two years after the event are not reflected in the figures below.

8.2 Summary of Agency Reports to the ISC

A total of 149 agencies have reported data for January 2016 to June 2016. The parsing of these reports into the ISC database is summarised in Table 8.1.

Table 8.1: *Summary of the parsing of reports received by the ISC from a total of 149 agencies, containing data for this summary period.*

	Number of reports
Total collected	3808
Automatically parsed	2799
Manually parsed	1009

Data collected by the ISC consists of multiple data types. These are typically one of:

- Bulletin, hypocentres with associated phase arrival observations.

- Catalogue, hypocentres only.
- Unassociated phase arrival observations.

In Table 8.2, the number of different data types reported to the ISC by each agency is listed. The number of each data type reported by each agency is also listed. Agencies reporting indirectly have their data type additionally listed for the agency that reported it. The agencies reporting indirectly may also have ‘hypocentres with associated phases’ but with no associated phases listed - this is because the association is being made by the agency reporting directly to the ISC. Summary maps of the agencies and the types of data reported are shown in Figure 8.1 and Figure 8.2.

Table 8.2: Agencies reporting to the ISC for this summary period. Entries in bold are for new or renewed reporting by agencies since the previous six-month period.

Agency	Country	Directly or indirectly reporting (D/I)	Hypocentres with associated phases	Hypocentres without associated phases	Associated phases	Unassociated phases	Amplitudes
TIR	Albania	D	275	15	4337	197	896
CRAAG	Algeria	D	458	0	2093	116	0
LPA	Argentina	D	0	0	0	707	0
SJA	Argentina	D	321	90	16112	0	3315
NSSP	Armenia	D	40	0	420	0	0
AUST	Australia	D	832	66	18737	0	0
CUPWA	Australia	D	37	0	552	0	0
IDC	Austria	D	17699	0	472774	0	409514
VIE	Austria	D	4018	37	37356	658	37146
AZER	Azerbaijan	D	197	0	7033	0	0
UCC	Belgium	D	661	259	6985	48	1611
SCB	Bolivia	D	474	0	8783	0	1845
RHSSO	Bosnia and Herzegovina	D	738	0	14159	5320	0
VAO	Brazil	D	1117	20	33381	0	0
SOF	Bulgaria	D	98	0	654	2179	0
SOMC	Cameroon	D	0	0	0	18	0
OTT	Canada	D	1828	23	42743	0	2912
PGC	Canada	I OTT	1352	0	32125	0	0
GUC	Chile	D	3126	375	104763	2495	30211
BJI	China	D	1469	59	112564	39750	80576
ASIES	Chinese Taipei	D	0	59	0	0	0
TAP	Chinese Taipei	D	30465	58	1191527	0	0
RSNC	Colombia	D	6664	13	179930	24833	56084
HDC	Costa Rica	I NEIC	0	1	0	0	0
UCR	Costa Rica	D	550	15	15569	0	1060
ZAG	Croatia	D	0	0	0	70643	0
SSNC	Cuba	D	1494	1	19298	0	7572
NIC	Cyprus	D	490	5	12471	0	6526
IPEC	Czech Republic	D	514	0	3252	25447	1488
PRU	Czech Republic	D	5933	2	51536	229	13980
WBNET	Czech Republic	D	215	0	4142	0	4105
KEA	Democratic People's Republic of Korea	D	171	0	3197	0	0
DNK	Denmark	D	1778	1071	20683	25742	6469
OSPL	Dominican Republic	D	932	6	10414	0	3666
IGQ	Ecuador	D	9	298	13153	0	0
HLW	Egypt	D	821	3	6252	0	0
SNET	El Salvador	D	1218	40	25217	58	4322
SSS	El Salvador	I UCR	0	7	0	0	0
EST	Estonia	I HEL	156	3	0	0	0
AAE	Ethiopia	D	163	1	1645	1129	247
SKO	FYR Macedonia	D	682	3	7819	3454	1466

Table 8.2: (continued)

Agency	Country	Directly or indirectly reporting (D/I)	Hypocentres with associated phases	Hypocentres without associated phases	Associated phases	Unassociated phases	Amplitudes
FIAO	Finland	I HEL	16	1	0	0	0
HEL	Finland	D	7978	4053	167116	13	24248
CSEM	France	I LIT	1819	796	0	0	0
LDG	France	D	2208	93	48756	0	19054
STR	France	D	1191	0	18942	0	0
PPT	French Polynesia	D	951	0	6438	592	6809
TIF	Georgia	D	0	241	0	3912	0
AWI	Germany	D	1685	0	7138	2236	0
BGR	Germany	D	479	240	13471	0	4686
BNS	Germany	I BGR	3	34	0	0	0
BRG	Germany	D	0	0	0	7070	3500
BUG	Germany	I BGR	22	7	0	0	0
CLL	Germany	D	5	0	210	8207	2925
GDNRW	Germany	I BGR	0	26	0	0	0
GFZ	Germany	I PRE	106	1	0	0	0
HLUG	Germany	I BGR	2	4	0	0	0
LEDBW	Germany	I BGR	10	4	0	0	0
LER	Germany	I BGR	1	0	0	0	0
ATH	Greece	D	8958	41	220096	0	70690
THE	Greece	D	4035	39	76048	6104	24783
UPSL	Greece	D	0	5	0	0	0
GCG	Guatemala	D	470	0	2761	0	0
HKC	Hong Kong	D	0	0	0	29	0
BUD	Hungary	D	0	0	0	5061	0
KRSZO	Hungary	D	285	25	3158	0	969
REY	Iceland	D	34	0	1316	0	0
HYB	India	D	685	18	5170	33	484
NDI	India	D	519	409	13389	1927	3300
DJA	Indonesia	D	4043	76	73949	0	97423
TEH	Iran	D	535	41	24491	0	5642
THR	Iran	D	7	1	182	0	52
ISN	Iraq	D	295	0	1969	0	763
GII	Israel	D	505	0	8450	0	0
GEN	Italy	D	543	0	13145	0	0
MED_RCMT	Italy	D	0	154	0	0	0
RISSC	Italy	D	3	0	30	0	0
ROM	Italy	D	6321	90	426334	184269	274385
TRI	Italy	D	0	0	0	6032	0
LIC	Ivory Coast	D	775	0	2340	0	1682
JSN	Jamaica	D	141	0	716	10	0
JMA	Japan	D	75042	1591	538399	257	6451
MAT	Japan	D	0	0	0	2526	0
NIED	Japan	D	0	867	0	0	0
SYO	Japan	D	0	0	0	1328	0
JSO	Jordan	D	15	13	149	0	152
NNC	Kazakhstan	D	8863	0	105415	0	96954
SOME	Kazakhstan	D	4556	163	83815	0	74606
KNET	Kyrgyzstan	D	1327	0	10811	0	2427
KRNET	Kyrgyzstan	D	3673	0	60348	0	0
LVSN	Latvia	D	180	0	2493	0	1377
GRAL	Lebanon	D	389	0	2590	488	0
LIT	Lithuania	D	503	496	4811	1817	206
ECGS	Luxembourg	D	473	0	4333	0	0
MCO	Macao, China	D	0	0	0	46	0
TAN	Madagascar	D	0	0	0	211	0
GSDM	Malawi	D	0	0	0	200	0
KLM	Malaysia	D	132	0	657	0	0
ECX	Mexico	D	538	1	12490	0	2040
MEX	Mexico	D	7129	147	98658	0	0
MOLD	Moldova	D	0	0	0	1888	990
PDG	Montenegro	D	240	0	5151	0	2405
CNRM	Morocco	D	6726	645	74030	0	0
NAM	Namibia	D	65	1	408	2	0
DMN	Nepal	D	1365	0	14001	0	9289

Table 8.2: (continued)

Agency	Country	Directly or indirectly reporting (D/I)	Hypocentres with associated phases	Hypocentres without associated phases	Associated phases	Unassociated phases	Amplitudes
DBN	Netherlands	I BGR	0	1	0	0	0
NOU	New Caledonia	D	3549	9	52490	0	5209
WEL	New Zealand	D	6094	95	234816	1352	200517
INET	Nicaragua	D	1526	25	10591	0	496
BER	Norway	D	2656	1778	51179	3699	11779
NAO	Norway	D	2388	1160	6805	1	1983
OMAN	Oman	D	577	0	19584	0	0
MSSP	Pakistan	D	0	0	0	991	0
UPA	Panama	D	492	0	9867	15	50
ARE	Peru	I NEIC	17	83	0	0	0
LIM	Peru	I HYB	2	0	0	0	0
MAN	Philippines	D	0	2364	0	30745	7796
WAR	Poland	D	0	0	0	10431	507
IGIL	Portugal	D	875	0	3640	0	1183
INMG	Portugal	D	1604	0	52039	2546	16155
PDA	Portugal	I NEIC	0	2	35	0	0
SVSA	Portugal	D	452	0	9178	2020	4003
BELR	Republic of Belarus	D	0	0	0	21357	5839
CFUSG	Republic of Crimea	D	8	0	190	201	233
KMA	Republic of Korea	D	31	0	651	0	0
BUC	Romania	D	897	5	15913	51984	4776
ASRS	Russia	D	137	0	4385	0	1376
BYKL	Russia	D	58	0	7388	0	2362
DRS	Russia	I MOS	141	157	0	0	0
IEPN	Russia	D	206	0	2214	4929	1812
KOLA	Russia	D	327	0	2710	0	0
KRSC	Russia	D	577	0	19644	0	0
MIRAS	Russia	D	113	0	3146	0	1242
MOS	Russia	D	1905	312	304605	0	108102
NERS	Russia	D	22	0	773	0	375
NORS	Russia	I MOS	33	150	0	0	0
SKHL	Russia	D	789	768	20323	0	9742
YARS	Russia	D	539	0	8151	0	5433
SGS	Saudi Arabia	D	32	0	352	0	0
BEO	Serbia	D	1066	1	17237	1387	0
BRA	Slovakia	D	0	0	0	21688	0
LJU	Slovenia	D	1261	427	17554	2405	5755
HNR	Solomon Islands	D	0	0	0	1367	0
PRE	South Africa	D	629	1	13147	0	4837
MDD	Spain	D	2677	12	68198	0	20334
MRB	Spain	D	524	0	11758	0	4540
SFS	Spain	D	1720	0	10772	3098	0
SSN	Sudan	D	104	1	469	0	58
UPP	Sweden	D	1348	2936	15047	0	0
ZUR	Switzerland	D	417	2	7522	0	4958
TRN	Trinidad and Tobago	D	0	1519	0	35600	0
DDA	Turkey	D	10044	2	218360	0	75951
ISK	Turkey	D	8420	17	117056	3378	67806
AEIC	U.S.A.	I NEIC	1659	531	66707	0	0
ANF	U.S.A.	I IRIS	81	932	0	0	0
BUT	U.S.A.	I NEIC	36	6	747	0	0
GCMT	U.S.A.	D	0	2138	0	0	0
HVO	U.S.A.	I NEIC	148	6	62	0	0
IRIS	U.S.A.	D	2484	932	232552	0	0
LDO	U.S.A.	I NEIC	12	2	13	0	0
NCEDC	U.S.A.	I NEIC	144	12	1720	0	0
NEIC	U.S.A.	D	15614	9073	1393632	0	643752
OGSO	U.S.A.	I NEIC	2	0	4	0	0
PAS	U.S.A.	I NEIC	57	14	1004	0	0
PNSN	U.S.A.	D	0	85	0	0	0

Table 8.2: (continued)

Agency	Country	Directly or indirectly reporting (D/I)	Hypocentres with associated phases	Hypocentres without associated phases	Associated phases	Unassociated phases	Amplitudes
REN	U.S.A.	I NEIC	183	20	706	0	0
RSPR	U.S.A.	D	2879	9	35254	0	0
SCEDC	U.S.A.	I IRIS	2	0	0	0	0
SEA	U.S.A.	I NEIC	32	2	2389	0	0
SLM	U.S.A.	I NEIC	34	0	930	0	0
TUL	U.S.A.	I NEIC	1129	4	0	0	0
UUS	U.S.A.	I NEIC	28	1	455	0	0
MCSM	Ukraine	D	58	0	1131	0	0
SIGU	Ukraine	D	35	27	902	0	392
DSN	United Arab Emirates	D	473	0	6088	0	0
BGS	United Kingdom	D	307	26	9259	9	3499
EAF	Unknown	D	1634	6	13536	6855	75
ISU	Uzbekistan	D	328	0	2963	0	0
CAR	Venezuela	I NEIC	0	4	0	0	0
FUNV	Venezuela	D	165	0	3711	0	0
PLV	Vietnam	D	4	0	48	0	26
LSZ	Zambia	D	58	1	204	33	15
BUL	Zimbabwe	D	1047	3	9152	544	0

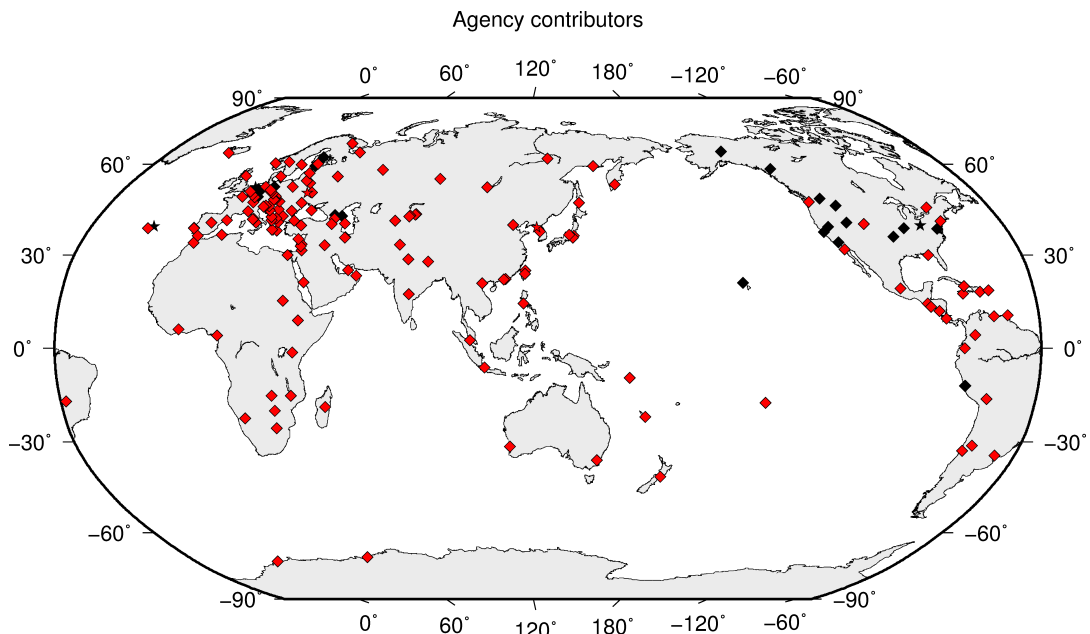


Figure 8.1: Map of agencies that have contributed data to the ISC for this summary period. Agencies that have reported directly to the ISC are shown in red. Those that have reported indirectly (via another agency) are shown in black. Any new or renewed agencies, since the last six-month period, are shown by a star. Each agency is listed in Table 8.2.

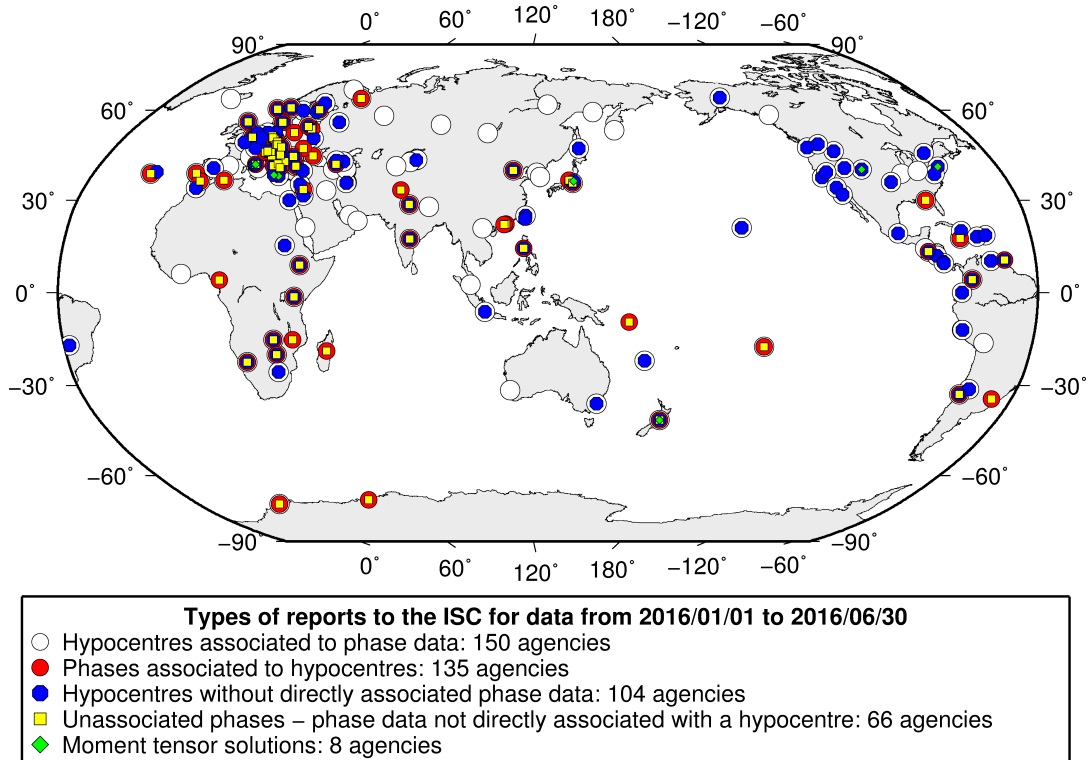


Figure 8.2: Map of the different data types reported by agencies to the ISC. A full list of the data types reported by each agency is shown in Table 8.2.

8.3 Arrival Observations

The collection of phase arrival observations at the ISC has increased dramatically with time. The increase in reported phase arrival observations is shown in Figure 8.3.

The reports with phase data are summarised in Table 8.3. This table is split into three sections, providing information on the reports themselves, the phase data, and the stations reporting the phase data. A map of the stations contributing these phase data is shown in Figure 8.4.

The ISC encourages the reporting of phase arrival times together with amplitude and period measurements whenever feasible. Figure 8.5 shows the percentage of events for which phase arrival times from each station are accompanied with amplitude and period measurements.

Figure 8.6 indicates the number of amplitude and period measurement for each station.

Together with the increase in the number of phases (Figure 8.3), there has been an increase in the number of stations reported to the ISC. The increase in the number of stations is shown in Figure 8.7. This increase can also be seen on the maps for stations reported each decade in Figure 8.8.

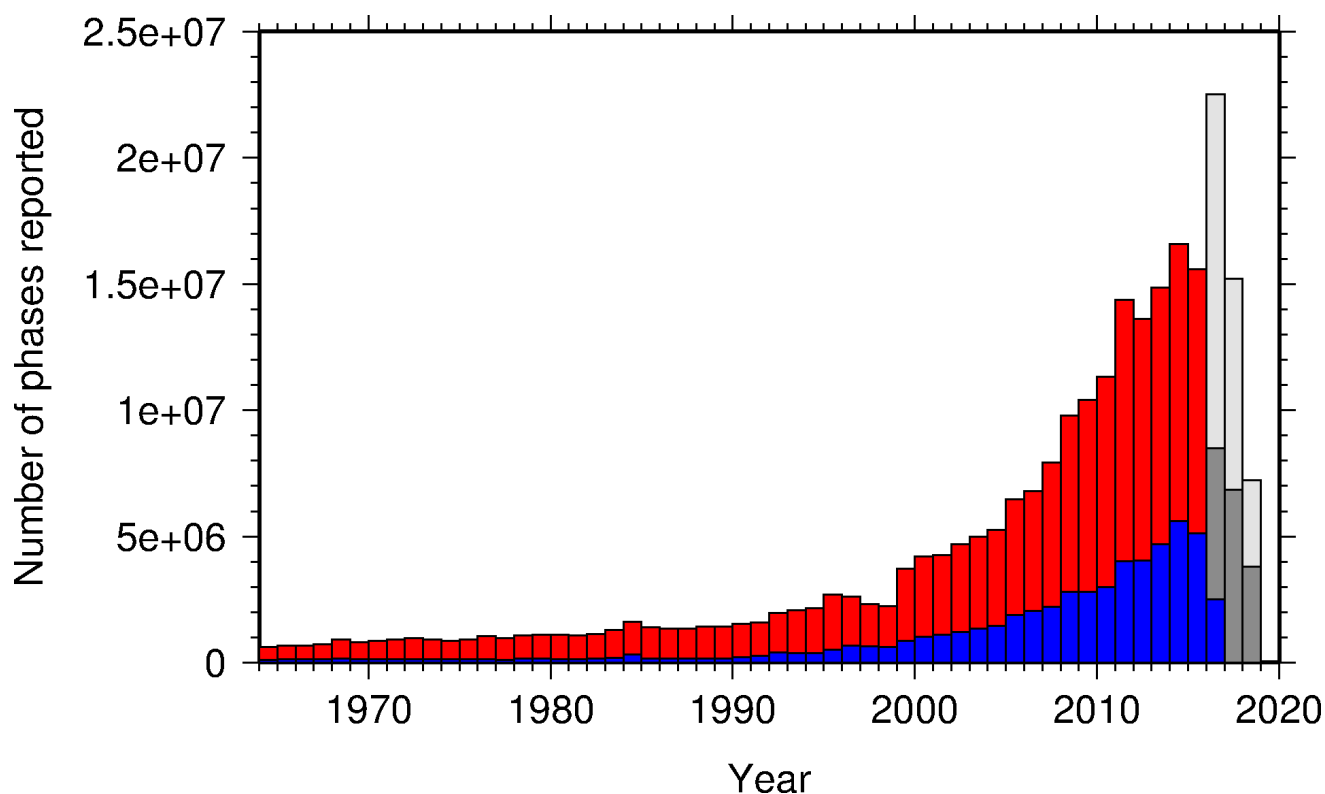


Figure 8.3: Histogram showing the number of phases (red) and number of amplitudes (blue) collected by the ISC for events each year since 1964. The data in grey covers the current period where data are still being collected before the ISC review takes place and is accurate at the time of publication.

Table 8.3: Summary of reports containing phase arrival observations.

Reports with phase arrivals	3579
Reports with phase arrivals including amplitudes	1170
Reports with only phase arrivals (no hypocentres reported)	255
Total phase arrivals received	8135872
Total phase arrival-times received	7672959
Number of duplicate phase arrival-times	535049 (7.0%)
Number of amplitudes received	2603751
Stations reporting phase arrivals	8087
Stations reporting phase arrivals with amplitude data	4902
Max number of stations per report	1886

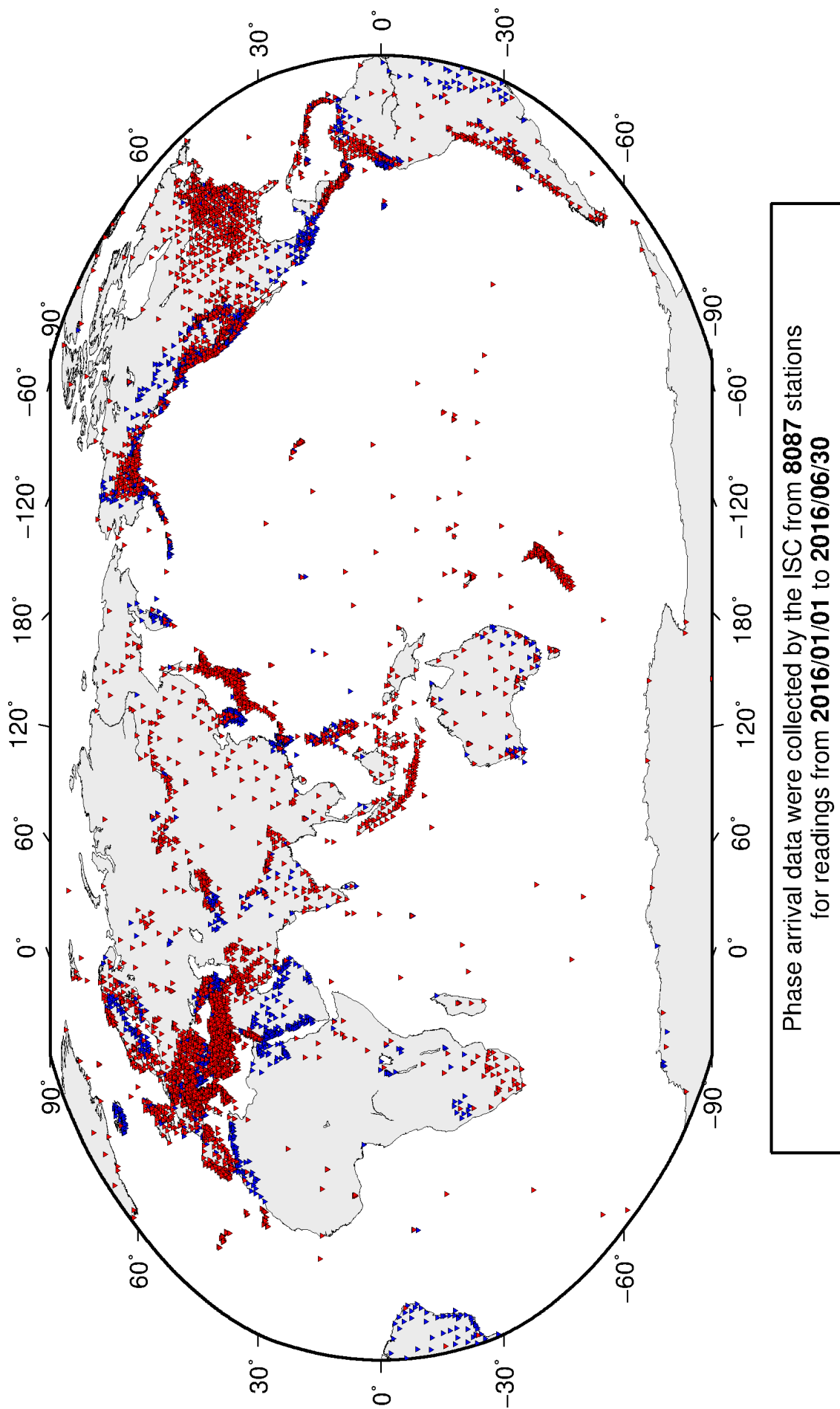


Figure 8.4: Stations contributing phase data to the ISC for readings from January 2016 to the end of July 2016. Stations in blue provided phase arrival times only; stations in red provided both phase arrival times and amplitude data.

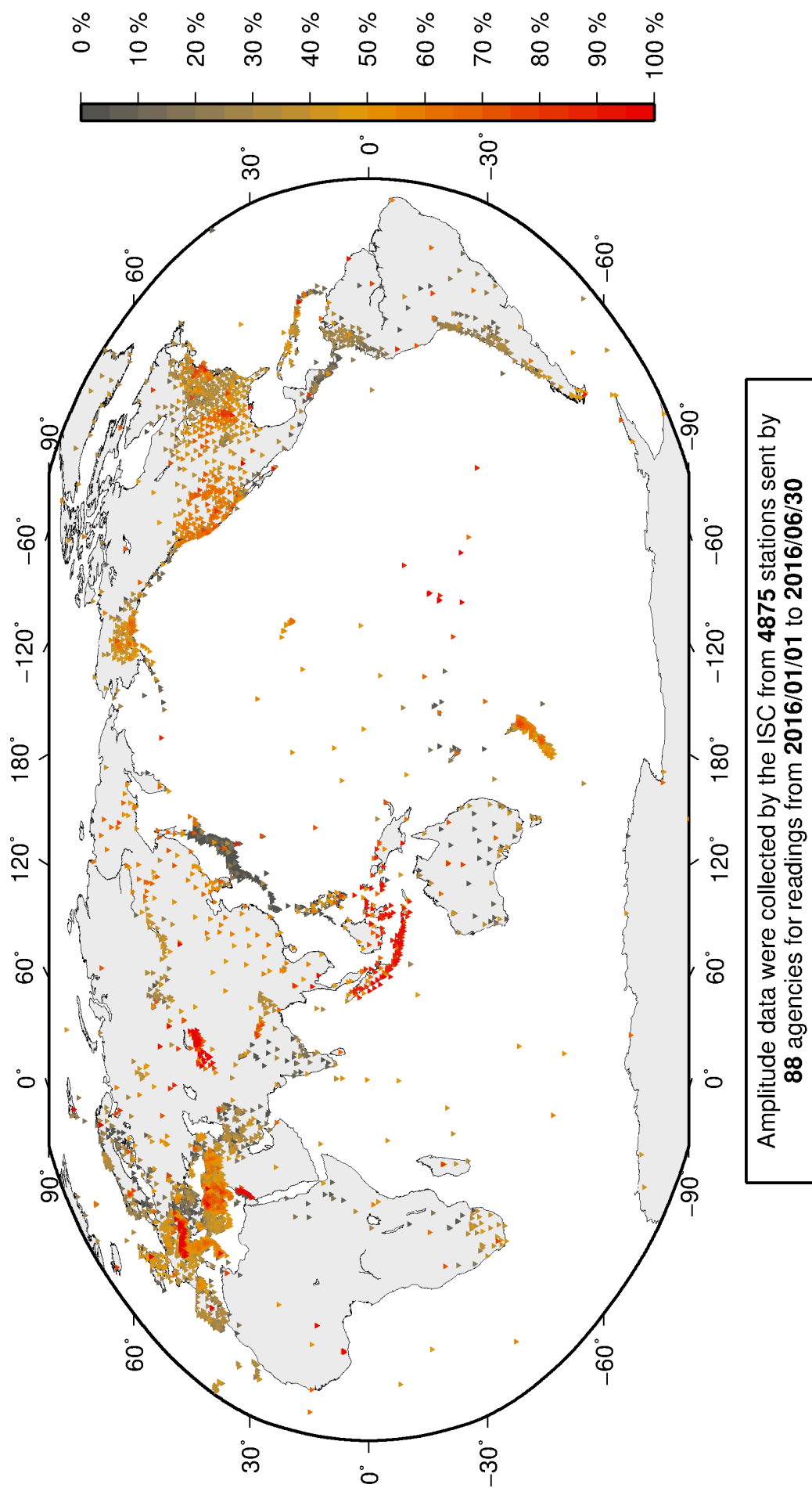


Figure 8.5: Percentage of events for which phase arrival times from each station are accompanied with amplitude and period measurements.

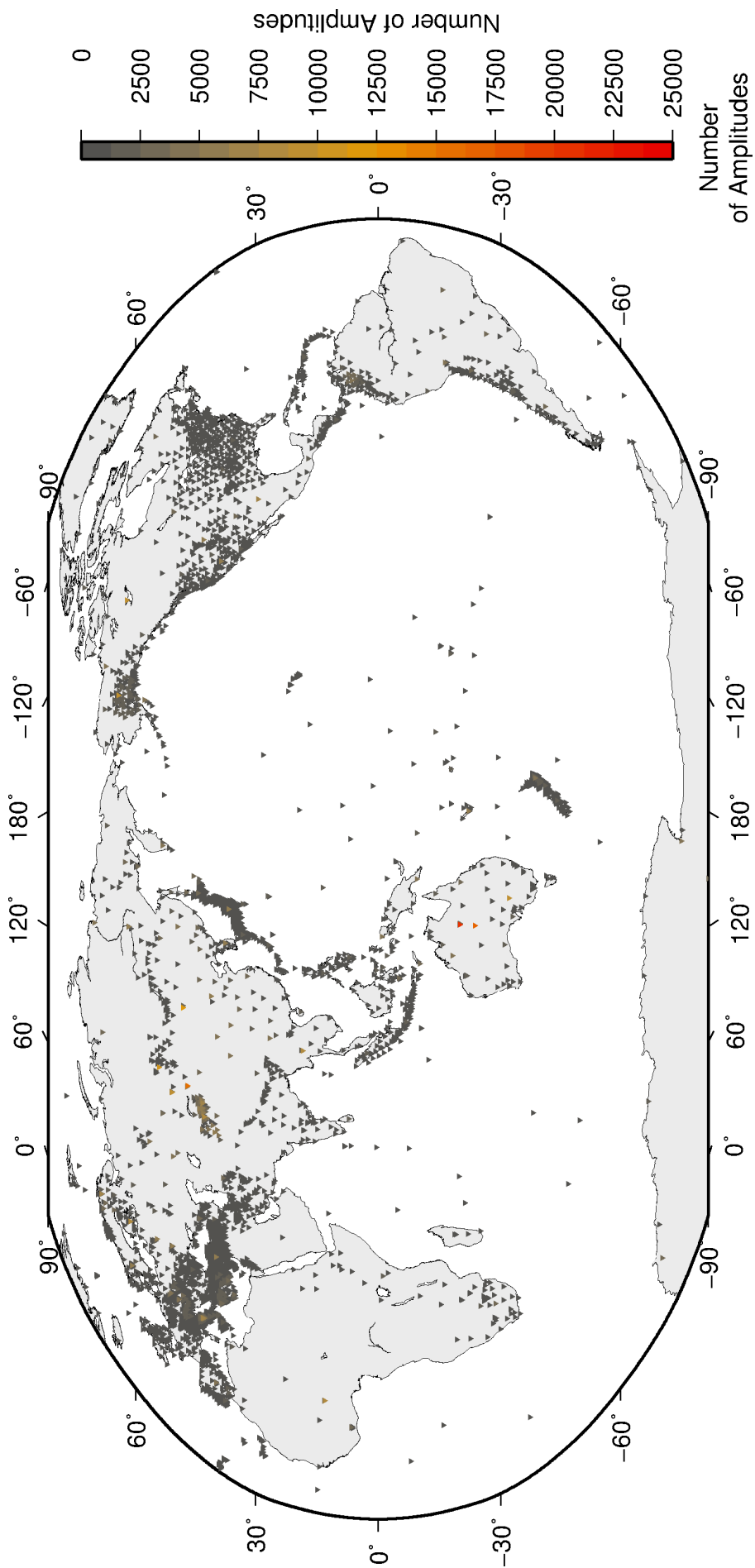


Figure 8.6: Number of amplitude and period measurements for each station.

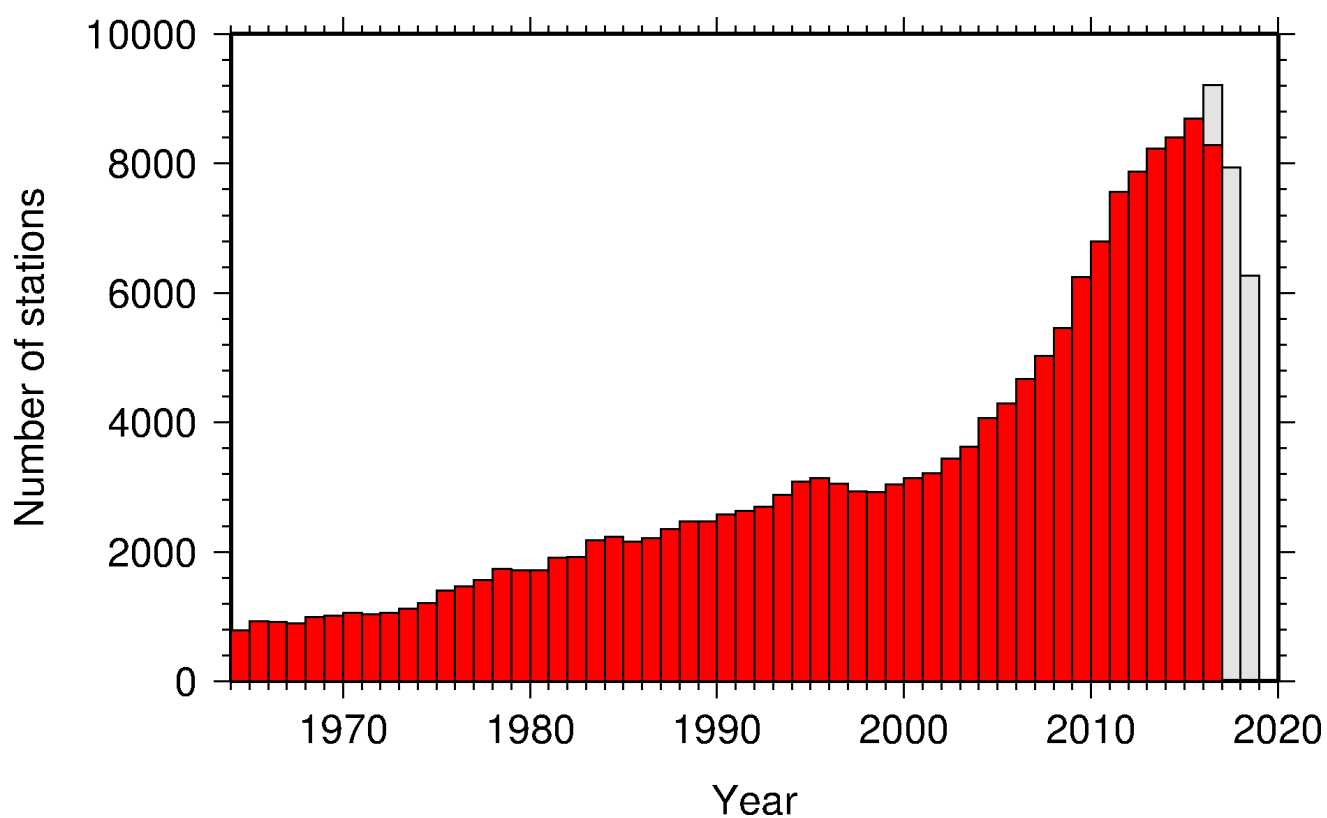


Figure 8.7: Histogram showing the number of stations reporting to the ISC each year since 1964. The data in grey covers the current period where station information is still being collected before the ISC review of events takes place and is accurate at the time of publication.

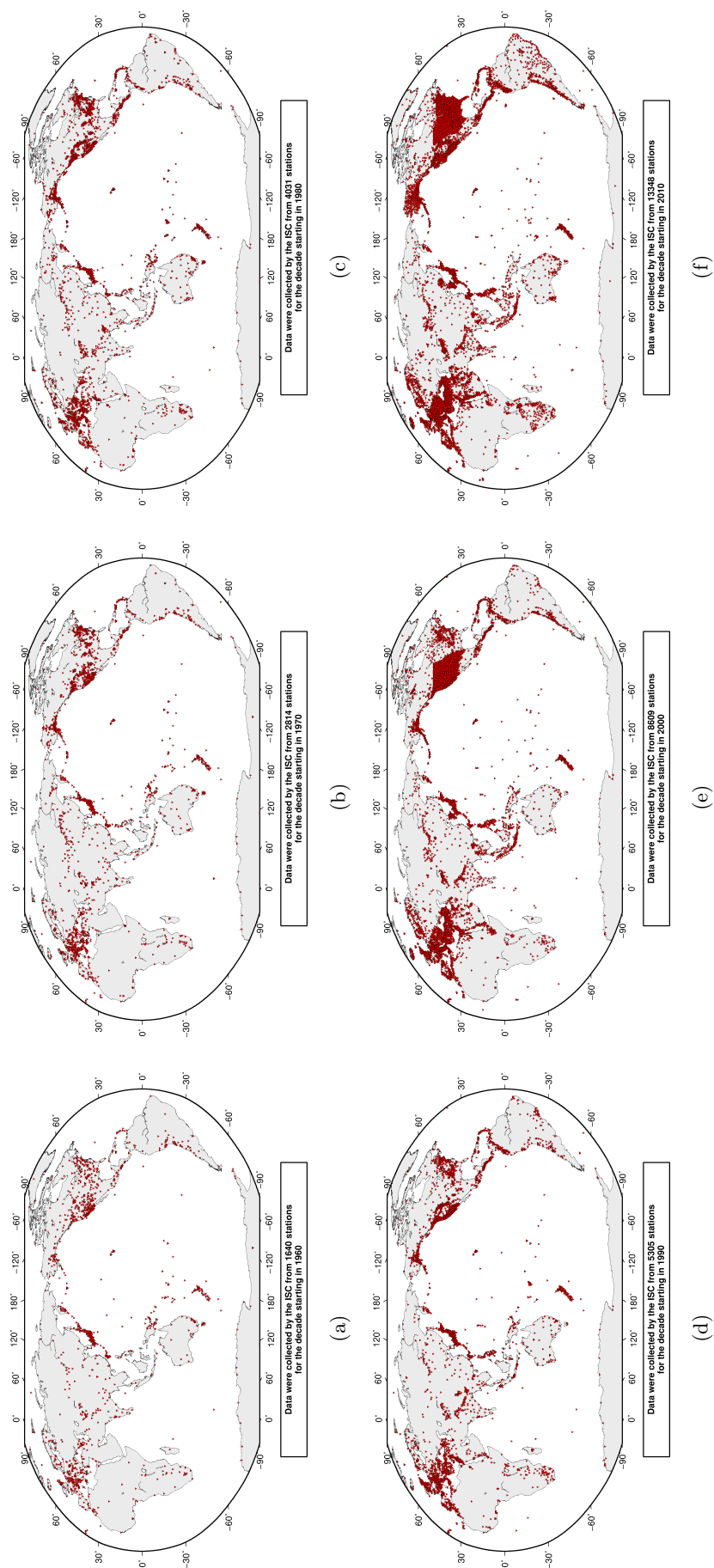


Figure 8.8: Maps showing the stations reported to the ISC for each decade since 1960. Note that the last map covers a shorter time period.

8.4 Hypocentres Collected

The ISC Bulletin groups multiple estimates of hypocentres into individual events, with an appropriate prime hypocentre solution selected. The collection of these hypocentre estimates are described in this section.

The reports containing hypocentres are summarised in Table 8.4. The number of hypocentres collected by the ISC has also increased significantly since 1964, as shown in Figure 8.9. A map of all hypocentres reported to the ISC for this summary period is shown in Figure 8.10. Where a network magnitude was reported with the hypocentre, this is also shown on the map, with preference given to reported values, first of M_W followed by M_S , m_b and M_L respectively (where more than one network magnitude was reported).

Table 8.4: Summary of the reports containing hypocentres.

Reports with hypocentres	3471
Reports of hypocentres only (no phase readings)	147
Total hypocentres received	342351
Number of duplicate hypocentres	9815 (2.9%)
Agencies determining hypocentres	165

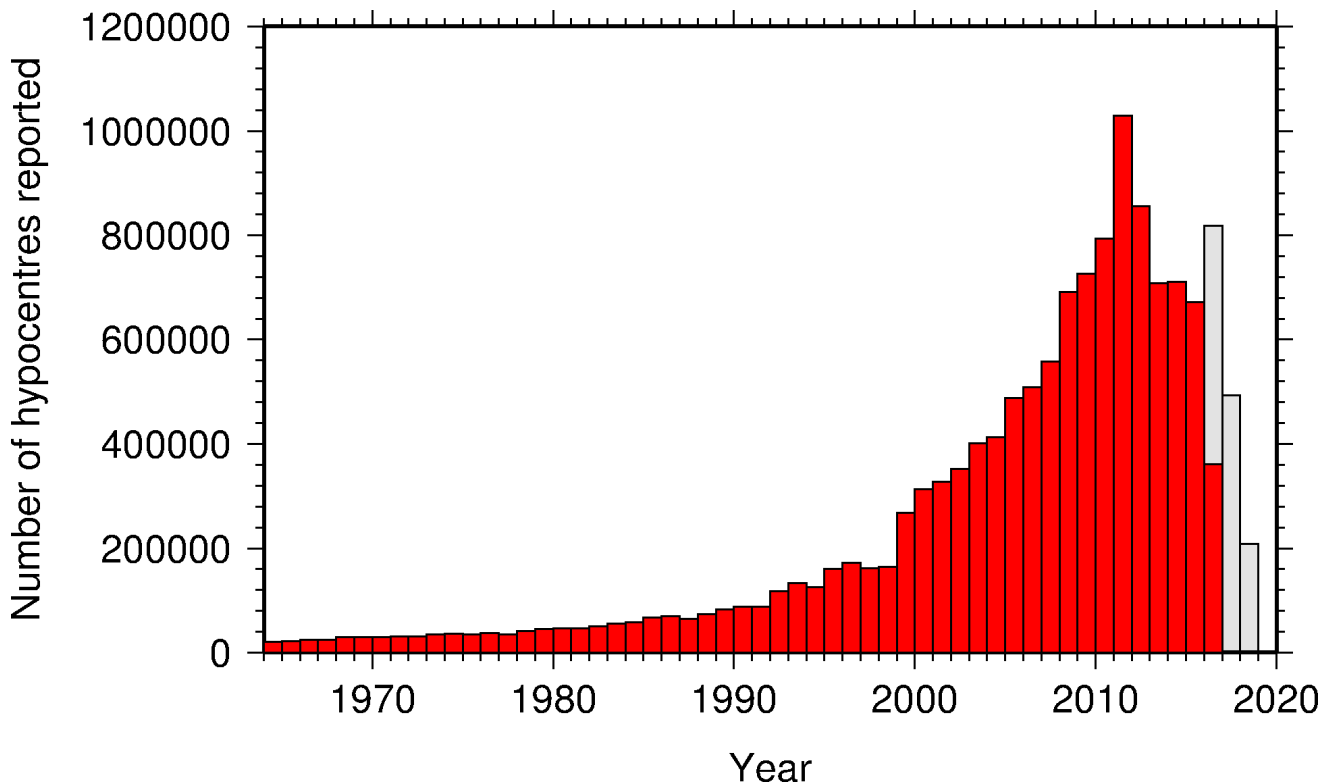


Figure 8.9: Histogram showing the number of hypocentres collected by the ISC for events each year since 1964. For each event, multiple hypocentres may be reported.

All the hypocentres that are reported to the ISC are automatically grouped into events, which form the basis of the ISC Bulletin. For this summary period 361567 hypocentres (including ISC) were grouped into 243606 events, the largest of these having 50 hypocentres in one event. The total number of events

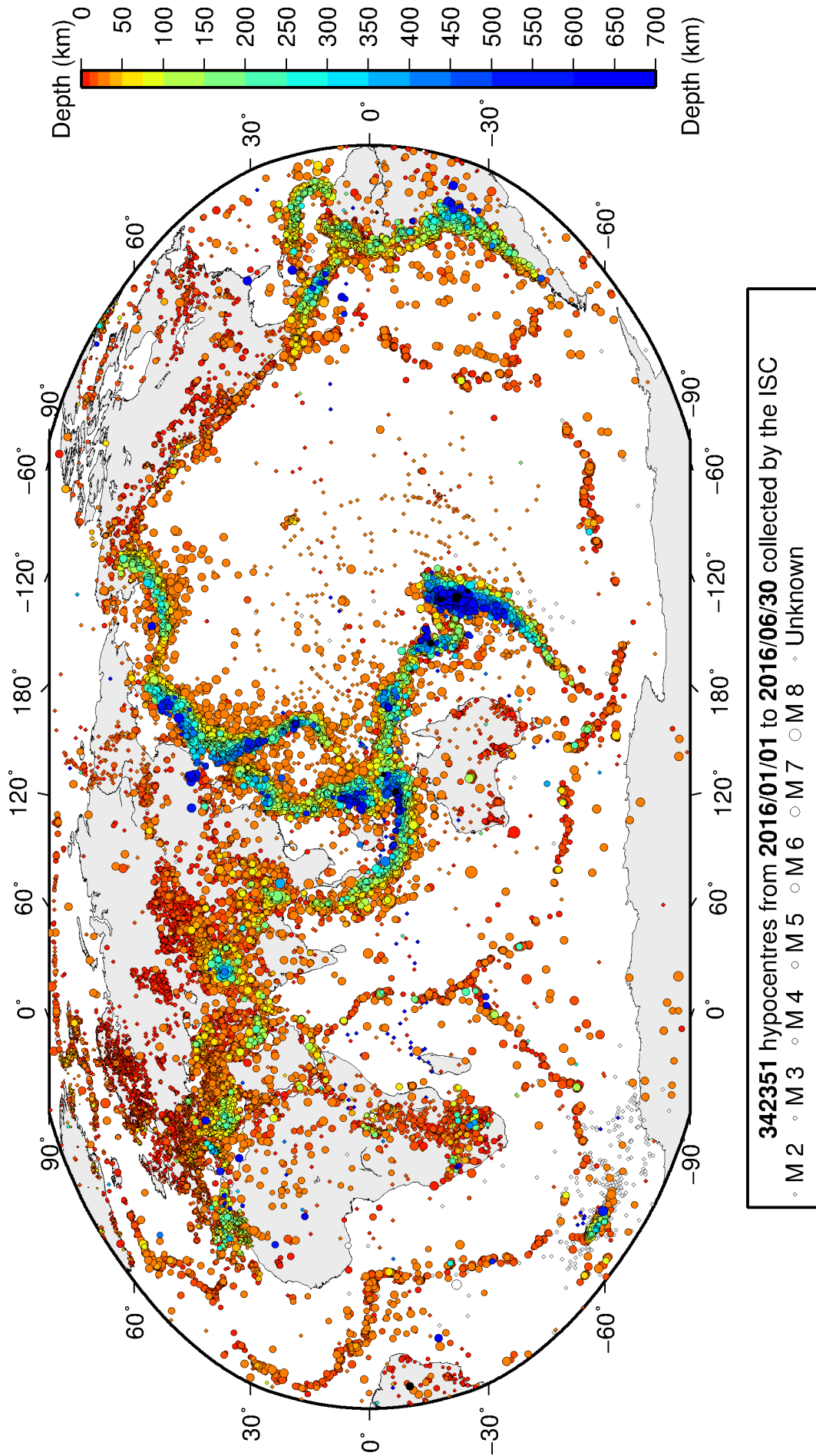


Figure 8.10: Map of all hypocentres collected by the ISC. The scatter shows the large variation of the multiple hypocentres that are reported for each event. The magnitude corresponds with the reported network magnitude. If more than one network magnitude type was reported, preference was given to values of M_W , M_S , m_b and M_L respectively. Compare with Figure 9.2

shown here is the result of an automatic grouping algorithm, and will differ from the total events in the published ISC Bulletin, where both the number of events and the number of hypocentre estimates will have changed due to further analysis. The process of grouping is detailed in Section 11.1.3. Figure 9.2 on page 73 shows a map of all prime hypocentres.

8.5 Collection of Network Magnitude Data

Data contributing agencies normally report earthquake hypocentre solutions along with magnitude estimates. For each seismic event, each agency may report one or more magnitudes of the same or different types. This stems from variability in observational practices at regional, national and global level in computing magnitudes based on a multitude of wave types. Differences in the amplitude measurement algorithm, seismogram component(s) used, frequency range, station distance range as well as the instrument type contribute to the diversity of magnitude types. Table 8.5 provides an overview of the complexity of reported network magnitudes reported for seismic events during the summary period.

Table 8.5: Statistics of magnitude reports to the ISC; M – average magnitude of estimates reported for each event.

	$M < 3.0$	$3.0 \leq M < 5.0$	$M \geq 5.0$
Number of seismic events	185081	38925	383
Average number of magnitude estimates per event	1.3	4.0	21.5
Average number of magnitudes (by the same agency) per event	1.2	2.3	3.1
Average number of magnitude types per event	1.2	3.3	11.3
Number of magnitude types	30	41	36

Table 8.6 gives the basic description, main features and scientific paper references for the most commonly reported magnitude types.

Table 8.6: Description of the most common magnitude types reported to the ISC.

Magnitude type	Description	References	Comments
M	Unspecified		Often used in real or near-real time magnitude estimations
mB	Medium-period and Broad-band body-wave magnitude	<i>Gutenberg</i> (1945a); <i>Gutenberg</i> (1945b); <i>IASPEI</i> (2005); <i>IASPEI</i> (2013); <i>Bormann et al.</i> (2009); <i>Bormann and Dewey</i> (2012)	
mb	Short-period body-wave magnitude	<i>IASPEI</i> (2005); <i>IASPEI</i> (2013); <i>Bormann et al.</i> (2009); <i>Bormann and Dewey</i> (2012)	Classical mb based on stations between 21°-100° distance

Table 8.6: *continued*

Magnitude type	Description	References	Comments
mb1	Short-period body-wave magnitude	<i>IDC</i> (1999) and references therein	Reported only by the IDC; also includes stations at distances less than 21°
mb1mx	Maximum likelihood short-period body-wave magnitude	<i>Ringdal</i> (1976); <i>IDC</i> (1999) and references therein	Reported only by the IDC
mbtmp	short-period body-wave magnitude with depth fixed at the surface	<i>IDC</i> (1999) and references therein	Reported only by the IDC
mbLg	Lg-wave magnitude	<i>Nuttli</i> (1973); <i>IASPEI</i> (2005); <i>IASPEI</i> (2013); <i>Bormann and Dewey</i> (2012)	Also reported as MN
Mc	Coda magnitude		
MD (Md)	Duration magnitude	<i>Bisztricsany</i> (1958); <i>Lee et al.</i> (1972)	
ME (Me)	Energy magnitude	<i>Choy and Boatwright</i> (1995)	Reported only by NEIC
MJMA	JMA magnitude	<i>Tsuboi</i> (1954)	Reported only by JMA
ML (Ml)	Local (Richter) magnitude	<i>Richter</i> (1935); <i>Hutton and Boore</i> (1987); <i>IASPEI</i> (2005); <i>IASPEI</i> (2013)	
MLS _n	Local magnitude calculated for S _n phases	<i>Balfour et al.</i> (2008)	Reported by PGC only for earthquakes west of the Cascadia subduction zone
ML _v	Local (Richter) magnitude computed from the vertical component		Reported only by DJA and BKK
MN (Mn)	Lg-wave magnitude	<i>Nuttli</i> (1973); <i>IASPEI</i> (2005)	Also reported as mbLg
MS (Ms)	Surface-wave magnitude	<i>Gutenberg</i> (1945c); <i>Vaněk et al.</i> (1962); <i>IASPEI</i> (2005)	Classical surface-wave magnitude computed from station between 20°-160° distance
Ms1	Surface-wave magnitude	<i>IDC</i> (1999) and references therein	Reported only by the IDC; also includes stations at distances less than 20°
ms1mx	Maximum likelihood surface-wave magnitude	<i>Ringdal</i> (1976); <i>IDC</i> (1999) and references therein	Reported only by the IDC

Table 8.6: *continued*

Magnitude type	Description	References	Comments
Ms7	Surface-wave magnitude	<i>Bormann et al.</i> (2007)	Reported only by BJI and computed from records of a Chinese-made long-period seismograph in the distance range 3°-177°
MW (Mw)	Moment magnitude	<i>Kanamori</i> (1977); <i>Dziewonski et al.</i> (1981)	Computed according to the <i>IASPEI</i> (2005) and <i>IASPEI</i> (2013) standard formula
Mw(mB)	Proxy Mw based on mB	<i>Bormann and Saul</i> (2008)	Reported only by DJA and BKK
Mwp	Moment magnitude from P-waves	<i>Tsuboi et al.</i> (1995)	Reported only by DJA and BKK and used in rapid response
mbh	Unknown		
mbv	Unknown		
MG	Unspecified type		Contact contributor
Mm	Unknown		
msh	Unknown		
MSV	Unknown		

Table 8.7 lists all magnitude types reported, the corresponding number of events in the ISC Bulletin and the agency codes along with the number of earthquakes.

Table 8.7: *Summary of magnitude types in the ISC Bulletin for this summary period. The number of events with values for each magnitude type is listed. The agencies reporting these magnitude types are listed, together with the total number of values reported.*

Magnitude type	Events	Agencies reporting magnitude type (number of values)
M	5754	WEL (5559), RSPR (134), KRSZO (45), PRU (16), MDD (1)
mb	26656	IDC (16300), NEIC (7314), NNC (4789), KRNET (3661), MAN (2081), VIE (1669), MOS (1480), DJA (1346), BJI (1174), VAO (504), NOU (412), BGR (182), MDD (127), OMAN (71), GII (44), DSN (44), CRAAG (40), NDI (25), SIGU (21), MCSM (14), PRE (5), ROM (4), PGC (4), DNK (3), DMN (3), GCG (1), INMG (1), STR (1), IASPEI (1), BER (1)
mB	1957	BJI (1204), DJA (786), WEL (208), NOU (8)
MB	3	IPEC (3)
mb1	12116	IDC (12116)
mb1mx	12116	IDC (12116)
mB_BB	19	BGR (19)
mb_Lg	3762	MDD (2486), NEIC (1240), TEH (41), OTT (5)
mbLg	64	MDD (64)
mbR	172	VAO (172)

Table 8.7: Continued.

Magnitude type	Events	Agencies reporting magnitude type (number of values)
mbtmp	17525	IDC (17525)
Mc	90	DNK (85), BER (3), JSO (3), OSPL (2), SIGU (2)
MC	30	DDA (30)
MD	10047	LDG (1604), RSPR (1396), TRN (1351), SSNC (1312), ROM (802), HLW (795), ECX (492), GCG (465), GRAL (389), TIR (251), EAF (239), BUL (191), GII (188), JMA (149), MEX (143), SNET (114), JSN (99), INMG (95), SOF (94), SJA (84), PNSN (75), PDG (67), LSZ (42), SLM (34), BUG (29), INET (28), UPA (14), NAM (10), NIC (9), NCEDC (5), SIGU (4), ISK (2), HVO (2), IGQ (1), USS (1), CAR (1), OGSO (1), HDC (1)
Mjma	1	JSO (1)
MJMA	38869	JMA (38869)
ML	121026	TAP (30515), IDC (9634), DDA (9485), ATH (8872), ISK (8424), HEL (8273), RSNC (6646), CNRM (5741), ROM (5586), WEL (5102), THE (4054), UPP (3503), GUC (3344), VIE (2514), NEIC (2282), AEIC (2149), MAN (2098), BER (2069), LDG (1984), SFS (1598), INMG (1594), SSNC (1425), LJU (1184), SNET (1143), TUL (1129), PGC (1084), BEO (1065), ANF (1026), DNK (992), OSPL (924), BUC (898), RHSSO (737), IGIL (591), KRSC (576), GEN (533), TEH (526), MRB (524), PRE (522), ECX (519), IPEC (513), NIC (490), NAO (481), SCB (472), ECGS (472), INET (421), KOLA (324), OMAN (300), ISN (292), CRAAG (268), BJI (268), SJA (266), TIR (263), HLW (233), UCR (227), WBNET (213), NDI (192), KNET (188), DSN (180), PDG (178), LVSN (176), KRSZO (162), HVO (152), BGS (133), REN (120), BGR (118), MIRAS (108), ARE (99), NOU (78), OTT (71), KEA (70), UCC (69), PPT (47), PAS (45), NCEDC (40), BUT (39), BNS (37), MCSM (35), DMN (35), SEA (33), UPA (31), BUG (29), SGS (29), USS (21), FIAO (17), CUPWA (15), LDO (13), AAE (12), HYB (10), THR (8), LSZ (6), SSS (6), CSEM (5), JSO (5), PLV (4), CLL (3), RISSC (3), DRS (3), EAF (3), SKO (3), PDA (2), ALG (2), AUST (1), RSPR (1), IGQ (1), OGSO (1), MOS (1), SSN (1), MEX (1), VAO (1)
MLh	532	ZUR (398), ASRS (135)
MLS _n	371	PGC (371)
ML _v	11232	WEL (5567), DJA (3106), NOU (1763), STR (960), KRSZO (27), MCSM (17), JSO (10), MDD (1)
Mm	373	GII (373)
MN	317	OTT (317)
mpv	5187	NNC (5187)
MPVA	260	MOS (224), NORS (173)
MS	9705	IDC (7813), MAN (2097), BJI (948), MOS (424), BGR (86), SOME (76), NSSP (40), VIE (16), KEA (16), OMAN (15), DSN (8), DNK (4), IPEC (3), UPA (2), BER (2), LDG (2), AAE (1), NDI (1), JSO (1), RSNC (1)

Table 8.7: Continued.

Magnitude type	Events	Agencies reporting magnitude type (number of values)
Ms1	5222	IDC (5222)
mslmx	5222	IDC (5222)
Ms7	941	BJI (941)
Ms_20	198	NEIC (198)
msh	4	SIGU (4)
MV	34283	JMA (34283)
MW	6218	INET (1190), SSNC (1147), GCMT (1069), NIED (867), UPA (453), PGC (400), RSNC (348), UCR (299), SJA (260), DDA (194), FUNV (165), SCB (105), MED_RCMT (77), JMA (61), ASIES (58), BER (57), WEL (47), GUC (35), ROM (15), ATH (13), DJA (11), DNK (9), SNET (6), IEC (5), UPSL (5), MOS (5), ECX (2), CRAAG (1), GFZ (1)
Mw(mB)	208	WEL (208)
Mwb	196	NEIC (196)
Mwc	47	NEIC (29), GCMT (18)
Mwp	122	DJA (113), OMAN (6), ROM (2), NEIC (1)
Mwr	422	NEIC (308), GUC (58), SLM (42), NCEDC (17), PAS (12), OTT (10), REN (10), RSNC (8), CAR (3), UCR (2), MDD (1)
Mww	290	NEIC (290)

The most commonly reported magnitude types are short-period body-wave, surface-wave, local (or Richter), moment, duration and JMA magnitude type. For a given earthquake, the number and type of reported magnitudes greatly vary depending on its size and location. The large earthquake of October 25, 2010 gives an example of the multitude of reported magnitude types for large earthquakes (Listing 8.1). Different magnitude estimates come from global monitoring agencies such as the IDC, NEIC and GCMT, a local agency (GUC) and other agencies, such as MOS and BJI, providing estimates based on the analysis of their networks. The same agency may report different magnitude types as well as several estimates of the same magnitude type, such as NEIC estimates of Mw obtained from W-phase, centroid and body-wave inversions.

Listing 8.1: Example of reported magnitudes for a large event

```

Event 15264887 Southern Sumatera
Date 2010/10/25 Time 14:42:22.18 Err 0.27 RMS 1.813 Latitude -3.5248 Longitude 100.1042 Smaj 4.045 Smin 3.327 Az 54 Depth 20.0 Err Ndef 2102 Nsta 2149 Gap 23 mdist 0.76 Mdlist 176.43 m i de ISC Author OrigID
(#PRIME)

Magnitude Err Nsta Author OrigID
mb 6.1 61 BJI 15548963
mB 6.9 68 BJI 15548963
Ms 7.7 85 BJI 15548963
Ms7 7.5 86 BJI 15548963
mb 5.3 0.1 48 IDC 16686694
mb1 5.3 0.1 51 IDC 16686694
mbmx 5.3 0.0 52 IDC 16686694
mbtmp 5.3 0.1 51 IDC 16686694
ML 5.1 0.2 2 IDC 16686694
MS 7.1 0.0 31 IDC 16686694
Ms1 7.1 0.0 31 IDC 16686694
mslmx 6.9 0.1 44 IDC 16686694
mb 6.1 243 ISCJB 01677901
MS 7.3 228 ISCJB 01677901
M 7.1 117 DJA 01268475
mb 6.1 0.2 115 DJA 01268475
mB 7.1 0.1 117 DJA 01268475
MLv 7.0 0.2 26 DJA 01268475
7.1 0.4 117 DJA 01268475
Mwp 6.9 0.2 102 DJA 01268475
mb 6.4 49 MOS 16742129
MS 7.2 70 MOS 16742129
mb 6.5 110 NEIC 01288303
ME 7.3 NEIC 01288303
MS 7.3 143 NEIC 01288303

```

MW	7.7		NEIC	01288303
MW	7.8	130	GCMT	00125427
mb	5.9		KLM	00255772
ML	6.7		KLM	00255772
MS	7.6		KLM	00255772
mb	6.4	20	BGR	16815854
Mb	7.2	2	BGR	16815854
mb	6.3	0.3	250	ISC
MS	7.3	0.1	237	ISC

An example of a relatively small earthquake that occurred in northern Italy for which we received magnitude reports of mostly local and duration type from six agencies in Italy, France and Austria is given in Listing 8.2.

Listing 8.2: Example of reported magnitudes for a small event

Event 15089710 Northern Italy																		
Date	Time	Err	RMS	Latitude	Longitude	Smaj	Smin	Az	Depth	Err	Ndef	Nsta	Gap	mdist	Mdist	Qual	Author	OrigID
2010/08/08	15:20:46.22	0.94	0.778	45.4846	8.3212	2.900	2.539	110	28.6	9.22	172	110	82	0.41	5.35	m i ke	ISC	01249414
(#PRIME)																		
Magnitude	Err	Nsta	Author	OrigID														
ML	2.4	10	ZUR	15925566														
Md	2.6	0.2	19	ROM	16861451													
M1	2.2	0.2	9	ROM	16861451													
ML	2.5		GEN	00554757														
ML	2.6	0.3	28	CSEM	00554756													
Md	2.3	0.0	3	LDG	14797570													
M1	2.6	0.3	32	LDG	14797570													

Figure 8.11 shows a distribution of the number of agencies reporting magnitude estimates to the ISC according to the magnitude value. The peak of the distribution corresponds to small earthquakes where many local agencies report local and/or duration magnitudes. The number of contributing agencies rapidly decreases for earthquakes of approximately magnitude 5.5 and above, where magnitudes are mostly given by global monitoring agencies.

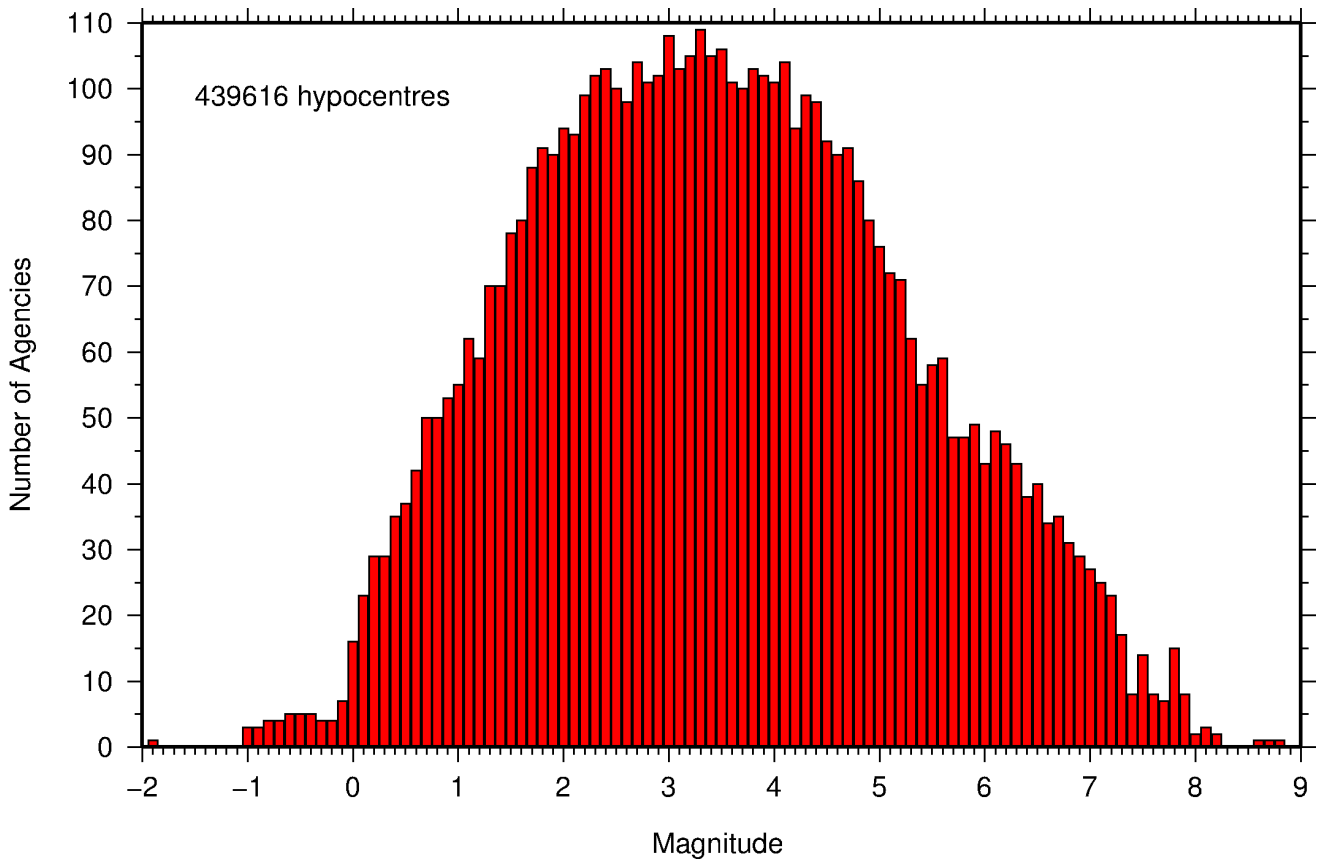


Figure 8.11: Histogram showing the number of agencies that reported network magnitude values. All magnitude types are included.

8.6 Moment Tensor Solutions

The ISC Bulletin publishes moment tensor solutions, which are reported to the ISC by other agencies. The collection of moment tensor solutions is summarised in Table 8.8. A histogram showing all moment tensor solutions collected throughout the ISC history is shown in Figure 8.12. Several moment tensor solutions from different authors and different moment tensor solutions calculated by different methods from the same agency may be present for the same event.

Table 8.8: Summary of reports containing moment tensor solutions.

Reports with Moment Tensors	64
Total moment tensors received	6676
Agencies reporting moment tensors	8

The number of moment tensors for this summary period, reported by each agency, is shown in Table 8.9. The moment tensor solutions are plotted in Figure 8.13.

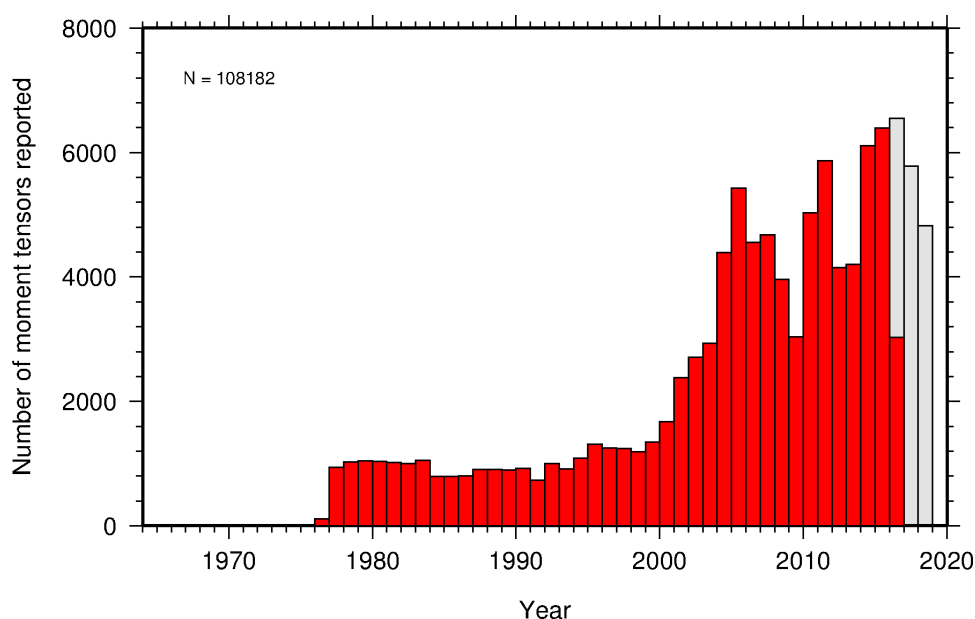
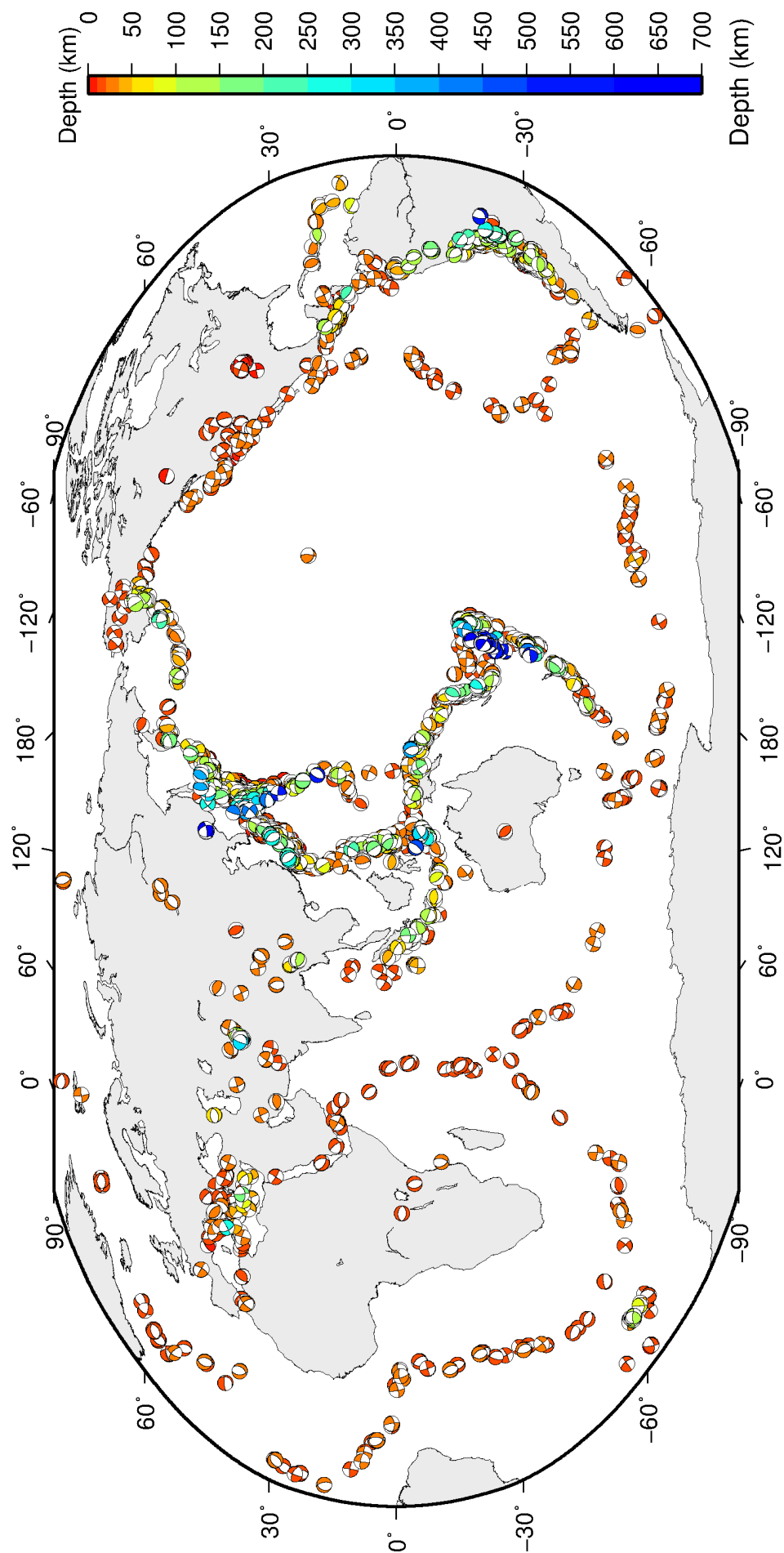


Figure 8.12: Histogram showing the number of moment tensors reported to the ISC since 1964. The regions in grey represent data that are still being actively collected.



ISC Bulletin: **3018** focal mechanism solutions for **2220** events from **2016/01/01** to **2016/06/30**

Figure 8.13: Map of all moment tensor solutions in the ISC Bulletin for this summary period.

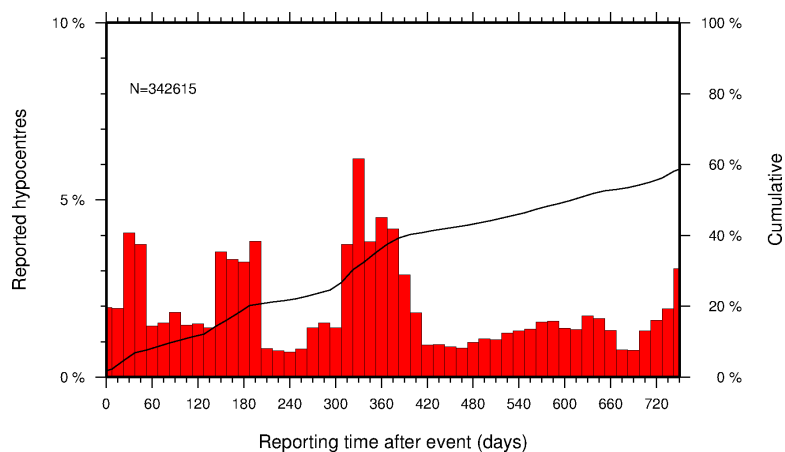
Table 8.9: Summary of moment tensor solutions in the ISC Bulletin reported by each agency.

Agency	Number of moment tensor solutions
GCMT	1069
NEIC	927
NIED	867
ISC	790
JMA	544
RSNC	93
MED_RCMT	77
PNSN	75
WEL	47
ECX	33
OSPL	20
MOS	18
ROM	13
UPA	13
ATH	13
IEC	10
UCR	6
UPSL	5
INET	2
SNET	2
DNK	1
GUC	1

8.7 Timing of Data Collection

Here we present the timing of reports to the ISC. Please note, this does not include provisional alerts, which are replaced at a later stage. Instead, it reflects the final data sent to the ISC. The absolute timing of all hypocentre reports, regardless of magnitude, is shown in Figure 8.14. In Figure 8.15 the reports are grouped into one of six categories - from within three days of an event origin time, to over one year. The histogram shows the distribution with magnitude (for hypocentres where a network magnitude was reported) for each category, whilst the map shows the geographic distribution of the reported hypocentres.

Figure 8.14: Histogram showing the timing of final reports of the hypocentres (total of N) to the ISC. The cumulative frequency is shown by the solid line.



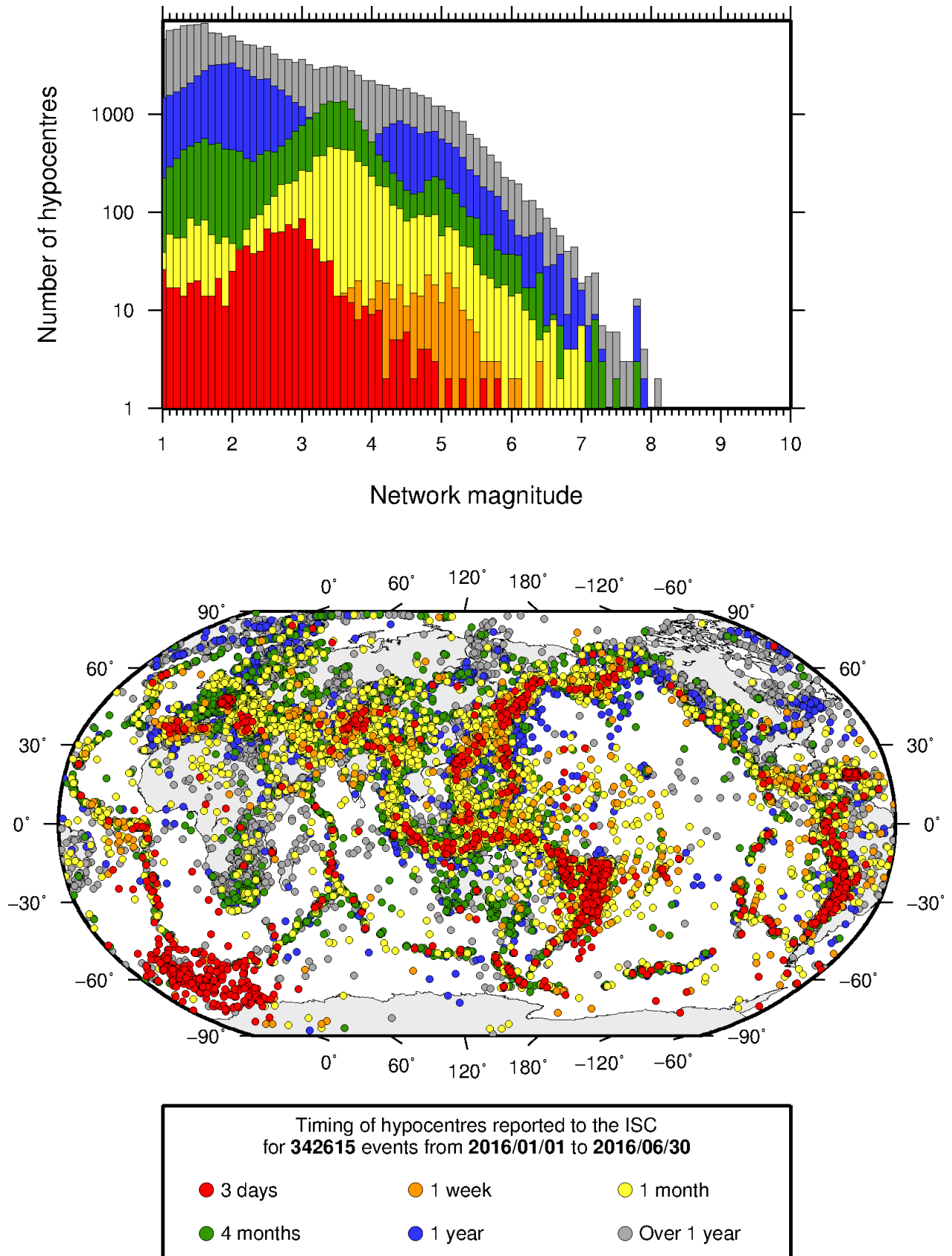


Figure 8.15: Timing of hypocentres reported to the ISC. The colours show the time after the origin time that the corresponding hypocentre was reported. The histogram shows the distribution with magnitude. If more than one network magnitude was reported, preference was given to a value of M_W followed by M_S , m_b and M_L respectively; all reported hypocentres are included on the map. Note: early reported hypocentres are plotted over later reported hypocentres, on both the map and histogram.

9

Overview of the ISC Bulletin

This chapter provides an overview of the seismic event data in the ISC Bulletin. We indicate the differences between all ISC events and those ISC events that are reviewed or located. We describe the wealth of phase arrivals and phase amplitudes and periods observed at seismic stations worldwide, reported in the ISC Bulletin and often used in the ISC location and magnitude determination. Finally, we make some comparisons of the ISC magnitudes with those reported by other agencies, and discuss magnitude completeness of the ISC Bulletin.

9.1 Events

The ISC Bulletin had 236949 reported events in the summary period between January and June 2016. Some 91% (216507) of the events were identified as earthquakes, the rest (20442) were of anthropogenic origin (including mining and other chemical explosions, rockbursts and induced events) or of unknown origin. As discussed in Section 11.1.3, typically about 15% of the events are selected for ISC review, and about half of the events selected for review are located by the ISC. In this summary period 11% of the events were reviewed and 7% of the events were located by the ISC. For events that are not located by the ISC, the prime hypocentre is identified according to the rules described in Section 11.1.3.

Of the 8296874 reported phase observations, 38% are associated to ISC-reviewed events, and 36% are associated to events selected for ISC location. Note that all large events are reviewed and located by the ISC. Since large events are globally recorded and thus reported by stations worldwide, they will provide the bulk of observations. This explains why only about one-fifth of the events in any given month is reviewed although the number of phases associated to reviewed events has increased nearly exponentially in the past decades.

Figure 9.1 shows the daily number of events throughout the summary period. Figure 9.2 shows the locations of the events in the ISC Bulletin; the locations of ISC-reviewed and ISC-located events are shown in Figures 9.3 and 9.4, respectively.

Figure 9.5 shows the hypocentral depth distributions of events in the ISC Bulletin for the summary period. The vast majority of events occur in the Earth's crust. Note that the peaks at 0, 10, 35 km, and at every 50 km intervals deeper than 100 km are artifacts of analyst practices of fixing the depth to a nominal value when the depth cannot be reliably resolved.

Figure 9.6 shows the depth distribution of free-depth solutions in the ISC Bulletin. The depth of a hypocentre reported to the ISC is assumed to be determined as a free parameter, unless it is explicitly labelled as a fixed-depth solution. On the other hand, as described in Section 11.1.4, the ISC locator attempts to get a free-depth solution if, and only if, there is resolution for the depth in the data, i.e. if

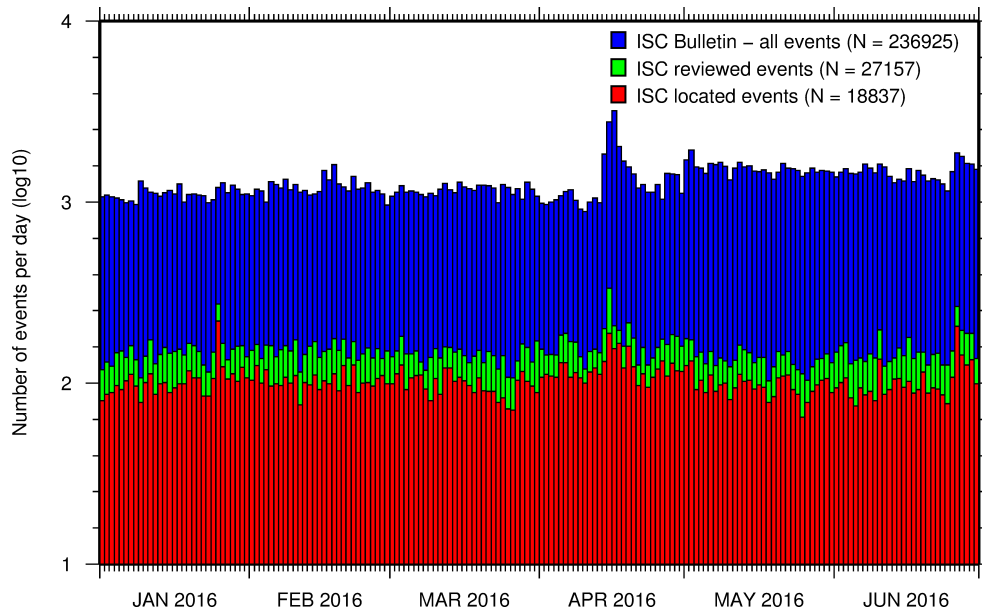


Figure 9.1: Histogram showing the number of events in the ISC Bulletin for the current summary period. The vertical scale is logarithmic.

there is a local network and/or sufficient depth-sensitive phases are reported.

Figure 9.7 shows the depth distribution of fixed-depth solutions in the ISC Bulletin. Except for a fraction of events whose depth is fixed to a shallow depth, this set comprises mostly ISC-located events. If there is no resolution for depth in the data, the ISC locator fixes the depth to a value obtained from the ISC default depth grid file, or if no default depth exists for that location, to a nominal default depth assigned to each Flinn-Engdahl region (see details in Section 11.1.4). During the ISC review editors are inclined to accept the depth obtained from the default depth grid, but they typically change the depth of those solutions that have a nominal (10 or 35 km) depth. When doing so, they usually fix the depth to a round number, preferably divisible by 50.

For events selected for ISC location, the number of stations typically increases as arrival data reported by several agencies are grouped together and associated to the prime hypocentre. Consequently, the network geometry, characterised by the secondary azimuthal gap (the largest azimuthal gap a single station closes), is typically improved. Figure 9.8 illustrates that the secondary azimuthal gap is indeed generally smaller for ISC-located events than that for all events in the ISC Bulletin. Figure 9.9 shows the distribution of the number of associated stations. For large events the number of associated stations is usually larger for ISC-located events than for any of the reported event bulletins. On the other hand, events with just a few reporting stations are rarely selected for ISC location. The same is true for the number of defining stations (stations with at least one defining phase that were used in the location). Figure 9.10 indicates that because the reported observations from multiple agencies are associated to the prime, large ISC-located events typically have a larger number of defining stations than any of the reported event bulletins.

The formal uncertainty estimates are also typically smaller for ISC-located events. Figure 9.11 shows the distribution of the area of the 90% confidence error ellipse for ISC-located events during the summary period. The distribution suffers from a long tail indicating a few poorly constrained event locations. Nevertheless, half of the events are characterised by an error ellipse with an area less than 186 km², 90%

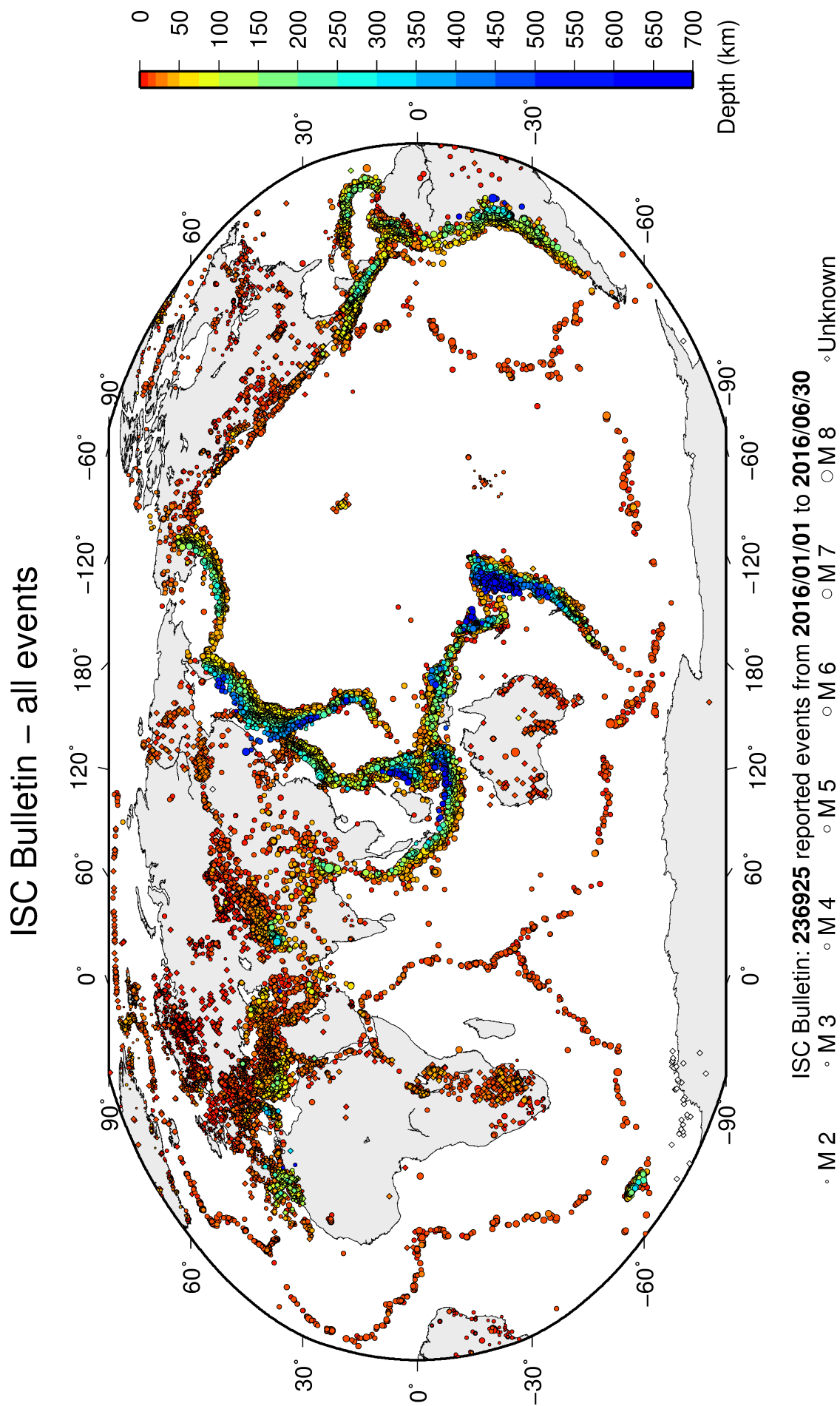


Figure 9.2: Map of all events in the ISC Bulletin. Prime hypocentre locations are shown. Compare with Figure 8.10.

ISC Bulletin – reviewed events

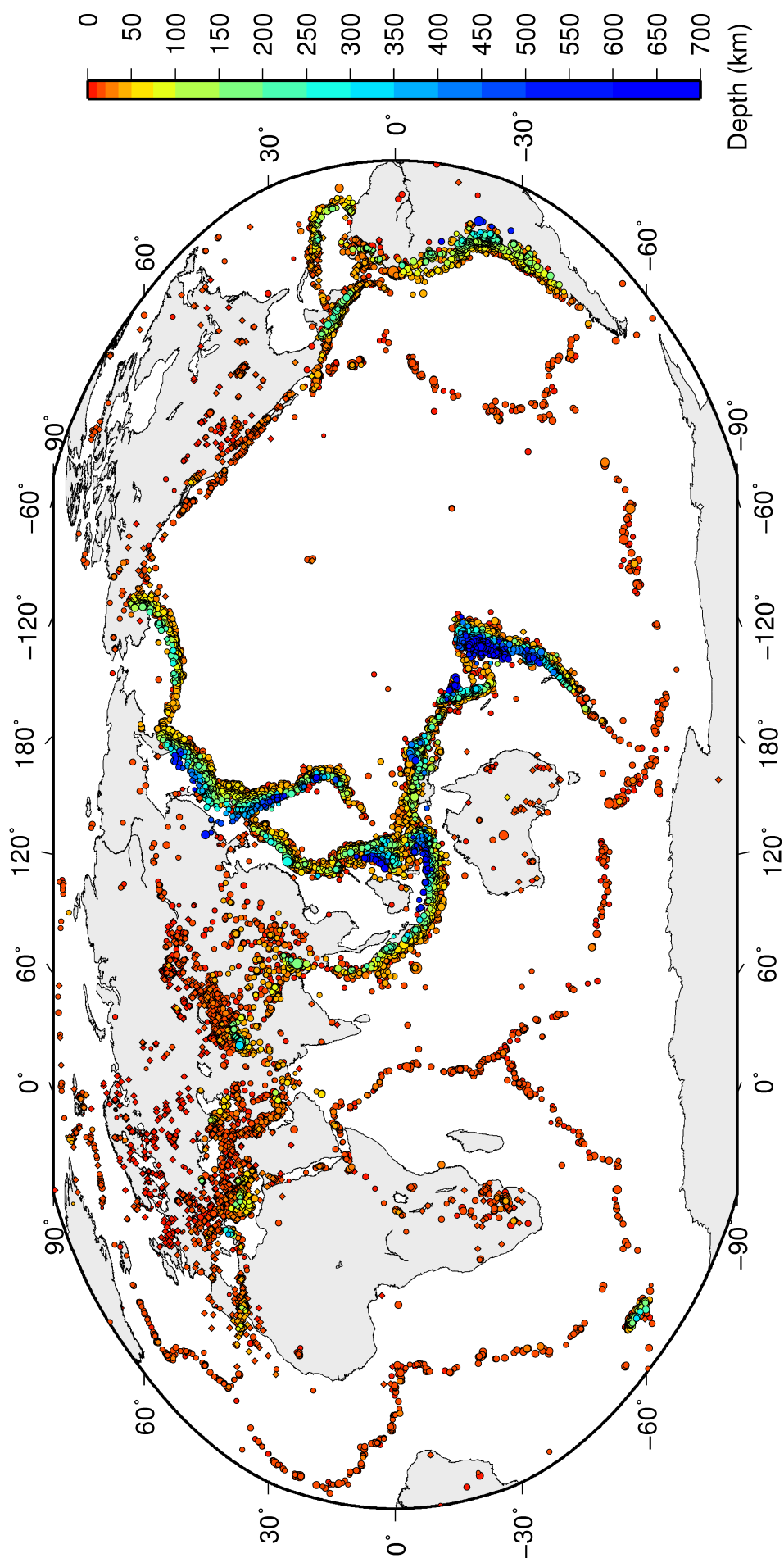


Figure 9.3: Map of all events reviewed by the ISC for this time period. Prime hypocentre locations are shown.

ISC Bulletin – ISC located events

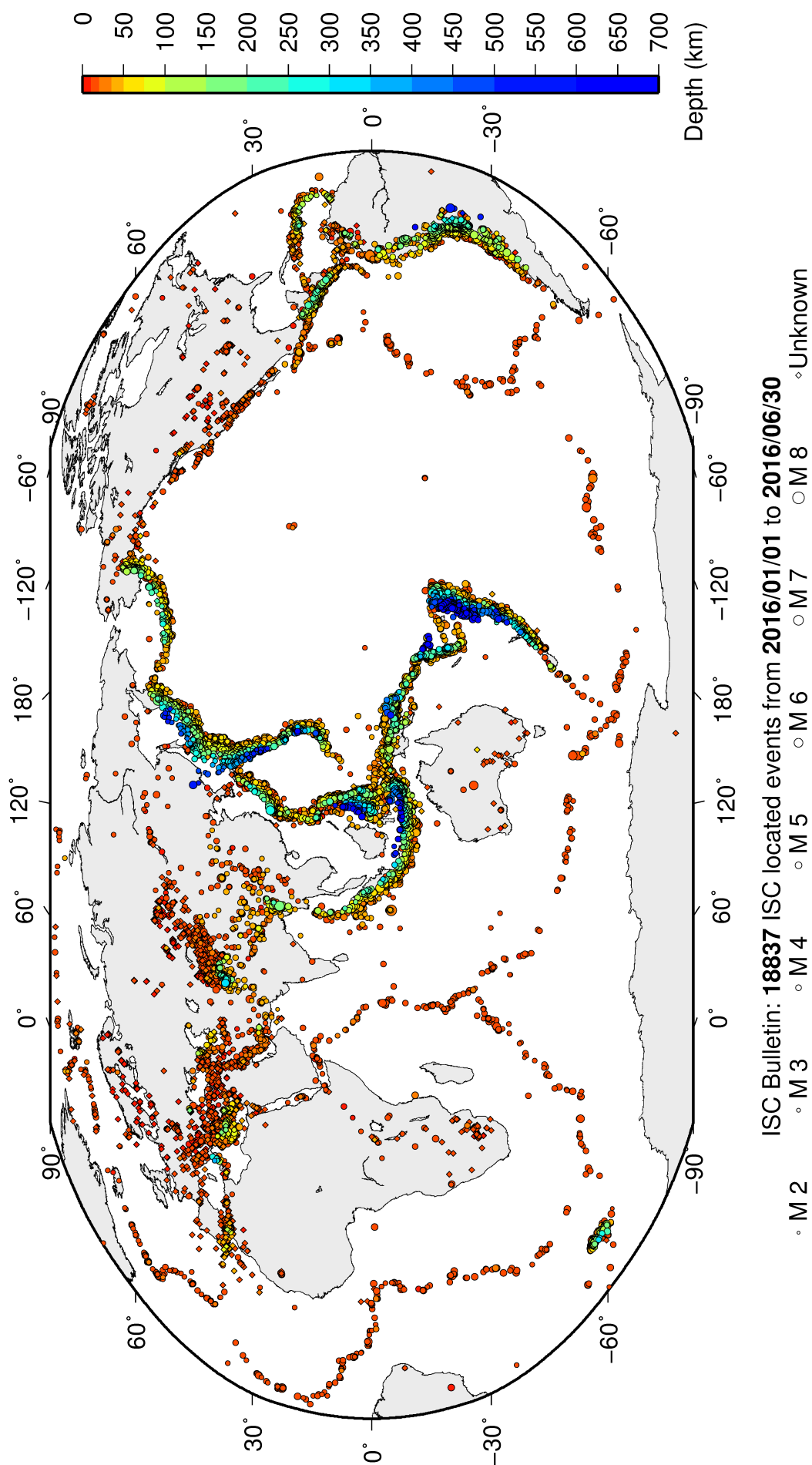


Figure 9.4: Map of all events located by the ISC for this time period. ISC determined hypocentre locations are shown.

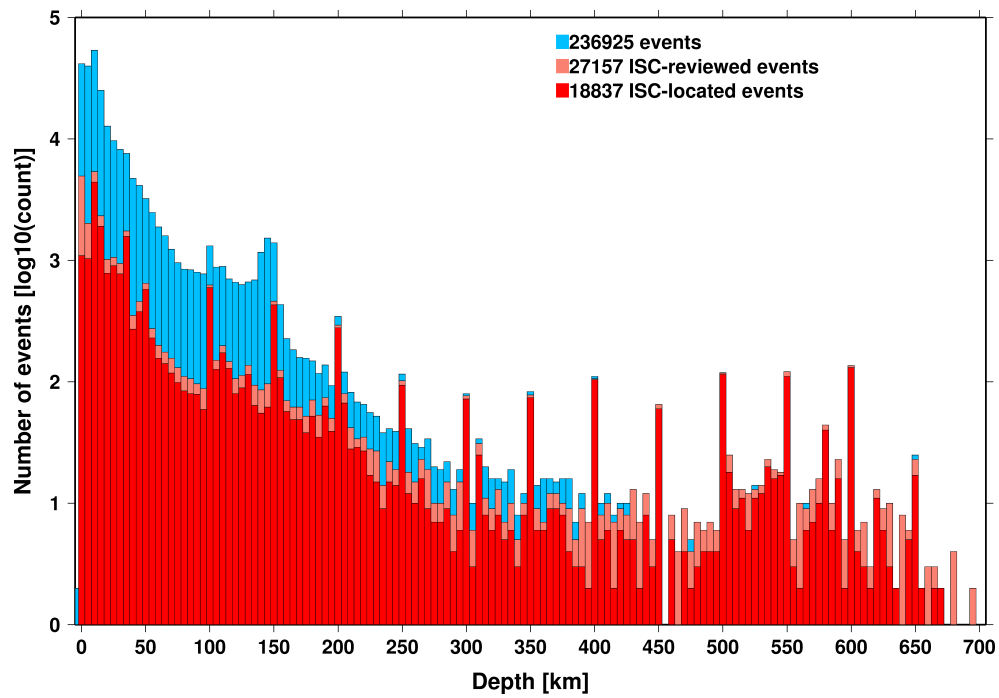


Figure 9.5: Distribution of event depths in the ISC Bulletin (blue) and for the ISC-reviewed (pink) and the ISC-located (red) events during the summary period. All ISC-located events are reviewed, but not all reviewed events are located by the ISC. The vertical scale is logarithmic.

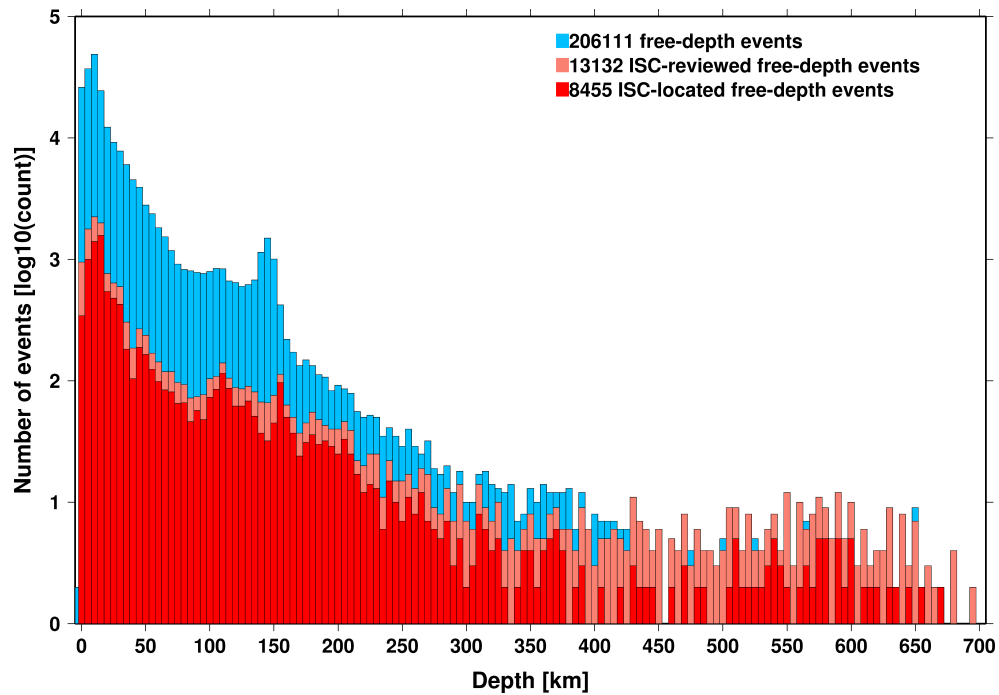


Figure 9.6: Hypocentral depth distribution of events where the prime hypocentres are reported/located with a free-depth solution in the ISC Bulletin. The vertical scale is logarithmic.

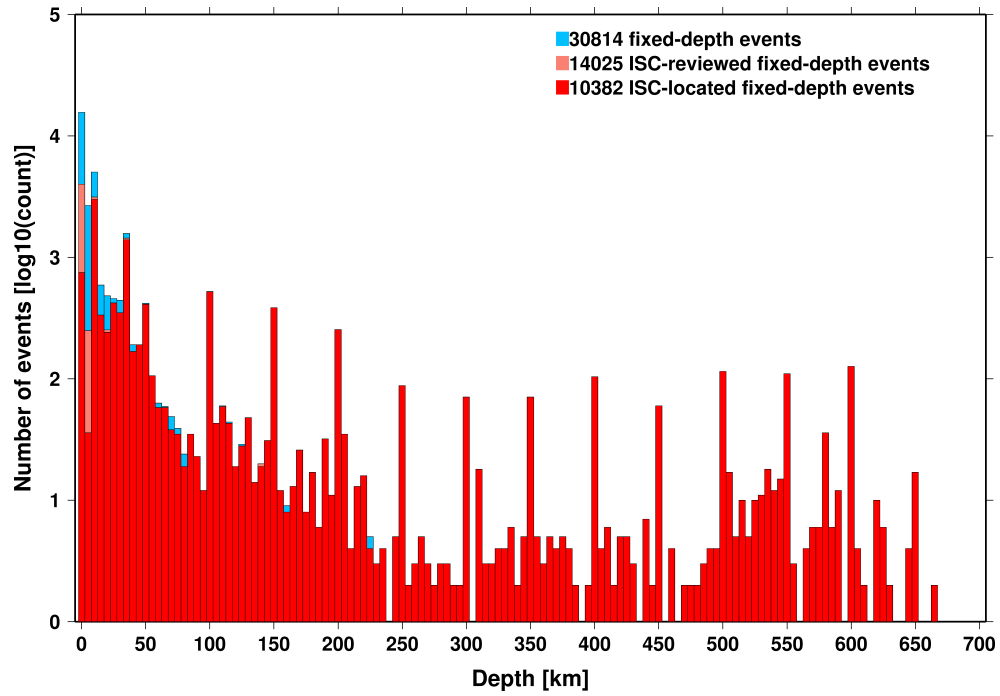


Figure 9.7: Hypocentral depth distribution of events where the prime hypocentres are reported/located with a fixed-depth solution in the ISC Bulletin. The vertical scale is logarithmic.

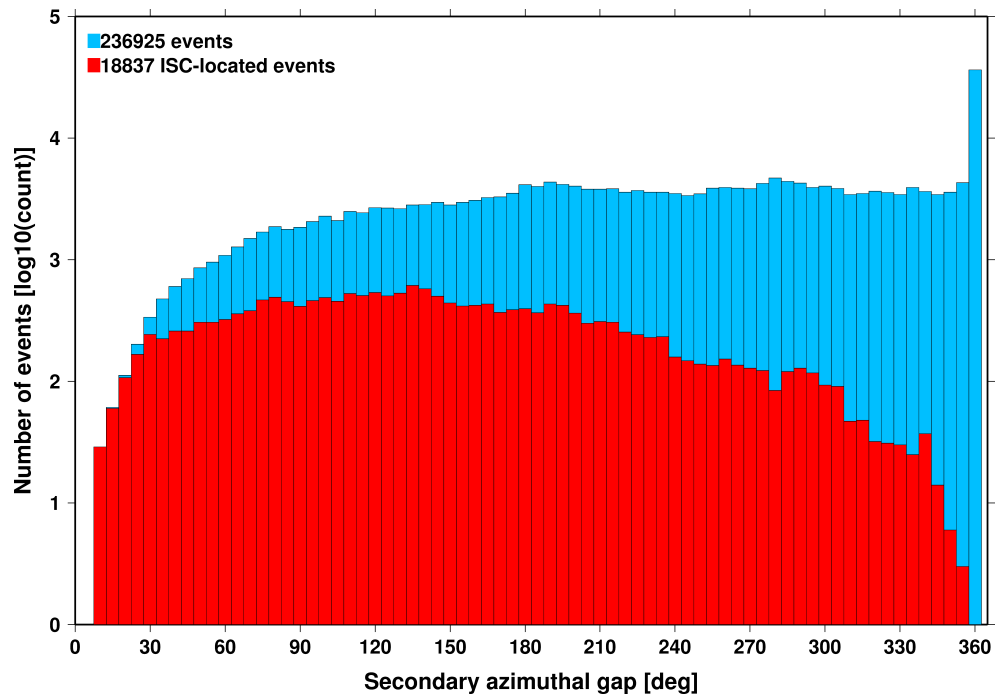


Figure 9.8: Distribution of secondary azimuthal gap for events in the ISC Bulletin (blue) and those selected for ISC location (red). The vertical scale is logarithmic.

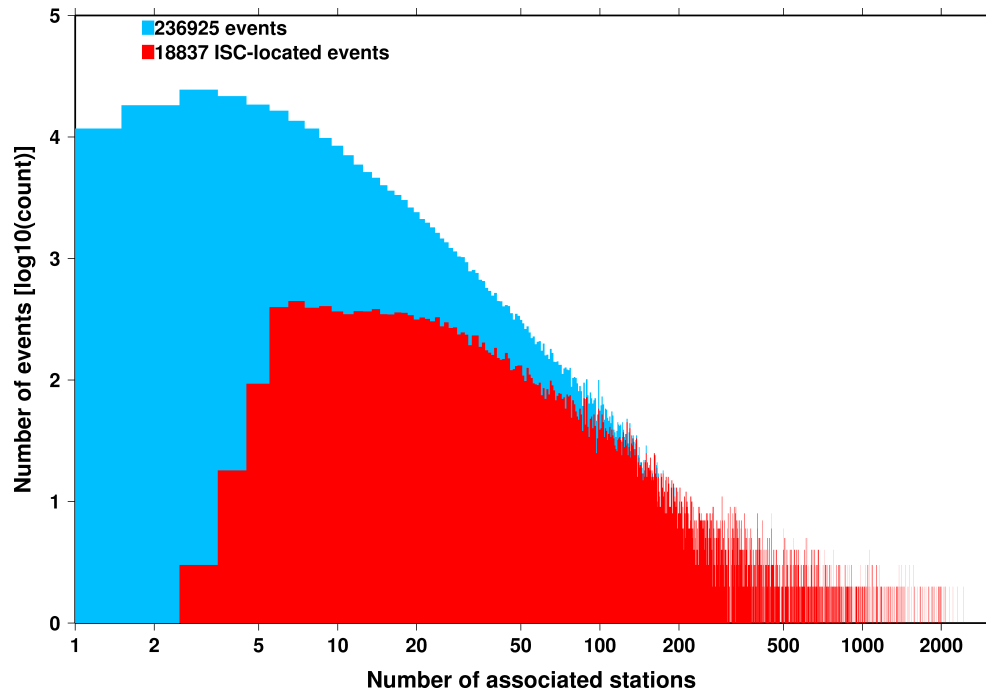


Figure 9.9: Distribution of the number of associated stations for events in the ISC Bulletin (blue) and those selected for ISC location (red). The vertical scale is logarithmic.

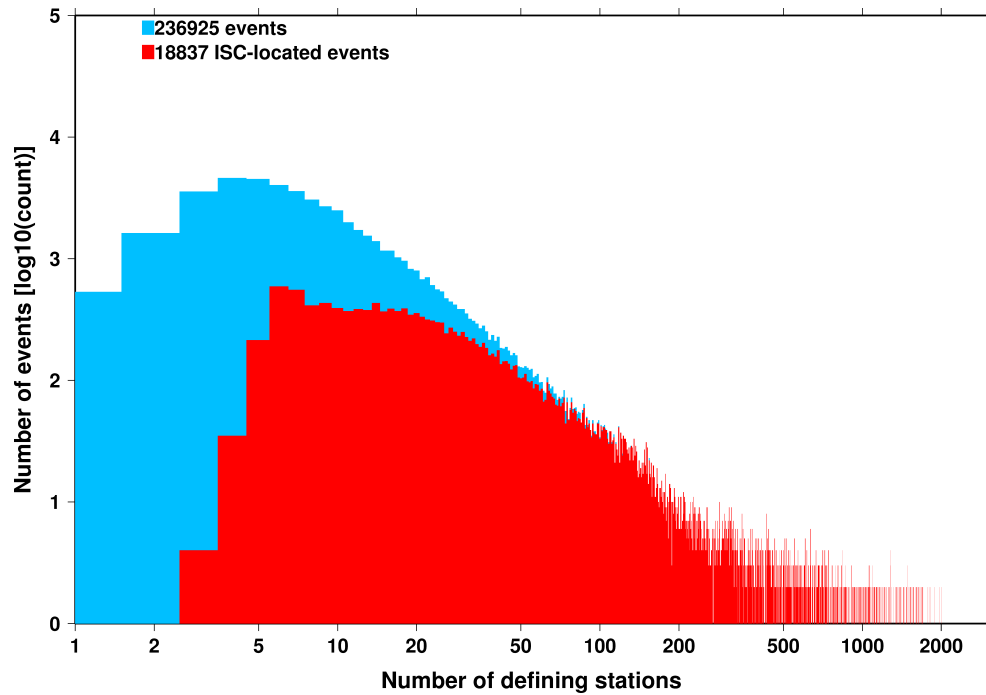


Figure 9.10: Distribution of the number of defining stations for events in the ISC Bulletin (blue) and those selected for ISC location (red). The vertical scale is logarithmic.

of the events have an error ellipse area less than 1169 km^2 , and 95% of the events have an error ellipse area less than 2006 km^2 .

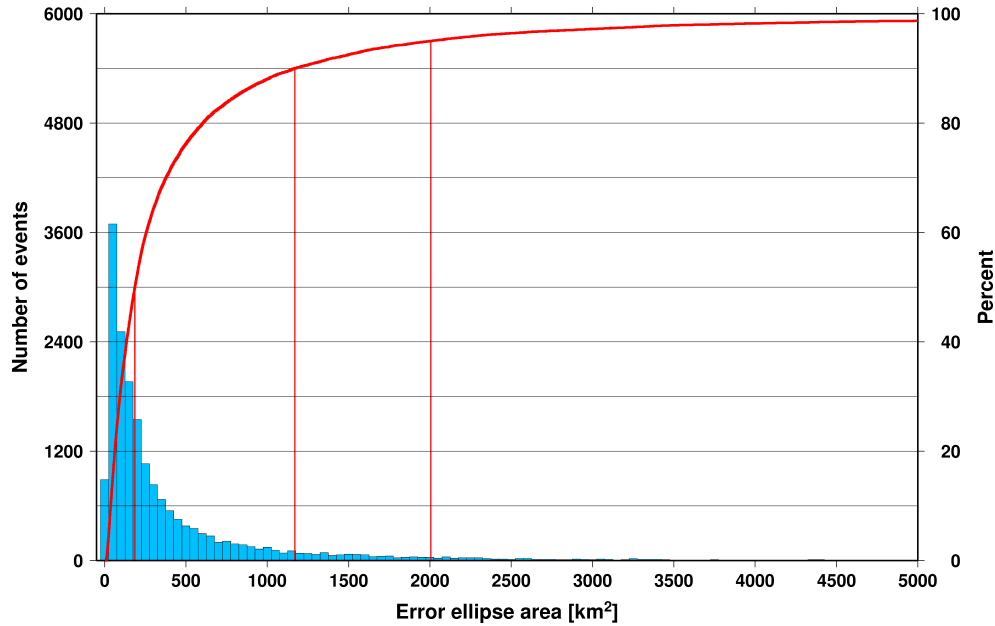


Figure 9.11: Distribution of the area of the 90% confidence error ellipse of the ISC-located events. Vertical red lines indicate the 50th, 90th and 95th percentile values.

Figure 9.12 shows one of the major characteristic features of the ISC location algorithm (Bondár and Storchak, 2011). Because the ISC locator accounts for correlated travel-time prediction errors due to unmodelled velocity heterogeneities along similar ray paths, the area of the 90% confidence error ellipse does not decrease indefinitely with increasing number of stations, but levels off once the information carried by the network geometry is exhausted, thus providing more realistic uncertainty estimates.

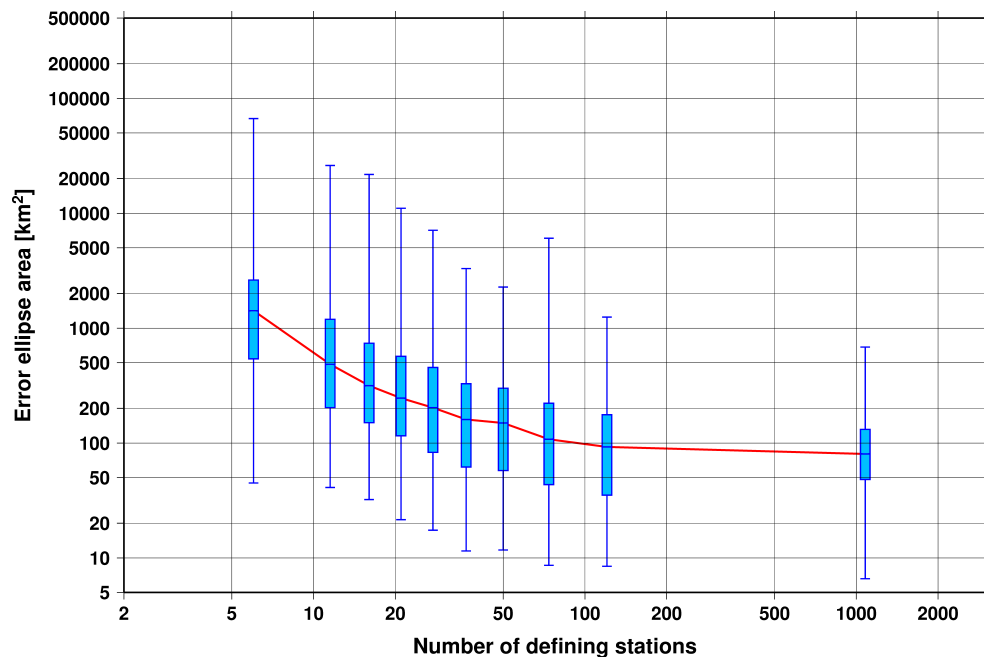


Figure 9.12: Box-and-whisker plot of the area of the 90% confidence error ellipse of the ISC-located events as a function of the number of defining stations. Each box represents one-tenth-worth of the total number of data. The red line indicates the median 90% confidence error ellipse area.

9.2 Seismic Phases and Travel-Time Residuals

The number of phases that are associated to events over the summary period in the ISC Bulletin is shown in Figure 9.13. Phase types and their total number in the ISC Bulletin is shown in the Appendix, Table 11.3. A summary of phase types is indicated in Figure 9.14.

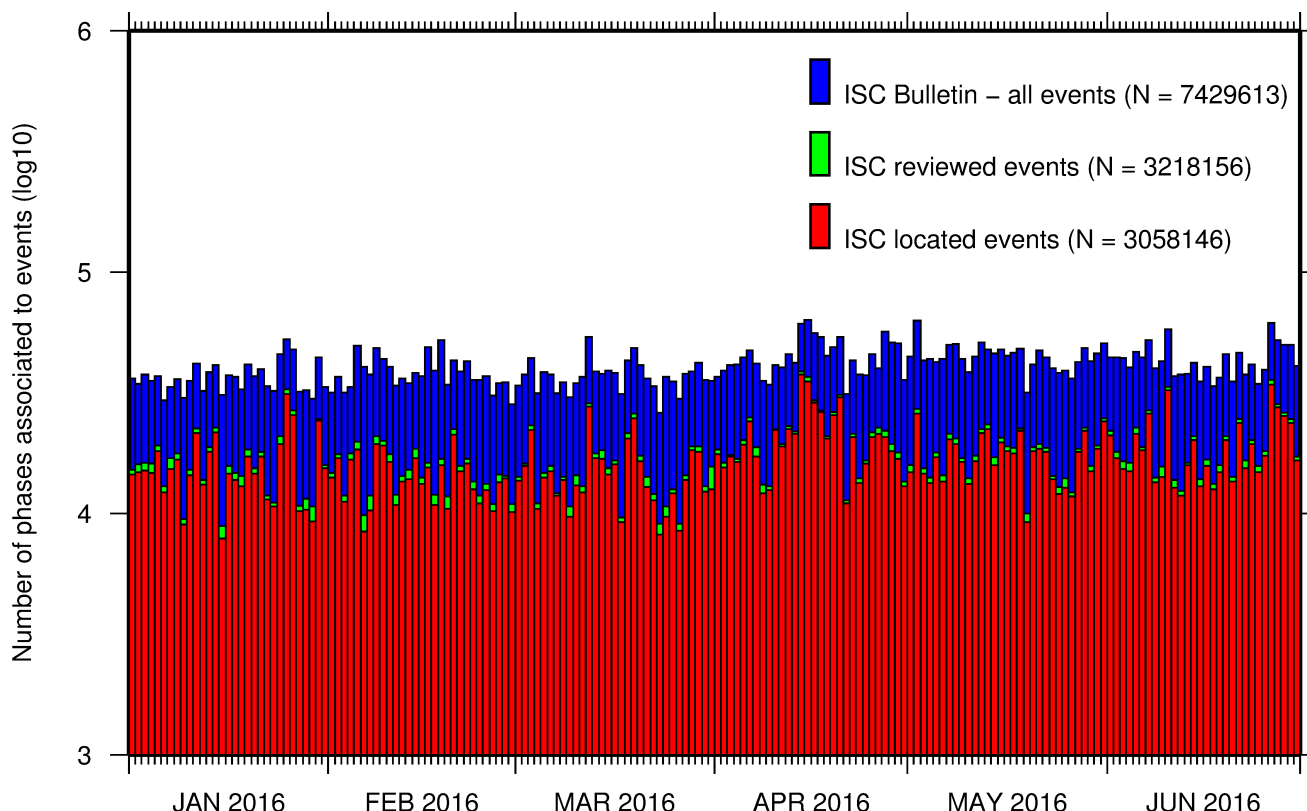


Figure 9.13: Histogram showing the number of phases (N) that the ISC has associated to events within the ISC Bulletin for the current summary period.

In computing ISC locations, the current (for events since 2009) ISC location algorithm (*Bondár and Storchak, 2011*) uses all *ak135* phases where possible. Within the Bulletin, the phases that contribute to an ISC location are labelled as *time defining*. In this section, we summarise these time defining phases.

In Figure 9.15, the number of defining phases is shown in a histogram over the summary period. Each defining phase is listed in Table 9.1, which also provides a summary of the number of defining phases per event. A pie chart showing the proportion of defining phases is shown in Figure 9.16. Figure 9.17 shows travel times of seismic waves. The distribution of residuals for these defining phases is shown for the top five phases in Figures 9.18 through 9.22.

Table 9.1: Numbers of ‘time defining’ phases (N) within the ISC Bulletin for 18837 ISC located events.

Phase	Number of ‘defining’ phases	Number of events	Max per event	Median per event
P	929024	13611	2232	14
Pn	569239	17461	553	17
Sn	166783	14810	213	6
Pb	84800	8045	115	5
Pg	63958	6347	147	5
PKPdf	59268	4099	718	2
S	55191	3287	708	3
Sg	53245	6049	107	4

Table 9.1: (continued)

Phase	Number of 'defining' phases	Number of events	Max per event	Median per event
Sb	53228	7424	86	4
PKiKP	32295	3146	535	2
PKPbc	24659	3308	229	2
PKPab	15244	2483	290	2
PcP	12008	3517	68	2
Pdif	10664	972	784	2
pP	9158	1295	309	3
PP	8114	1130	133	2
SS	4035	939	42	2
ScP	4019	1173	112	2
sP	3747	898	110	2
SKSac	2860	378	143	2
PKKPbc	1973	440	59	2
pwP	1588	493	34	2
SKPbc	1055	307	54	2
ScS	1029	323	25	2
SnSn	982	481	12	1
PnPn	948	470	23	1
pPKPdf	846	335	24	1
sS	755	336	27	1
SKiKP	743	313	34	1
P'P'df	646	148	44	2
PKKPab	474	200	53	1
PS	469	173	14	2
pPKPab	455	159	26	1
pPKPbc	447	203	28	1
PKKPdf	417	231	18	1
SKPab	303	149	16	1
SKSdf	282	186	12	1
sPKPdf	258	170	10	1
SKKSac	226	130	11	1
PcS	226	161	5	1
PnS	193	128	5	1
SKPdf	160	79	15	1
SKKPbc	156	34	16	2
PKSdf	146	79	9	1
sPKPbc	136	98	7	1
sPKPab	104	58	17	1
Sdif	101	61	13	1
SP	81	46	8	1
pS	80	66	5	1
SKKSdf	60	51	4	1
pPdif	51	25	22	1
P'P'bc	42	15	12	1
SKKPab	33	10	13	1
PbPb	31	24	4	1
sPdif	27	9	13	1
SPn	24	19	3	1
pPKiKP	22	21	2	1
sPKiKP	17	13	4	1
SbSb	11	11	1	1
PKSab	7	7	1	1
S'S'ac	7	7	1	1
PKSbc	6	5	2	1
SKKPdf	6	6	1	1
P'P'ab	5	3	2	2
sPn	5	5	1	1
sSKSac	4	3	2	1
PgS	2	2	1	1
pPn	2	1	2	2
PgPg	2	2	1	1
pSKSac	2	2	1	1
sSdif	1	1	1	1

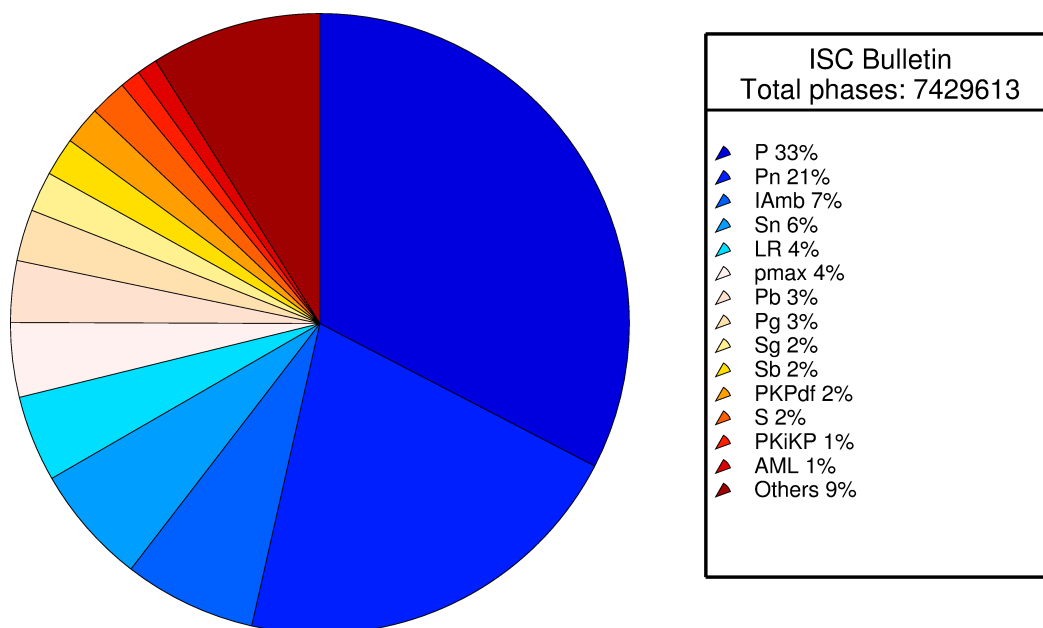


Figure 9.14: Pie chart showing the fraction of various phase types in the ISC Bulletin for this summary period.

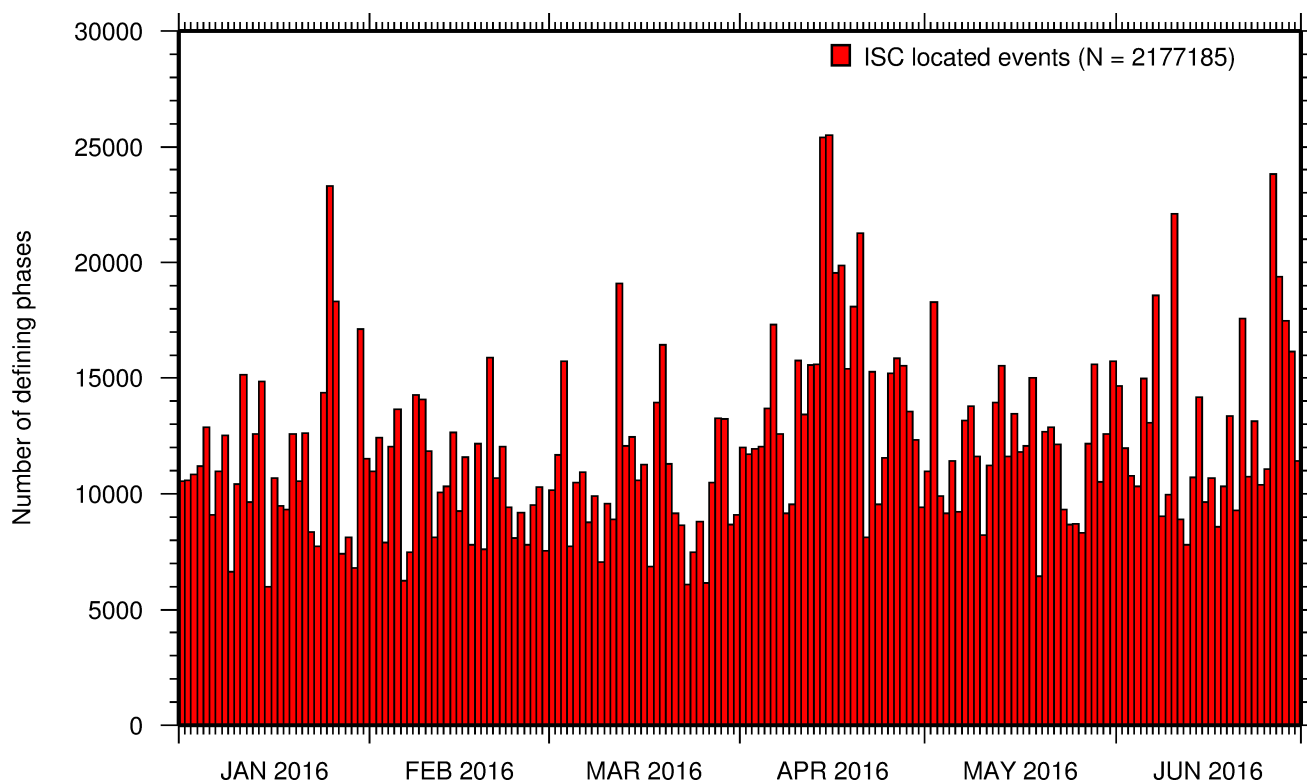


Figure 9.15: Histogram showing the number of defining phases in the ISC Bulletin, for events located by the ISC.

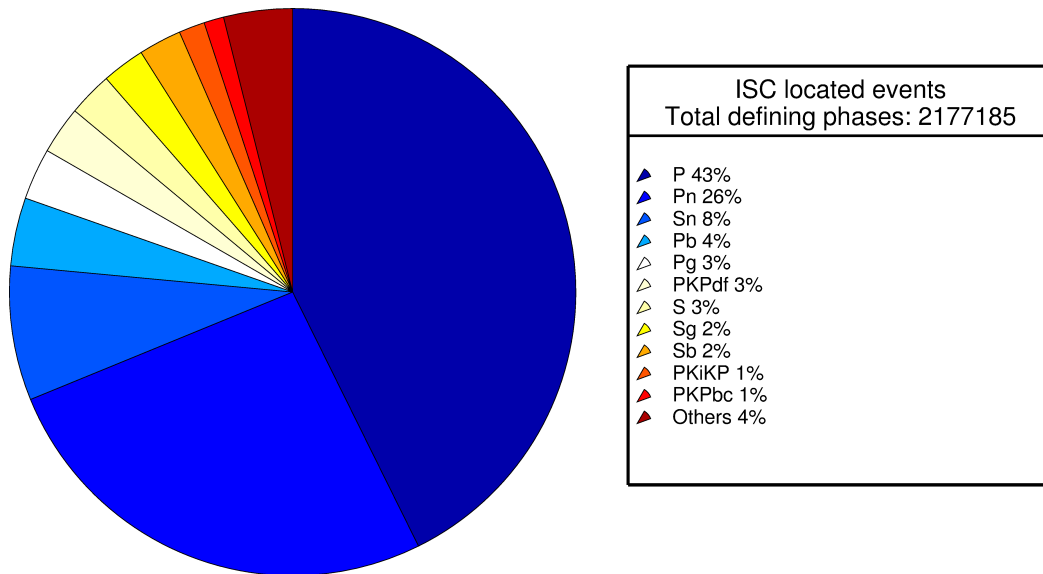


Figure 9.16: Pie chart showing the defining phases in the ISC Bulletin, for events located by the ISC. A complete list of defining phases is shown in Table 9.1.

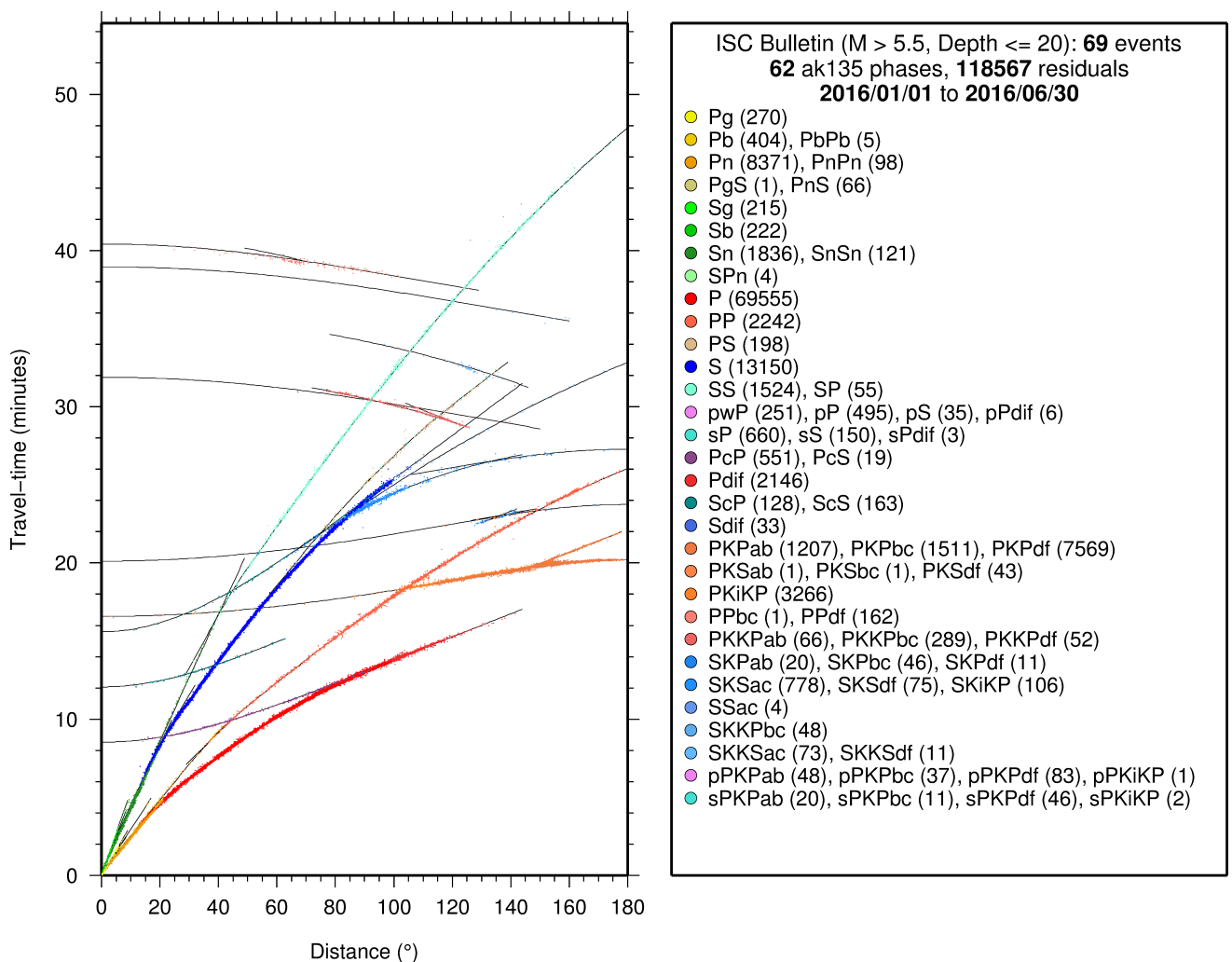


Figure 9.17: Distribution of travel-time observations in the ISC Bulletin for events with $M > 5.5$ and depth less than 20 km. The travel-time observations are shown relative to a 0 km source and compared with the theoretical ak135 travel-time curves (solid lines). The legend lists the number of each phase plotted.

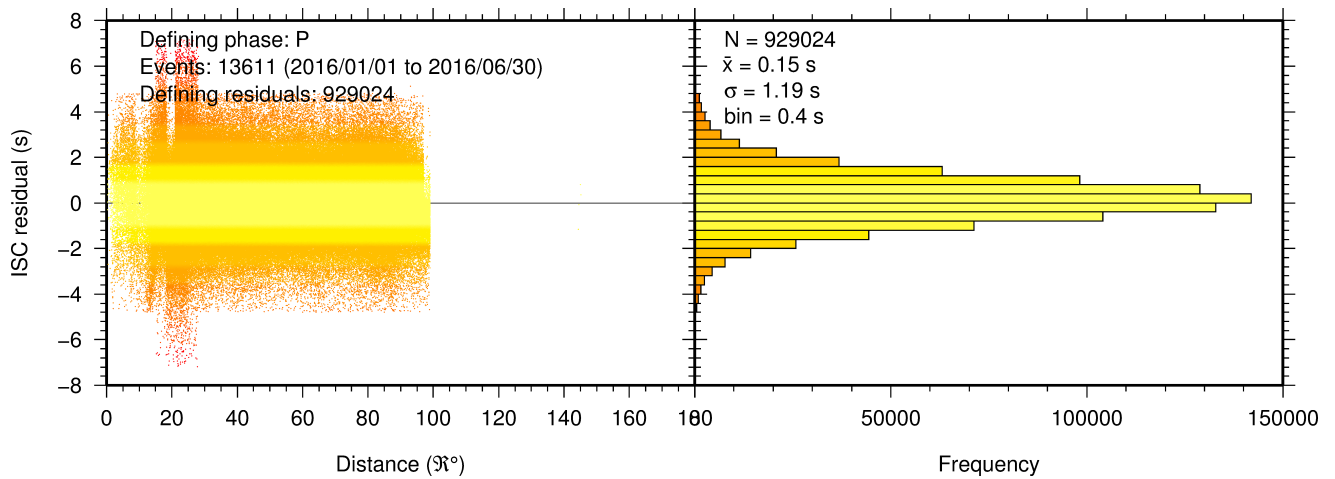


Figure 9.18: Distribution of travel-time residuals for the defining P phases used in the computation of ISC located events in the Bulletin.

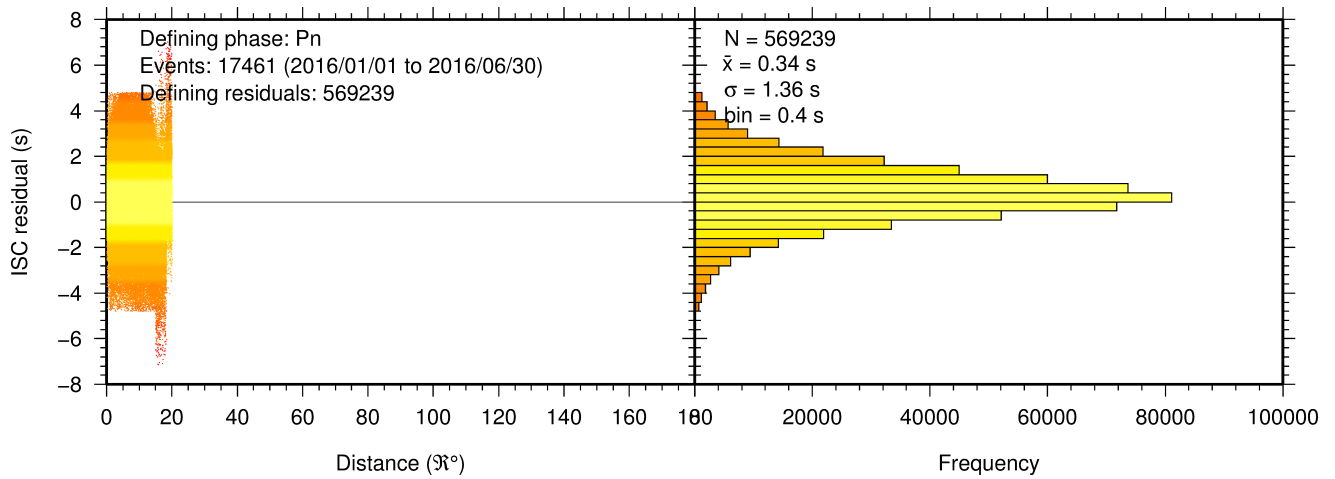


Figure 9.19: Distribution of travel-time residuals for the defining Pn phases used in the computation of ISC located events in the Bulletin.

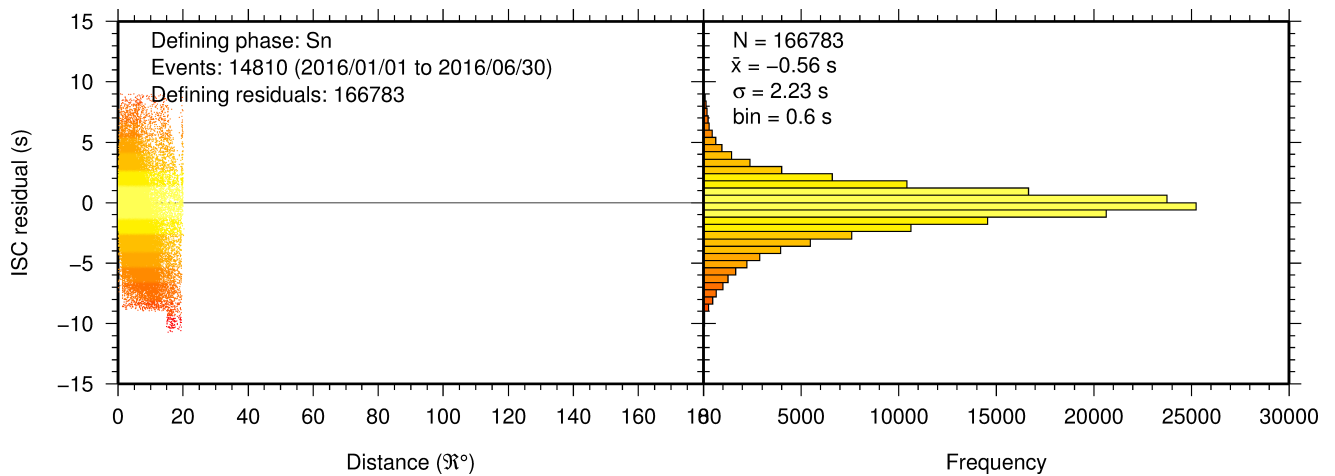


Figure 9.20: Distribution of travel-time residuals for the defining Sn phases used in the computation of ISC located events in the Bulletin.

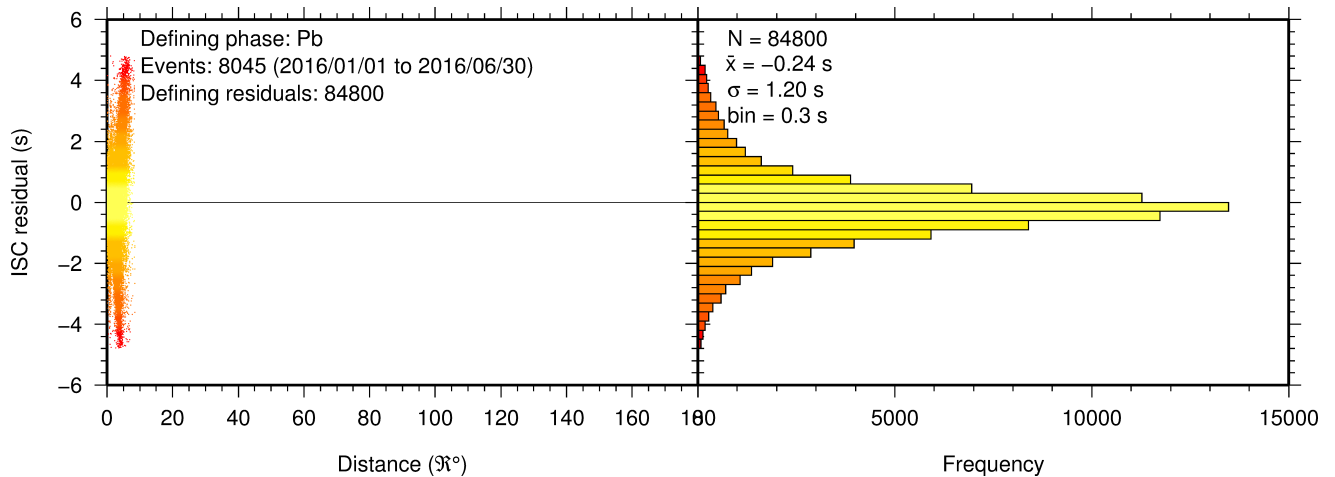


Figure 9.21: Distribution of travel-time residuals for the defining *Pb* phases used in the computation of ISC located events in the Bulletin.

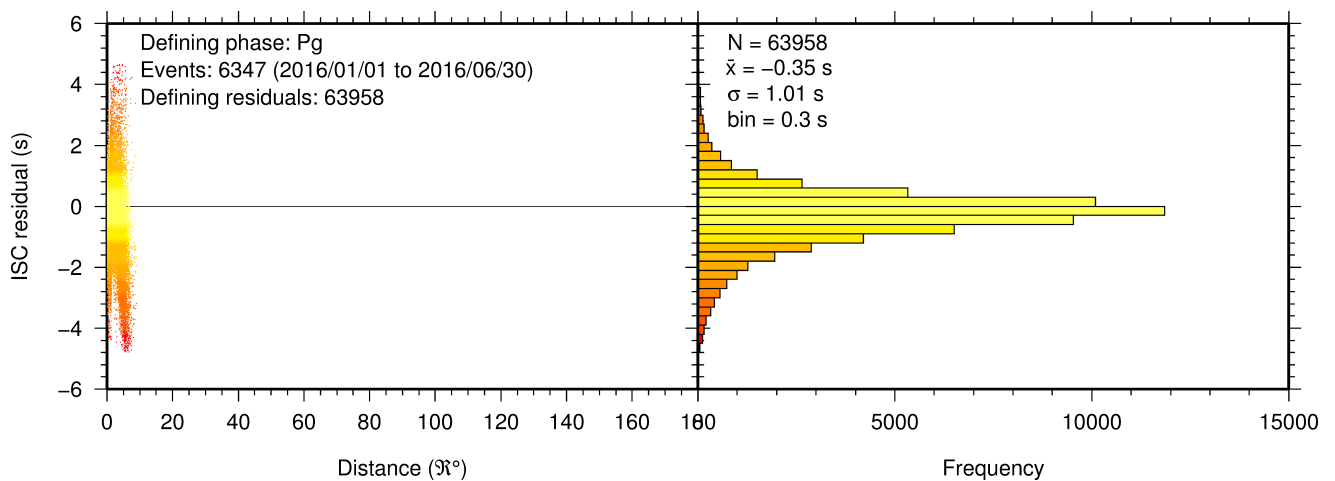


Figure 9.22: Distribution of travel-time residuals for the defining *Pg* phases used in the computation of ISC located events in the Bulletin.

9.3 Seismic Wave Amplitudes and Periods

The ISC Bulletin contains a variety of seismic wave amplitudes and periods measured by reporting agencies. For this Bulletin Summary, the total of collected amplitudes and periods is 2,638,209 (see Section 8.3). For the determination of the ISC magnitudes *MS* and *mb*, only a fraction of such data can be used. Indeed, the ISC network magnitudes are computed only for ISC located events. Here we recall the main features of the ISC procedure for *MS* and *mb* computation (see detailed description in Section 11.1.4). For each amplitude-period pair in a reading the ISC algorithm computes the magnitude (a reading can include several amplitude-period measurements) and the reading magnitude is assigned to the maximum A/T in the reading. If more than one reading magnitude is available for a station, the station magnitude is the median of the reading magnitudes. The network magnitude is computed then as the 20% alpha-trimmed median of the station magnitudes (at least three required). *MS* is computed for shallow earthquakes (depth ≤ 60 km) only and using amplitudes and periods on all three components (when available) if the period is within 10-60 s and the epicentral distance is between 20° and 160° . *mb* is computed also for deep earthquakes (depth down to 700 km) but only with amplitudes on the vertical

component measured at periods ≤ 3 s in the distance range 21° - 100° .

Table 9.2 is a summary of the amplitude and period data that contributed to the computation of station and ISC *MS* and *mb* network magnitudes for this Bulletin Summary.

Table 9.2: Summary of the amplitude-period data used by the ISC Locator to compute *MS* and *mb*.

	<i>MS</i>	<i>mb</i>
Number of amplitude-period data	140535	437266
Number of readings	121726	433193
Percentage of readings in the ISC located events with qualifying data for magnitude computation	15.0	43.3
Number of station magnitudes	116655	393007
Number of network magnitudes	3341	11907

A small percentage of the readings with qualifying data for *MS* and *mb* calculation have more than one amplitude-period pair. Notably, only 15% of the readings for the ISC located (shallow) events included qualifying data for *MS* computation, whereas for *mb* the percentage is much higher at 43%. This is due to the seismological practice of reporting agencies. Agencies contributing systematic reports of amplitude and period data are listed in Appendix Table 11.4. Obviously the ISC Bulletin would benefit if more agencies included surface wave amplitude-period data in their reports.

Figure 9.23 shows the distribution of the number of station magnitudes versus distance. For *mb* there is a significant increase in the distance range 70° - 90° , whereas for *MS* most of the contributing stations are below 100° . The increase in number of station magnitude between 70° - 90° for *mb* is partly due to the very dense distribution of seismic stations in North America and Europe with respect to earthquake occurring in various subduction zones around the Pacific Ocean.

Finally, Figure 9.24 shows the distribution of network *MS* and *mb* as well as the median number of stations for magnitude bins of 0.2. Clearly with increasing magnitude the number of events is smaller but with a general tendency of having more stations contributing to the network magnitude.

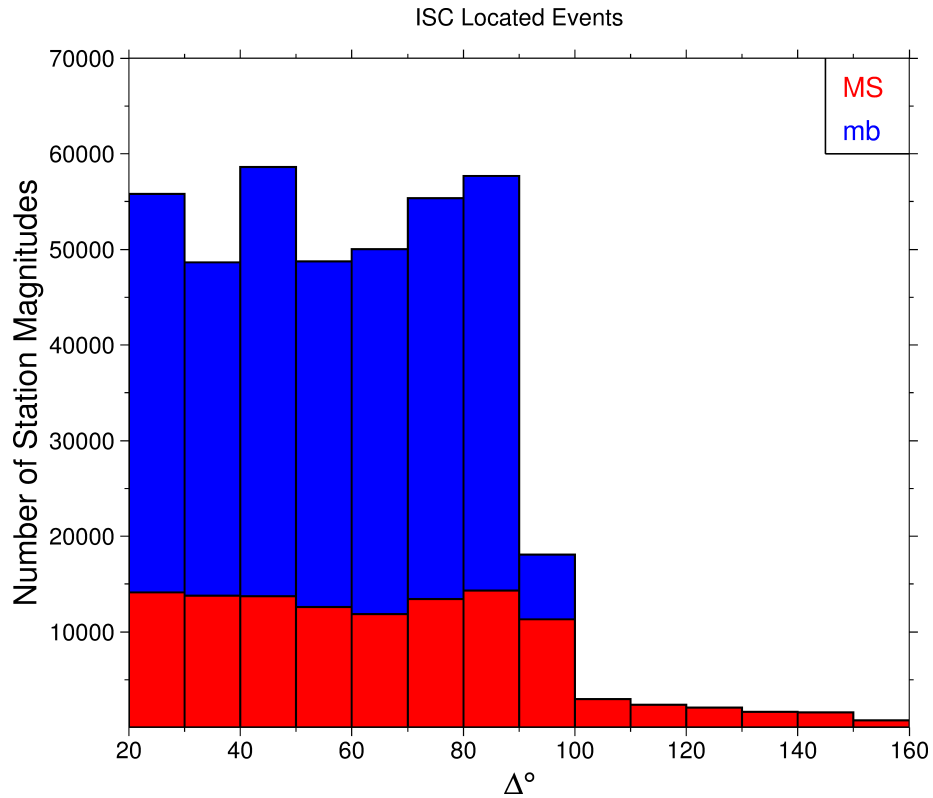


Figure 9.23: Distribution of the number of station magnitudes computed by the ISC Locator for mb (blue) and MS (red) versus distance.

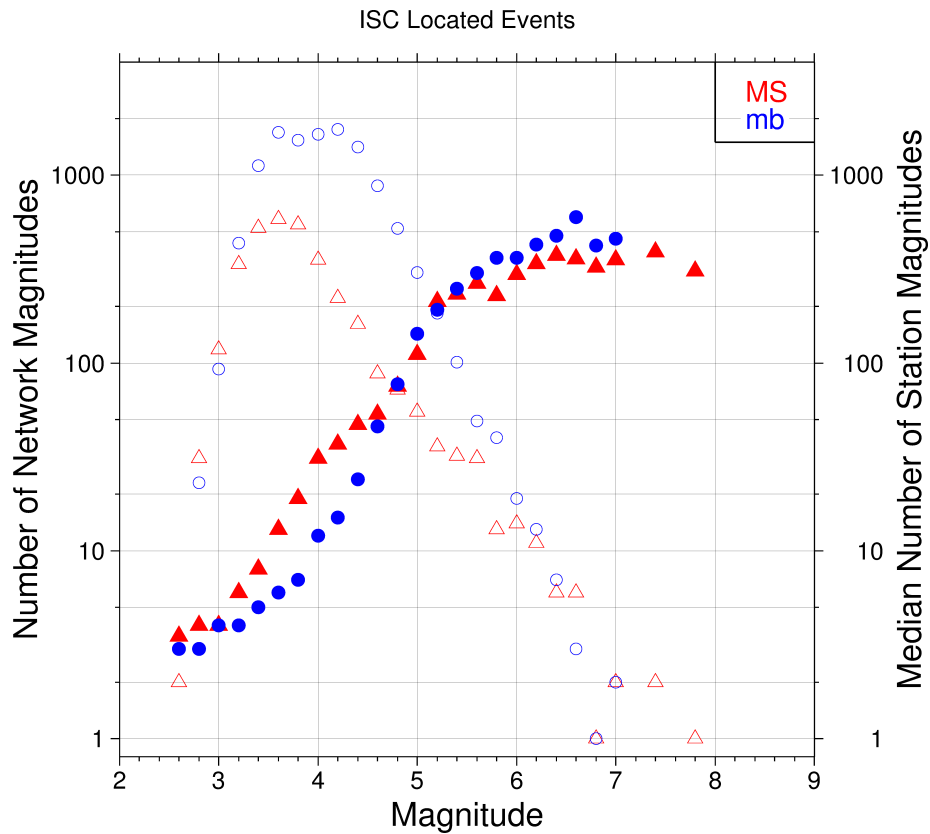


Figure 9.24: Number of network magnitudes (open symbols) and median number of stations magnitudes (filled symbols). Blue circles refer to mb and red triangles to MS. The width of the magnitude interval δM is 0.2, and each symbol includes data with magnitude in $M \pm \delta M/2$.

9.4 Completeness of the ISC Bulletin

The completeness of the ISC Bulletin can be expressed as a magnitude value, above which we expect the Bulletin to contain 100% of events. This magnitude of completeness, M_C can be measured as the point where the seismicity no longer follows the Gutenberg-Richter relationship. We compute an estimate of M_C using the maximum curvature technique of *Woessner and Wiemer (2005)*.

The completeness of the ISC Bulletin for this summary period is shown in Figure 9.25. A history of completeness for the ISC Bulletin is shown in Figure 9.26. The step change in 1996 corresponds with the inclusion of the Prototype IDC (EIDC) Bulletin, followed by the Reviewed Event Bulletin (REB) of the IDC.

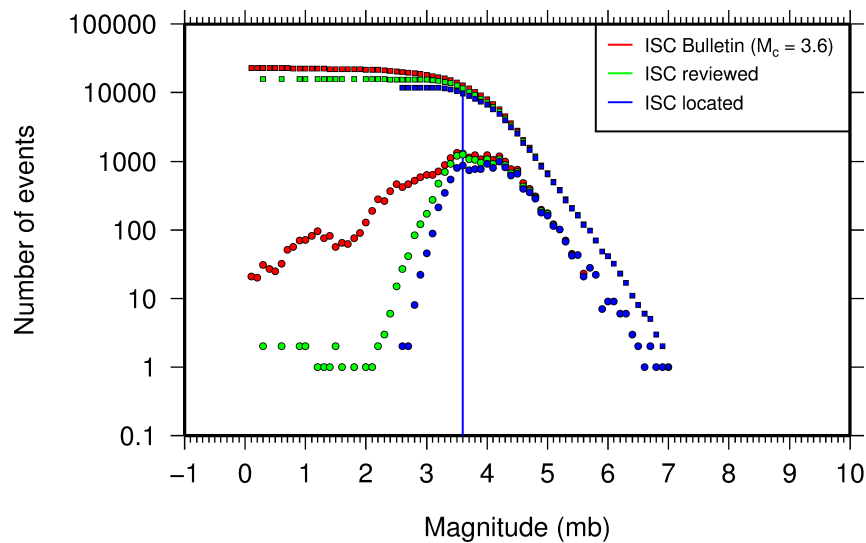


Figure 9.25: Frequency and cumulative frequency magnitude distribution for all events in the ISC Bulletin, ISC reviewed events and events located by the ISC. The magnitude of completeness (M_C) is shown for the ISC Bulletin. Note: only events with values of mb are represented in the figure.

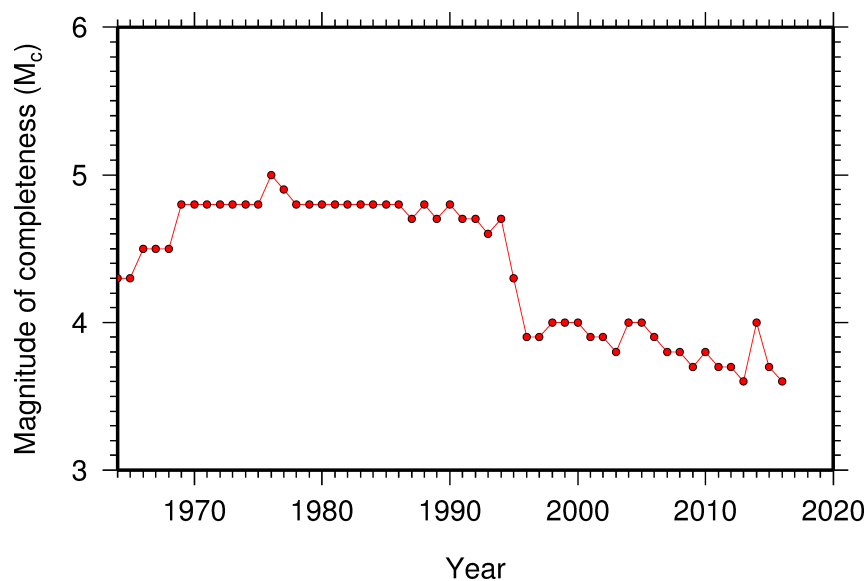


Figure 9.26: Variation of magnitude of completeness (M_C) for each year in the ISC Bulletin. Note: M_C is calculated only using those events with values of mb.

9.5 Magnitude Comparisons

The ISC Bulletin publishes network magnitudes reported by multiple agencies to the ISC. For events that have been located by the ISC, where enough amplitude data has been collected, the MS and mb magnitudes are calculated by the ISC (MS is computed only for depths ≤ 60 km). In this section, ISC magnitudes and some other reported magnitudes in the ISC Bulletin are compared.

The comparison between MS and mb computed by the ISC locator for events in this summary period is shown in Figure 9.27, where the large number of data pairs allows a colour coding of the data density. The scatter in the data reflects the fundamental differences between these magnitude scales.

Similar plots are shown in Figure 9.28 and 9.29, respectively, for comparisons of ISC mb and ISC MS with M_W from the GCMT catalogue. Since M_W is not often available below magnitude 5, these distributions are mostly for larger, global events. Not surprisingly, the scatter between mb and M_W is larger than the scatter between MS and M_W . Also, the saturation effect of mb is clearly visible for earthquakes with $M_W > 6.5$. In contrast, MS scales well with $M_W > 6$, whereas for smaller magnitudes MS appears to be systematically smaller than M_W .

In Figure 9.30 ISC values of mb are compared with all reported values of mb , values of mb reported by NEIC and values of mb reported by IDC. Similarly in Figure 9.31, ISC values of MS are compared with all reported values of MS , values of MS reported by NEIC and values of MS reported by IDC. There is a large scatter between the ISC magnitudes and the mb and MS reported by all other agencies.

The scatter decreases both for mb and MS when ISC magnitudes are compared just with NEIC and IDC magnitudes. This is not surprising as the latter two agencies provide most of the amplitudes and periods used by the ISC locator to compute MS and mb . However, ISC mb appears to be smaller than NEIC mb for $mb < 4$ and larger than IDC mb for $mb > 4$. Since NEIC does not include IDC amplitudes, it seems these features originate from observations at the high-gain, low-noise sites reported by the IDC. For the MS comparisons between ISC and NEIC a similar but smaller effect is observed for $MS < 4.5$, whereas a good scaling is generally observed for the MS comparisons between ISC and IDC.

Figure 9.27: Comparison of ISC values of MS with mb for common event pairs.

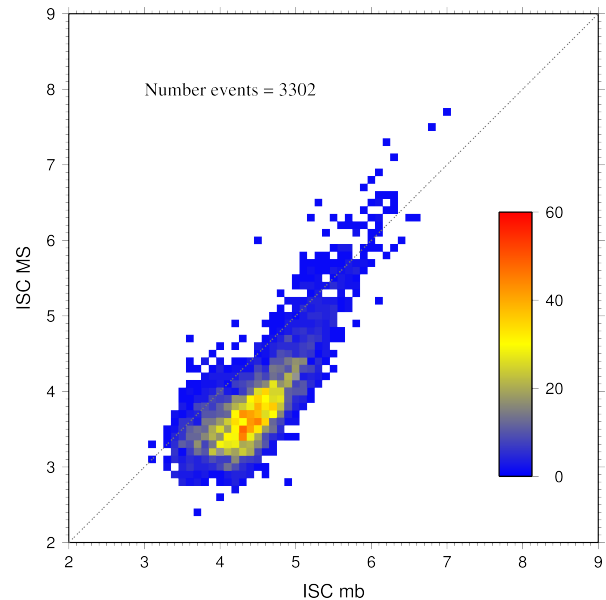


Figure 9.28: Comparison of ISC values of m_b with GCMT M_W for common event pairs.

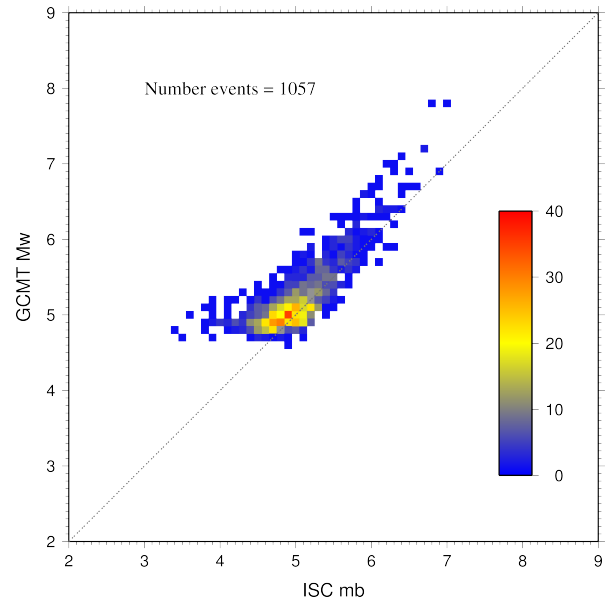
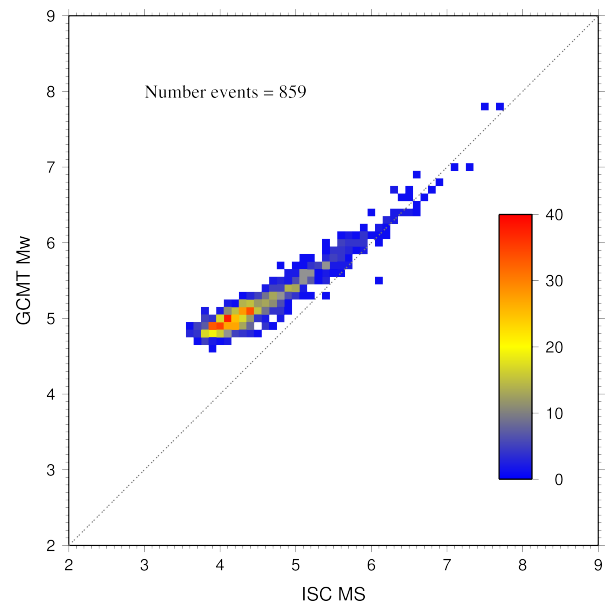


Figure 9.29: Comparison of ISC values of M_S with GCMT M_W for common event pairs.



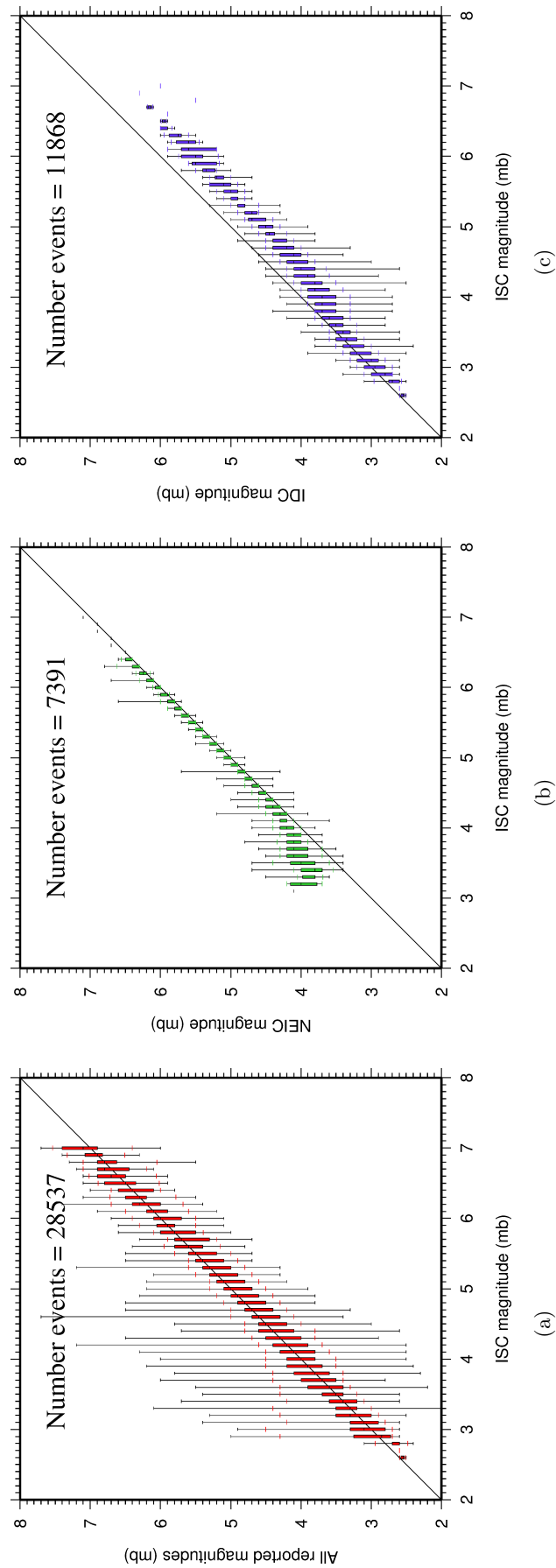


Figure 9.30: Comparison of ISC magnitude data (mb) with additional agency magnitudes (mb). The statistical summary is shown in box-and-whisker plots where the 10th and 90th percentiles are shown in addition to the max and min values. (a): All magnitudes reported; (b): NEIC magnitudes; (c): IDC magnitudes.

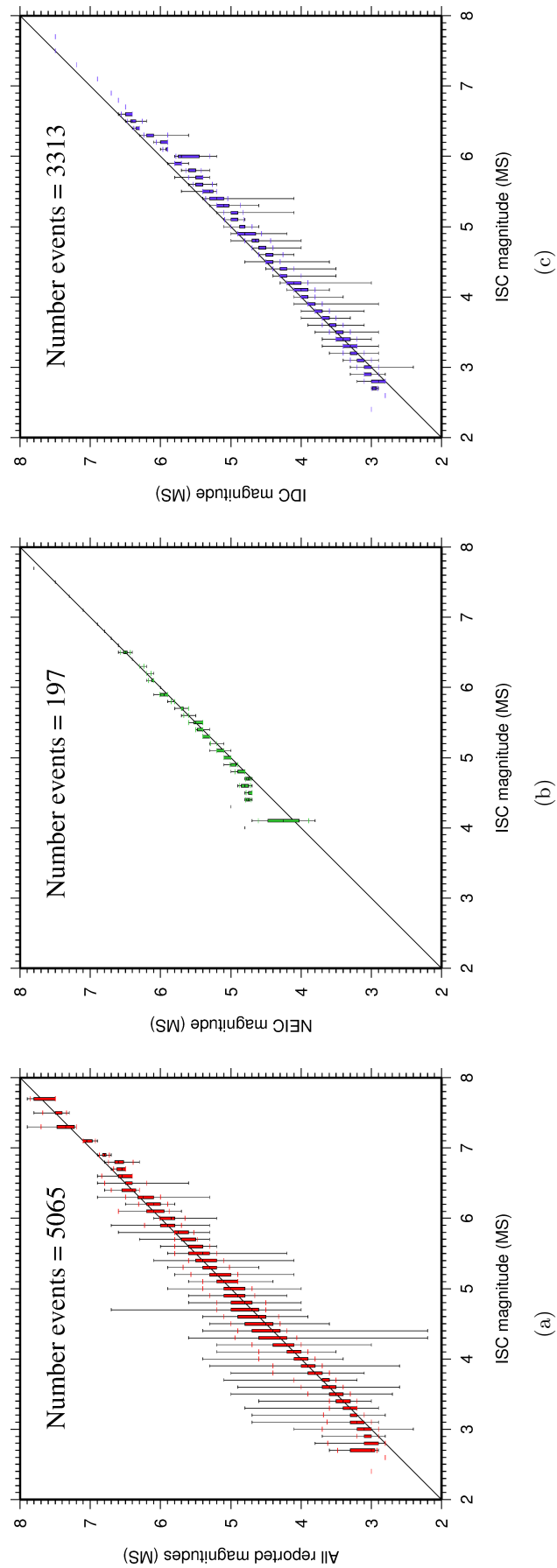


Figure 9.31: Comparison of ISC magnitude data (MS) with additional agency magnitudes (MS). The statistical summary is shown in the box-and-whisker plots where the 10th and 90th percentiles are shown in addition to the max and min values. (a): All magnitudes reported; (b): NEIC magnitudes; (c): IDC magnitudes.

10

The Leading Data Contributors

For the current six-month period, 149 agencies reported related bulletin data. Although we are grateful for every report, we nevertheless would like to acknowledge those agencies that made the most useful or distinct contributions to the contents of the ISC Bulletin. Here we note those agencies that:

- provided a comparatively large volume of parametric data (see Section 10.1),
- reported data that helped quite considerably to improve the quality of the ISC locations or magnitude determinations (see Section 10.2),
- helped the ISC by consistently reporting data in one of the standard recognised formats and in-line with the ISC data collection schedule (see Section 10.3).

We do not aim to discourage those numerous small networks who provide comparatively smaller yet still most essential volumes of regional data regularly, consistently and accurately. Without these reports the ISC Bulletin would not be as comprehensive and complete as it is today.

10.1 The Largest Data Contributors

We acknowledge the contribution of IDC, NEIC, BJI, MOS, DJA, GCMT, CLL and a few others (Figure 10.1) that reported the majority of moderate to large events recorded at teleseismic distances. The contributions of IDC, NEIC, MEX, JMA and several others are also acknowledged with respect to smaller seismic events. The contributions of JMA, TAP, NEIC, IDC, DDA, ATH, HEL and a number of others are also acknowledged with respect to small seismic events. Note that the NEIC bulletin accumulates a contribution of all regional networks in the USA. Several agencies monitoring highly seismic regions routinely report large volumes of small to moderate magnitude events, such as those in Japan, Chinese Taipei, Turkey, Italy, Greece, New Zealand, Mexico and Columbia. Contributions of small magnitude events by agencies in regions of low seismicity, such as Finland are also gratefully received.

We also would like to acknowledge contributions of those agencies that report a large portion of arrival time and amplitude data (Figure 10.2). For small magnitude events, these are local agencies in charge of monitoring local and regional seismicity. For moderate to large events, contributions of IDC, USArray, NEIC, MOS are especially acknowledged. Notably, three agencies (IDC, NEIC and MOS) together reported over 70% of all amplitude measurements made for teleseismically recorded events. We hope that other agencies would also be able to update their monitoring routines in the future to include the amplitude reports for teleseismic events compliant with the IASPEI standards.

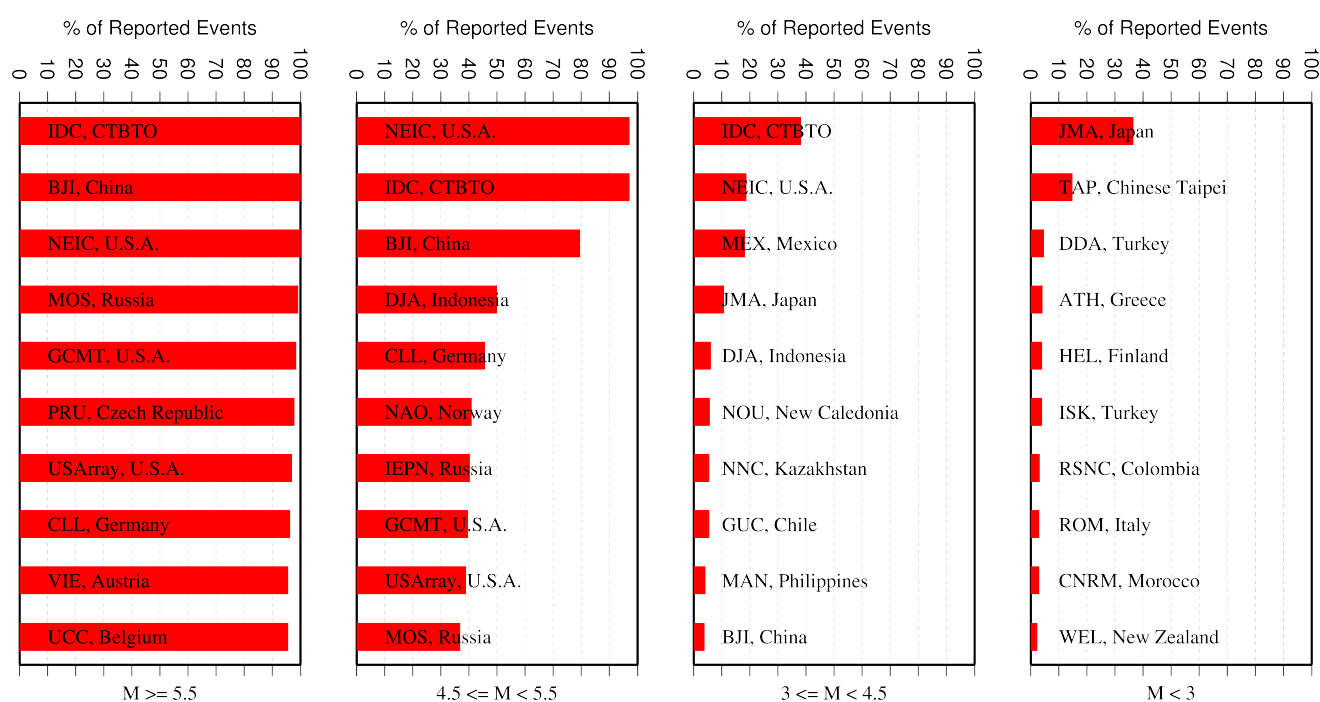


Figure 10.1: Frequency of events in the ISC Bulletin for which an agency reported at least one item of data: a moment tensor, a hypocentre, a station arrival time or an amplitude. The top ten agencies are shown for four magnitude intervals.

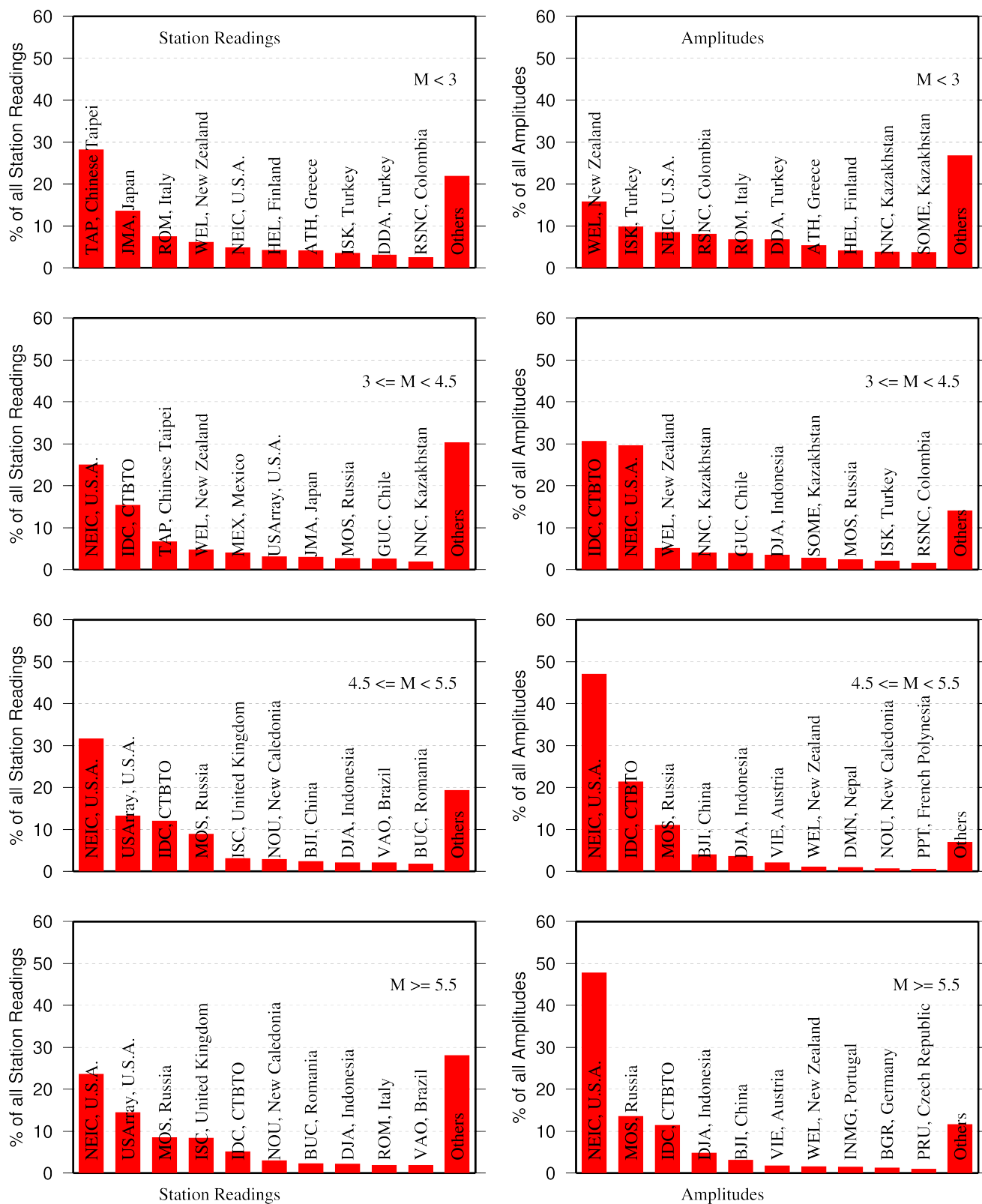


Figure 10.2: Contributions of station arrival time readings (left) and amplitudes (right) of agencies to the ISC Bulletin. Top ten agencies are shown for four magnitude intervals.

10.2 Contributors Reporting the Most Valuable Parameters

One of the main ISC duties is to re-calculate hypocentre estimates for those seismic events where a collective wealth of all station reports received from all agencies is likely to improve either the event location or depth compared to the hypocentre solution from each single agency. For areas with a sparse local seismic network or an unfavourable station configuration, readings made by other networks at teleseismic distances are very important. All events near mid-oceanic ridges as well as those in the majority of subduction zones around the world fall into this category. Hence we greatly appreciate the effort made by many agencies that report data for remote earthquakes (Figure 10.3). For some agencies, such as the IDC and the NEIC, it is part of their mission. For instance, the IDC reports almost every seismic event that is large enough to be recorded at teleseismic distance (20 degrees and beyond). This is largely because the International Monitoring System of primary arrays and broadband instruments is distributed at quiet sites around the world in order to be able to detect possible violations of the Comprehensive Nuclear-Test-Ban Treaty. The NEIC reported over 45% of those events as their mission requires them to report events above magnitude 4.5 outside the United States of America. For other agencies reporting distant events it is an extra effort that they undertake to notify their governments and relief agencies as well as to help the ISC and academic research in general. Hence these agencies usually report on the larger magnitude events. BJI, NAO, CLL, MOS, IEPN, NOU, PRU and AWI each reported individual station arrivals for several percent of all relevant events. We encourage other agencies to report distant events to us.

In addition to the first arriving phase we encourage reporters to contribute observations of secondary seismic phases that help constrain the event location and depth: S, Sn, Sg and pP, sP, PcP (Figure 10.4). We expect though that these observations are actually made from waveforms, rather than just predicted by standard velocity models and modern software programs. It is especially important that these arrivals are manually reviewed by an operator (as we know takes place at the IDC and NEIC), as opposed to some lesser attempts to provide automatic phase readings that are later rejected by the ISC due to a generally poor quality of unreviewed picking.

Another important long-term task that the ISC performs is to compute the most definitive values of

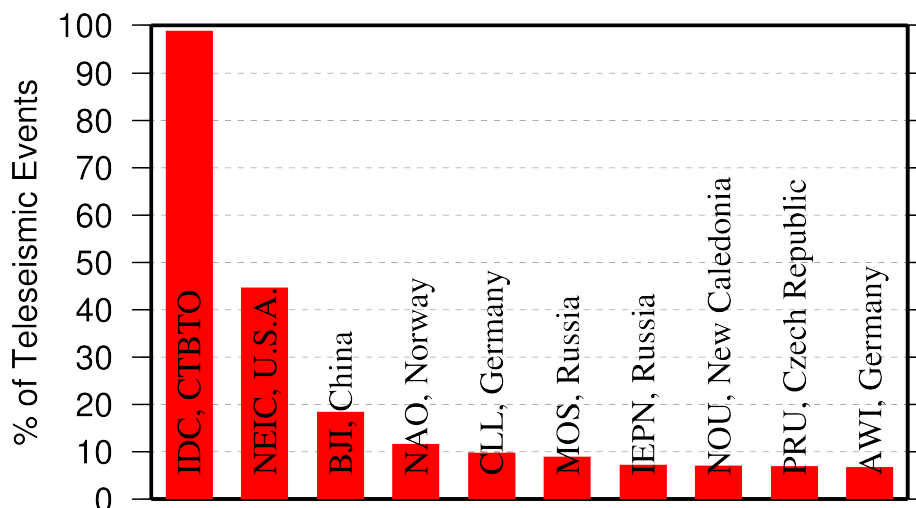


Figure 10.3: Top ten agencies that reported teleseismic phase arrivals for a large portion of ISC events.

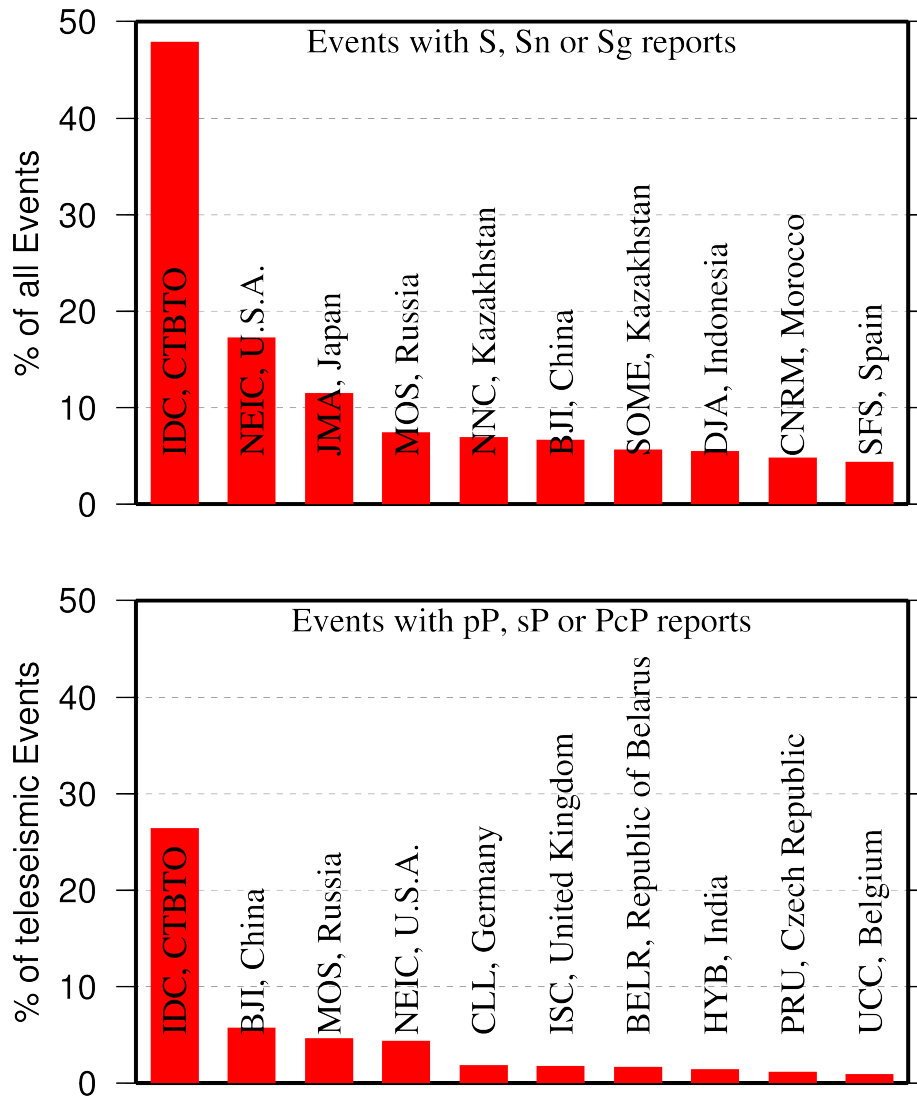


Figure 10.4: Top ten agencies that reported secondary phases important for an accurate epicentre location (top) and focal depth determination (bottom).

MS and mb network magnitudes that are considered reliable due to removal of outliers and consequent averaging (using alpha-trimmed median) across the largest network of stations, generally not feasible for a single agency. Despite concern over the bias at the lower end of mb introduced by the body wave amplitude data from the IDC, other agencies are also known to bias the results. This topic is further discussed in Section 9.5.

Notably, the IDC reports almost 100% of all events for which *MS* and *mb* are estimated. This is due to the standard routine that requires determination of body and surface wave magnitudes useful for discrimination purposes. NEIC, BJI, MOS, NAO, PPT and a few other agencies (Figure 10.5) are also responsible for the majority of the amplitude and period reports that contribute towards the ISC magnitudes.

Since the ISC does not routinely process waveforms, we rely on other agencies to report moment magnitudes as well as moment tensor determinations (Figure 10.6).

Among other event parameters the ISC Bulletin also contains information on event type. We cannot

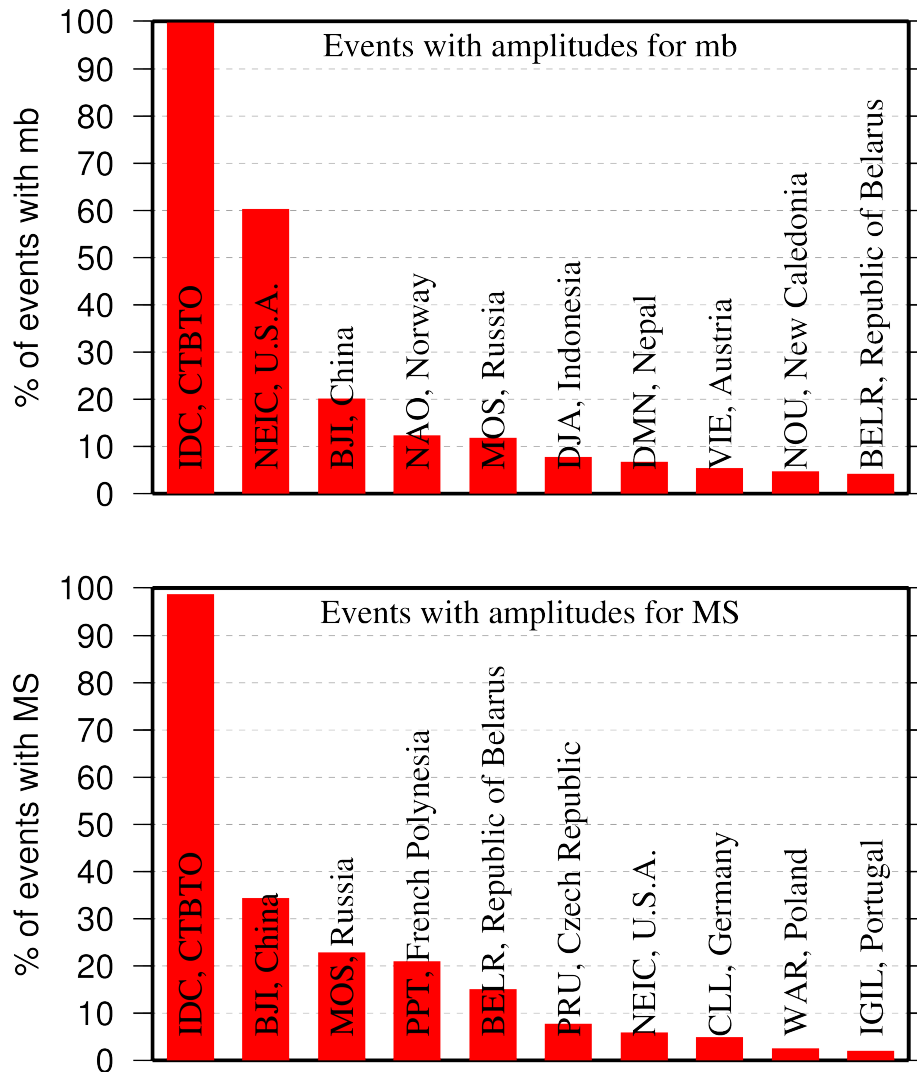


Figure 10.5: Agencies that report defining body (top) and surface (bottom) wave amplitudes and periods for the largest fraction of those ISC Bulletin events with MS/mb determinations.

independently verify the type of each event in the Bulletin and thus rely on other agencies to report the event type to us. Practices of reporting non-tectonic events vary greatly from country to country. Many agencies do not include anthropogenic events in their reports. Suppression of such events from reports to the ISC may lead to a situation where a neighbouring agency reports the anthropogenic event as an earthquake for which expected data are missing. This in turn is detrimental to ISC Bulletin users studying natural seismic hazard. Hence we encourage all agencies to join the agencies listed on Figure 10.7 and several others in reporting both natural and anthropogenic events to the ISC.

The ISC Bulletin also contains felt and damaging information when local agencies have reported it to us. Agencies listed on Figure 10.8 provide such information for the majority of all felt or damaging events in the ISC Bulletin.

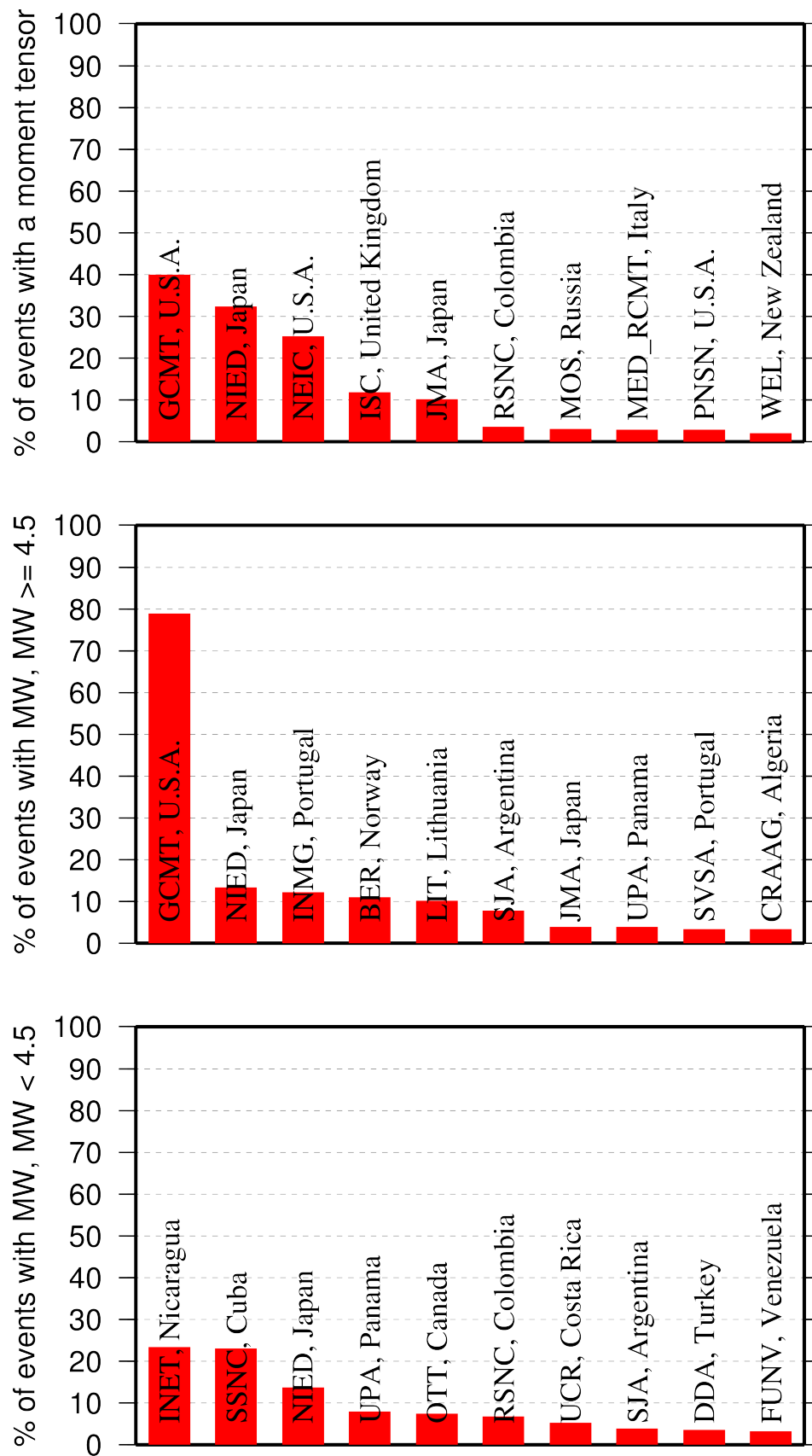


Figure 10.6: Top ten agencies that most frequently report determinations of seismic moment tensor (top) and moment magnitude (middle/bottom for M greater/smaller than 4.5).

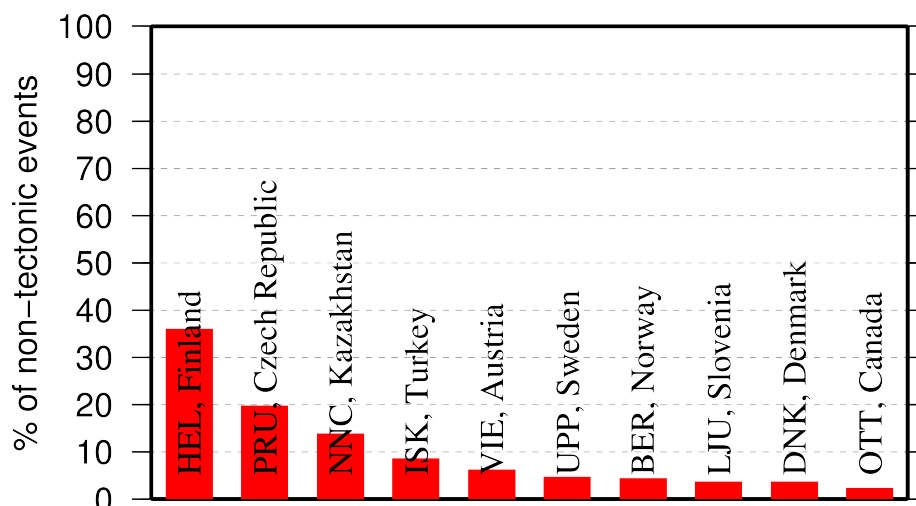


Figure 10.7: Top ten agencies that most frequently report non-tectonic seismic events to the ISC.

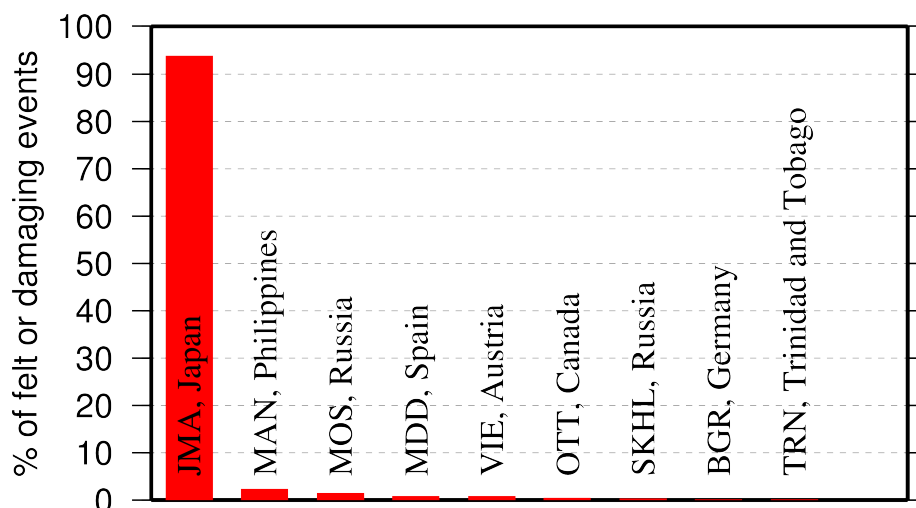


Figure 10.8: Top ten agencies that most frequently report macroseismic information to the ISC.

10.3 The Most Consistent and Punctual Contributors

During this six-month period, 43 agencies reported their bulletin data in one of the standard seismic formats (ISF, IMS, GSE, Nordic or QuakeML) and within the current 12-month deadline. Here we must reiterate that the ISC accepts reviewed bulletin data after a final analysis as soon as they are ready. These data, even if they arrive before the deadline, are immediately parsed into the ISC database, grouped with other data and become available to the ISC users on-line as part of the preliminary ISC Bulletin. There is no reason to wait until the deadline to send the data to the ISC. Table 10.1 lists all agencies that have been helpful to the ISC in this respect during the six-month period.

Table 10.1: Agencies that contributed reviewed bulletin data to the ISC in one of the standard international formats before the submission deadline.

Agency Code	Country	Average Delay from real time (days)
ZUR	Switzerland	13
PPT	French Polynesia	22
LIC	Ivory Coast	30
IGIL	Portugal	32
NAO	Norway	32
ATH	Greece	36
ECX	Mexico	38
NAM	Namibia	40
BUC	Romania	42
PRE	South Africa	43
ISN	Iraq	43
IDC	Austria	60
TIR	Albania	63
INMG	Portugal	67
SVSA	Portugal	74
ISK	Turkey	83
AUST	Australia	103
BEO	Serbia	117
BJI	China	127
VIE	Austria	133
KRSC	Russia	144
INET	Nicaragua	173
THE	Greece	213
KNET	Kyrgyzstan	226
STR	France	233
NERS	Russia	245
BGS	United Kingdom	247
UCR	Costa Rica	247
DSN	United Arab Emirates	254
SNET	El Salvador	258
THR	Iran	258
DDA	Turkey	259
MIRAS	Russia	275
DMN	Nepal	285
ASRS	Russia	290
YARS	Russia	298
SSNC	Cuba	303
BYKL	Russia	304
RHSSO	Bosnia and Herzegovina	316
LIT	Lithuania	328
IPEC	Czech Republic	332
UPA	Panama	336
SOME	Kazakhstan	356

11

Appendix

11.1 ISC Operational Procedures

11.1.1 Introduction

The relational database at the ISC is the primary source for the ISC Bulletin. This database is also the source for the ISC web-based search, the ISC CD-ROMs and this printed Summary. The ISC database is also mirrored at several institutions such as the Data Management Center of the Incorporated Research Institutions for Seismology (IRIS DMC), Earthquake Research Institute (ERI) of the University of Tokyo and a few others.

The database holds information about ISC events, both natural and anthropogenic. Information on each event may include hypocentre estimates, moment tensors, event type, felt and damaging reports and associated station observations reported by different agencies and grouped together per physical event.

The majority of the ISC events ($\sim 80\%$) are small and are not reviewed by the ISC analysts. Those that are reviewed ($\sim 20\%$, usually magnitude greater than 3.5) may or may not include an ISC hypocentre solution and magnitude estimates. The decision depends on whether the wealth of combined information from several agencies as compared to the data of each single agency alone warrants the ISC location. The events are called ISC events regardless of whether they have been reviewed or located by the ISC or not.

All events located by the ISC are reviewed by the ISC analysts but not the other way round. Analyst review involves an examination of the integrity of all reported parametric information. It does not involve review of waveforms. Even if waveforms from all of the $\sim 6,000$ stations included in a typical recent month of the ISC Bulletin were freely available, it would be an unmanageable task to inspect them all.

We shall now describe briefly current processes and procedures involved in producing the Bulletin of the International Seismological Centre. These have been developed from former practices described in the Introduction to earlier issues of the ISC Bulletin to account for modern methods and technologies of data collection and analysis.

11.1.2 Data Collection

Parametric data, mainly comprising seismic event hypocentre solutions, phase arrival observations and associated magnitude data, are now mostly emailed to the ISC (seismo@isc.ac.uk) by agencies around the world. Other macroseismic and source information associated with seismic events may also be incorporated in accordance with modern standards. The process of data collection at the ISC involves

the automatic parsing of these data into the ISC relational database. The ISC now has over 200 individual parsers to account for legacy and current bulletin data formats used by data reporters.

Figure 11.1 shows the 313 agencies that have reported bulletin data to the ISC, directly or via regional data centres, during the entire period of the ISC existence: these agencies are also listed in Table 11.2 of the Appendix. In Figure 11.1, corresponding countries are shown shaded in red. Please note that the continent of Antarctica appears white on the map despite a steady stream of bulletin data from Antarctic stations: the agencies that run these stations are based elsewhere.

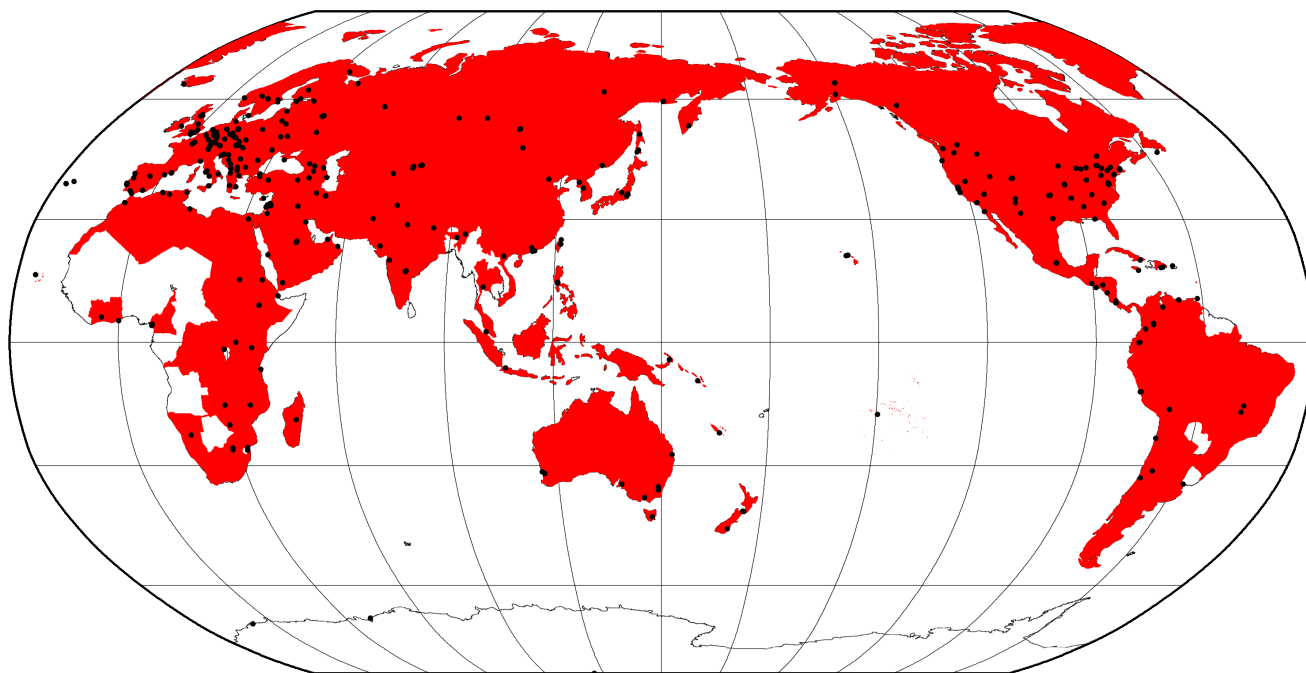


Figure 11.1: Map of 313 agencies and corresponding countries that have reported seismic bulletin data to the ISC at least once during the entire period of the ISC operations, either directly or via regional data centres. Corresponding countries are shaded in red.

11.1.3 ISC Automatic Procedures

Grouping

Grouping is the automatic process by which the many hypocentre solutions sent by the agencies reporting to the ISC for the same physical event are merged together into a single ISC event. This process possibly begins with an alert message and ends before a final review by ISC analysts. The process periodically runs through a set time interval of the input data stream, typically one day, looking for hypocentres in newly received data that are not yet grouped into an ISC event. Thus it considers only data more recent than the last data month reviewed by the ISC analysts. Immediately after grouping the seismic arrival associator is run on the same time interval, dealing with new phase arrival data not associated with any hypocentre.

The first stage of grouping gets a score where possible for each hypocentre to determine whether the reported hypocentre will be considered to be the primary estimate, or prime, for an ISC event. This score is based on the station arrival times reported in association with the hypocentre in four epicentral

distance zones that characterise the networks of stations reporting:

1. Whole network
2. Local, 0 - 150 km
3. Near-regional, 3° - 10°
4. Teleseismic, 28° - 180°

For each distance zone, the azimuthal gap, the secondary azimuthal gap (the largest azimuthal gap filled by a single station), the minimum and maximum epicentral distance and number of stations are all used to calculate the value of dU , the normalised absolute deviation from best fitting uniformly distributed stations (*Bondár and McLaughlin, 2009a*). Clearly, this procedure can only use:

1. Bulletin data with hypocentres and sufficient associated seismic arrivals
2. Data for stations that are in the International Registry (IR)
3. Station data that are actually reported to ISC: CENC (China), for example, reports at most 24 stations, whilst many more may have been used to determine the hypocentre.

The hypocentres are then each considered in turn for grouping using one of two methods, the first by searching for a similar hypocentre, and the second by searching for the best fit of the reported phase arrival data that are associated with the candidate hypocentre. The method chosen for a reporter is based on feedback gained from ISC analysts.

For finding similar hypocentres, three sets of limits for origin-time difference and epicentral separation are used according to the type of bulletin data, be it alert, provisional or final: these limits are, respectively:

- ± 2 minutes and 10°
- ± 2 minutes and 4°
- ± 1 minutes and 2°

If there is no overlap with the hypocentre of an existing ISC event, a new event is formed. For each candidate hypocentre, a proximity score is otherwise calculated based on differences in time, t , and distance, s , between the candidate hypocentre and a hypocentre in an event with which it could potentially be grouped.

$$\text{Proximity score} = 2 - (dt/dt_{max}) - (ds/ds_{max})$$

where ds_{max} is the maximum distance between hypocentres and dt_{max} the maximum difference in origin time.

As long as there is no duplication of hypocentre (with the same author, origin time and location within tight limits) the candidate hypocentre together with the associated phase data is grouped with the prime

hypocentre of the event and the initial dU score is used to reassess the prime hypocentre designation. Apparent duplicated hypocentre estimations, including preliminary solutions relayed by other agencies, need to be assessed to determine whether they should really be split between different events. Should there be two or more equally valid events, these can be assessed in turn and may eventually be merged together.

Grouping by fit of the associated phase arrival data is simpler. The residuals of the arrival data are calculated using ak135 travel times for all suitable prime hypocentres within the widest proximity limits given above for similar hypocentres. The hypocentre and associated phase arrival data is then grouped with the event with the best fitting prime hypocentre, which may similarly be re-designated according to the dU scores. Associations of phase arrival data are updated to be with the prime hypocentre estimate of each ISC event.

It follows that a hypocentre and associated phase arrival data submitted by a reporter will have the reported hypocentre set as the prime hypocentre in the ISC event if no other submitted hypocentre estimate is a closer match. It follows also that a hypocentre submitted without phase data can only be grouped with a similar hypocentre. Generally, early arriving data may be superseded by later arriving data: the data will still be in the ISC database but be deprecated, that is, marked as being no longer useful for further processes.

Association

Association is the automatic procedure, run routinely after grouping, that links reported phase arrivals at IR stations with the prime hypocentres of ISC events. As grouping took care of those phases associated with reported hypocentres, by associating the phases to the respective prime hypocentres of the ISC events without further checks, this procedure is only required for phase arrival observations that were sent without any association of event made for them by the reporter. Currently only 5% of arrival data is sent unassociated compared with 25% ten years ago.

If a phase arrival is found to be very similar to another already reported, it is placed in the same event, otherwise the procedure below is followed.

For associating a phase arrival, suitable events are sought with prime hypocentre origin-times in the window 40 minutes before and 100 s after the arrival time. For each phase arrival and prime hypocentre an ak135 travel-time residual is calculated for either the reported arrival phase name or an alternative from a default list if appropriate. Possible timing errors that are multiples of 60 s (a minute) are considered if the phase arrival is at a station not known to be digitally recording. A reporting likelihood is then determined based on the reported event magnitude: a magnitude default of 3.0 is used if no magnitude is given.

A final score is calculated from the residuals, from the likelihood of the phase observations for the magnitude of the event and from the S-P misfit. A phase arrival along with all other phase arrivals in that reading for the station is then associated with the prime hypocentre with the best score. If no suitable match is found, the reading remains unassociated but may be used at some later stage.

Thresholding

Thresholding is the process determining which events are to be reviewed by the ISC analysts. In former times, before email transmission of data was convenient, all events were reviewed, with magnitudes nearly always 3.5 or above. Nowadays, data contributors are encouraged to send all their data, which are stored in the ISC database. The overwhelming amount of data, including that for many more smaller events and from many more seismograph stations, led to the advent of ISC Comprehensive Bulletin, for all events, and the ISC Reviewed Bulletin, for selected events reviewed by ISC analysts. Thresholding has been under constant review since the start of the 1999 data year.

Several criteria are considered to decide which events merit review. Once a decision is made, whether or not an event is to be reviewed, further criteria are not considered.

In this section, M is the maximum magnitude reported by any agency for the event. The sequence of tests in the automatic decision process for reviewing events is currently:

- All events reported by the International Data Centre (IDC) of the Comprehensive Nuclear-Test-Ban Treaty Organization (CTBTO) are reviewed.
- If M is greater than or equal to 3.5, the event is reviewed.
- If M is less than 2.5, the event is not reviewed.
- If M is unknown, the number of data sources of hypocentres and phase arrivals is used. Care is taken here to avoid counting indirect reports arriving via agencies such as NEIC, CSEM and CASC, which compile regional and global data:
 - If the number of hypocentre authors is greater than two and the maximum epicentral distance of arrival data is greater than 10° , the event is reviewed.
 - If the number of arrival authors is greater than two and the maximum epicentral distance of arrival data is greater than 10° , the event is reviewed.
 - Otherwise the event is not reviewed.
- If M is between 2.5 and 3.5:
 - If the number of hypocentre and seismic arrival authors is less than two, the event is not reviewed.
 - If any bulletin contributing to the event has at least ten stations within 3° and the secondary azimuthal gap (the largest azimuthal gap filled by a single station) is less than 135° , the event is not reviewed.

Location by the ISC

The automatic processes group and associate incoming data into ISC events as indicated above. These data are available to users before review by the ISC analysts but there will be no ISC hypocentre solutions for any of the events. The candidate events due for review by the ISC analysts are determined by the

thresholding process, which is why many smaller events remain without an ISC hypocentre solution even after the analyst review.

Several further checks of the data are made in preparation for the analyst review, and initial trial estimates for ISC hypocentres are then generated using the accumulated data. If sufficiently robust, the ISC hypocentre estimation will be retained and be made the prime solution for the event, but this, of course, will itself be subject to the analyst review.

It is important to note that not all reviewed events will have an ISC hypocentre. For the reviewed events certain criteria must be met for an initial ISC location of an event to be made. These criteria are shown below:

- All events with an IDC hypocentre, unless IDC is the only hypocentre author and there are less than six associated phases.
- Two or more reporters of data
- Phase data at epicentral distance $\geq 20^\circ$

The ISC locator also needs an initial seed location; in all events except those with eight or more reporters of data where the existing prime is used, this is calculated using a Neighbourhood Algorithm (NA) (*Sambridge, 1999; Sambridge and Kennett, 2001*). More information about the ISC location algorithm and initial seed is given in the next section.

11.1.4 ISC Location Algorithm

The new ISC location algorithm is described in detail in *Bondár and Storchak (2011)* (doi: 10.1111/j.1365-246X.2011.05107.x, Manual www.isc.ac.uk/iscbulletin/iscloc/); here we give a short summary of the major features. Ever since the ISC came into existence in 1964, it has been committed to providing a homogeneous bulletin that benefits scientific research. Hence the location algorithm used by the ISC, except for some minor modifications, has remained largely unchanged for the past 40 years (*Adams et al., 1982; Bolt, 1960*). While the ISC location procedures have served the scientific community well in the past, they can certainly be improved.

Linearised location algorithms are very sensitive to the initial starting point for the location. The old procedures made the assumption that a good initial hypocentre is available among the reported hypocentres. However, there is no guarantee that any of the reported hypocentres are close to the global minimum in the search space. Furthermore, attempting to find a free-depth solution was futile when the data had no resolving power for depth (e.g. when the first arrival is not within the inflection point of the P travel-time curve). When there was no depth resolution, the algorithm would simply pick a point on the origin time – depth trade-off curve. The old ISC locator assumed that the observational errors are independent. The recent years have seen a phenomenal growth both in the number of reported events and phases, owing to the ever-increasing number of stations worldwide. Similar ray paths will produce correlated travel-time prediction errors due to unmodelled heterogeneities in the Earth, resulting in underestimated location uncertainties and for unfavourable network geometries, location bias. Hence,

accounting for correlated travel-time prediction errors becomes imperative if we want to improve (or simply maintain) location accuracy as station networks become progressively denser. Finally, publishing network magnitudes that may have been derived from a single station measurement was rather prone to producing erroneous event magnitude estimates.

To meet the challenge imposed by the ever-increasing data volume from heavily unbalanced networks we introduced a new ISC location algorithm to ensure the efficient handling of data and to further improve the location accuracy of events reviewed by the ISC. The new ISC location algorithm

- Uses all ak135 (*Kennett et al.*, 1995) predicted phases (including depth phases) in the location;
- Obtains the initial hypocentre guess via the Neighbourhood Algorithm (NA) (*Sambridge*, 1999; *Sambridge and Kennett*, 2001);
- Performs iterative linearised inversion using an *a priori* estimate of the full data covariance matrix to account for correlated model errors (*Bondár and McLaughlin*, 2009b);
- Attempts a free-depth solution if and only if there is depth resolution, otherwise it fixes the depth to a region-dependent default depth;
- Scales uncertainties to 90% confidence level and calculates location quality metrics for various distance ranges;
- Obtains a depth-phase depth estimate based on reported surface reflections via depth-phase stacking (*Murphy and Barker*, 2006);
- Provides robust network magnitude estimates with uncertainties.

Seismic Phases

One of the major advantages of using the ak135 travel-time predictions (*Kennett et al.*, 1995) is that they do not suffer from the baseline difference between P, S and PKP phases compared with the Jeffreys-Bullen tables (*Jeffreys and Bullen*, 1940). Furthermore, ak135 offers an abundance of phases from the IASPEI Standard Seismic List (*Storchak et al.*, 2003; 2011) that can be used in the location, most notably the PKP branches and depth-sensitive phases. Elevation and ellipticity corrections (*Dziewonski and Gilbert*, 1976; *Engdahl et al.*, 1998; *Kennett et al.*, 1996), using the WG84 ellipsoid parameters, are added to the ak135 predictions. For depth phases, bounce point (elevation correction at the surface reflection point) and water depth (for pwP) corrections are calculated using the algorithm of *Engdahl et al.* (1998). We use the ETOPO1 global relief model (*Amante and Eakins*, 2009) to obtain the elevation or the water depth at the bounce point.

Phase picking errors are described by *a priori* measurement error estimates derived from the inspection of the distribution of ground truth residuals (residuals calculated with respect to the ground truth location) from the IASPEI Reference Event List (*Bondár and McLaughlin*, 2009a). For phases that do not have a sufficient number of observations in the ground truth database we establish *a priori* measurement errors so that the consistency of the relative weighting schema is maintained. First-arriving P-type phases (P, Pn, Pb, Pg) are picked more accurately than later phases, so their measurement error estimates are

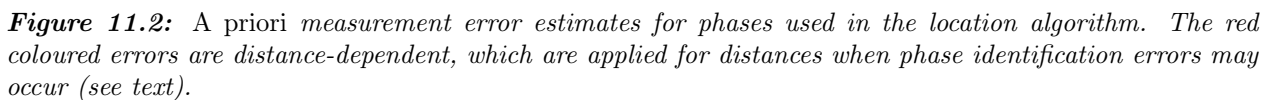
the smallest, 0.8 s. The measurement error for first-arriving S-phases (S, Sn, Sb, Sg) is set to 1.5 s. Phases traversing through or reflecting from the inner/outer core of the Earth have somewhat larger (1.3 s for PKP, PKS, PKKP, PKKS and P'P' branches as well as PKiKP, PcP and PcS, and 1.8 s for SKP, SKS, SKKP, SKKS and S'S' branches as well as SKiKP, ScP and ScS) measurement error estimates to account for possible identification errors among the various branches. Free-surface reflections and conversions (PnPn, PbPb, PgPg, PS, PnS, PgS and SnSn, SbSb, SgSg, SP, SPn, SPg) are observed less frequently and with larger uncertainty, and therefore suffer from large, 2.5 s, measurement errors. Similarly, a measurement error of 2.8 s is assigned to the longer period and typically emergent diffracted phases (Pdif, Sdif, PKPdif). The *a priori* measurement error for the commonly observed depth phases (pP, sP, pS, sS and pwP) is set to 1.3 s, while the remaining depth phases (pPKP, sPKP, pSKS, sSKS branches and pPb, sPb, sSb, pPn, sPn, sSn) have the measurement error estimate set to 1.8 s. We set the measurement error estimate to 2.5 s for the less reliable depth phases (pPg, sPg, sSg, pPdif, pSdif, sPdif and sSdif). Note that we also allow for distance-dependent measurement errors. For instance, to account for possible phase identification errors at far-regional distances the *a priori* measurement error for Pn and P is increased from 0.8 s to 1.2 s and for Sn and S from 1.5 s to 1.8 s between 15° and 28°. The measurement errors between 40° and 180° are set to 1.3 s and 1.8 s for the prominent PP and SS arrivals respectively, but they are increased to 1.8 s and 2.5 s between 25° and 40°.

The relative weighting scheme (Figure 11.2) described above ensures that arrivals picked less reliably or prone to phase identification errors are down-weighted in the location algorithm. Since the ISC works with reported parametric data with wildly varying quality, we opted for a rather conservative set of *a priori* measurement error estimates.

Correlated Travel-Time Prediction Error Structure

Most location algorithms, either linearised or non-linear, assume that all observational errors are independent. This assumption is violated when the separation between stations is less than the scale length of local velocity heterogeneities. When correlated travel-time prediction errors are present, the data covariance matrix is no longer diagonal, and the redundancy in the observations reduces the effective number of degrees of freedom. Thus, ignoring the correlated error structure inevitably results in underestimated location uncertainty estimates. For events located by an unbalanced seismic network this may also lead to a biased location estimate. *Chang et al.* (1983) demonstrated that accounting for correlated error structure in a linearised location algorithm is relatively straightforward once an estimate of the non-diagonal data covariance matrix is available. To determine the data covariance matrix we follow the approach described by *Bondár and McLaughlin* (2009b). They assume that the similarity between ray paths is well approximated by the station separation. This simplifying assumption allows for the estimation of covariances between station pairs from a generic P variogram model derived from ground truth residuals. Because the overwhelming number of phases in the ISC Bulletin is teleseismic P, we expect that the generic variogram model will perform reasonably well anywhere on the globe.

Since in this representation the covariances depend only on station separations, the covariance matrix (and its inverse) needs to be calculated only once. We assume that different phases owing to the different ray paths they travel along as well as station pairs with a separation larger than 1000 km are uncorrelated. Hence, the data covariance matrix is a sparse, block-diagonal matrix. Furthermore, if the stations in



each phase block are ordered by their nearest neighbour distance, the phase blocks themselves become block-diagonal. To reduce the computational time of inverting large matrices we exploit the inherent block-diagonal structure by inverting the covariance matrix block-by-block. The *a priori* measurement error variances are added to the diagonal of the data covariance matrix.

Depth Resolution

In principle, depth can be resolved if there is a mixture of upgoing and downgoing waves emanating from the source, that is, if there are stations covering the distance range where the vertical partial derivative of the travel-time of the first-arriving phase changes sign (local networks), or if there are phases with vertical slowness of opposite sign (depth phases). Core reflections, such as PcP, and to a lesser extent, secondary phases (S in particular) could also help in resolving the depth.

We developed a number of criteria to test whether the reported data for an event have sufficient depth resolution:

- local network: one or more stations within 0.2° with time-defining phases
- depth phases: five or more time-defining depth phases reported by at least two agencies (to reduce a chance of misinterpretation by a single inexperienced analyst)
- core reflections: five or more time-defining core reflections (PcP, ScS) reported by at least two agencies
- local/near regional S: five or more time-defining S and P pairs within 3°

We attempt a free-depth solution if any of the above criteria are satisfied; otherwise we fix the depth to a default depth dependent on the epicentre location. The default depth grid was derived from the EHB (*Engdahl et al.*, 1998) free-depth solutions, including the fixed-depth EHB earthquakes that were flagged as having reliable depth estimate (personal communication with Bob Engdahl), as well as from free-depth solutions obtained by the new locator when locating the entire ISC Bulletin data-set. As Figure 11.3 indicates, the default depth grid provides a reasonable depth estimate where seismicity is well established. Note that the depths of known anthropogenic events and landslides are fixed to the surface.

Depth-Phase Stack

While we use depth phases directly in the location, the depth-phase stacking method (*Murphy and Barker*, 2006) provides an independent means to obtain robust depth estimates. Because the depth obtained from the depth-phase stacking method implicitly depends on the epicentre itself, we perform the depth-phase stack only twice: first, with respect to the initial location in order to obtain a reasonable starting point for the depth in the grid search described in the following section; second, with respect to the final location to obtain the final estimate for the depth-phase constrained depth.

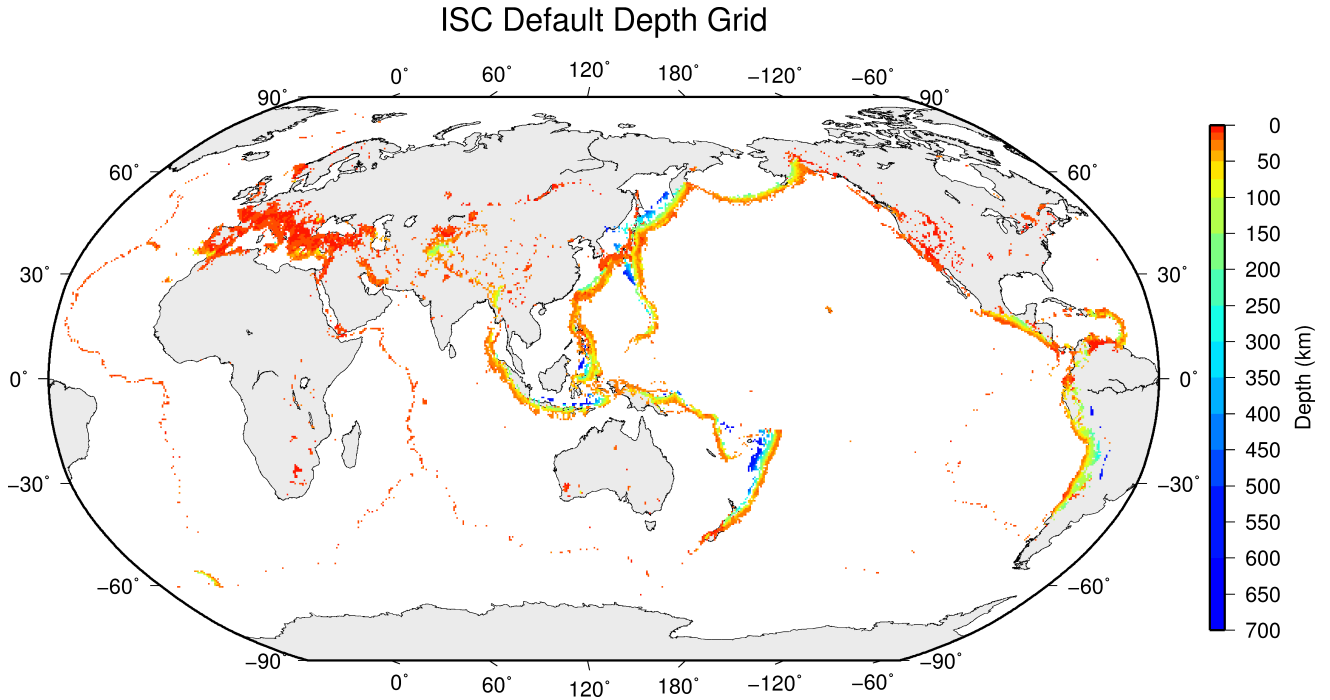


Figure 11.3: Default depths on a 0.5×0.5 degree grid derived from EHB free-depth solutions and EHB events flagged as reliable depth, as well as free-depth solutions from the entire ISC Bulletin located with the new locator.

Initial Hypocentre

For poorly recorded events the reported hypocentres may exhibit a large scatter and they could suffer from large location errors, especially if they are only recorded teleseismically. In order to obtain a good initial hypocentre guess for the linearised location algorithm we employ the Neighbourhood Algorithm (NA) (Sambridge, 1999; Sambridge and Kennett, 2001). NA is a nonlinear grid search method capable of exploring a large search space and rapidly closing in on the global optimum. Kennett (2006) discusses in detail the NA algorithm and its use for locating earthquakes.

We perform a search around the median of reported hypocentre parameters with a generously defined search region – within a 2° radius circle around the median epicentre, 10 s around the median origin time and 150 km around the median reported depth. These default search parameters were obtained by trial-and-error runs to achieve a compromise between execution time and allowance for gross errors in the median reported hypocentre parameters. Note that if our test for depth resolution fails, we fix the depth to the region-dependent default depth. The initial hypocentre estimate will be the one with the smallest L1-norm misfit among the NA trial hypocentres. Once close to the global optimum, we proceed with the linearised location algorithm to obtain the final solution and corresponding formal uncertainties.

Iterative Linearised Location Algorithm

We adopt the location algorithm described in detail in Bondár and McLaughlin (2009b). Recall that in the presence of correlated travel-time prediction errors the data covariance matrix is no longer diagonal. Using the singular value decomposition of the data covariance matrix we construct a projection matrix

that orthogonalises the data set and projects redundant observations into the null space. In other words, we solve the inversion problem in the eigen coordinate system in which the transformed observations are independent.

The model covariance matrix yields the four-dimensional error ellipsoid whose projections provide the two-dimensional error ellipse and one-dimensional errors for depth and origin time. These uncertainties are scaled to the 90% confidence level. Note that since we projected the system of equations into the eigen coordinate system, the number of independent observations is less than the total number of observations. Hence, the estimated location error ellipses necessarily become larger, providing a more realistic representation of the location uncertainties. The major advantage of this approach is that the projection matrix is calculated only once for each event location.

Validation Tests

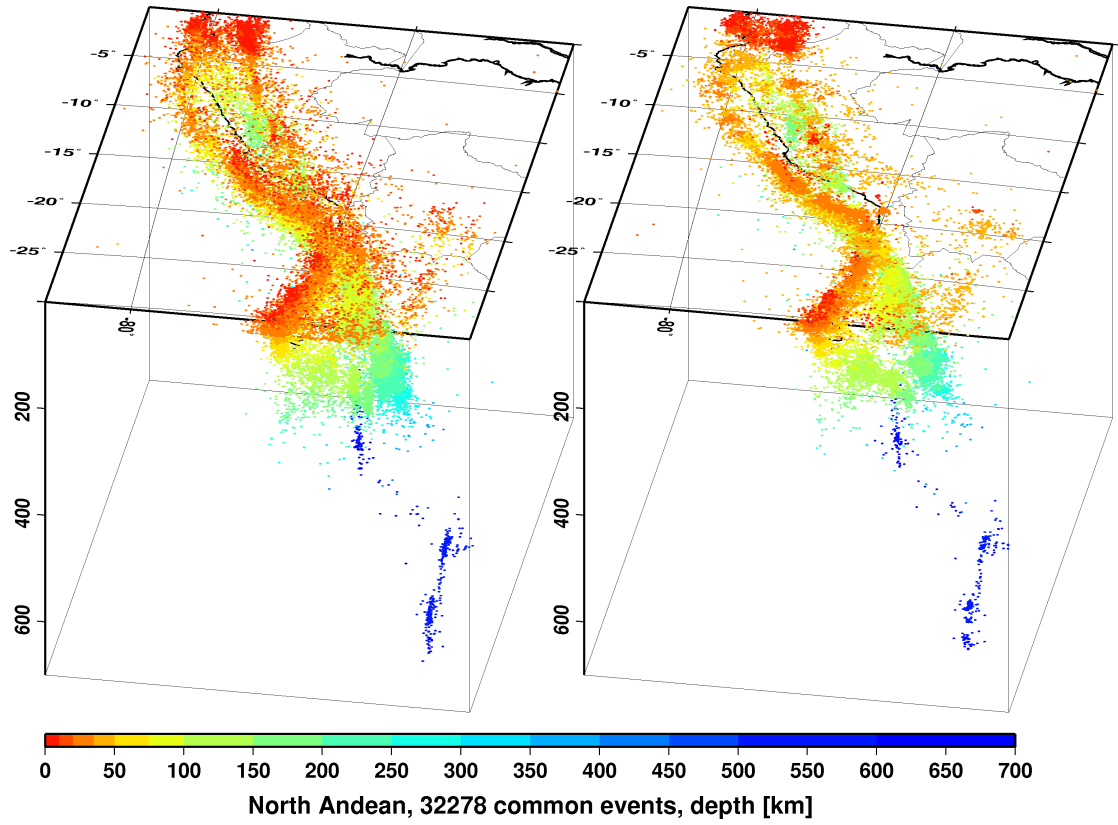
To demonstrate improvements due to the new location procedures, we located some 7,200 GT0-5 events in the IASPEI Reference Event List (*Bondár and McLaughlin, 2009a*) both with the old ISC locator (which constitutes the baseline) and with the new location algorithm. We also located the entire (1960-2010) ISC Bulletin, including four years of the International Seismological Summary (ISS, the predecessor of the ISC) catalogue (*Villaseñor and Engdahl, 2005; 2007*).

The location of GT events demonstrated that the new ISC location algorithm provides small but consistent location improvements, considerable improvements in depth determination and significantly more accurate formal uncertainty estimates. Even using a 1-D model and a variogram model that fits teleseismic observations we could achieve realistic uncertainty estimates, as the 90% confidence error ellipses cover the true locations 80-85% of the time. The default depth grid provides reasonable depth estimates where there is seismicity. We have shown that the location and depth accuracy obtained by the new algorithm matches or surpasses the EHB accuracy.

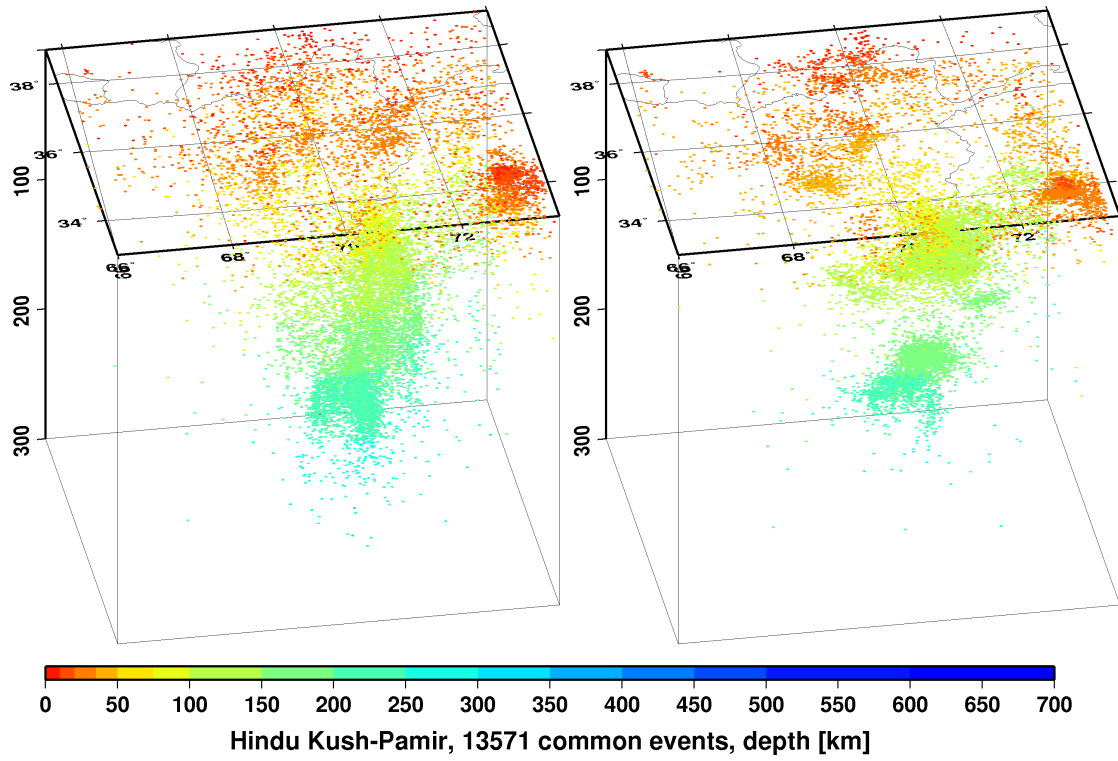
We noted above that the location improvements for the ground truth events are consistent, but minor. This is not surprising as most of the events in the IASPEI Reference Event List are very well-recorded with a small azimuthal gap and dominated by P-type phases. In these circumstances we could expect significant location improvements only for heavily unbalanced networks where large numbers of correlated ray paths conspire to introduce location bias. On the other hand, the ISC Bulletin represents a plethora of station configurations ranging from reasonable to the most unfavourable network geometries. Hence, we could expect more dramatic location improvements when locating the entire ISC Bulletin. Although in this case we cannot measure the improvement in location accuracy due to the lack of ground truth information, we show that with the new locator we obtain significantly better clustering of event locations (Figure 11.4), thus providing an improved view of the seismicity of the Earth.

Magnitude Calculation

Currently the ISC locator calculates body and surface wave magnitudes. MS is calculated for shallow events (depth < 60 km) only. At least three station magnitudes are required for a network (mb or MS) magnitude. The network magnitude is defined as the median of the station magnitudes, and its



(a)



(b)

Figure 11.4: Comparison of seismicity maps for common events in the reviewed ISC Bulletin (old locator, left) and the located ISC Bulletin (new locator, right) for the North Andean (a) and Hindu Kush - Pamir regions (b). The events are better clustered when located with the new locator.

uncertainty is defined as the standard median absolute deviation (SMAD) of the alpha-trimmed ($\alpha = 20\%$) station magnitudes.

The station magnitude is defined as the median of reading magnitudes for a station. The reading magnitude is defined as the magnitude computed from the maximal $\log(A/T)$ in a reading. Amplitude magnitudes are calculated for each reported amplitude-period pair.

Body-Wave Magnitudes

Body-wave magnitudes are calculated for each reported amplitude-period pair, provided that the phase is in the list of phases that can contribute to mb (P, pP, sP, AMB, IAmb, pmax), the station is between the epicentral distances $21 - 100^\circ$ and the period is less than 3 s.

A reading contains all parametric data reported by a single agency for an event at a station, and it may have several reported amplitude and periods. The amplitudes are measured as zero-to-peak values in nanometres. For each pair an amplitude mb is calculated.

$$mb_{amp} = \log(A/T) + Q(\Delta, h) - 3 \quad (11.1)$$

If no amplitude-period pairs are reported for a reading, the body-wave magnitude is calculated using the reported \logat values for $\log(A/T)$.

$$mb_{amp} = \logat + Q(\Delta, h) - 3 \quad (11.2)$$

where the magnitude attenuation $Q(\Delta, h)$ value is calculated using the Gutenberg-Richter tables (*Gutenberg and Richter, 1956*).

For each reading the ISC locator finds the reported amplitude-period pair for which A/T is maximal:

$$mb_{rd} = \log(\max(A/T)) + Q(\Delta, h) - 3 \quad (11.3)$$

Or, if no amplitude-period pairs were reported for the reading:

$$mb_{rd} = \max(\logat) + Q(\Delta, h) - 3 \quad (11.4)$$

Several agencies may report data from the same station. The station magnitude is defined as the median of the reading magnitudes for a station.

$$mb_{sta} = \text{median}(mb_{rd}) \quad (11.5)$$

Once all station mb values are determined, the station magnitudes are sorted and the lower and upper alpha percentiles are made non-defining. The network mb and its uncertainty are then calculated as the median and the standard median absolute deviation (SMAD) of the alpha-trimmed station magnitudes, respectively.

Surface-Wave Magnitudes

Surface-wave magnitudes are calculated for each reported amplitude-period pair, provided that the phase is in the list of phases that can contribute to MS (AMS , $IAMS_{20}$, LR , MLR , M , L), the station is between the epicentral distances $20 - 160^\circ$ and the period is between $10 - 60$ s.

For each reported amplitude-period pair MS is calculated using the Prague formula (*Vaněk et al.*, 1962). Amplitude MS is calculated for each component (Z, E, N) separately.

$$MS_{amp} = \log(A/T) + 1.66 * \log(\Delta) + 0.3 \quad (11.6)$$

To calculate the reading MS , the ISC locator first finds the reported amplitude-period pair for which A/T is maximal on the vertical component.

$$MS_Z = \log(\max(A_Z/T_Z)) + 1.66 * \log(\Delta) + 0.3 \quad (11.7)$$

Then it finds the $\max(A/T)$ for the E and N components for which the period measured on the horizontal components is within ± 5 s from the period measured on the vertical component.

$$MS_E = \log(\max(A_E/T_E)) + 1.66 * \log(\Delta) + 0.3 \quad (11.8)$$

$$MS_N = \log(\max(A_N/T_N)) + 1.66 * \log(\Delta) + 0.3 \quad (11.9)$$

The horizontal MS is calculated as

$$\max(A/T)_h = \begin{cases} \sqrt{2(\max(A_E/T_E))^2} & \text{if } MS_N \text{ does not exist} \\ \sqrt{(\max(A_E/T_E))^2 + (\max(A_N/T_N))^2} & \text{if } MS_E \text{ and } MS_N \text{ exist} \\ \sqrt{2(\max(A_N/T_N))^2} & \text{if } MS_E \text{ does not exist} \end{cases} \quad (11.10)$$

$$MS_H = \log(\max(A/T)_h) + 1.66 * \log(\Delta) + 0.3 \quad (11.11)$$

The reading MS is defined as

$$MS = \begin{cases} (MS_Z + MS_H)/2 & \text{if } MS_Z \text{ and } MS_H \text{ exist} \\ MS_H & \text{if } MS_Z \text{ does not exist} \\ MS_Z & \text{if } MS_H \text{ does not exist} \end{cases} \quad (11.12)$$

Several agencies may report data from the same station. The station magnitude is defined as the median of the reading magnitudes for a station.

$$MS_{sta} = \text{median}(MS_{rd}) \quad (11.13)$$

Once all station MS values are determined, the station magnitudes are sorted and the lower and upper alpha percentiles are made non-defining. The network MS and its uncertainty are calculated as the median and the standard median absolute deviation (SMAD) of the alpha-trimmed station magnitudes, respectively.

11.1.5 Review Process

Typically, for each month, the ISC analysts now review approximately 20% of the events in the ISC database, currently 3,500-5,000 per data month. This review is done about 24 months behind real time to allow for the comprehensive collection of data from networks and data centres worldwide.

Users of the ISC Bulletin can be assured that all ISC Bulletin events with an ISC hypocentre solution have been reviewed by the ISC analysts. Not all reviewed events will end up having an ISC hypocentre solution, but events that have not been reviewed are flagged accordingly.

An automatic process creates a monthly listing of the events for the analysts to review. The analysis is performed in batches: thus, events are generally not finalised one at a time, and a completed month of events is published after all the analysis is finished.

The first batch of editing involves careful examination of all events selected for review for the month. The entire month is then reprocessed incorporating the editing changes deemed necessary by the analysts. The analysts next review the same events again in a second pass through the data, checking for each event where there is a change that the result was as could be expected by comparing the revised solution against the initial solution. When the analysts are satisfied with an event, it is no longer revised in a subsequent pass but analysis continues in several passes until all events are considered satisfactory.

The analysts initially print the entire monthly listing, which is split into sections each with about 150 events. Each event, uniquely identified in the monthly printout, shows the reported hypocentres, magnitudes and phase arrivals grouped and associated for the event, as well as an ISC solution of hypocentre, if there is one, along with quality metrics, error estimates, redetermined magnitudes and phase arrival-time residuals. Ancillary information including the geographic region and reported macroseismic observations is also present in the listing for each pass.

The analysts have the capability to execute a variety of commands that can be used to merge or split events, to move phase arrivals or hypocentres from one event to another or to modify the reported phase names. Each of these changes initiates a new revision of the relevant events and ISC hypocentre solutions. There are also several commands to change the starting depth or location in the location algorithm.

The main tasks in reviewing the ISC Bulletin are to:

1. Check that the grouping of hypocentres and association of phase arrivals is appropriate.
2. Check that the depth and location is appropriate for the region and reported phase arrivals.
3. Check that no data are missing for an event, given the region and magnitude, and that included data are appropriate.

4. Examine the phase arrival-time residuals to check that the ISC hypocentre solution is appropriate.
5. Look for outliers in the observations and for misassociated phases.

As well as examining each event closely, it is also important to scan the hypocentres and phase arrivals of adjacent events, close in time and space, to ensure that there is uniformity in the composition of the events. In some cases, two events should be merged into one event, as apparent in some other case. In other cases, one apparent event needs to be split into two events, when the automatic grouping has erroneously created one event with more than one reported hypocentre out of the observations for two real events that are distinct but closely occurring.

Misassociated phase arrivals are returned to the unassociated data stream, if not immediately placed by the analyst in another event where they belong. These unassociated phases are then available to be associated with some other event if the time and location is appropriate. The analysts also check that no phase is associated to more than one event.

Towards the end of the monthly analysis, the ISC ‘Search’ procedure runs, attempting to build events from the remaining set of unassociated phase arrivals. The algorithm is based on the methodology of *Engdahl and Gunst* (1966). Candidate events are validated or rejected by attempting to find ISC hypocentres for them using the ISC locator. The surviving events are then reviewed. Those events with phase arrival observations reported by stations from at least two networks are added to the ISC Bulletin if the solutions meet the standards set by the ISC analysts. These events have only an ISC determination of hypocentre.

At the end of analysis for a data month, a set of final checks is run for quality control, with the results reviewed by an analyst and the defects rectified. These are checks for inconsistencies and errors to ensure the general integrity of the ISC Bulletin.

11.1.6 History of Operational Changes

- From data-month January 2001 onwards, both P and S groups of arrival times are used in location.
- From data-month September 2002 onwards, the printed ISC Bulletins have been generated directly from the ISC Relational Database.
- From data-month October 2002, a new location program ISCloc has been used in operations. Also, the IASPEI standard phase list has now been adopted by the ISC. Please see Section 11.2.1 for details.
- From data-month January 2003 onwards, an updated regionalisation scheme has been adopted (*Young et al.*, 1996).
- From data-month January 2006 the ISC hypocentres are computed using the *ak135* earth velocity model (*Kennett et al.*, 1995) and then reviewed by ISC seismologists. The ISC still produces the hypocentre solutions based on Jeffreys-Bullen travel time tables (agency code ISCJB), yet these solutions are no longer reviewed.

Currently, the ISC is re-computing the entire ISC Bulletin as part of the Rebuild Project using *ak135* and the new location program (Section 11.1.4) in order to assure homogeneity and consistency of the data in the ISC Bulletin.

- From data-month January 2009, a new location program (*Bondár and Storchak, 2011*) has been used in operations. The new program uses all predicted *ak135* phases and accounts for correlated model errors. An overview of the location algorithm is provided in this volume (Section 11.1.4).

11.2 IASPEI Standards

11.2.1 Standard Nomenclature of Seismic Phases

The following list of seismic phases was approved by the IASPEI Commission on Seismological Observation and Interpretation (CoSOI) and adopted by IASPEI on 9th July 2003. More details can be found in *Storchak et al. (2003)* and *Storchak et al. (2011)*. Ray paths for some of these phases are shown in Figures 11.5–11.10.

Crustal Phases

Pg	At short distances, either an upgoing P wave from a source in the upper crust or a P wave bottoming in the upper crust. At larger distances also, arrivals caused by multiple P-wave reverberations inside the whole crust with a group velocity around 5.8 km/s.
Pb	Either an upgoing P wave from a source in the lower crust or a P wave bottoming in the lower crust (alt: P*)
Pn	Any P wave bottoming in the uppermost mantle or an upgoing P wave from a source in the uppermost mantle
PnPn	Pn free-surface reflection
PgPg	Pg free-surface reflection
PmP	P reflection from the outer side of the Moho
PmPN	PmP multiple free surface reflection; <i>N</i> is a positive integer. For example, PmP2 is PmPPmP.
PmS	P to S reflection/conversion from the outer side of the Moho
Sg	At short distances, either an upgoing S wave from a source in the upper crust or an S wave bottoming in the upper crust. At larger distances also, arrivals caused by superposition of multiple S-wave reverberations and SV to P and/or P to SV conversions inside the whole crust.
Sb	Either an upgoing S wave from a source in the lower crust or an S wave bottoming in the lower crust (alt: S*)
Sn	Any S wave bottoming in the uppermost mantle or an upgoing S wave from a source in the uppermost mantle
SnSn	Sn free-surface reflection
SgSg	Sg free-surface reflection
SmS	S reflection from the outer side of the Moho
SmSN	SmS multiple free-surface reflection; <i>N</i> is a positive integer. For example, SmS2 is SmSSmS.
SmP	S to P reflection/conversion from the outer side of the Moho
Lg	A wave group observed at larger regional distances and caused by superposition of multiple S-wave reverberations and SV to P and/or P to SV conversions inside the whole crust. The maximum energy travels with a group velocity of approximately 3.5 km/s
Rg	Short-period crustal Rayleigh wave

Mantle Phases

P	A longitudinal wave, bottoming below the uppermost mantle; also an upgoing longitudinal wave from a source below the uppermost mantle
PP	Free-surface reflection of P wave leaving a source downward
PS	P, leaving a source downward, reflected as an S at the free surface. At shorter distances the first leg is represented by a crustal P wave.
PPP	Analogous to PP
PPS	PP which is converted to S at the second reflection point on the free surface; travel time matches that of PSP
PSS	PS reflected at the free surface
PcP	P reflection from the core-mantle boundary (CMB)
PcS	P converted to S when reflected from the CMB
PcPN	PcP reflected from the free surface $N - 1$ times; N is a positive integer. For example PcP2 is PcPPcP.
Pz+P	(alt: PzP) P reflection from outer side of a discontinuity at depth z ; z may be a positive numerical value in km. For example, P660+P is a P reflection from the top of the 660 km discontinuity.
Pz-P	P reflection from inner side of a discontinuity at depth z . For example, P660-P is a P reflection from below the 660 km discontinuity, which means it is precursory to PP.
Pz+S	(alt:PzS) P converted to S when reflected from outer side of discontinuity at depth z
Pz-S	P converted to S when reflected from inner side of discontinuity at depth z
PScS	P (leaving a source downward) to ScS reflection at the free surface
Pdif	P diffracted along the CMB in the mantle (old: Pdiff)
S	Shear wave, bottoming below the uppermost mantle; also an upgoing shear wave from a source below the uppermost mantle
SS	Free-surface reflection of an S wave leaving a source downward
SP	S, leaving a source downward, reflected as P at the free surface. At shorter distances the second leg is represented by a crustal P wave.
SSS	Analogous to SS
SSP	SS converted to P when reflected from the free surface; travel time matches that of SPS
SPP	SP reflected at the free surface
ScS	S reflection from the CMB
ScP	S converted to P when reflected from the CMB
ScSN	ScS multiple free-surface reflection; N is a positive integer. For example ScS2 is ScSScS.
Sz+S	S reflection from outer side of a discontinuity at depth z ; z may be a positive numerical value in km. For example S660+S is an S reflection from the top of the 660 km discontinuity. (alt: SzS)
Sz-S	S reflection from inner side of discontinuity at depth z . For example, S660-S is an S reflection from below the 660 km discontinuity, which means it is precursory to SS.
Sz+P	(alt: SzP) S converted to P when reflected from outer side of discontinuity at depth z
Sz-P	S converted to P when reflected from inner side of discontinuity at depth z
ScSP	ScS to P reflection at the free surface
Sdif	S diffracted along the CMB in the mantle (old: Sdiff)

Core Phases

PKP	Unspecified P wave bottoming in the core (alt: P')
PKPab	P wave bottoming in the upper outer core; ab indicates the retrograde branch of the PKP caustic (old: PKP2)
PKPbc	P wave bottoming in the lower outer core; bc indicates the prograde branch of the PKP caustic (old: PKP1)
PKPdf	P wave bottoming in the inner core (alt: PKIKP)

PKPpre	A precursor to PKPdf due to scattering near or at the CMB (old: PKhKP)
PKPdif	P wave diffracted at the inner core boundary (ICB) in the outer core
PKS	Unspecified P wave bottoming in the core and converting to S at the CMB
PKSab	PKS bottoming in the upper outer core
PKSbc	PKS bottoming in the lower outer core
PKSdf	PKS bottoming in the inner core
P'P'	Free-surface reflection of PKP (alt: PKPPKP)
P'N	PKP reflected at the free surface $N - 1$ times; N is a positive integer. For example, P'3 is P'P'P'. (alt: PKPN)
P'z-P'	PKP reflected from inner side of a discontinuity at depth z outside the core, which means it is precursory to P'P'; z may be a positive numerical value in km
P'S'	(alt: PKPSKS) PKP converted to SKS when reflected from the free surface; other examples are P'PKS, P'SKP
PS'	P (leaving a source downward) to SKS reflection at the free surface (alt: PSKS)
PKKP	Unspecified P wave reflected once from the inner side of the CMB
PKKPab	PKKP bottoming in the upper outer core
PKKPbc	PKKP bottoming in the lower outer core
PKKPdf	PKKP bottoming in the inner core
PNKP	P wave reflected $N - 1$ times from inner side of the CMB; N is a positive integer.
PKKPpre	A precursor to PKKP due to scattering near the CMB
PKiKP	P wave reflected from the inner core boundary (ICB)
PKNIKP	P wave reflected $N - 1$ times from the inner side of the ICB
PKJKP	P wave traversing the outer core as P and the inner core as S
PKKS	P wave reflected once from inner side of the CMB and converted to S at the CMB
PKKSab	PKKS bottoming in the upper outer core
PKKSbc	PKKS bottoming in the lower outer core
PKKSdf	PKKS bottoming in the inner core
PcPP'	PcP to PKP reflection at the free surface; other examples are PcPS', PcSP', PcSS', PcPSKP, PcSSKP. (alt: PcPPKP)
SKS	unspecified S wave traversing the core as P (alt: S')
SKSac	SKS bottoming in the outer core
SKSdf	SKS bottoming in the inner core (alt: SKIKS)
SPdifKS	SKS wave with a segment of mantleside Pdif at the source and/or the receiver side of the ray path (alt: SKPdifS)
SKP	Unspecified S wave traversing the core and then the mantle as P
SKPab	SKP bottoming in the upper outer core
SKPbc	SKP bottoming in the lower outer core
SKPdf	SKP bottoming in the inner core
S'S'	Free-surface reflection of SKS (alt: SKSSKS)
S'N	SKS reflected at the free surface $N - 1$ times; N is a positive integer
S'z-S'	SKS reflected from inner side of discontinuity at depth z outside the core, which means it is precursory to S'S'; z may be a positive numerical value in km.
S'P'	(alt: SKSPKP) SKS converted to PKP when reflected from the free surface; other examples are S'SKP, S'PKS.
S'P	(alt: SKSP) SKS to P reflection at the free surface
SKKS	Unspecified S wave reflected once from inner side of the CMB
SKKSac	SKKS bottoming in the outer core
SKKSdf	SKKS bottoming in the inner core
SNKS	S wave reflected $N - 1$ times from inner side of the CMB; N is a positive integer.
SKiKS	S wave traversing the outer core as P and reflected from the ICB
SKJKS	S wave traversing the outer core as P and the inner core as S
SKKP	S wave traversing the core as P with one reflection from the inner side of the CMB and then continuing as P in the mantle

SKKPab	SKKP bottoming in the upper outer core
SKKPbc	SKKP bottoming in the lower outer core
SKKPdf	SKKP bottoming in the inner core
ScSS'	ScS to SKS reflection at the free surface; other examples are ScPS', ScSP', ScPP', ScSSKP, ScPSKP. (alt: ScSSKS)

Near-source Surface reflections (Depth Phases)

pPy	All P-type onsets (<i>Py</i>), as defined above, which resulted from reflection of an upgoing P wave at the free surface or an ocean bottom. WARNING: The character <i>y</i> is only a wild card for any seismic phase, which could be generated at the free surface. Examples are pP, pPKP, pPP, pPcP, etc.
sPy	All <i>Py</i> resulting from reflection of an upgoing S wave at the free surface or an ocean bottom; for example, sP, sPKP, sPP, sPcP, etc.
pSy	All S-type onsets (<i>Sy</i>), as defined above, which resulted from reflection of an upgoing P wave at the free surface or an ocean bottom; for example, pS, pSKS, pSS, pScP, etc.
sSy	All <i>Sy</i> resulting from reflection of an upgoing S wave at the free surface or an ocean bottom; for example, sSn, sSS, sScS, sSdif, etc.
pwPy	All <i>Py</i> resulting from reflection of an upgoing P wave at the ocean's free surface
pmPy	All <i>Py</i> resulting from reflection of an upgoing P wave from the inner side of the Moho

Surface Waves

L	Unspecified long-period surface wave
LQ	Love wave
LR	Rayleigh wave
G	Mantle wave of Love type
GN	Mantle wave of Love type; <i>N</i> is integer and indicates wave packets traveling along the minor arcs (odd numbers) or major arc (even numbers) of the great circle
R	Mantle wave of Rayleigh type
RN	Mantle wave of Rayleigh type; <i>N</i> is integer and indicates wave packets traveling along the minor arcs (odd numbers) or major arc (even numbers) of the great circle
PL	Fundamental leaking mode following P onsets generated by coupling of P energy into the waveguide formed by the crust and upper mantle SPL S wave coupling into the PL waveguide; other examples are SSPL, SSSPL.

Acoustic Phases

H	A hydroacoustic wave from a source in the water, which couples in the ground
HPg	H phase converted to Pg at the receiver side
HSg	H phase converted to Sg at the receiver side
HRg	H phase converted to Rg at the receiver side
I	An atmospheric sound arrival which couples in the ground
IPg	I phase converted to Pg at the receiver side
ISg	I phase converted to Sg at the receiver side
IRg	I phase converted to Rg at the receiver side
T	A tertiary wave. This is an acoustic wave from a source in the solid earth, usually trapped in a low-velocity oceanic water layer called the SOFAR channel (SOund Fixing And Ranging).
TPg	T phase converted to Pg at the receiver side
TSg	T phase converted to Sg at the receiver side
TRg	T phase converted to Rg at the receiver side

Amplitude Measurement Phases

The following set of amplitude measurement names refers to the IASPEI Magnitude Standard (see www.iaspei.org/commissions/CSOI/Summary_of_WG_recommendations.pdf)

compliance to which is indicated by the presence of leading letter I. The absence of leading letter I indicates that a measurement is non-standard. Letter A indicates a measurement in *nm* made on a displacement seismogram, whereas letter V indicates a measurement in *nm/s* made on a velocity seismogram.

IAML	Displacement amplitude measured according to the IASPEI standard for local magnitude <i>ML</i>
IAMs_20	Displacement amplitude measured according to IASPEI standard for surface-wave magnitude <i>MS</i> (20)
IVMs_BB	Velocity amplitude measured according to IASPEI standard for broadband surface-wave magnitude <i>MS</i> (<i>BB</i>)
IAMB	Displacement amplitude measured according to IASPEI standard for short-period teleseismic body-wave magnitude <i>mb</i>
IVmB_BB	Velocity amplitude measured according to IASPEI standard for broadband teleseismic body-wave magnitude <i>mB</i> (<i>BB</i>)
AX_IN	Displacement amplitude of phase of type <i>X</i> (e.g., PP, S, etc), measured on an instrument of type IN (e.g., SP - short-period, LP - long-period, BB - broadband)
VX_IN	Velocity amplitude of phase of type <i>X</i> and instrument of type IN (as above)
A	Unspecified displacement amplitude measurement
V	Unspecified velocity amplitude measurement
AML	Displacement amplitude measurement for nonstandard local magnitude
AMs	Displacement amplitude measurement for nonstandard surface-wave magnitude
Amb	Displacement amplitude measurement for nonstandard short-period body-wave magnitude
AmB	Displacement amplitude measurement for nonstandard medium to long-period body-wave magnitude
END	Time of visible end of record for duration magnitude

Unidentified Arrivals

x	unidentified arrival (old: i, e, NULL)
rx	unidentified regional arrival (old: i, e, NULL)
tx	unidentified teleseismic arrival (old: i, e, NULL)
Px	unidentified arrival of P type (old: i, e, NULL, (P), P?)
Sx	unidentified arrival of S type (old: i, e, NULL, (S), S?)

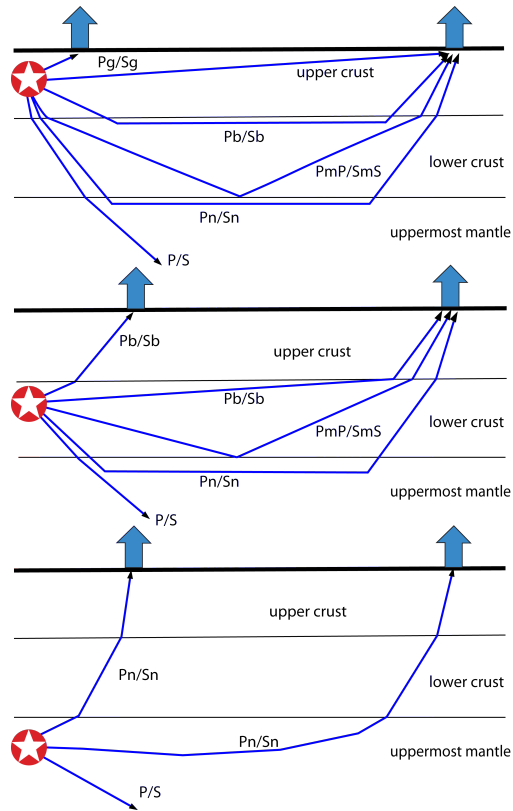


Figure 11.5: Seismic ‘crustal phases’ observed in the case of a two-layer crust in local and regional distance ranges ($0^\circ < D < \text{about } 20^\circ$) from the seismic source in the: upper crust (top); lower crust (middle); and uppermost mantle (bottom).

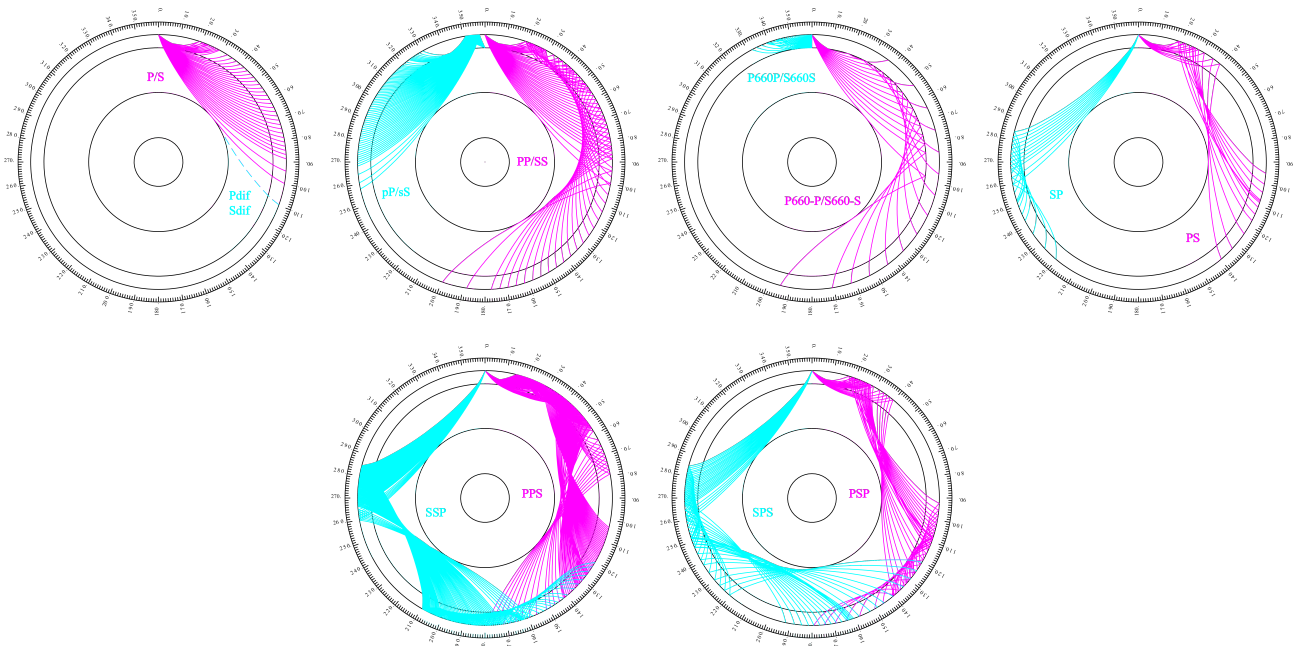


Figure 11.6: Mantle phases observed at the teleseismic distance range $D > \text{about } 20^\circ$.

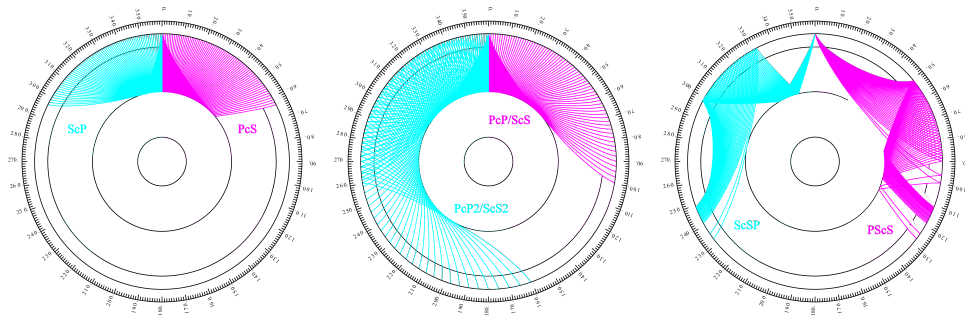


Figure 11.7: Reflections from the Earth's core.

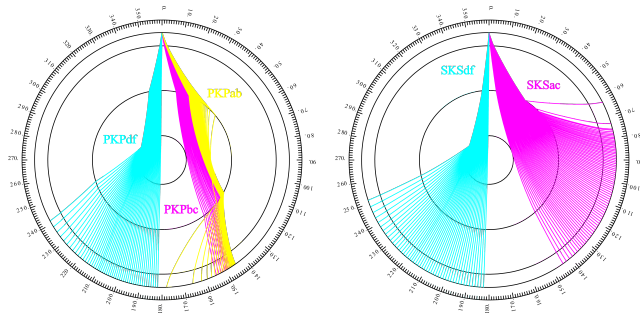


Figure 11.8: Seismic rays of direct core phases.

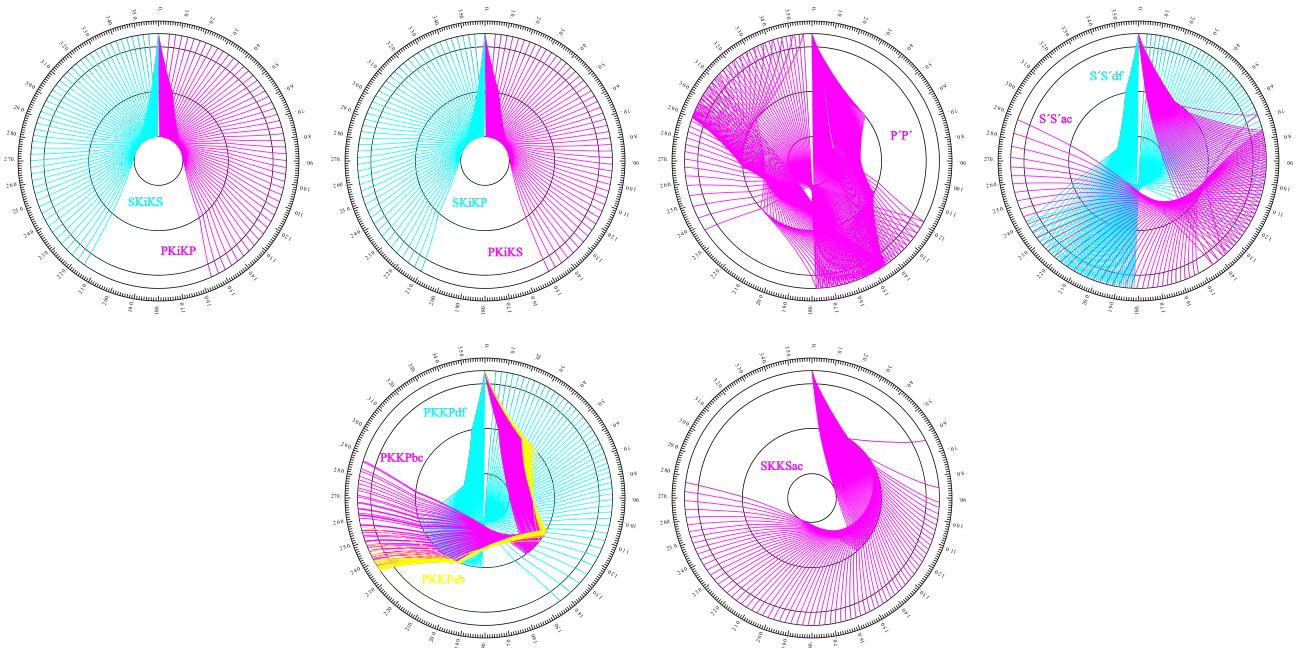


Figure 11.9: Seismic rays of single-reflected core phases.

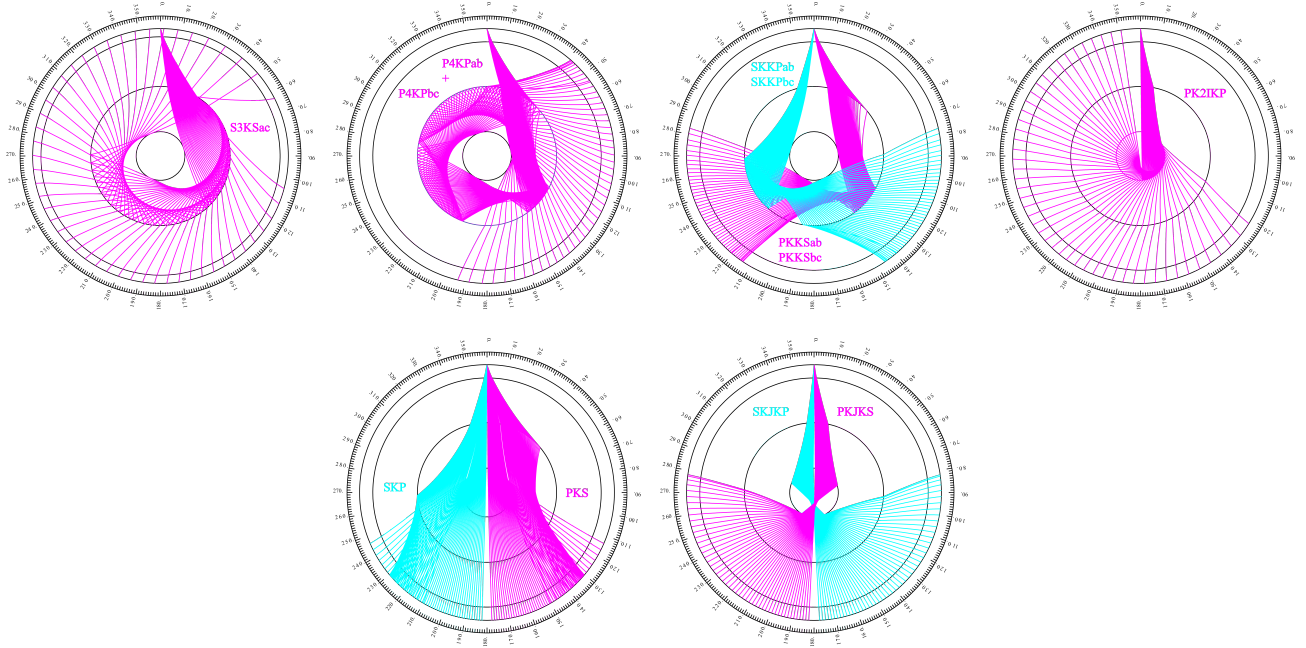


Figure 11.10: Seismic rays of multiple-reflected and converted core phases.

11.2.2 Flinn-Engdahl Regions

The Flinn-Engdahl regions were first proposed by *Flinn and Engdahl* (1965), with the standard defined by *Flinn et al.* (1974). The latest version of the schema, published by *Young et al.* (1996), divides the Earth into 50 seismic regions (Figure 11.11), which are further subdivided producing a total of 754 geographical regions (listed below). The geographic regions are numbered 1 to 757 with regions 172, 299 and 550 no longer in use. The boundaries of these regions are defined at one-degree intervals.

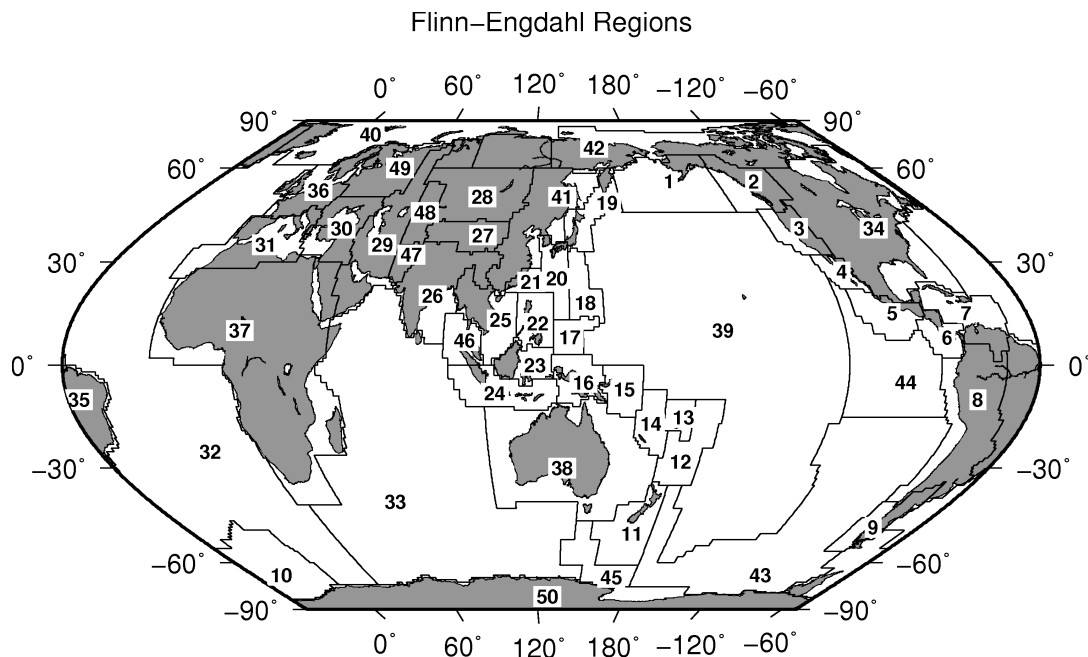


Figure 11.11: Map of all Flinn-Engdahl seismic regions.

Seismic Region 1

Alaska-Aleutian Arc

1. Central Alaska
2. Southern Alaska
3. Bering Sea
4. Komandorsky Islands region
5. Near Islands
6. Rat Islands
7. Andreanof Islands
8. Pribilof Islands
9. Fox Islands
10. Unimak Island region
11. Bristol Bay
12. Alaska Peninsula
13. Kodiak Island region
14. Kenai Peninsula
15. Gulf of Alaska
16. South of Aleutian Islands
17. South of Alaska

Seismic Region 2

Eastern Alaska to Vancouver Island

18. Southern Yukon Territory
19. Southeastern Alaska
20. Off coast of southeastern Alaska
21. West of Vancouver Island
22. Queen Charlotte Islands region
23. British Columbia
24. Alberta
25. Vancouver Island region
26. Off coast of Washington
27. Near coast of Washington
28. Washington-Oregon border region
29. Washington

Seismic Region 3

California-Nevada Region

30. Off coast of Oregon
31. Near coast of Oregon
32. Oregon
33. Western Idaho
34. Off coast of northern California
35. Near coast of northern California
36. Northern California
37. Nevada
38. Off coast of California
39. Central California
40. California-Nevada border region
41. Southern Nevada
42. Western Arizona
43. Southern California
44. California-Arizona border region
45. California-Baja California border region
46. Western Arizona-Sonora border

region

Seismic Region 4

Lower California and Gulf of California

47. Off west coast of Baja California
48. Baja California
49. Gulf of California
50. Sonora
51. Off coast of central Mexico
52. Near coast of central Mexico

Seismic Region 5

Mexico-Guatemala Area

53. Revilla Gigedo Islands region
54. Off coast of Jalisco
55. Near coast of Jalisco
56. Near coast of Michoacan
57. Michoacan
58. Near coast of Guerrero
59. Guerrero
60. Oaxaca
61. Chiapas
62. Mexico-Guatemala border region
63. Off coast of Mexico
64. Off coast of Michoacan
65. Off coast of Guerrero
66. Near coast of Oaxaca
67. Off coast of Oaxaca
68. Off coast of Chiapas
69. Near coast of Chiapas
70. Guatemala
71. Near coast of Guatemala
730. Northern East Pacific Rise

Seismic Region 6

Central America

72. Honduras
73. El Salvador
74. Near coast of Nicaragua
75. Nicaragua
76. Off coast of central America
77. Off coast of Costa Rica
78. Costa Rica
79. North of Panama
80. Panama-Costa Rica border region
81. Panama
82. Panama-Colombia border region
83. South of Panama

Seismic Region 7

Caribbean Loop

84. Yucatan Peninsula
85. Cuba region
86. Jamaica region

87. Haiti region
88. Dominican Republic region
89. Mona Passage
90. Puerto Rico region
91. Virgin Islands
92. Leeward Islands
93. Belize
94. Caribbean Sea
95. Windward Islands
96. Near north coast of Colombia
97. Near coast of Venezuela
98. Trinidad
99. Northern Colombia
100. Lake Maracaibo
101. Venezuela
731. North of Honduras

Seismic Region 8

Andean South America

102. Near west coast of Colombia
103. Colombia
104. Off coast of Ecuador
105. Near coast of Ecuador
106. Colombia-Ecuador border region
107. Ecuador
108. Off coast of northern Peru
109. Near coast of northern Peru
110. Peru-Ecuador border region
111. Northern Peru
112. Peru-Brazil border region
113. Western Brazil
114. Off coast of Peru
115. Near coast of Peru
116. Central Peru
117. Southern Peru
118. Peru-Bolivia border region
119. Northern Bolivia
120. Central Bolivia
121. Off coast of northern Chile
122. Near coast of northern Chile
123. Northern Chile
124. Chile-Bolivia border region
125. Southern Bolivia
126. Paraguay
127. Chile-Argentina border region
128. Jujuy Province
129. Salta Province
130. Catamarca Province
131. Tucuman Province
132. Santiago del Estero Province
133. Northeastern Argentina
134. Off coast of central Chile
135. Near coast of central Chile
136. Central Chile
137. San Juan Province
138. La Rioja Province
139. Mendoza Province

140. San Luis Province
141. Cordoba Province
142. Uruguay

Seismic Region 9

Extreme South America

143. Off coast of southern Chile
144. Southern Chile
145. Southern Chile-Argentina border region
146. Southern Argentina

Seismic Region 10

Southern Antilles

147. Tierra del Fuego
148. Falkland Islands region
149. Drake Passage
150. Scotia Sea
151. South Georgia Island region
152. South Georgia Rise
153. South Sandwich Islands region
154. South Shetland Islands
155. Antarctic Peninsula
156. Southwestern Atlantic Ocean
157. Weddell Sea
732. East of South Sandwich Islands

Seismic Region 11

New Zealand Region

158. Off west coast of North Island
159. North Island
160. Off east coast of North Island
161. Off west coast of South Island
162. South Island
163. Cook Strait
164. Off east coast of South Island
165. North of Macquarie Island
166. Auckland Islands region
167. Macquarie Island region
168. South of New Zealand

Seismic Region 12

Kermadec-Tonga-Samoa Area

169. Samoa Islands region
170. Samoa Islands
171. South of Fiji Islands
172. West of Tonga Islands (REGION NOT IN USE)
173. Tonga Islands
174. Tonga Islands region
175. South of Tonga Islands
176. North of New Zealand
177. Kermadec Islands region
178. Kermadec Islands
179. South of Kermadec Islands

Seismic Region 13

Fiji Area

180. North of Fiji Islands
181. Fiji Islands region
182. Fiji Islands

Seismic Region 14

Vanuatu (New Hebrides)

183. Santa Cruz Islands region
184. Santa Cruz Islands
185. Vanuatu Islands region
186. Vanuatu Islands
187. New Caledonia
188. Loyalty Islands
189. Southeast of Loyalty Islands

Seismic Region 15

Bismarck and Solomon Islands

190. New Ireland region
191. North of Solomon Islands
192. New Britain region
193. Bougainville-Solomon Islands region
194. D'Entrecasteaux Islands region
195. South of Solomon Islands

Seismic Region 16

New Guinea

196. Irian Jaya region
197. Near north coast of Irian Jaya
198. Ninigo Islands region
199. Admiralty Islands region
200. Near north coast of New Guinea
201. Irian Jaya
202. New Guinea
203. Bismarck Sea
204. Aru Islands region
205. Near south coast of Irian Jaya
206. Near south coast of New Guinea
207. Eastern New Guinea region
208. Arafura Sea

Seismic Region 17

Caroline Islands to Guam

209. Western Caroline Islands
210. South of Mariana Islands

Seismic Region 18

Guam to Japan

211. Southeast of Honshu
212. Bonin Islands region
213. Volcano Islands region
214. West of Mariana Islands
215. Mariana Islands region
216. Mariana Islands

Seismic Region 19

Japan-Kurils-Kamchatka

217. Kamchatka Peninsula
218. Near east coast of Kamchatka Peninsula
219. Off east coast of Kamchatka Peninsula
220. Northwest of Kuril Islands
221. Kuril Islands
222. East of Kuril Islands
223. Eastern Sea of Japan
224. Hokkaido region
225. Off southeast coast of Hokkaido
226. Near west coast of eastern Honshu
227. Eastern Honshu
228. Near east coast of eastern Honshu
229. Off east coast of Honshu
230. Near south coast of eastern Honshu

Seismic Region 20

Southwestern Japan and Ryukyu Islands

231. South Korea
232. Western Honshu
233. Near south coast of western Honshu
234. Northwest of Ryukyu Islands
235. Kyushu
236. Shikoku
237. Southeast of Shikoku
238. Ryukyu Islands
239. Southeast of Ryukyu Islands
240. West of Bonin Islands
241. Philippine Sea

Seismic Region 21

Taiwan

242. Near coast of southeastern China
243. Taiwan region
244. Taiwan
245. Northeast of Taiwan
246. Southwestern Ryukyu Islands
247. Southeast of Taiwan

Seismic Region 22

Philippines

248. Philippine Islands region
249. Luzon
250. Mindoro
251. Samar
252. Palawan
253. Sulu Sea
254. Panay

- 255. Cebu
- 256. Leyte
- 257. Negros
- 258. Sulu Archipelago
- 259. Mindanao
- 260. East of Philippine Islands

Seismic Region 23

Borneo-Sulawesi

- 261. Borneo
- 262. Celebes Sea
- 263. Talaud Islands
- 264. North of Halmahera
- 265. Minahassa Peninsula, Sulawesi
- 266. Northern Molucca Sea
- 267. Halmahera
- 268. Sulawesi
- 269. Southern Molucca Sea
- 270. Ceram Sea
- 271. Buru
- 272. Seram

Seismic Region 24

Sunda Arc

- 273. Southwest of Sumatera
- 274. Southern Sumatera
- 275. Java Sea
- 276. Sunda Strait
- 277. Jawa
- 278. Bali Sea
- 279. Flores Sea
- 280. Banda Sea
- 281. Tanimbar Islands region
- 282. South of Jawa
- 283. Bali region
- 284. South of Bali
- 285. Sumbawa region
- 286. Flores region
- 287. Sumba region
- 288. Savu Sea
- 289. Timor region
- 290. Timor Sea
- 291. South of Sumbawa
- 292. South of Sumba
- 293. South of Timor

Seismic Region 25

Myanmar and Southeast Asia

- 294. Myanmar-India border region
- 295. Myanmar-Bangladesh border region
- 296. Myanmar
- 297. Myanmar-China border region
- 298. Near south coast of Myanmar
- 299. Southeast Asia (REGION NOT IN USE)
- 300. Hainan Island

- 301. South China Sea
- 733. Thailand
- 734. Laos
- 735. Kampuchea
- 736. Vietnam
- 737. Gulf of Tongking

Seismic Region 26

India-Xizang-Szechwan-Yunnan

- 302. Eastern Kashmir
- 303. Kashmir-India border region
- 304. Kashmir-Xizang border region
- 305. Western Xizang-India border region
- 306. Xizang
- 307. Sichuan
- 308. Northern India
- 309. Nepal-India border region
- 310. Nepal
- 311. Sikkim
- 312. Bhutan
- 313. Eastern Xizang-India border region
- 314. Southern India
- 315. India-Bangladesh border region
- 316. Bangladesh
- 317. Northeastern India
- 318. Yunnan
- 319. Bay of Bengal

Seismic Region 27

Southern Xinjiang to Gansu

- 320. Kyrgyzstan-Xinjiang border region
- 321. Southern Xinjiang
- 322. Gansu
- 323. Western Nei Mongol
- 324. Kashmir-Xinjiang border region
- 325. Qinghai

Seismic Region 28

Alma-Ata to Lake Baikal

- 326. Southwestern Siberia
- 327. Lake Baykal region
- 328. East of Lake Baykal
- 329. Eastern Kazakhstan
- 330. Lake Issyk-Kul region
- 331. Kazakhstan-Xinjiang border region
- 332. Northern Xinjiang
- 333. Tuva-Buryatia-Mongolia border region
- 334. Mongolia

Seismic Region 29

Western Asia

- 335. Ural Mountains region
- 336. Western Kazakhstan
- 337. Eastern Caucasus
- 338. Caspian Sea
- 339. Northwestern Uzbekistan
- 340. Turkmenistan
- 341. Iran-Turkmenistan border region
- 342. Turkmenistan-Afghanistan border region
- 343. Turkey-Iran border region
- 344. Iran-Armenia-Azerbaijan border region
- 345. Northwestern Iran
- 346. Iran-Iraq border region
- 347. Western Iran
- 348. Northern and central Iran
- 349. Northwestern Afghanistan
- 350. Southwestern Afghanistan
- 351. Eastern Arabian Peninsula
- 352. Persian Gulf
- 353. Southern Iran
- 354. Southwestern Pakistan
- 355. Gulf of Oman
- 356. Off coast of Pakistan

Seismic Region 30

Middle East-Crimea-Eastern Balkans

- 357. Ukraine-Moldova-Southwestern Russia region
- 358. Romania
- 359. Bulgaria
- 360. Black Sea
- 361. Crimea region
- 362. Western Caucasus
- 363. Greece-Bulgaria border region
- 364. Greece
- 365. Aegean Sea
- 366. Turkey
- 367. Turkey-Georgia-Armenia border region
- 368. Southern Greece
- 369. Dodecanese Islands
- 370. Crete
- 371. Eastern Mediterranean Sea
- 372. Cyprus region
- 373. Dead Sea region
- 374. Jordan-Syria region
- 375. Iraq

Seismic Region 31

Western Mediterranean Area

- 376. Portugal
- 377. Spain

378. Pyrenees
379. Near south coast of France
380. Corsica
381. Central Italy
382. Adriatic Sea
383. Northwestern Balkan Peninsula
384. West of Gibraltar
385. Strait of Gibraltar
386. Balearic Islands
387. Western Mediterranean Sea
388. Sardinia
389. Tyrrhenian Sea
390. Southern Italy
391. Albania
392. Greece-Albania border region
393. Madeira Islands region
394. Canary Islands region
395. Morocco
396. Northern Algeria
397. Tunisia
398. Sicily
399. Ionian Sea
400. Central Mediterranean Sea
401. Near coast of Libya

Seismic Region 32

Atlantic Ocean

402. North Atlantic Ocean
403. Northern Mid-Atlantic Ridge
404. Azores Islands region
405. Azores Islands
406. Central Mid-Atlantic Ridge
407. North of Ascension Island
408. Ascension Island region
409. South Atlantic Ocean
410. Southern Mid-Atlantic Ridge
411. Tristan da Cunha region
412. Bouvet Island region
413. Southwest of Africa
414. Southeastern Atlantic Ocean
738. Reykjanes Ridge
739. Azores-Cape St. Vincent Ridge

Seismic Region 33

Indian Ocean

415. Eastern Gulf of Aden
416. Socotra region
417. Arabian Sea
418. Lakshadweep region
419. Northeastern Somalia
420. North Indian Ocean
421. Carlsberg Ridge
422. Maldive Islands region
423. Laccadive Sea
424. Sri Lanka
425. South Indian Ocean
426. Chagos Archipelago region

427. Mauritius-Reunion region
428. Southwest Indian Ridge
429. Mid-Indian Ridge
430. South of Africa
431. Prince Edward Islands region
432. Crozet Islands region
433. Kerguelen Islands region
434. Broken Ridge
435. Southeast Indian Ridge
436. Southern Kerguelen Plateau
437. South of Australia
740. Owen Fracture Zone region
741. Indian Ocean Triple Junction
742. Western Indian-Antarctic Ridge

Seismic Region 34

Eastern North America

438. Saskatchewan
439. Manitoba
440. Hudson Bay
441. Ontario
442. Hudson Strait region
443. Northern Quebec
444. Davis Strait
445. Labrador
446. Labrador Sea
447. Southern Quebec
448. Gaspé Peninsula
449. Eastern Quebec
450. Anticosti Island
451. New Brunswick
452. Nova Scotia
453. Prince Edward Island
454. Gulf of St. Lawrence
455. Newfoundland
456. Montana
457. Eastern Idaho
458. Hebgen Lake region, Montana
459. Yellowstone region
460. Wyoming
461. North Dakota
462. South Dakota
463. Nebraska
464. Minnesota
465. Iowa
466. Wisconsin
467. Illinois
468. Michigan
469. Indiana
470. Southern Ontario
471. Ohio
472. New York
473. Pennsylvania
474. Vermont-New Hampshire region
475. Maine
476. Southern New England

477. Gulf of Maine
478. Utah
479. Colorado
480. Kansas
481. Iowa-Missouri border region
482. Missouri-Kansas border region
483. Missouri
484. Missouri-Arkansas border region
485. Missouri-Illinois border region
486. New Madrid region, Missouri
487. Cape Girardeau region, Missouri
488. Southern Illinois
489. Southern Indiana
490. Kentucky
491. West Virginia
492. Virginia
493. Chesapeake Bay region
494. New Jersey
495. Eastern Arizona
496. New Mexico
497. Northwestern Texas-Oklahoma border region
498. Western Texas
499. Oklahoma
500. Central Texas
501. Arkansas-Oklahoma border region
502. Arkansas
503. Louisiana-Texas border region
504. Louisiana
505. Mississippi
506. Tennessee
507. Alabama
508. Western Florida
509. Georgia
510. Florida-Georgia border region
511. South Carolina
512. North Carolina
513. Off east coast of United States
514. Florida Peninsula
515. Bahama Islands
516. Eastern Arizona-Sonora border region
517. New Mexico-Chihuahua border region
518. Texas-Mexico border region
519. Southern Texas
520. Near coast of Texas
521. Chihuahua
522. Northern Mexico
523. Central Mexico
524. Jalisco
525. Veracruz
526. Gulf of Mexico
527. Bay of Campeche

Seismic Region 35

Eastern South America

- 528. Brazil
- 529. Guyana
- 530. Suriname
- 531. French Guiana

Seismic Region 36

Northwestern Europe

- 532. Eire
- 533. United Kingdom
- 534. North Sea
- 535. Southern Norway
- 536. Sweden
- 537. Baltic Sea
- 538. France
- 539. Bay of Biscay
- 540. The Netherlands
- 541. Belgium
- 542. Denmark
- 543. Germany
- 544. Switzerland
- 545. Northern Italy
- 546. Austria
- 547. Czech and Slovak Republics
- 548. Poland
- 549. Hungary

Seismic Region 37

Africa

- 550. Northwest Africa (REGION NOT IN USE)
- 551. Southern Algeria
- 552. Libya
- 553. Egypt
- 554. Red Sea
- 555. Western Arabian Peninsula
- 556. Chad region
- 557. Sudan
- 558. Ethiopia
- 559. Western Gulf of Aden
- 560. Northwestern Somalia
- 561. Off south coast of northwest Africa
- 562. Cameroon
- 563. Equatorial Guinea
- 564. Central African Republic
- 565. Gabon
- 566. Congo
- 567. Zaire
- 568. Uganda
- 569. Lake Victoria region
- 570. Kenya
- 571. Southern Somalia
- 572. Lake Tanganyika region
- 573. Tanzania
- 574. Northwest of Madagascar

- 575. Angola
- 576. Zambia
- 577. Malawi
- 578. Namibia
- 579. Botswana
- 580. Zimbabwe
- 581. Mozambique
- 582. Mozambique Channel
- 583. Madagascar
- 584. South Africa
- 585. Lesotho
- 586. Swaziland
- 587. Off coast of South Africa
- 743. Western Sahara
- 744. Mauritania
- 745. Mali
- 746. Senegal-Gambia region
- 747. Guinea region
- 748. Sierra Leone
- 749. Liberia region
- 750. Cote d'Ivoire
- 751. Burkina Faso
- 752. Ghana
- 753. Benin-Togo region
- 754. Niger
- 755. Nigeria

Seismic Region 38

Australia

- 588. Northwest of Australia
- 589. West of Australia
- 590. Western Australia
- 591. Northern Territory
- 592. South Australia
- 593. Gulf of Carpentaria
- 594. Queensland
- 595. Coral Sea
- 596. Northwest of New Caledonia
- 597. New Caledonia region
- 598. Southwest of Australia
- 599. Off south coast of Australia
- 600. Near coast of South Australia
- 601. New South Wales
- 602. Victoria
- 603. Near southeast coast of Australia
- 604. Near east coast of Australia
- 605. East of Australia
- 606. Norfolk Island region
- 607. Northwest of New Zealand
- 608. Bass Strait
- 609. Tasmania region
- 610. Southeast of Australia

Seismic Region 39

Pacific Basin

- 611. North Pacific Ocean

- 612. Hawaiian Islands region
- 613. Hawaiian Islands
- 614. Eastern Caroline Islands region
- 615. Marshall Islands region
- 616. Enewetak Atoll region
- 617. Bikini Atoll region
- 618. Gilbert Islands region
- 619. Johnston Island region
- 620. Line Islands region
- 621. Palmyra Island region
- 622. Kiritimati region
- 623. Tuvalu region
- 624. Phoenix Islands region
- 625. Tokelau Islands region
- 626. Northern Cook Islands
- 627. Cook Islands region
- 628. Society Islands region
- 629. Tubuai Islands region
- 630. Marquesas Islands region
- 631. Tuamotu Archipelago region
- 632. South Pacific Ocean

Seismic Region 40

Arctic Zone

- 633. Lomonosov Ridge
- 634. Arctic Ocean
- 635. Near north coast of Kalaallit Nunaat
- 636. Eastern Kalaallit Nunaat
- 637. Iceland region
- 638. Iceland
- 639. Jan Mayen Island region
- 640. Greenland Sea
- 641. North of Svalbard
- 642. Norwegian Sea
- 643. Svalbard region
- 644. North of Franz Josef Land
- 645. Franz Josef Land
- 646. Northern Norway
- 647. Barents Sea
- 648. Novaya Zemlya
- 649. Kara Sea
- 650. Near coast of northwestern Siberia
- 651. North of Severnaya Zemlya
- 652. Severnaya Zemlya
- 653. Near coast of northern Siberia
- 654. East of Severnaya Zemlya
- 655. Laptev Sea

Seismic Region 41

Eastern Asia

- 656. Southeastern Siberia
- 657. Priamurye-Northeastern China border region
- 658. Northeastern China
- 659. North Korea

660. Sea of Japan
661. Primorye
662. Sakhalin Island
663. Sea of Okhotsk
664. Southeastern China
665. Yellow Sea
666. Off east coast of southeastern China

Seismic Region 42
Northeastern Asia, Northern Alaska to Greenland

667. North of New Siberian Islands
668. New Siberian Islands
669. Eastern Siberian Sea
670. Near north coast of eastern Siberia
671. Eastern Siberia
672. Chukchi Sea
673. Bering Strait
674. St. Lawrence Island region
675. Beaufort Sea
676. Northern Alaska
677. Northern Yukon Territory
678. Queen Elizabeth Islands
679. Northwest Territories
680. Western Kalaallit Nunaat
681. Baffin Bay
682. Baffin Island region

Seismic Region 43
Southeastern and Antarctic Pacific Ocean

683. Southeastcentral Pacific Ocean
684. Southern East Pacific Rise
685. Easter Island region
686. West Chile Rise

687. Juan Fernandez Islands region
688. East of North Island
689. Chatham Islands region
690. South of Chatham Islands
691. Pacific-Antarctic Ridge
692. Southern Pacific Ocean
756. Southeast of Easter Island

Seismic Region 44
Galapagos Area

693. Eastcentral Pacific Ocean
694. Central East Pacific Rise
695. West of Galapagos Islands
696. Galapagos Islands region
697. Galapagos Islands
698. Southwest of Galapagos Islands
699. Southeast of Galapagos Islands
757. Galapagos Triple Junction region

Seismic Region 45
Macquarie Loop

700. South of Tasmania
701. West of Macquarie Island
702. Balleny Islands region

Seismic Region 46
Andaman Islands to Sumatera

703. Andaman Islands region
704. Nicobar Islands region
705. Off west coast of northern Sumatera
706. Northern Sumatera
707. Malay Peninsula
708. Gulf of Thailand

Seismic Region 47
Baluchistan

709. Southeastern Afghanistan
710. Pakistan
711. Southwestern Kashmir
712. India-Pakistan border region

Seismic Region 48
Hindu Kush and Pamir

713. Central Kazakhstan
714. Southeastern Uzbekistan
715. Tajikistan
716. Kyrgyzstan
717. Afghanistan-Tajikistan border region
718. Hindu Kush region
719. Tajikistan-Xinjiang border region
720. Northwestern Kashmir

Seismic Region 49
Northern Eurasia

721. Finland
722. Norway-Murmansk border region
723. Finland-Karelia border region
724. Baltic States-Belarus-Northwestern Russia
725. Northwestern Siberia
726. Northern and central Siberia

Seismic Region 50
Antarctica

727. Victoria Land
728. Ross Sea
729. Antarctica

11.2.3 IASPEI Magnitudes

The ISC publishes a diversity of magnitude data. Although trying to be as complete and specific as possible, preference is now given to magnitudes determined according to standard procedures recommended by the Working Group on Magnitude Measurements of the IASPEI Commission on Seismological Observation and Interpretation (CoSOI). So far, such standards have been agreed upon for the local magnitude ML , the local-regional mb_Lg , and for two types each of body-wave (mb and mB_BB) and surface-wave magnitudes (Ms_20 and Ms_BB). With the exception of ML , all other standard magnitudes are measured on vertical-component records only. BB stands for direct measurement on unfiltered velocity broadband records in a wide range of periods, provided that their passband covers at least the period range within which mB_BB and Ms_BB are supposed to be measured. Otherwise, a deconvolution has to be applied prior to the amplitude and period measurement so as to assure that this specification is met. In contrast, mb_Lg , mb and Ms_20 are based on narrowband amplitude measurements around periods of 1 s and 20 s, respectively.

ML is consistent with the original definition of the local magnitude by *Richter* (1935) and mB_BB in close agreement with the original definition of medium-period body-wave magnitude mB measured in a wide range of periods between some 2 to 20 s and calibrated with the *Gutenberg and Richter* (1956) Q -function for vertical-component P waves. Similarly, Ms_BB is best tuned to the unbiased use of the IASPEI (1967) recommended standard magnitude formula for surface-wave amplitudes in a wide range of periods and distances, as proposed by its authors *Vaněk et al.* (1962). In contrast, mb and Ms_20 are chiefly based on measurement standards defined by US agencies in the 1960s in conjunction with the global deployment of the World-Wide Standard Seismograph Network (WWSSN), which did not include medium or broadband recordings. Some modifications were made in the 1970s to account for IASPEI recommendations on extended measurement time windows for mb . Although not optimal for calibrating narrow-band spectral amplitudes measured around 1 s and 20 s only, mb and Ms_20 use the same original calibrations functions as mB_BB and Ms_BB . But mb and Ms_20 data constitute by far the largest available magnitude data sets. Therefore they continue to be used, with appreciation for their advantages (e.g., mb is by far the most frequently measured teleseismic magnitude and often the only available and reasonably good magnitude estimator for small earthquakes) and their shortcomings (see section 3.2.5.2 of Chapter 3 in NMSOP-2).

Abbreviated descriptions of the standard procedures for ML , mb_Lg , mb , mB_BB and Ms_BB are summarised below. For more details, including also the transfer functions of the simulation filters to be used, see www.iaspei.org/commissions/CSOI/Summary_WG-Recommendations_20130327.pdf.

All amplitudes used in the magnitude formulas below are in most circumstances to be measured as one-half the maximum deflection of the seismogram trace, peak-to-adjacent-trough or trough-to-adjacent-peak, where the peak and trough are separated by one crossing of the zero-line: this measurement is sometimes described as “one-half peak-to-peak amplitude.” The periods are to be measured as twice the time-intervals separating the peak and adjacent-trough from which the amplitudes are measured. The amplitude-phase arrival-times are to be measured and reported too as the time of the zero-crossing between the peak and adjacent-trough from which the amplitudes are measured. The issue of amplitude and period measuring procedures, and circumstances under which alternative procedures are acceptable or preferable, is discussed further in Section 5 of IS 3.3 and in section 3.2.3.3 of Chapter 3 of NMSOP-2.

Amplitudes measured according to recommended IASPEI standard procedures should be reported with the following ISF amplitude “phase names”: IAML, IAmb_Lg, IAmb, IAMs_20, IVmB_BB and IVMs_BB. “T” stands for “International” or “IASPEI”, “A” for displacement amplitude, measured in nm, and “V” for velocity amplitude, measured in nm/s. Although the ISC will calculate standard surface-wave magnitudes only for earthquakes shallower than 60 km, contributing agencies or stations are encouraged to report standard amplitude measurements of IAMs_20 and IVMs_BB for deeper earthquakes as well.

Note that the commonly known classical calibration relationships have been modified in the following to be consistent with displacements measured in nm, and velocities in nm/s, which is now common with high-resolution digital data and analysis tools. With these general definitions of the measurement parameters, where R is hypocentral distance in km (typically less than 1000 km), Δ is epicentral distance in degrees and h is hypocentre depth in km, the standard formulas and procedures read as follows:

ML :

$$ML = \log_{10}(A) + 1.11 \log_{10} R + 0.00189R - 2.09 \quad (11.14)$$

for crustal earthquakes in regions with attenuative properties similar to those of southern California, and with A being the maximum trace amplitude in nm that is measured on output from a horizontal-component instrument that is filtered so that the response of the seismograph/filter system replicates that of a Wood-Anderson standard seismograph (but with a static magnification of 1). For the normalised simulated response curve and related poles and zeros see Figure 1 and Table 1 in IS 3.3 of NMSOP-2.

Equation (11.14) is an expansion of that of *Hutton and Boore* (1987). The constant term in equation (11.14), -2.09 , is based on an experimentally determined static magnification of the Wood-Anderson of 2080 (see *Uhrhammer and Collins* (1990)), rather than the theoretical magnification of 2800 that was specified by the seismograph’s manufacturer. The formulation of equation (11.14) assures that reported ML amplitude data are not affected by uncertainty in the static magnification of the Wood-Anderson seismograph.

For seismographic stations containing two horizontal components, amplitudes are measured independently from each horizontal component and each amplitude is treated as a single datum. There is no effort to measure the two observations at the same time, and there is no attempt to compute a vector average. For crustal earthquakes in regions with attenuative properties that are different from those of coastal California and for measuring magnitudes with vertical-component seismographs the constants in the above equation have to be re-determined to adjust for the different regional attenuation and travel paths as well as for systematic differences between amplitudes measured on horizontal and vertical seismographs.

mb_Lg :

$$mb_Lg = \log_{10}(A) + 0.833 \log_{10} R + 0.434\gamma(R - 10) - 0.87 \quad (11.15)$$

where A = “sustained ground-motion amplitude” in nm, defined as the third largest amplitude in the time window corresponding to group velocities of 3.6 to 3.2 km/s, in the period (T) range 0.7 s to 1.3

s; R = epicentral distance in km, γ = coefficient of attenuation in km^{-1} . γ is related to the quality factor Q through the equation $\gamma = \pi/(QU T)$, where U is group velocity and T is the wave period of the L_g wave. γ is a strong function of crustal structure and should be determined specifically for the region in which the mb_Lg is to be used. A and T are measured on output from a vertical-component instrument that is filtered so that the frequency response of the seismograph/filter system replicates that of a WWSSN short-period seismograph (see Figure 1 and Table 1 in IS 3.3 of NMSOP-2). Arrival times with respect to the origin of the seismic disturbance are used, along with epicentral distance, to compute group velocity U .

mb :

$$mb = \log_{10}(A/T) + Q(\Delta, h) - 3.0 \quad (11.16)$$

where A = vertical component P-wave ground amplitude in nm measured at distances $20^\circ \leq \Delta \leq 100^\circ$ and calculated from the maximum trace-amplitude with $T < 3$ s in the entire P-phase train (time spanned by P, pP, sP, and possibly PcP and their codas, and ending preferably before PP). A and T are measured on output from an instrument that is filtered so that the frequency response of the seismograph/filter system replicates that of a WWSSN short-period seismograph (see Figure 1 and Table 1 in IS 3.3 of NMSOP-2). A is determined by dividing the maximum trace amplitude by the magnification of the simulated WWSSN-SP response at period T .

$Q(\Delta, h)$ = attenuation function for PZ (P-waves recorded on vertical component seismographs) established by *Gutenberg and Richter* (1956) in the tabulated or algorithmic form as used by the U.S. Geological Survey/National Earthquake Information Center (USGS/NEIC) (see Table 2 in IS 3.3 and program description PD 3.1 in NMSOP-2);

mB_BB :

$$mB_BB = \log_{10}(Vmax/2\pi) + Q(\Delta, h) - 3.0 \quad (11.17)$$

where $Vmax$ = vertical component ground velocity in nm/s at periods between $0.2 \text{ s} < T < 30 \text{ s}$, measured in the range $20^\circ \leq \Delta \leq 100^\circ$. $Vmax$ is calculated from the maximum trace-amplitude in the entire P-phase train (see mb), as recorded on a seismogram that is proportional to velocity at least in the period range of measurements. $Q(\Delta, h)$ = attenuation function for PZ established by *Gutenberg and Richter* (1956) (see 11.16). Equation (11.16) differs from the equation for mB of *Gutenberg and Richter* (1956) by virtue of the $\log_{10}(Vmax/2\pi)$ term, which replaces the classical $\log_{10}(A/T)_{max}$ term. Contributors should continue to send observations of A and T to ISC.

Ms_20 :

$$Ms_20 = \log_{10}(A/T) + 1.66 \log_{10} \Delta + 0.3 \quad (11.18)$$

where A = vertical-component ground displacement in nm at $20^\circ \leq \Delta \leq 160^\circ$ epicentral distance measured from the maximum trace amplitude of a surface-wave phase having a period T between 18 s and 22 s on a waveform that has been filtered so that the frequency response of the seismograph/filter

replicates that of a WWSSN long-period seismograph (see Figure 1 and Table 1 in IS 3.3 of NMSOP-2). A is determined by dividing the maximum trace amplitude by the magnification of the simulated WWSSN-LP response at period T . Equation (11.18) is formally equivalent to the Ms equation proposed by *Vaněk et al.* (1962) but is here applied to vertical motion measurements in a narrow range of periods.

Ms_BB :

$$Ms_BB = \log_{10} (Vmax/2\pi) + 1.66 \log_{10} \Delta + 0.3 \quad (11.19)$$

where $Vmax$ = vertical-component ground velocity in nm/s associated with the maximum trace-amplitude in the surface-wave train at periods between $3 \text{ s} < T < 60 \text{ s}$ as recorded at distances $2^\circ \leq \Delta \leq 160^\circ$ on a seismogram that is proportional to velocity in that range of considered periods. Equation (11.19) is based on the Ms equation proposed by *Vaněk et al.* (1962), but is here applied to vertical motion measurements and is used with the $\log_{10} (Vmax/2\pi)$ term replacing the $\log_{10} (A/T)_{max}$ term of the original. As for mB_BB , observations of A and T should be reported to ISC.

Mw :

$$Mw = (\log_{10} M_0 - 9.1) / 1.5 \quad (11.20)$$

Moment magnitude Mw is calculated from data of the scalar seismic moment M_0 (when given in Nm), or

$$Mw = (\log_{10} M_0 - 16.1) / 1.5 \quad (11.21)$$

its CGS equivalent when M_0 is in dyne-cm.

Please note that the magnitude nomenclature used in this Section uses the IASPEI standards as the reference. However, the magnitude type is typically written in plain text in most typical data reports and so it is in this document. Moreover, writing magnitude types in plain text allows us to reproduce the magnitude type as stored in the database and provides a more direct identification of the magnitude type reported by different agencies. A short description of the common magnitude types available in this Summary is given in table 8.6.

11.2.4 The IASPEI Seismic Format (ISF)

The ISF is the IASPEI approved standard format for the exchange of parametric seismological data (hypocentres, magnitudes, phase arrivals, moment tensors etc.) and is one of the formats used by the ISC. It was adopted as standard in August 2001 and is an extension of the International Monitoring System 1.0 (IMS1.0) standard, which was developed for exchanging data used to monitor the Comprehensive Nuclear-Test-Ban Treaty. An example of the ISF is shown in Listing 11.1.

Bulletins which use the ISF are comprised of origin and arrival information, provided in a series of data blocks. These include: a bulletin title block; an event title block; an origin block; a magnitude sub-block; an effect block; a reference block; and a phase block.

Within these blocks an important extension of the IMS1.0 standard is the ability to add additional comments and thus provide further parametric information. The ISF comments are distinguishable within the open parentheses required for IMS1.0 comments by beginning with a hash mark (#) followed by a keyword identifying the type of formatted comment. Each additional line required in the ISF comment begins with the hash (within the comment parentheses) followed by blank spaces at least as long as the keyword. Optional lines within the comment are signified with a plus sign (+) instead of a hash mark. The keywords include **PRIME** (to designate a prime origin of a hypocentre); **CENTROID** (to indicate the centroid origin); **MOMTENS** (moment tensor solution); **FAULT_PLANE** (fault plane solution); **PRINAX** (principal axes); **PARAM** (an origin parameter e.g. hypocentre depth given by a depth phase).

The full documentation for the ISF is maintained at the ISC and can be downloaded from:
www.isc.ac.uk/doc/code/isf/isf.pdf

The documentation for the IMS1.0 standard can be downloaded from:
www.isc.ac.uk/doc/code/isf/ims1_0.pdf

Listing 11.1: Example of an ISF formatted event

```

Event 15146084 Near east coast of eastern Honshu
Date Time Err RMS Latitude Longitude Smaj Smin Az Depth Err Ndef Nsta Gap mdist Mdlist Qual Author OrigID
2010/09/01 07:32:00 37.9000 141.9000f 37.0 44.0 71 281 11.00 51.10 uk BJI 15275482
(#MOMTENS sc MO fCLVD MRR MTT MPP MRT MTP MPR NST1 NST2 Author )
(# eMO eCLVD eRR eTT ePP eRT eTP ePR NCO1 NCO2 Duration )
(# 16 5.760 NIED )
(# )
(#FAULT_PLANE Typ Strike Dip Rake NP NS Plane Author )
(# BDC 199.00 19.00 86.00 NIED )
(+ 23.00 71.00 91.00 )
(Epicenter information from JMA Focal Mechanism Solution Determined Manually Variance reduction = 96.98%)
2010/09/01 07:32:47.50 1.470 37.8300 142.2400 6.7 4.5 110 44.0 114 490 478 122 0.65 92.01 m i fe ISCJB 16741494
2010/09/01 07:32:52.20 0.92 38.0320 141.8090 6.7 4.5 110 44.0 114 490 478 122 0.65 92.01 m i fe ISCJB 16741494
2010/09/01 07:32:52.53 0.35 0.889 37.9202 141.8229 4.090 2.740 145 49.7 2.76 490 478 122 0.65 92.01 m i fe ISCJB 16741494
(#PARAM pP_DEPTH=41.11021)
2010/09/01 07:32:52.60 0.10 37.9100 141.8700 1.1 0.9 -1 43.0 1.0 fe JMA 16271222
(Felt I=III-III J1)
2010/09/01 07:32:53.66 0.42 0.770 37.9250 141.7880 5.1 3.4 140 44.4 3.9 102 127 3.17 127.67 fe NEIC 01134459
(#MOMTENS sc MO fCLVD MRR MTT MPP MRT MTP MPR NST1 NST2 Author )
(# eMO eCLVD eRR eTT ePP eRT eTP ePR NCO1 NCO2 Duration )
(# 16 5.800 3.600 -0.550 -3.040 1.850 -1.140 4.150 NIED )
(# )
(#FAULT_PLANE Typ Strike Dip Rake NP NS Plane Author )
(# BDC 199.00 19.00 86.00 NIED )
(+ 23.00 71.00 91.00 )
(Recorded [3 JMA] in Miyagi; [2 JMA] in Fukushima and Iwate; [1 JMA] in Akita, Aomori, Ibaraki, Tochigi and Yamagata.)
2010/09/01 07:32:53.70 0.20 37.9300 142.0600 2.224 1.112 -1 50.3 1.0 262 89 GCMT 00124877
(#CENTROID)
(#MOMTENS sc MO fCLVD MRR MTT MPP MRT MTP MPR NST1 NST2 Author )
(# eMO eCLVD eRR eTT ePP eRT eTP ePR NCO1 NCO2 Duration )
(# 16 6.891 5.430 -0.440 -4.990 1.500 -2.070 3.710 64 89 GCMT )
(# 0.173 0.118 0.120 0.100 0.094 0.110 102 160 0.90 )
(#FAULT_PLANE Typ Strike Dip Rake NP NS Plane Author )
(# BDC 22.00 63.00 91.00 GCMT )
(+ 201.00 27.00 89.00 )
(#PRINAX sc T_val T_azim T_pl B_val B_azim B_pl P_val P_azim P_pl Author )
(# 16 6.711 293.00 72.00 0.360 201.00 0.00 -7.072 111.00 18.00 GCMT )
(nsta1 refers to body waves, cutoff=40s. nsta2 refers to surface waves, cutoff=50s.)
2010/09/01 07:32:55.05 1.77 1.070 37.8692 141.9450 12.9 10.4 100 63.6 16.8 36 127 3.24 117.04 uk IDC 16680924
2010/09/01 07:32:52.23 0.30 1.333 37.8836 141.9148 5.558 4.001 142 38.9 2.33 542 478 61 0.72 141.68 m i se ISC 01237353
(#PRIME)
(#PARAM pP_DEPTH=39.00000)

Magnitude Err Nsta Author OrigID
Mw 5.1 NIED 17047453
Ms 4.8 61 BJI 15275482
Ms7 4.6 58 BJI 15275482
mb 5.1 48 BJI 15275482
mb 5.0 63 BJI 15275482
MS 4.7 19 MOS 16741494
mb 5.2 49 MOS 16741494
MS 4.6 43 ISCJB 01631732
mb 4.9 138 ISCJB 01631732
mb 5.0 JMA 16271222
mb 5.0 55 NEIC 01134459
MW 5.1 NIED 01134459
MW 5.2 89 GCMT 00124877
MS 4.4 0.1 28 IDC 16680924
Msl 4.4 0.1 28 IDC 16680924
mb 4.4 0.1 27 IDC 16680924
mbi 4.5 0.0 33 IDC 16680924
mbimx 4.4 0.0 37 IDC 16680924
mbtmp 4.7 0.1 33 IDC 16680924
mslmx 4.3 0.1 31 IDC 16680924
MS 4.7 0.2 43 ISC 01237353
mb 4.9 0.2 145 ISC 01237353

Sta Dist EvAz Phase Time TRes Azim AzRes Slow SRes Def SNR Amp Per Qual Magnitude ArrID
JIO 0.72 322.1 Pn 07:33:05.9 -0.06 90.9 T-- 49540510
JIO 0.72 322.1 Sn 07:33:15.0 -0.82 T-- 49540511
JMM 0.89 269.2 Sn 07:33:08.4 0.2 T-- 49540512
JMM 0.89 269.2 Sn 07:33:19.2 -0.68 T-- 49540513
JFK 0.97 238.3 Pn 07:33:09.5 0.1 T-- 49540514
JFK 0.97 238.3 Sn 07:33:21.5 -0.54 T-- 49540515
JOU 1.10 296.4 Pn 07:33:11.5 0.4 T-- 49540516
JOU 1.10 296.4 Sn 07:33:25.4 0.3 T-- 49540517
UNAJ 1.18 229.0 Pn 07:33:12.4 0.1 T-- 49540530
JMK 1.20 333.1 Pn 07:33:12.5 0.0 T-- 49540518
JMK 1.20 333.1 Sn 07:33:27.1 -0.39 T-- 49540519
OFUJ 1.21 350.9 Pn 07:33:12.3 -0.34 T-- 49540531
.
.
532A 91.05 49.8 P 07:45:52.799 -0.00 90.9 T-- 05504129
334A 91.18 47.9 P 07:45:54.012 0.7 91.0 T-- 05504128
H06N1 91.36 64.9 T 09:27:33.559 --- 6.0 --- 58438458
MIAR 91.43 42.9 P 07:45:54.85 0.5 91.2 T-- 05504179
Y39A 91.60 43.6 P 07:45:55.543 0.4 91.4 T-- 05504214
534A 91.98 49.0 P 07:45:57.308 0.2 91.8 T-- 05504130
KEST 94.59 323.1 LR 08:33:52.432 320.5 38.70 --- 466.5 18.65 --- 58438480
ESDC 96.70 334.2 LR 08:34:40.011 345.0 38.30 --- 375.8 20.18 --- 58438449
TORO 117.01 315.6 PKPdf 07:51:32.55 -0.82 17.7 2.30 T-- 5.1 0.4 0.70 --- 58438504
TORO 117.01 315.6 PP 07:52:39.3 -2.90 31.2 6.30 T-- 6.5 1.3 0.68 --- 58438505
QSPA 127.62 180.0 PKPdf 07:51:52.02 -0.16 T-- 23535420
SNA4 141.68 197.1 PKPdf 07:52:13.761 -4.52 T-- 20375340
VNA2 143.24 196.3 PKPbc 07:52:18.562 0.4 122.0 2.31 --- 20375338
VNA1 143.64 196.2 PKPbc 07:52:19.77 0.6 --- 20375339

```

11.2.5 Ground Truth (GT) Events

Accurate locations are crucial in testing Earth models derived from body and surface wave tomography as well as in location calibration studies. ‘Ground Truth’ (GT) events are well-established source locations and origin times. A database of IASPEI reference events (GT earthquakes and explosions) is hosted at the ISC (www.isc.ac.uk). A full description of GT selection criteria can be found in *Bondár and McLaughlin* (2009a).

The events are coded by category GT0, GT1, GT2 or GT5, where the epicentre of a GT X event is known to within X km to a 95% confidence level. A map of all IASPEI reference events is shown in Figure 11.12 and the types of event are categorised in Figure 11.13. GT0 are explosions with announced locations and origin times. GT1 and GT2 are typically explosions, mine blasts or rock bursts either associated to explosion phenomenology located upon overhead imagery with seismically determined origin times, or precisely located by in-mine seismic networks. GT1-2 events are assumed to be shallow, but depth is unknown.

The database consists of nuclear explosions of GT0–5 quality, adopted from the Nuclear Explosion Database (*Bennett et al.*, 2010); GT0–5 chemical explosions, rock bursts, mine-induced events, as well as a few earthquakes, inherited from the reference event set by *Bondár et al.* (2004); GT5 events (typically earthquakes with crustal depths) which have been identified using either the method of *Bondár et al.* (2008) (2,275 events) or *Bondár and McLaughlin* (2009a) (updated regularly from the EHB catalogue (*Engdahl et al.*, 1998)), which uses the following criteria:

- 10 or more stations within 150 km from the epicentre
- one or more stations within 10 km
- $\Delta U \leq 0.35$
- a secondary azimuthal gap $\leq 160^\circ$

where ΔU is the network quality metric defined as the mean absolute deviation between the best-fitting uniformly distributed network of stations and the actual network:

$$\Delta U = \frac{4 \sum |esaz_i - (unif_i + b)|}{360N}, 0 \leq \Delta U \leq 1 \quad (11.22)$$

where N is the number of stations, $esaz_i$ is the i th event-to-station azimuth, $unif_i = 360i/N$ for $i = 0, \dots, N - 1$, and $b = \text{avg}(esaz_i) - \text{avg}(unif_i)$. ΔU is normalised so that it is 0 when the stations are uniformly distributed in azimuth and 1 when all the stations are at the same azimuth.

The seismological community is invited to participate in this project by nominating seismic events for the reference event database. Submitters may be contacted for further confirmation and for arrival time data. The IASPEI Reference Event List will be periodically published both in written and electronic form with proper acknowledgement of all submitters.

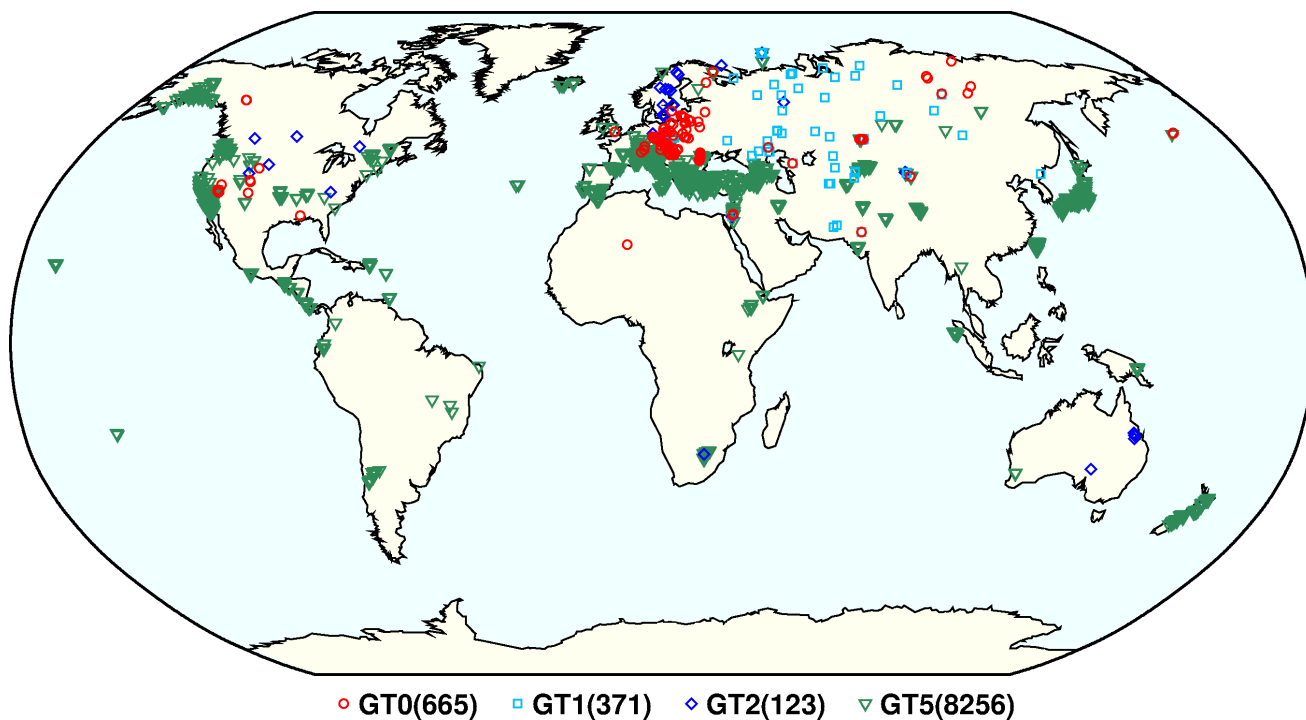


Figure 11.12: Map of all IASPEI Reference Events as of May 2018.

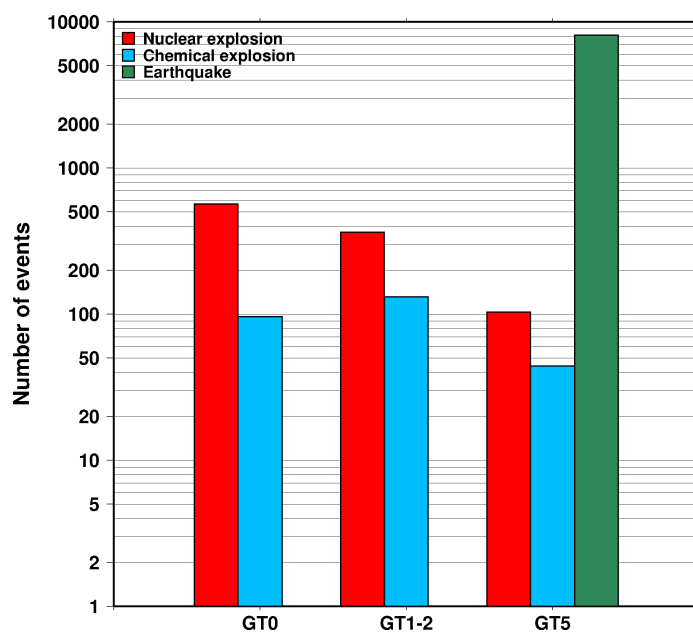


Figure 11.13: Histogram showing the event types within the IASPEI Reference Event list as of May 2018.

11.2.6 Nomenclature of Event Types

The nomenclature of event types currently used in the ISC Bulletin takes its origin from the IASPEI International Seismic Format (ISF).

Event type codes are composed of a leading character that generally indicates the confidence with which the type of the event is asserted and a trailing character that generally gives the type of the event. The leading and trailing characters may be used in any combination.

The **leading** characters are:

- s = suspected
- k = known
- f = felt (implies known)
- d = damaging (implies felt and known)

The **trailing** characters are:

- c = meteoritic event
- e = earthquake
- h = chemical explosion
- i = induced event
- l = landslide
- m = mining explosion
- n = nuclear explosion
- r = rock burst
- x = experimental explosion

A chemical explosion might be for mining or experimental purposes, and it is conceivable that other types of event might be assigned two or more different event type codes. This is deliberate, and matches the ambiguous identification of events in existing databases.

In addition, the code **uk** is used for events of unknown type and **ls** is used for known landslides.

The frequency of the different event types designated in the ISC Bulletin since 1964 is indicated in Figure 11.14.

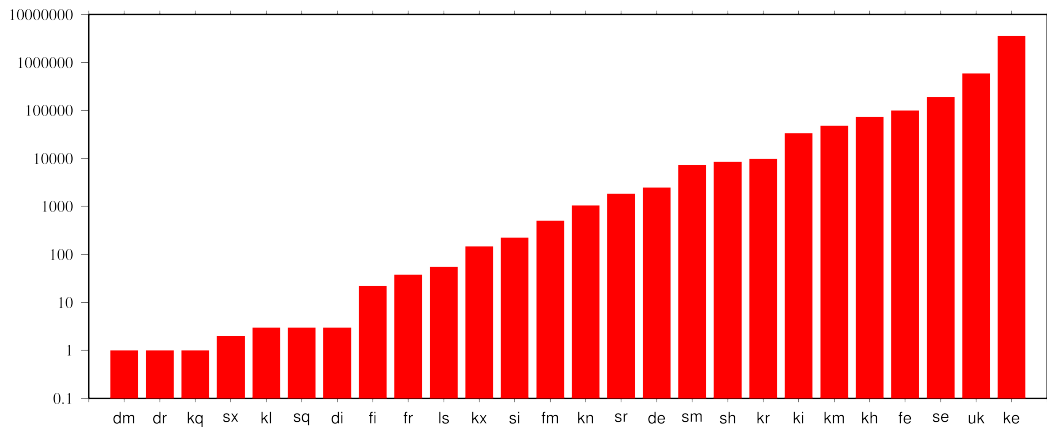


Figure 11.14: Event types in the ISC Bulletin

There are currently plans to revise this nomenclature as part of the coordination process between the National Earthquake Information Center (NEIC/USGS), European-Mediterranean Seismological Centre (CSEM) and the ISC.

11.3 Tables

Table 11.2: Listing of all 377 agencies that have directly reported to the ISC. The 149 agencies highlighted in bold have reported data to the ISC Bulletin for the period of this Bulletin Summary.

Agency Code	Agency Name
AAA	Alma-ata, Kazakhstan
AAE	University of Addis Ababa, Ethiopia
AAM	University of Michigan, USA
ADE	Primary Industries and Resources SA, Australia
ADH	Observatorio Afonso Chaves, Portugal
AEIC	Alaska Earthquake Information Center, USA
AFAR	The Afar Depression: Interpretation of the 1960-2000 Earthquakes, Israel
AFUA	University of Alabama, USA
ALG	Algiers University, Algeria
ANDRE	USSR
ANF	USArray Array Network Facility, USA
ANT	Antofagasta, Chile
ARE	Instituto Geofisico del Peru, Peru
ARO	Observatoire Géophysique d'Arta, Djibouti
ASIES	Institute of Earth Sciences, Academia Sinica, Chinese Taipei
ASL	Albuquerque Seismological Laboratory, USA
ASM	University of Asmara, Eritrea
ASRS	Altai-Sayan Seismological Centre, GS SB RAS, Russia
ATA	The Earthquake Research Center Ataturk University, Turkey
ATH	National Observatory of Athens, Greece
AUST	Geoscience Australia, Australia
AVETI	USSR
AWI	Alfred Wegener Institute for Polar and Marine Research, Germany

Table 11.2: Continued.

Agency Code	Agency Name
AZER	Republican Seismic Survey Center of Azerbaijan National Academy of Sciences, Azerbaijan
BCIS	Bureau Central International de Sismologie, France
BDF	Observatório Sismológico da Universidade de Brasília, Brazil
BELR	Centre of Geophysical Monitoring of the National Academy of Sciences of Belarus, Republic of Belarus
BEO	Seismological Survey of Serbia, Serbia
BER	University of Bergen, Norway
BERK	Berkheimer H, Germany
BGR	Bundesanstalt für Geowissenschaften und Rohstoffe, Germany
BGS	British Geological Survey, United Kingdom
BGSI	Botswana Geoscience Institute, Botswana
BHUI2	Study of Aftershocks of the Bhuj Earthquake by Japanese Research Team, Japan
BIAK	Biak earthquake aftershocks (17-Feb-1996), USA
BJI	China Earthquake Networks Center, China
BKK	Thai Meteorological Department, Thailand
BNS	Erdbebenstation, Geologisches Institut der Universität, Köl, Germany
BOG	Universidad Javeriana, Colombia
BRA	Geophysical Institute, Slovak Academy of Sciences, Slovakia
BRG	Seismological Observatory Berggießhübel, TU Bergakademie Freiberg, Germany
BRK	Berkeley Seismological Laboratory, USA
BRS	Brisbane Seismograph Station, Australia
BUC	National Institute for Earth Physics, Romania
BUD	Geodetic and Geophysical Research Institute, Hungary
BUEE	Earth & Environment, USA
BUG	Institute of Geology, Mineralogy & Geophysics, Germany
BUL	Goetz Observatory, Zimbabwe
BUT	Montana Bureau of Mines and Geology, USA
BYKL	Baykal Regional Seismological Centre, GS SB RAS, Russia
CADCG	Central America Data Centre, Costa Rica
CAN	Australian National University, Australia
CANSK	Canadian and Scandinavian Networks, Sweden
CAR	Instituto Sismologico de Caracas, Venezuela
CASC	Central American Seismic Center, Costa Rica
CENT	Centennial Earthquake Catalog, USA
CERI	Center for Earthquake Research and Information, USA
CFUSG	Inst. of Seismology and Geodynamics, V.I. Vernadsky Crimean Federal University, Republic of Crimea
CLL	Geophysikalisches Observatorium Collm, Germany
CMWS	Laboratory of Seismic Monitoring of Caucasus Mineral Water Region, GSRAS, Russia
CNG	Seismographic Station Changanane, Mozambique
CNRM	Centre National de Recherche, Morocco
COSMOS	Consortium of Organizations for Strong Motion Observations, USA

Table 11.2: Continued.

Agency Code	Agency Name
CRAAG	Centre de Recherche en Astronomie, Astrophysique et Géophysique, Algeria
CSC	University of South Carolina, USA
CSEM	Centre Sismologique Euro-Méditerranéen (CSEM/EMSC), France
CUPWA	Curtin University, Australia
DASA	Defense Atomic Support Agency, USA
DBN	Koninklijk Nederlands Meteorologisch Instituut, Netherlands
DDA	Disaster and Emergency Management Presidency, Turkey
DHMR	Yemen National Seismological Center, Yemen
DIAS	Dublin Institute for Advanced Studies, Ireland
DJA	Badan Meteorologi, Klimatologi dan Geofisika, Indonesia
DMN	National Seismological Centre, Nepal, Nepal
DNAG	USA
DNK	Geological Survey of Denmark and Greenland, Denmark
DRS	Dagestan Branch, Geophysical Survey, Russian Academy of Sciences, Russia
DSN	Dubai Seismic Network, United Arab Emirates
DUSS	Damascus University, Syria, Syria
EAF	East African Network, Unknown
EAGLE	Ethiopia-Afar Geoscientific Lithospheric Experiment, Unknown
EBR	Observatori de l'Ebre, Spain
EBSE	Ethiopian Broadband Seismic Experiment, Unknown
ECGS	European Center for Geodynamics and Seismology, Luxembourg
ECX	Centro de Investigación Científica y de Educación Superior de Ensenada, Mexico
EFATE	OBS Experiment near Efate, Vanuatu, USA
EHB	Engdahl, van der Hilst and Buland, USA
EIDC	Experimental (GSETT3) International Data Center, USA
EKA	Eskdalemuir Array Station, United Kingdom
ENT	Geological Survey and Mines Department, Uganda
EPSI	Reference events computed by the ISC for EPSI project, United Kingdom
ERDA	Energy Research and Development Administration, USA
EST	Geological Survey of Estonia, Estonia
EVBIB	Data from publications listed in the ISC Event Bibliography, Unknown
FBR	Fabra Observatory, Spain
FDF	Fort de France, Martinique
FIA0	Finessa Array, Finland
FOR	Unknown Historical Agency, Unknown - historical agency
FUBES	Earth Science Dept., Geophysics Section, Germany
FUNV	Fundación Venezolana de Investigaciones Sismológicas, Venezuela
FUR	Geophysikalisches Observatorium der Universität München, Germany
GBZT	Marmara Research Center, Turkey
GCG	INSIVUMEH, Guatemala
GCMT	The Global CMT Project, USA
GDNRW	Geologischer Dienst Nordrhein-Westfalen, Germany

Table 11.2: Continued.

Agency Code	Agency Name
GEN	Dipartimento per lo Studio del Territorio e delle sue Risorse (RSNI), Italy
GEOAZ	UMR Géoazur, France
GEOMR	GEOMAR, Germany
GFZ	Helmholtz Centre Potsdam GFZ German Research Centre For Geosciences, Germany
GII	The Geophysical Institute of Israel, Israel
GOM	Observatoire Volcanologique de Goma, Democratic Republic of the Congo
GRAL	National Council for Scientific Research, Lebanon
GSDM	Geological Survey Department Malawi, Malawi
GTFE	German Task Force for Earthquakes, Germany
GUC	Centro Sismológico Nacional, Universidad de Chile, Chile
HAN	Hannover, Germany
HDC	Observatorio Vulcanológico y Sismológico de Costa Rica, Costa Rica
HEL	Institute of Seismology, University of Helsinki, Finland
HFS	Hagfors Observatory, Sweden
HFS1	Hagfors Observatory, Sweden
HFS2	Hagfors Observatory, Sweden
HIMNT	Himalayan Nepal Tibet Experiment, USA
HKC	Hong Kong Observatory, Hong Kong
HLUG	Hessisches Landesamt für Umwelt und Geologie, Germany
HLW	National Research Institute of Astronomy and Geophysics, Egypt
HNR	Ministry of Mines, Energy and Rural Electrification, Solomon Islands
HON	Pacific Tsunami Warning Center - NOAA, USA
HRVD	Harvard University, USA
HRVD_LR	Department of Geological Sciences, Harvard University, USA
HVO	Hawaiian Volcano Observatory, USA
HYB	National Geophysical Research Institute, India
HYD	National Geophysical Research Institute, India
IAG	Instituto Andaluz de Geofísica, Spain
IASBS	Institute for Advanced Studies in Basic Sciences, Iran
IASPEI	IASPEI Working Group on Reference Events, USA
ICE	Instituto Costarricense de Electricidad, Costa Rica
IDC	International Data Centre, CTBTO, Austria
IDG	Institute of Dynamics of Geosphere, Russian Academy of Sciences, Russia
IEC	Institute of the Earth Crust, SB RAS, Russia
IEPN	Institute of Environmental Problems of the North, Russian Academy of Sciences, Russia
IGGSL	Seismology Lab, Institute of Geology & Geophysics, Chinese Academy of Sciences, China
IGIL	Instituto Geofísico do Infante Dom Luiz, Portugal
IGQ	Servicio Nacional de Sismología y Vulcanología, Ecuador
IGS	Institute of Geological Sciences, United Kingdom

Table 11.2: Continued.

Agency Code	Agency Name
INDEPTH3	International Deep Profiling of Tibet and the Himalayas, USA
INET	Instituto Nicaraguense de Estudios Territoriales - INETER, Nicaragua
INMG	Instituto Português do Mar e da Atmosfera, I.P., Portugal
INMGC	Instituto Nacional de Meteorologia e Geofísica, Cape Verde
IPEC	The Institute of Physics of the Earth (IPEC), Czech Republic
IPER	Institute of Physics of the Earth, Academy of Sciences, Moscow, Russia
IPGP	Institut de Physique du Globe de Paris, France
IPRG	Institute for Petroleum Research and Geophysics, Israel
IRIS	IRIS Data Management Center, USA
IRSM	Institute of Rock Structure and Mechanics, Czech Republic
ISK	Kandilli Observatory and Research Institute, Turkey
ISN	Iraqi Meteorological and Seismology Organisation, Iraq
ISS	International Seismological Summary, United Kingdom
IST	Institute of Physics of the Earth, Technical University of Istanbul, Turkey
ISU	Institute of Seismology, Academy of Sciences, Republic of Uzbekistan, Uzbekistan
ITU	Faculty of Mines, Department of Geophysical Engineering, Turkey
JEN	Geodynamisches Observatorium Moxa, Germany
JMA	Japan Meteorological Agency, Japan
JOH	Bernard Price Institute of Geophysics, South Africa
JSN	Jamaica Seismic Network, Jamaica
JSO	Jordan Seismological Observatory, Jordan
KBC	Institut de Recherches Géologiques et Minières, Cameroon
KEA	Korea Earthquake Administration, Democratic People's Republic of Korea
KEW	Kew Observatory, United Kingdom
KHC	Geofysikalni Ustav, Ceske Akademie Ved, Czech Republic
KISR	Kuwait Institute for Scientific Research, Kuwait
KLM	Malaysian Meteorological Service, Malaysia
KMA	Korea Meteorological Administration, Republic of Korea
KNET	Kyrgyz Seismic Network, Kyrgyzstan
KOLA	Kola Regional Seismic Centre, GS RAS, Russia
KRAR	Krasnoyarsk Scientific Research Inst. of Geology and Mineral Resources, Russia, Russia
KRL	Geodätisches Institut der Universität Karlsruhe, Germany
KRNET	Institute of Seismology, Academy of Sciences of Kyrgyz Republic, Kyrgyzstan
KRSC	Kamchatkan Experimental and Methodical Seismological Department, GS RAS, Russia
KRSZO	Geodetic and Geophysical Research Institute, Hungarian Academy of Sciences, Hungary
KSA	Observatoire de Ksara, Lebanon
KUK	Geological Survey Department of Ghana, Ghana
LAO	Large Aperture Seismic Array, USA
LDG	Laboratoire de Détection et de Géophysique/CEA, France
LDN	University of Western Ontario, Canada

Table 11.2: Continued.

Agency Code	Agency Name
LDO	Lamont-Doherty Earth Observatory, USA
LED	Landeserdbebendienst Baden-Württemberg, Germany
LEDBW	Landeserdbebendienst Baden-Württemberg, Germany
LER	Besucherbergwerk Binweide Station, Germany
LIB	Tripoli, Libya
LIC	Station Géophysique de Lamto, Ivory Coast
LIM	Lima, Peru
LIS	Instituto de Meteorologia, Portugal
LIT	Geological Survey of Lithuania, Lithuania
LJU	Slovenian Environment Agency, Slovenia
LPA	Universidad Nacional de La Plata, Argentina
LPZ	Observatorio San Calixto, Bolivia
LRSM	Long Range Seismic Measurements Project, Unknown
LSZ	Geological Survey Department of Zambia, Zambia
LVSN	Latvian Seismic Network, Latvia
MAN	Philippine Institute of Volcanology and Seismology, Philippines
MAT	The Matsushiro Seismological Observatory, Japan
MATSS	USSR
MCO	Macao Meteorological and Geophysical Bureau, Macao, China
MCSM	Main Centre for Special Monitoring, Ukraine
MDD	Instituto Geográfico Nacional, Spain
MED_RCMT	MedNet Regional Centroid - Moment Tensors, Italy
MERI	Maharashtra Engineering Research Institute, India
MES	Messina Seismological Observatory, Italy
MEX	Instituto de Geofísica de la UNAM, Mexico
MIRAS	Mining Institute of the Ural Branch of the Russian Academy of Sciences, Russia
MNH	Institut für Angewandte Geophysik der Universität München, Germany
MOLD	Institute of Geophysics and Geology, Moldova
MOS	Geophysical Survey of Russian Academy of Sciences, Russia
MOZ	Direccao Nacional de Geologia, Mozambique
MOZAR	, Mozambique
MRB	Institut Cartogràfic i Geològic de Catalunya, Spain
MSI	Messina Seismological Observatory, Italy
MSSP	Micro Seismic Studies Programme, PINSTECH, Pakistan
MSUGS	Michigan State University, Department of Geological Sciences, USA
MUN	Mundaring Observatory, Australia
NAI	University of Nairobi, Kenya
NAM	The Geological Survey of Namibia, Namibia
NAO	Stiftelsen NORSAR, Norway
NCEDC	Northern California Earthquake Data Center, USA
NDI	National Centre for Seismology of the Ministry of Earth Sciences of India, India
NEIC	National Earthquake Information Center, USA
NEIS	National Earthquake Information Service, USA
NERS	North Eastern Regional Seismological Centre, GS RAS, Russia
NIC	Cyprus Geological Survey Department, Cyprus

Table 11.2: Continued.

Agency Code	Agency Name
NIED	National Research Institute for Earth Science and Disaster Prevention, Japan
NKSZ	USSR
NNC	National Nuclear Center, Kazakhstan
NORS	North Ossetia (Alania) Branch, Geophysical Survey, Russian Academy of Sciences, Russia
NOU	IRD Centre de Nouméa, New Caledonia
NSSC	National Syrian Seismological Center, Syria
NSSP	National Survey of Seismic Protection, Armenia
OBM	Research Centre of Astronomy and Geophysics, Mongolia
OGAUC	Centro de Investigação da Terra e do Espaço da Universidade de Coimbra, Portugal
OGSO	Ohio Geological Survey, USA
OMAN	Sultan Qaboos University, Oman
ORF	Orfeus Data Center, Netherlands
OSPL	Observatorio Sismologico Politecnico Loyola, Dominican Republic
OSUB	Osservatorio Sismologico Universita di Bari, Italy
OTT	Canadian Hazards Information Service, Natural Resources Canada, Canada
PAL	Palisades, USA
PAS	California Institute of Technology, USA
PDA	Universidade dos Açores, Portugal
PDG	Seismological Institute of Montenegro, Montenegro
PEK	Peking, China
PGC	Pacific Geoscience Centre, Canada
PLV	National Center for Scientific Research, Vietnam
PMEL	Pacific seismicity from hydrophones, USA
PMR	Alaska Tsunami Warning Center,, USA
PNNL	Pacific Northwest National Laboratory, USA
PNSN	Pacific Northwest Seismic Network, USA
PPT	Laboratoire de Géophysique/CEA, French Polynesia
PRE	Council for Geoscience, South Africa
PRU	Geophysical Institute, Academy of Sciences of the Czech Republic, Czech Republic
PTO	Instituto Geofísico da Universidade do Porto, Portugal
PTWC	Pacific Tsunami Warning Center, USA
QCP	Manila Observatory, Philippines
QUE	Pakistan Meteorological Department, Pakistan
QUI	Escuela Politécnica Nacional, Ecuador
RAB	Rabaul Volcanological Observatory, Papua New Guinea
RBA	Université Mohammed V, Morocco
REN	MacKay School of Mines, USA
REY	Icelandic Meteorological Office, Iceland
RHSSO	Republic Hydrometeorological Service, Seismological Observatory, Banja Luka, Bosnia and Herzegovina

Table 11.2: Continued.

Agency Code	Agency Name
RISSC	Laboratory of Research on Experimental and Computational Seimology, Italy
RMIT	Royal Melbourne Institute of Technology, Australia
ROC	Odenbach Seismic Observatory, USA
ROM	Istituto Nazionale di Geofisica e Vulcanologia, Italy
RRLJ	Regional Research Laboratory Jorhat, India
RSMAC	Red Sísmica Mexicana de Apertura Continental, Mexico
RSNC	Red Sismológica Nacional de Colombia, Colombia
RSPR	Red Sísmica de Puerto Rico, USA
RYD	King Saud University, Saudi Arabia
SAPSE	Southern Alps Passive Seismic Experiment, New Zealand
SAR	Sarajevo Seismological Station, Bosnia and Herzegovina
SBDV	USSR
SCB	Observatorio San Calixto, Bolivia
SCEDC	Southern California Earthquake Data Center, USA
SCSIO	Key Laboratory of Ocean and Marginal Sea Geology, South China Sea, China
SDD	Universidad Autonoma de Santo Domingo, Dominican Republic
SEA	Geophysics Program AK-50, USA
SET	Setif Observatory, Algeria
SFS	Real Instituto y Observatorio de la Armada, Spain
SGS	Saudi Geological Survey, Saudi Arabia
SHL	Central Seismological Observatory, India
SIGU	Subbotin Institute of Geophysics, National Academy of Sciences, Ukraine
SIK	Seismic Institute of Kosovo, Unknown
SIO	Scripps Institution of Oceanography, USA
SJA	Instituto Nacional de Prevención Sísmica, Argentina
SJS	Instituto Costarricense de Electricidad, Costa Rica
SKHL	Sakhalin Experimental and Methodological Seismological Expedition, GS RAS, Russia
SKL	Sakhalin Complex Scientific Research Institute, Russia
SKO	Seismological Observatory Skopje, FYR Macedonia
SLC	Salt Lake City, USA
SLM	Saint Louis University, USA
SNET	Servicio Nacional de Estudios Territoriales, El Salvador
SNM	New Mexico Institute of Mining and Technology, USA
SNSN	Saudi National Seismic Network, Saudi Arabia
SOF	Geophysical Institute, Bulgarian Academy of Sciences, Bulgaria
SOMC	Seismological Observatory of Mount Cameroon, Cameroon
SOME	Seismological Experimental Methodological Expedition, Kazakhstan
SPA	USGS - South Pole, Antarctica
SPGM	Service de Physique du Globe, Morocco
SPITAK	, Armenia
SRI	Stanford Research Institute, USA
SSN	Sudan Seismic Network, Sudan

Table 11.2: Continued.

Agency Code	Agency Name
SSNC	Servicio Sismológico Nacional Cubano, Cuba
SSS	Centro de Estudios y Investigaciones Geotecnicas del San Salvador, El Salvador
STK	Stockholm Seismological Station, Sweden
STR	EOST / RéNaSS, France
STU	Stuttgart Seismological Station, Germany
SVSA	Sistema de Vigilância Sismológica dos Açores, Portugal
SYO	National Institute of Polar Research, Japan
SZGRF	Seismologisches Zentralobservatorium Gräfenberg, Germany
TAC	Estación Central de Tacubaya, Mexico
TAN	Antananarivo, Madagascar
TANZANIA	Tanzania Broadband Seismic Experiment, USA
TAP	CWB, Chinese Taipei
TAU	University of Tasmania, Australia
TEH	Tehran University, Iran
TEIC	Center for Earthquake Research and Information, USA
THE	Department of Geophysics, Aristotle University of Thessaloniki, Greece
THR	International Institute of Earthquake Engineering and Seismology (IIEES), Iran
TIF	Institute of Earth Sciences/ National Seismic Monitoring Center, Georgia
TIR	The Institute of Seismology, Academy of Sciences of Albania, Albania
TRI	Istituto Nazionale di Oceanografia e di Geofisica Sperimentale (OGS), Italy
TRN	The Seismic Research Centre, Trinidad and Tobago
TTG	Titograd Seismological Station, Montenegro
TUL	Oklahoma Geological Survey, USA
TUN	Institut National de la Météorologie, Tunisia
TVA	Tennessee Valley Authority, USA
TZN	University of Dar Es Salaam, Tanzania
UAF	Department of Geosciences, USA
UATDG	The University of Arizona, Department of Geosciences, USA
UAV	Red Sismológica de Los Andes Venezolanos, Venezuela
UCB	University of Colorado, Boulder, USA
UCC	Royal Observatory of Belgium, Belgium
UCDES	Department of Earth Sciences, United Kingdom
UCR	Sección de Sismología, Vulcanología y Exploración Geofísica, Costa Rica
UCSC	Earth & Planetary Sciences, USA
UESG	School of Geosciences, United Kingdom
UGN	Institute of Geonics AS CR, Czech Republic
ULE	University of Leeds, United Kingdom
UNAH	Universidad Nacional Autonoma de Honduras, Honduras
UPA	Universidad de Panama, Panama
UPIES	Institute of Earth- and Environmental Science, Germany

Table 11.2: Continued.

Agency Code	Agency Name
UPP	University of Uppsala, Sweden
UPSL	University of Patras, Department of Geology, Greece
UREES	Department of Earth and Environmental Science, USA
USAEC	United States Atomic Energy Commission, USA
USCGS	United States Coast and Geodetic Survey, USA
USGS	United States Geological Survey, USA
UTEP	Department of Geological Sciences, USA
UUSS	The University of Utah Seismograph Stations, USA
UVC	Universidad del Valle, Colombia
UWMDG	University of Wisconsin-Madison, Department of Geoscience, USA
VAO	Instituto Astronomico e Geofisico, Brazil
VIE	Zentralanstalt für Meteorologie und Geodynamik (ZAMG), Austria
VKMS	Lab. of Seismic Monitoring, Voronezh region, GSRAS & Voronezh State University, Russia
VLA	Vladivostok Seismological Station, Russia
VSI	University of Athens, Greece
VUW	Victoria University of Wellington, New Zealand
WAR	Institute of Geophysics, Polish Academy of Sciences, Poland
WASN	USA
WBNET	Institute of Geophysics, Czech Academy of Sciences, Czech Republic
WEL	Institute of Geological and Nuclear Sciences, New Zealand
WES	Weston Observatory, USA
WUSTL	Washington University Earth and Planetary Sciences, USA
YARS	Yakutiya Regional Seismological Center, GS SB RAS, Russia
ZAG	Seismological Survey of the Republic of Croatia, Croatia
ZEMSU	USSR
ZUR	Swiss Seismological Service (SED), Switzerland
ZUR_RMT	Zurich Moment Tensors, Switzerland

Table 11.3: Phases reported to the ISC. These include phases that could not be matched to an appropriate ak135 phases. Those agencies that reported at least 10% of a particular phase are also shown.

Reported Phase	Total	Agencies reporting
P	3475961	TAP (18%)
S	1674479	TAP (33%), JMA (15%)
AML	425070	ROM (64%), DDA (18%), ATH (17%)
IAmb	417705	NEIC (98%)
NULL	362717	NEIC (32%), AEIC (18%), IDC (18%), RSNC (15%)
Pn	246449	NEIC (45%)
IAML	215986	NEIC (63%), GUC (14%)
Pg	179040	NEIC (15%), NNC (13%), ZAG (13%)
Sg	148492	ZAG (16%), NEIC (12%)
LR	140133	IDC (67%), BJI (29%)
pmax	121453	MOS (69%), BJI (31%)
PG	103931	ISK (45%), HEL (25%), PRU (14%)
SG	91976	HEL (31%), ISK (28%), PRU (22%), IPEC (11%)
Sn	85476	INMG (13%), MDD (12%), IDC (12%), ZAG (11%)
PN	69305	ISK (59%), MOS (16%), HEL (13%)
IAMs_20	53967	NEIC (98%)
IAmb_Lg	46039	NEIC (100%)
Lg	41835	NNC (71%), IDC (17%)
PKP	27453	IDC (54%)
A	24961	INMG (49%), SKHL (23%), SVSA (15%), JMA (13%)
MSG	24270	HEL (100%)
T	23998	IDC (96%)
SN	22734	HEL (65%), ISK (16%)
pP	17833	BJI (47%), IDC (17%)
Vmb_Lg	16128	MDD (100%)
MLR	15685	MOS (100%)
PKPbc	15163	IDC (60%), BGR (12%), NEIC (12%)
PKIKP	14773	MOS (96%)
PKPdf	11654	NEIC (58%)
PcP	11477	IDC (67%), BJI (12%)
PP	11477	BJI (27%), IDC (20%), BELR (15%)
SB	11245	HEL (100%)
PB	10059	HEL (100%)
sP	8726	BJI (77%)
SS	8483	MOS (34%), BJI (28%), BELR (20%)
smax	7533	MOS (74%), BJI (26%)
PKPab	6401	IDC (44%), NEIC (20%), INMG (12%)
x	4942	NDI (28%), PRU (22%), CLL (20%), BRG (15%)
AMB	4537	SKHL (79%), BJI (21%)
AMS	4448	PRU (69%), KEA (22%)
END	4368	ROM (100%)
PKiKP	4103	IDC (39%), IRIS (29%)
Sb	3916	IRIS (76%), BELR (20%)
ScP	3755	IDC (76%), BJI (11%)
Amp	3500	BRG (100%)
SPECP	3473	DDA (100%)
PPP	3374	MOS (49%), BELR (45%)
LG	3319	BRA (80%), OTT (14%)
Trac	2913	OTT (100%)
SSS	2799	BELR (55%), MOS (33%)
PKP2	2597	MOS (91%)
LQ	2515	BELR (48%), INMG (21%), IEPN (16%), PPT (13%)
*PP	2448	MOS (100%)
LRM	2429	BELR (87%), MOLD (13%)
AMP	2411	IEPN (56%), TIR (37%)
Pb	2333	IRIS (55%), BELR (35%)
sS	2320	BJI (86%), BELR (11%)
PKKPbc	2244	IDC (96%)
Pdiff	1810	IRIS (55%), IDC (29%)
PKhKP	1576	IDC (100%)
Vmb_V	1397	MDD (100%)
SKS	1381	BJI (41%), BELR (31%), PRU (17%)
PS	1358	MOS (40%), BELR (27%), CLL (11%)
SKPbc	1333	IDC (92%)
L	1227	WAR (40%), BGR (34%), MOLD (20%)

Table 11.3: (continued)

Reported Phase	Total	Agencies reporting
AMl	1149	NIC (100%)
pPKP	1096	BJI (35%), IDC (34%), PRU (13%)
Smax	1085	BYKL (100%)
ScS	1016	BJI (66%), BELR (14%), IDC (11%)
IVMs_BB	1008	BER (75%), HYB (19%)
IVmB_BB	968	BER (57%), HYB (22%), DNK (13%)
X	930	JMA (71%), ISC1 (13%), SYO (12%)
Pdif	885	BER (34%), NEIC (19%), INMG (13%), BJI (11%)
Pmax	843	BYKL (93%)
PKPPKP	840	IDC (93%)
PKHKP	772	MOS (99%)
SKSac	768	BER (41%), INMG (12%), CLL (11%)
PKPDF	743	PRU (79%), BUD (21%)
*SP	585	MOS (100%)
SKP	557	IDC (50%), BELR (20%), PRU (13%)
SKKS	548	BELR (48%), BJI (47%)
pPKPbc	515	IDC (67%), BGR (21%)
sPKP	509	BJI (83%), BELR (13%)
max	474	BYKL (100%)
PKPAB	463	PRU (100%)
s	442	ROM (100%)
*SS	436	MOS (100%)
PKP1	420	LIC (96%)
Lm	410	CLL (100%)
PKKP	409	IDC (79%)
SP	397	BER (39%), MOS (27%)
p	386	ROM (99%)
PKKPab	296	IDC (92%)
PDIFF	281	BRA (45%), PRU (39%), IPEC (15%)
Sgmax	269	NERS (100%)
PcS	263	BJI (90%)
PKS	251	BJI (45%), BELR (42%)
AmB	249	KEA (100%)
LmV	247	CLL (100%)
PPS	246	CLL (57%), MOS (33%)
SKKPbc	246	IDC (93%)
PKP2bc	241	IDC (100%)
E	221	ZAG (94%)
pPKPdf	220	NEIC (19%), CLL (18%), OMAN (14%)
P3KPbc	207	IDC (100%)
PKPpre	204	NEIC (59%), PRU (31%)
Sm	189	SIGU (62%), CFUSG (38%)
Rg	187	IDC (48%), NNC (21%), NAO (16%), DNK (13%)
LmH	187	CLL (100%)
pPKPab	164	IDC (40%), CLL (22%), INMG (21%)
SKPdf	160	BER (48%), CLL (31%), NEIC (14%)
Pm	160	SIGU (75%), CFUSG (25%)
IVmBBB	151	BER (73%), HYB (25%)
P4KPbc	143	IDC (100%)
SSSS	127	CLL (100%)
pwP	116	ISC1 (79%), NEIC (21%)
ATPG	106	OSPL (98%)
ASSG	106	OSPL (98%)
ASPG	104	OSPL (98%)
PmP	103	BGR (63%), ZUR (37%)
ATSG	102	OSPL (98%)
PCP	102	PRU (56%), LPA (33%)
Pgmax	100	NERS (100%)
pPKiKP	99	OMAN (39%), CLL (25%), HYB (16%)
Pfiff	89	IRIS (100%)
SKKSac	82	CLL (46%), HYB (40%)
SKPab	79	IDC (70%), INMG (16%)
SmS	79	BGR (91%)
pPcP	78	IDC (94%)
H	72	IDC (100%)
Lmax	72	CLL (100%)
pPP	71	LPA (54%), CLL (38%)

Table 11.3: (continued)

Reported Phase	Total	Agencies reporting
PKP2ab	70	IDC (100%)
SKSdf	69	HYB (52%), BER (39%)
m	66	SIGU (100%)
(P)	64	BRG (100%)
PKPB	62	BUD (100%)
Snm	61	SIGU (87%), CFUSG (13%)
iAML	57	INMG (100%)
PKSdf	56	BER (59%), CLL (39%)
PKKPdf	52	AWI (50%), INMG (31%)
pPdiff	49	SYO (73%), BGR (18%)
AMd	48	NIC (100%)
P3KP	47	IDC (100%)
SKIKS	47	LPA (100%)
PnPn	45	UCC (96%)
Px	42	CLL (100%)
SKIKP	41	LPA (100%)
SKKP	40	IDC (40%), PRU (22%), AWI (12%)
MSN	39	HEL (64%), BER (36%)
PgPg	38	BYKL (97%)
PKIKS	38	LPA (100%)
pPxPxbc	36	BGR (100%)
Sdif	36	CLL (86%)
rx	35	SKHL (100%)
RG	35	IPEC (77%), HEL (23%)
LQM	34	MOLD (100%)
SCS	34	LPA (100%)
sPP	34	CLL (100%)
PPPP	33	CLL (100%)
pPdif	33	INMG (70%), CLL (12%)
PSKS	32	CLL (100%)
IVMsBB	30	BER (53%), HYB (30%)
PKPf	29	BRG (100%)
(sP)	27	CLL (100%)
sPKiKP	27	HYB (48%), CLL (30%), UCC (22%)
Sgm	25	SIGU (100%)
Plp	25	CLL (100%)
LMZ	23	WAR (100%)
sPKPbc	23	BGR (83%)
PKPpB	23	BUD (100%)
sSS	23	CLL (100%)
SCP	23	IPEC (52%), PRU (48%)
P*	23	MOS (52%), BGR (35%), BJI (13%)
P1	22	ZUR (100%)
SKSp	22	BRA (86%), WAR (14%)
PKPdif	21	CLL (86%), LJU (14%)
i	21	INMG (100%)
(SSS)	20	CLL (100%)
SPP	20	CLL (40%), BELR (40%), MOS (20%)
IAMb	20	LJU (100%)
SgSg	20	BYKL (100%)
Cod	19	SFS (100%)
Pnm	19	SIGU (95%)
sPKPpdf	17	CLL (47%), HYB (18%), IEPN (18%), SYO (18%)
SKiKP	17	IDC (59%), AWI (29%)
SDIFF	17	LPA (82%), IPEC (12%)
(SSSS)	16	CLL (100%)
sPdif	16	SYO (69%), LJU (25%)
(PP)	16	CLL (94%)
PKKS	16	IEPN (50%), PRU (44%)
PKPPKPpdf	16	CLL (100%)
Pgm	15	SIGU (100%)
SDIF	15	PRU (100%)
tx	14	SOME (79%), IEPN (21%)
PSPS	14	CLL (100%)
Sx	14	CLL (93%)
(pP)	13	CLL (100%)
PSP	13	LPA (100%)

Table 11.3: (continued)

Reported Phase	Total	Agencies reporting
LgX	12	MDD (100%)
sSKS	12	BELR (100%)
(Pg)	12	CLL (75%), SIGU (17%)
MPN	12	HEL (75%), BER (25%)
SKKPab	11	IDC (64%), LJU (18%), BGR (18%)
PxPxbc	11	BGR (100%)
P4KP	11	IDC (100%)
del	11	AUST (73%), KNET (27%)
(Sg)	10	CLL (50%), BRG (30%), SIGU (20%)
(PKPab)	10	CLL (100%)
SKKSdf	10	CLL (50%), HYB (50%)
PDIF	10	BUD (100%)
pPn	10	UCC (60%), HYB (30%)
(SS)	10	CLL (100%)
mb	10	KMA (100%)
Sglp	10	CLL (100%)
PKSab	9	CLL (100%)
iAmb	9	INMG (100%)
(pPKPdf)	9	CLL (100%)
(Pn)	9	SIGU (44%), BRG (33%), CLL (22%)
PPPprev	9	CLL (100%)
S*	8	BGR (88%), BJI (12%)
Sdiff	8	LJU (88%), SYO (12%)
EePg	8	ZAG (100%)
IAMs	8	EAF (100%)
SKKPdf	8	PPT (50%), HYB (38%), CLL (12%)
SKSSKSac	8	CLL (100%)
PbPb	8	UCC (100%)
pKP	8	BRA (100%)
sPKPab	8	CLL (88%), AWI (12%)
(PKPdf)	7	CLL (100%)
AMPN	7	INET (100%)
PKSbc	7	CLL (100%)
pPKIKP	7	IPEC (100%)
(PcP)	7	CLL (100%)
AMSN	7	INET (100%)
SKPa	7	NAO (86%), BER (14%)
M	7	MOLD (71%), LJU (29%)
PKKSbc	7	CLL (43%), HYB (29%), IEPN (29%)
(PKiKP)	7	CLL (100%)
R	7	LDG (100%)
PSS	6	CLL (100%)
sPS	6	CLL (100%)
(pPKiKP)	6	CLL (100%)
SKPb	6	NAO (67%), BER (33%)
Piff	6	BRG (100%)
PKPlp	6	CLL (100%)
SKPDF	6	BRA (100%)
PKPM	6	MOLD (100%)
pPKKPbc	5	CLL (100%)
(Sn)	5	CLL (60%), SIGU (40%)
(PPP)	5	CLL (100%)
LqM	5	MOLD (100%)
sSSS	5	CLL (100%)
(PPS)	5	CLL (100%)
sPcP	5	CLL (100%)
(SP)	5	CLL (100%)
sPdif	5	CLL (80%), HYB (20%)
sPn	5	HYB (40%), BJI (40%), UCC (20%)
pS	5	BELR (40%), CLL (40%), BRG (20%)
sSKSsac	5	CLL (80%), HYB (20%)
Siff	5	BRG (100%)
sPPS	5	CLL (100%)
sPPP	4	CLL (100%)
SSP	4	CLL (100%)
pSKPdf	4	CLL (100%)
(PS)	4	CLL (100%)

Table 11.3: (continued)

Reported Phase	Total	Agencies reporting
SKPPKPdf	4	CLL (100%)
(pPKPab)	4	CLL (100%)
(PKPbc)	4	CLL (100%)
SnSn	4	HYB (50%), UCC (50%)
PKPa	4	NAO (100%)
Lq	4	MOLD (100%)
I	4	SOME (100%)
(PKP)	4	BRG (75%), CLL (25%)
(sS)	4	CLL (100%)
sp	4	INMG (100%)
P'P'df	4	AWI (100%)
iAMs_20	4	INMG (100%)
PPPPrev	3	CLL (100%)
(PPPP)	3	CLL (100%)
SH	3	SYO (100%)
P2	3	ECX (100%)
PM	3	MOLD (100%)
PPmax	3	CLL (100%)
SKSP	3	CLL (100%)
EePn	3	ZAG (100%)
(sPP)	3	CLL (100%)
PSSrev	3	CLL (100%)
PP(2)	3	CLL (100%)
PPlp	3	CLL (100%)
(pSKPpdf)	3	CLL (100%)
sSKPpdf	3	CLL (100%)
(SKSac)	3	CLL (100%)
(SKPpdf)	3	CLL (100%)
PKPPKP'	3	BRG (100%)
(PKSdf)	2	CLL (100%)
sPKKKPpdf	2	CLL (100%)
pPS	2	CLL (100%)
sSKKSac	2	CLL (100%)
SKPPKPbc	2	CLL (100%)
sSdif	2	CLL (100%)
pSKSac	2	CLL (100%)
SSSrev	2	CLL (100%)
pScP	2	IDC (100%)
pPKKPab	2	CLL (100%)
(PKKSdf)	2	CLL (100%)
P(2)	2	CLL (100%)
(PSPS)	2	CLL (100%)
PKiK	2	HYB (100%)
(Pdif)	2	CLL (100%)
Sgc	2	WAR (100%)
(SKPbc)	2	CLL (100%)
SPKPDF	2	BUD (100%)
(sPKiKP)	2	CLL (100%)
pPKSab	2	CLL (100%)
LV	2	CLL (100%)
(SKSP)	2	CLL (100%)
LM	2	MOLD (100%)
sSSSS	2	CLL (100%)
PKPmax	2	CLL (100%)
pPKPdif	2	CLL (100%)
Sd2	2	ATH (100%)
(SKKSac)	2	CLL (100%)
sPSKS	2	CLL (100%)
PKP'PKP'	2	BRG (100%)
R2	2	CLL (100%)
(pPKPbc)	2	CLL (100%)
PKPbc(2)	2	CLL (100%)
PKPPKPbc	1	CLL (100%)
PPPPmax	1	CLL (100%)
pSKSP	1	CLL (100%)
pPKPPKP	1	CLL (100%)
pPSKS	1	CLL (100%)

Table 11.3: (continued)

Reported Phase	Total	Agencies reporting
SKKSa	1	BRG (100%)
pPDIFF	1	IPEC (100%)
SSrev	1	CLL (100%)
i-	1	INMG (100%)
pPmax	1	CLL (100%)
(PSS)	1	CLL (100%)
pPKPabm	1	CLL (100%)
pg	1	BRG (100%)
PC	1	SYO (100%)
SSmax	1	CLL (100%)
epPKPpdf	1	CLL (100%)
PV	1	MOLD (100%)
(PPPprev)	1	CLL (100%)
(pSKPbc)	1	CLL (100%)
p3PKPpdf	1	CLL (100%)
PSPSrev	1	CLL (100%)
PE	1	ECX (100%)
PPKPDF	1	BUD (100%)
sSP	1	CLL (100%)
AP	1	MOS (100%)
WSKS	1	MOS (100%)
(pPS)	1	CLL (100%)
sPKKPbc	1	CLL (100%)
pPKKPpdf	1	CLL (100%)
Pp	1	MOLD (100%)
3PKPab	1	CLL (100%)
(sSS)	1	CLL (100%)
PPP(3)	1	CLL (100%)
Sdiff(2)	1	CLL (100%)
SKPd	1	HYB (100%)
Lqm	1	MOLD (100%)
Amb	1	DNK (100%)
SSlp	1	CLL (100%)
(sPPS)	1	CLL (100%)
Pd0	1	ATH (100%)
LmV(360	1	CLL (100%)
P(4)	1	CLL (100%)
sg	1	BER (100%)
pPKSdf	1	CLL (100%)
AMLv	1	MDD (100%)
SSS(2)	1	CLL (100%)
pPPP	1	CLL (100%)
P5KP	1	IDC (100%)
pSKKPbc	1	CLL (100%)
SKSac(2)	1	CLL (100%)
XM	1	MOLD (100%)
PSKSrev	1	CLL (100%)
PKKSdf	1	HYB (100%)
(SPP)	1	CLL (100%)
(Sdif)	1	CLL (100%)
SbSb	1	UCC (100%)
h	1	KRSC (100%)
-	1	SVSA (100%)
pPPS	1	CLL (100%)
P9	1	EAF (100%)
On	1	SYO (100%)
Pdif(2)	1	CLL (100%)
sPSPS	1	CLL (100%)
PKPab(2)	1	CLL (100%)
pSKKSac	1	CLL (100%)
SSSmax	1	CLL (100%)
P(3)	1	CLL (100%)
pSKPab	1	CLL (100%)
PPPmax	1	CLL (100%)
(pPcP)	1	CLL (100%)
SKPPKP	1	BRG (100%)
(sPdif)	1	CLL (100%)

Table 11.3: *(continued)*

Reported Phase	Total	Agencies reporting
SS(2)	1	CLL (100%)
PKPabmax	1	CLL (100%)
EiPg	1	ZAG (100%)
(pPP)	1	CLL (100%)
(PKPdif)	1	CLL (100%)
(SKKPbc)	1	CLL (100%)
PKPRpre	1	CLL (100%)
3PKPdf	1	CLL (100%)
(SKPab)	1	CLL (100%)
pPKKSbc	1	CLL (100%)
qM	1	MOLD (100%)
PKPdf(2)	1	CLL (100%)
sPKKPab	1	CLL (100%)
(sPKPdf)	1	CLL (100%)

Table 11.4: Reporters of amplitude data

Agency	Number of reported amplitudes	Number of amplitudes in ISC located events	Number used for ISC <i>mb</i>	Number used for ISC <i>MS</i>
NEIC	643752	261424	182145	25040
IDC	409512	387913	126282	68910
ROM	274385	7216	0	0
WEL	200517	35186	0	0
MOS	108098	104245	52716	11359
DJA	97423	59530	12757	0
NNC	96954	36281	60	0
BJI	80576	76395	18946	24420
DDA	75951	7798	0	0
SOME	74606	28071	1983	0
ATH	70690	8526	0	0
ISK	67806	11743	0	0
RSNC	56084	5607	0	0
VIE	37146	20532	7825	0
GUC	30211	7739	26	5
THE	24783	4423	0	0
HEL	24248	579	0	0
MDD	20334	8493	0	0
LDG	19054	4613	4	0
INMG	16155	10295	2764	0
PRU	13980	4322	0	2551
BER	11779	2611	154	8
SKHL	9742	5145	0	0
DMN	9289	8910	5481	0
MAN	7796	2331	0	0
SSNC	7572	918	13	0
PPT	6809	5773	663	1994
NIC	6526	2809	0	0
DNK	6469	3654	2807	16
JMA	6451	6441	0	0
BELR	5839	4148	511	1292
LJU	5755	175	5	8
TEH	5642	3152	0	0
YARS	5433	117	0	0
NOU	5209	5009	3548	0
ZUR	4958	365	0	0
PRE	4837	2181	1274	85
BUC	4776	981	0	0
BGR	4686	4418	3229	0
MRB	4540	242	0	0
SNET	4322	1732	0	0
WBNET	4105	0	0	0
SVSA	4003	546	314	0
OSPL	3666	937	0	0

Table 11.4: *Continued.*

Agency	Number of reported amplitudes	Number of amplitudes in ISC located events	Number used for ISC <i>mb</i>	Number used for ISC <i>MS</i>
BRG	3500	2157	0	0
BGS	3499	2236	1267	504
SJA	3315	3288	0	0
NDI	3300	2869	1090	39
CLL	2925	2579	438	285
OTT	2912	369	0	0
KNET	2427	996	0	0
PDG	2405	1635	0	0
BYKL	2362	988	0	0
ECX	2040	352	0	0
NAO	1983	1958	1466	0
SCB	1845	575	0	0
IEPN	1811	1488	21	1
KEA	1709	1279	0	173
LIC	1682	1463	816	0
UCC	1611	1459	1205	0
IPEC	1488	278	0	0
SKO	1466	138	0	0
LVSN	1377	136	0	0
ASRS	1376	840	0	0
MIRAS	1242	113	0	0
IGIL	1183	784	121	159
UCR	1060	999	0	0
MOLD	990	658	135	0
KRSZO	969	190	0	0
TIR	896	412	0	0
ISN	763	283	0	0
WAR	507	499	0	389
INET	496	187	0	0
HYB	484	460	4	1
SIGU	392	120	0	0
NERS	375	123	0	0
AAE	247	149	0	55
MCSM	236	209	0	0
CFUSG	233	161	0	0
LIT	206	129	1	0
JSO	152	125	0	0
EAF	75	36	0	1
SSN	58	32	1	0
THR	52	52	0	0
UPA	50	14	0	3
PLV	26	22	0	0
LSZ	15	2	0	0

12

Glossary of ISC Terminology

- Agency/ISC data contributor

An academic or government institute, seismological organisation or company, geological/meteorological survey, station operator or author that reports or contributed data in the past to the ISC or one of its predecessors. Agencies may contribute data to the ISC directly, or indirectly through other ISC data contributors.

- Agency code

A unique, maximum eight-character code for a data reporting agency (e.g. NEIC, GFZ, BUD) or author (e.g. ISC, EHB, IASPEI). Often the agency code is the commonly used acronym of the reporting institute.

- Arrival

A phase pick at a station is characterised by a phase name and an arrival time.

- Associated phase

Associated phase arrival or amplitude measurements represent a collection of observations belonging to (i.e. generated by) an event. The complete set of observations are associated to the prime hypocentre.

- Azimuthal gap/Secondary azimuthal gap

The azimuthal gap for an event is defined as the largest angle between two stations with defining phases when the stations are ordered by their event-to-station azimuths. The secondary azimuthal gap is the largest azimuthal gap a single station closes.

- BAAS

Seismological bulletins published by the British Association for the Advancement of Science (1913-1917) under the leadership of H.H. Turner. These bulletins are the predecessors of the ISS Bulletins and include reports from stations distributed worldwide.

- Bulletin

An ordered list of event hypocentres, uncertainties, focal mechanisms, network magnitudes, as well as phase arrival and amplitude observations associated to each event. An event bulletin may list all the reported hypocentres for an event. The convention in the ISC Bulletin is that the preferred (prime) hypocentre appears last in the list of reported hypocentres for an event.

- Catalogue

An ordered list of event hypocentres, uncertainties and magnitudes. An event catalogue typically lists only the preferred (prime) hypocentres and network magnitudes.

- CoSOI/IASPEI

Commission on Seismological Observation and Interpretation, a commission of IASPEI that prepares and discusses international standards and procedures in seismological observation and interpretation.

- Defining/Non-defining phase

A defining phase is used in the location of the event (time-defining) or in the calculation of the network magnitude (magnitude-defining). Non-defining phases are not used in the calculations because they suffer from large residuals or could not be identified.

- Direct/Indirect report

A data report sent (e-mailed) directly to the ISC, or indirectly through another ISC data contributor.

- Duplicates

Nearly identical phase arrival time data reported by one or more agencies for the same station. Duplicates may be created by agencies reporting observations from other agencies, or several agencies independently analysing the waveforms from the same station.

- Event

A natural (e.g. earthquake, landslide, asteroid impact) or anthropogenic (e.g. explosion) phenomenon that generates seismic waves and its source can be identified by an event location algorithm.

- Grouping

The ISC algorithm that organises reported hypocentres into groups of events. Phases associated to any of the reported hypocentres will also be associated to the preferred (prime) hypocentre. The grouping algorithm also attempts to associate phases that were reported without an accompanying hypocentre to events.

- Ground Truth

An event with a hypocentre known to certain accuracy at a high confidence level. For instance, GT0 stands for events with exactly known location, depth and origin time (typically explosions); GT5 stands for events with their epicentre known to 5 km accuracy at the 95% confidence level, while their depth and origin time may be known with less accuracy.

- Ground Truth database

On behalf of IASPEI, the ISC hosts and maintains the IASPEI Reference Event List, a bulletin of ground truth events.

- IASPEI

International Association of Seismology and Physics of the Earth Interior, www.iaspei.org.

- International Registry of Seismograph Stations (IR)

Registry of seismographic stations, jointly run by the ISC and the World Data Center for Seismology, Denver (NEIC). The registry provides and maintains unique five-letter codes for stations participating in the international parametric and waveform data exchange.

- ISC Bulletin

The comprehensive bulletin of the seismicity of the Earth stored in the ISC database and accessible through the ISC website. The bulletin contains both natural and anthropogenic events. Currently the ISC Bulletin spans more than 50 years (1960-to date) and it is constantly extended by adding both recent and past data. Eventually the ISC Bulletin will contain all instrumentally recorded events since 1900.

- ISC Governing Council

According to the ISC Working Statutes the Governing Council is the governing body of the ISC, comprising one representative for each ISC Member.

- ISC-located events

A subset of the events selected for ISC review are located by the ISC. The rules for selecting an event for location are described in Section 11.1.3; ISC-located events are denoted by the author ISC.

- ISC Member

An academic or government institute, seismological organisation or company, geological/meteorological survey, station operator, national/international scientific organisation that contribute to the ISC budget by paying membership fees. ISC members have voting rights in the ISC Governing Council.

- ISC-reviewed events

A subset of the events reported to the ISC are selected for ISC analyst review. These events may or may not be located by the ISC. The rules for selecting an event for review are described in Section 11.1.3. Non-reviewed events are explicitly marked in the ISC Bulletin by the comment following the prime hypocentre "Event not reviewed by the ISC".

- ISF

International Seismic Format (www.isc.ac.uk/standards/isf). A standard bulletin format approved by IASPEI. The ISC Bulletin is presented in this format at the ISC website.

- ISS

International Seismological Summary (1918-1963). These bulletins are the predecessors of the ISC Bulletin and represent the major source of instrumental seismological data before the digital era. The ISS contains regionally and teleseismically recorded events from several hundreds of globally distributed stations.

- Network magnitude

The event magnitude reported by an agency or computed by the ISC locator. An agency can report several network magnitudes for the same event and also several values for the same magnitude type. The network magnitude obtained with the ISC locator is defined as the median of station magnitudes of the same magnitude type.

- Phase

A maximum eight-character code for a seismic, infrasonic, or hydroacoustic phase. During the ISC processing, reported phases are mapped to standard IASPEI phase names. Amplitude measurements are identified by specific phase names to facilitate the computation of body-wave and surface-wave magnitudes.

- Prime hypocentre

The preferred hypocentre solution for an event from a list of hypocentres reported by various agencies or calculated by the ISC.

- Reading

Parametric data that are associated to a single event and reported by a single agency from a single station. A reading typically includes one or more phase names, arrival time and/or amplitude/period measurements.

- Report/Data report

All data that are reported to the ISC are parsed and stored in the ISC database. These may include event bulletins, focal mechanisms, moment tensor solutions, macroseismic descriptions and other event comments, as well as phase arrival data that are not associated to events. Every single report sent to the ISC can be traced back in the ISC database via its unique report identifier.

- Shide Circulars

Collections of station reports for large earthquakes occurring in the period 1899-1912. These reports were compiled through the efforts of J. Milne. The reports are mainly for stations of the British Empire equipped with Milne seismographs. After Milne's death, the Shide Circulars were replaced by the Seismological Bulletins of the BAAS.

- Station code

A unique, maximum six-character code for a station. The ISC Bulletin contains data exclusively from stations registered in the International Registry of Seismograph Stations.

13

Acknowledgements

We thank our colleagues at the Kazakhstan National Data Centre in Almaty for kindly accepting our invitation and submitting the articles on their seismic network's history, current status and operational procedures for this issue of the Summary.

We are also grateful to the developers of the Generic Mapping Tools (GMT) suite of software (Wessel and Smith, 1998) that was used extensively for producing the graphical figures.


Finally, we thank the ISC Member Institutions, Data Contributors, Funding Agencies (including NSF Award EAR-1811737 and USGS Award G15AC00202) and Sponsors for supporting the long-term operation of the ISC.

References

- Adams, R. D., A. A. Hughes, and D. M. McGregor (1982), Analysis procedures at the International Seismological Centre, *Physics of the Earth and Planetary Interiors*, *30*, 85–93.
- Amante, C., and B. W. Eakins (2009), ETOPO1 1 arc-minute global relief model: procedures, data sources and analysis, *NOAA Technical Memorandum NESDIS NGDC-24*, NOAA.
- Balfour, N., R. Baldwin, and A. Bird (2008), Magnitude calculations in Antelope 4.10, *Analysis Group Note of Geological Survey of Canada*, pp. 1–13.
- Bennett, T. J., V. Oancea, B. W. Barker, Y.-L. Kung, M. Bahavar, B. C. Kohl, J. . Murphy, and I. K. Bondár (2010), The nuclear explosion database NEDB: a new database and web site for accessing nuclear explosion source information and waveforms, *Seismological Research Letters*, *81*, doi:10.1785/gssrl.81.1.12.
- Bisztricsany, E. A. (1958), A new method for the determination of the magnitude of earthquakes, *Geofiz. Kozl*, pp. 69–76.
- Bolt, B. A. (1960), The revision of earthquake epicentres, focal depths and origin time using a high-speed computer, *Geophysical Journal of the Royal Astronomical Society*, *3*, 434–440.
- Bondár, I., and K. McLaughlin (2009a), A new ground truth data set for seismic studies, *Seismological Research Letters*, *80*, 465–472.
- Bondár, I., and K. McLaughlin (2009b), Seismic location bias and uncertainty in the presence of correlated and non-Gaussian travel-time errors, *Bulletin of the Seismological Society of America*, *99*, 172–193.
- Bondár, I., and D. Storchak (2011), Improved location procedures at the International Seismological Centre, *Geophysical Journal International*, *186*, 1220–1244.
- Bondár, I., E. R. Engdahl, X. Yang, H. A. A. Ghalib, A. Hofstetter, V. Kirchenko, R. Wagner, I. Gupta, G. Ekström, E. Bergman, H. Israelsson, and K. McLaughlin (2004), Collection of a reference event set for regional and teleseismic location calibration, *Bulletin of the Seismological Society of America*, *94*, 1528–1545.
- Bondár, I., E. Bergman, E. R. Engdahl, B. Kohl, Y.-L. Kung, and K. McLaughlin (2008), A hybrid multiple event location technique to obtain ground truth event locations, *Geophysical Journal International*, *175*, doi:10.1111/j.1365.246X.2008.03,867x.
- Bormann, P., and J. W. Dewey (2012), The new iaspei standards for determining magnitudes from digital data and their relation to classical magnitudes, is 3.3, *New Manual of Seismological Observatory Practice 2 (NMSOP-2)*, P. Bormann (Ed.), pp. 1–44, doi:10.2312/GFZ.NMSOP-2_IS_3.3,10.2312/GFZ.NMSOP-2, <http://nmsop.gfz-postsdam.de>.
- Bormann, P., and J. Saul (2008), The new IASPEI standard broadband magnitude mB, *Seism. Res. Lett*, *79*(5), 698–705.
- Bormann, P., R. Liu, X. Ren, R. Gutdeutsch, D. Kaiser, and S. Castellaro (2007), Chinese national network magnitudes, their relation to NEIC magnitudes and recommendations for new IASPEI magnitude standards, *Bulletin of the Seismological Society of America*, *97*(1B), 114–127, doi:10.1785/012006007835.
- Bormann, P., R. Liu, Z. Xu, R. Ren, and S. Wendt (2009), First application of the new IASPEI teleseismic magnitude standards to data of the China National Seismographic Network, *Bulletin of the Seismological Society of America*, *99*, 1868–1891, doi:10.1785/0120080010.

- Chang, A. C., R. H. Shumway, R. R. Blandford, and B. W. Barker (1983), Two methods to improve location estimates - preliminary results, *Bulletin of the Seismological Society of America*, 73, 281–295.
- Choy, G. L., and J. L. Boatwright (1995), Global patterns of radiated seismic energy and apparent stress, *J. Geophys. Res.*, 100(B9), 18,205–18,228.
- Dziewonski, A. M., and F. Gilbert (1976), The effect of small, aspherical perturbations on travel times and a re-examination of the correction for ellipticity, *Geophysical Journal of the Royal Astronomical Society*, 44, 7–17.
- Dziewonski, A. M., T.-A. Chou, and J. H. Woodhouse (1981), Determination of earthquake source parameters from waveform data for studies of global and regional seismicity, *J. Geophys. Res.*, 86, 2825–2852.
- Engdahl, E. R., and R. H. Gunst (1966), Use of a high speed computer for the preliminary determination of earthquake hypocentres, *Bulletin of the Seismological Society of America*, 56, 325–336.
- Engdahl, E. R., and A. Villaseñor (2002), Global seismicity: 1900–1999, *International Handbook of Earthquake Engineering and Seismology, International Geophysics series*, 81A, 665–690.
- Engdahl, E. R., R. van der Hilst, and R. Buland (1998), Global teleseismic earthquake relocation with improved travel times and procedures for depth determination, *Bulletin of the Seismological Society of America*, 88, 722–743.
- Flinn, E. A., and E. R. Engdahl (1965), Proposed basis for geographical and seismic regionalization, *Reviews of Geophysics*, 3(1), 123–149.
- Flinn, E. A., E. R. Engdahl, and A. R. Hill (1974), Seismic and geographical regionalization, *Bulletin of the Seismological Society of America*, 64, 771–993.
- Gutenberg, B. (1945a), Amplitudes of P, PP and S and magnitude of shallow earthquakes, *Bulletin of the Seismological Society of America*, 35, 57–69.
- Gutenberg, B. (1945b), Magnitude determination of deep-focus earthquakes, *Bulletin of the Seismological Society of America*, 35, 117–130.
- Gutenberg, B. (1945c), Amplitudes of surface waves and magnitudes of shallow earthquakes, *Bulletin of the Seismological Society of America*, 35, 3–12.
- Gutenberg, B., and C. F. Richter (1956), Magnitude and Energy of earthquakes, *Ann. Geof.*, 9, 1–5.
- Hutton, L. K., and D. M. Boore (1987), The ML scale in southern California, *Bulletin of the Seismological Society of America*, 77, 2074–2094.
- IASPEI (2005), Summary of magnitude working group recommendations on standard procedures for determining earthquake magnitudes from digital data, <http://www.iaspei.org/commissions/CSOI.html#wgmm>, http://www.iaspei.org/commissions/CSOI/summary_of_WG_recommendations_2005.pdf.
- IASPEI (2013), Summary of magnitude working group recommendations on standard procedures for determining earthquake magnitudes from digital data, http://www.iaspei.org/commissions/CSOI/Summary_of_WG_recommendations_20130327.pdf.
- IDC (1999), IDC processing of seismic, hydroacoustic and infrasonic data, *IDC Documentation*.
- Jeffreys, H., and K. E. Bullen (1940), *Seismological Tables*, British Association for the Advancement of Science.
- Kanamori, H. (1977), The energy release in great earthquakes, *J. Geophys. Res.*, 82, 2981–2987.
- Kennett, B. L. N. (2006), Non-linear methods for event location in a global context, *Physics of the Earth and Planetary Interiors*, 158, 45–64.
- Kennett, B. L. N., E. R. Engdahl, and R. Buland (1995), Constraints on seismic velocities in the Earth from traveltimes, *Geophysical Journal International*, 122, 108–124.
- Kennett, B. L. N., E. R. Engdahl, and R. Buland (1996), Ellipticity corrections for seismic phases, *Geophysical Journal International*, 127, 40–48.

- Lee, W. H. K., R. Bennet, and K. Meagher (1972), A method of estimating magnitude of local earthquakes from signal duration, *U.S. Geol. Surv.*, Open-File Rep.
- Murphy, J. R., and B. W. Barker (2006), Improved focal-depth determination through automated identification of the seismic depth phases pP and sP, *Bulletin of the Seismological Society of America*, *96*, 1213–1229.
- NMSOP-2 (2012), *New Manual of Seismological Observatory Practice (NMSOP-2)*, IASPEI, GFZ, German Research Centre for Geosciences, Potsdam, doi:10.2312/GFZ.NMSOP-2, <http://nmsop.gfz-potsdam.de>, urn:nbn:de:kobv:b103-NMSOP-2.
- Nuttli, O. W. (1973), Seismic wave attenuation and magnitude relations for eastern North America, *J. Geophys. Res.*, *78*, 876–885.
- Richter, C. F. (1935), An instrumental earthquake magnitude scale, *Bulletin of the Seismological Society of America*, *25*, 1–32.
- Ringdal, F. (1976), Maximum-likelihood estimation of seismic magnitude, *Bulletin of the Seismological Society of America*, *66*(3), 789–802.
- Sambridge, M. (1999), Geophysical inversion with a neighbourhood algorithm, *Geophysical Journal International*, *138*, 479–494.
- Sambridge, M., and B. L. N. Kennett (2001), Seismic event location: non-linear inversion using a neighbourhood algorithm, *Pure and Applied Geophysics*, *158*, 241–257.
- Storchak, D. A., J. Schweitzer, and P. Bormann (2003), The IASPEI standard seismic phases list, *Seismological Research Letters*, *74*(6), 761–772.
- Storchak, D. A., J. Schweitzer, and P. Bormann (2011), Seismic phase names: IASPEI standard, in *Encyclopedia of Solid Earth Geophysics*, edited by H. Gupta, pp. 1162–1173, Springer.
- Tsuboi, C. (1954), Determination of the Gutenberg-Richter's magnitude of earthquakes occurring in and near Japan, *Zisin (J. Seism. Soc. Japan)*, *Ser. II*(7), 185–193.
- Tsuboi, S., K. Abe, K. Takano, and Y. Yamanaka (1995), Rapid determination of Mw from broadband P waveforms, *Bulletin of the Seismological Society of America*, *85*(2), 606–613.
- Uhrhammer, R. A., and E. R. Collins (1990), Synthesis of Wood-Anderson Seismograms from Broadband Digital Records, *Bulletin of the Seismological Society of America*, *80*(3), 702–716.
- Vaněk, J., A. Zapotek, V. Karnik, N. V. Kondorskaya, Y. V. Riznichenko, E. F. Savarensky, S. L. Solov'yov, and N. V. Shebalin (1962), Standardization of magnitude scales, *Izvestiya Akad. SSSR., Ser. Geofiz.*(2), 153–158, pages 108–111 in the English translation.
- Villaseñor, A., and E. R. Engdahl (2005), A digital hypocenter catalog for the International Seismological Summary, *Seismological Research Letters*, *76*, 554–559.
- Villaseñor, A., and E. R. Engdahl (2007), Systematic relocation of early instrumental seismicity: Earthquakes in the International Seismological Summary for 1960–1963, *Bulletin of the Seismological Society of America*, *97*, 1820–1832.
- Woessner, J., and S. Wiemer (2005), Assessing the quality of earthquake catalogues: estimating the magnitude of completeness and its uncertainty, *Bulletin of the Seismological Society of America*, *95*(2), doi:10.1785/012040.007.
- Young, J. B., B. W. Presgrave, H. Aichele, D. A. Wiens, and E. A. Flinn (1996), The Flinn-Engdahl regionalisation scheme: the 1995 revision, *Physics of the Earth and Planetary Interiors*, *96*, 223–297.



*Silence isn't empty,
it's full of answers.*

GeoSIG
swiss made to measure 

2 minutes

is all it takes to answer our survey about seismic instruments
and be entered into our prize draw. It's that simple.

One lucky winner will
receive an APPLE Watch!



**LAST
CHANCE!**

In order to encourage more participation, we've extended the deadline for this survey to March 15, 2019. If you've already entered: THANK YOU, your entry will be included; no need to enter again. The prize is an APPLE watch. Choice of this prize does not indicate endorsement or sponsorship by Apple. Full terms and conditions are available with the survey. If you have experience with seismometers, we value your feedback: it might help us with future product development.



SEISMOLOGY
RESEARCH
CENTRE

Easy-to-use, Affordable SEISMOGRAPHS & ACCELEROGRAPHS



Gecko Prism

120s-60Hz or 40s-90Hz
broadband seismograph

Gecko Tremor

0.5s to 1600Hz bandwidth
short period seismograph

Gecko SMA-HR

$\pm 2g$ high sensitivity structural
health monitor accelerograph

Gecko SMA

$\pm 2g$, $\pm 5g$, $\pm 10g$... up to $\pm 400g$
strong motion accelerograph

Gecko Blast

4.5-1600 Hz triaxial velocity
blast and vibration monitor

Gecko Rugged

3+1 channel waterproof
recorder for outdoor use

Gecko Compact

3+1 channel affordable casing
recorder for indoor installation



MADE IN
AUSTRALIA

GECKO PRICING
FROM LESS THAN
€3000

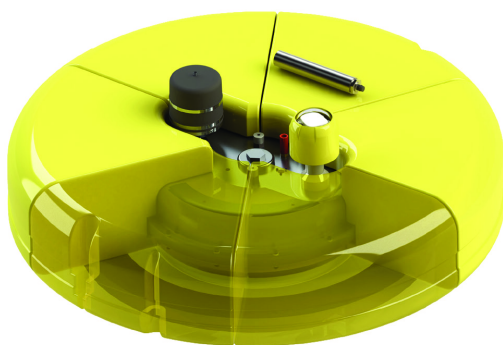


www.src.com.au

141 Palmer St, Richmond
Victoria 3121 Australia
T: +61 3 8420 8940
sales@src.com.au

AQUARIUS

Get near real-time seismic data from the ocean floor...
...without cables.



The Aquarius from Gralp is a compact freefall ocean bottom seismometer (OBS) with optional features for earthquake or tsunami early warning applications.

The Aquarius uses acoustic telemetry capability to deliver near real-time seismic data from the ocean floor to the surface without cables.

The Aquarius sensor is a digital feedback, triaxial, broadband seismometer with a flat response between 120 s and 100 Hz and is operational at any angle.

An additional sensor such as a hydrophone or a pressure sensor can also be incorporated.

AQUARIUS

RESEARCH OPTION:

- > Receive 'State of Health' parameters and noise performance data direct from the seabed following deployment, for confident seismic recording projects lasting up to 18 months
- > For when data transfer is needed only at the installation and at the recovery of the OBS
- > The OBS is equipped with an omni-directional transducer
- > The battery can be sized to record seismic data from 3 to 18 months

AQUARIUS+

RESEARCH AND ALERT OPTION:

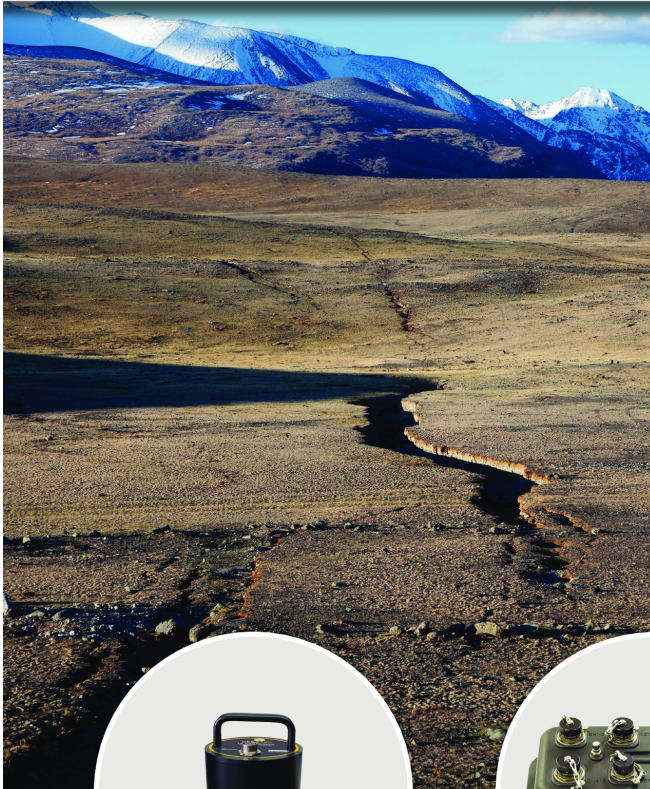
- > Receive triggered (STA/LTA) event notifications to the surface in near real time with options to receive more detailed data for further analysis selected by time frame or by event
- > Bi-directional communication and controls between the underwater system and the ocean surface infrastructure
- > The battery is sized to transfer 10-15 MB of data per month for a deployment lasting 12 months.



Want to find out more?

www.guralp.com/aquarius

If It Moves, You'll Know It. Immediately.



For over 40 years REF TEK®, a Trimble brand, has been the trusted partner for seismologists around the globe.

If it shakes, sinks or shifts our reliable sensors and recorders will know about it instantaneously. And you will too, anytime, as sophisticated application software informs you immediately. Always on the job, offering some peace of mind in an unstable world.



New! REF TEK COLT
High Performance Broadband Seismometer

Delivers exceptional low self noise performance to better measure ground motion, even at the quietest sites. Enables quick and easy deployment using unique alignment features in a small, robust form-factor.



REF TEK 130S-01
High Resolution Seismic Recorder

A compact and lightweight seismic recorder, with IP Communications, ultra-low latency data transmission and removeable data storage. Meets the requirements for Earthquake Early Warning (EEW) systems.



REF TEK 147A
Strong Motion Accelerometer

With high sensitivity, large linear range, high resolution and dynamic range the 147A is suitable for free field applications such as microzonation, site response, earthquake monitoring and more.

For more information visit www.reftek.com

Follow @REFTEK_Trimble 

REF TEK
A TRIMBLE BRAND

© 2019, Trimble Inc. All rights reserved. 022506-267A (01/19)

